

Principles of Modern Wireless Communication Systems

Theory and Practice

About the Author

Aditya K. Jagannatham received his bachelor's degree from the Indian Institute of Technology (IIT) Bombay, Mumbai, India; and MS and PhD degrees from the University of California, San Diego, USA. For two years he was employed as a senior wireless systems engineer at Qualcomm Inc., San Diego, California, where he worked on developing 3G UMTS/WCDMA/HSDPA mobile chipsets as part of the Qualcomm CDMA technologies division.

Dr Jagannatham has contributed to the 802.11n high-throughput wireless LAN standard and has published extensively in leading international journals and conferences. He was awarded the Calit2 Fellowship for pursuing graduate studies at the University of California, San Diego. In 2009, he received the Upendra Patel Achievement Award for his efforts towards developing HSDPA/HSUPA/HSPA + WCDMA technologies at Qualcomm. He is now a faculty member in the Electrical Engineering Department at IIT Kanpur and is also associated with the BSNL-IITK Telecom Center of Excellence (BITCOE). At IIT Kanpur, he has been awarded the P K Kelkar Young Faculty Research Fellowship (June 2012 to May 2015) for excellence in research.

Dr Jagannatham's research interests are in the area of next-generation wireless communications and networking, sensor and ad-hoc networks, digital video processing for wireless systems, wireless 3G/4G cellular standards, and CDMA/OFDM/MIMO wireless technologies. His popular video lectures for the NPTEL (National Programme on Technology Enhanced Learning) course on Advanced 3G and 4G Wireless Mobile Communications can be found on YouTube.

Principles of Modern Wireless Communication Systems

Theory and Practice

Aditya K. Jagannatham

*Department of Electrical Engineering
Indian Institute of Technology (IIT) Kanpur
Kanpur, Uttar Pradesh*



McGraw Hill Education (India) Private Limited
NEW DELHI

McGraw Hill Education Offices

New Delhi New York St Louis San Francisco Auckland Bogotá Caracas
Kuala Lumpur Lisbon London Madrid Mexico City Milan Montreal
San Juan Santiago Singapore Sydney Tokyo Toronto



McGraw Hill Education (India) Private Limited

Published by McGraw Hill Education (India) Private Limited,
P-24, Green Park Extension, New Delhi 110 016.

Principles of Modern Wireless Communication Systems

Copyright © 2016, by McGraw Hill Education (India) Private Limited.

No part of this publication may be reproduced or distributed in any form or by any means, electronic, mechanical, photocopying, recording, or otherwise or stored in a database or retrieval system without the prior written permission of the publishers. The program listing (if any) may be entered, stored and executed in a computer system, but they may not be reproduced for publication.

This edition can be exported from India only by the publishers,
McGraw Hill Education (India) Private Limited.

Print Edition:

ISBN (13): 978-1-259-02957-8

ISBN (10): 1-259-02957-3

Ebook Edition:

ISBN (13): 978-93-392-2003-7

ISBN (10): 93-392-2003-X

Managing Director: *Kaushik Bellani*

Director—Products (Higher Education & Professional): *Vibha Mahajan*

Manager—Product Development: *Koyel Ghosh*

Specialist—Product Development: *Sachin Kumar*

Head—Production (Higher Education & Professional): *Satinder S Baveja*

Manager—Editorial Services: *Sohini Mukherjee*

Assistant Manager—Production: *Anuj K Shrivastava*

Senior Graphic Designer—Cover: *Meenu Raghav*

Assistant General Manager—Product Management (Higher Education & Professional): *Shalini Jha*

Assistant Product Manager: *Tina Jajoriya*

General Manager—Production: *Rajender P Ghansela*

Manager—Production: *Reji Kumar*

Information contained in this work has been obtained by McGraw Hill Education (India), from sources believed to be reliable. However, neither McGraw Hill Education (India) nor its authors guarantee the accuracy or completeness of any information published herein, and neither McGraw Hill Education (India) nor its authors shall be responsible for any errors, omissions, or damages arising out of use of this information. This work is published with the understanding that McGraw Hill Education (India) and its authors are supplying information but are not attempting to render engineering or other professional services. If such services are required, the assistance of an appropriate professional should be sought.

Typeset at Script Makers, 19, A1-B, DDA Market, Paschim Vihar, New Delhi, India

Visit us at: www.mheducation.co.in

Contents

Preface

xi

Chapter 1	Introduction to 3G/4G Wireless Communications	1–5
1.1	Introduction	1
1.2	2G Wireless Standards	1
1.3	3G Wireless Standards	2
1.4	4G Wireless Standards	3
1.5	Overview of Cellular Service Progression	4
	<i>Problems</i>	5
Chapter 2	Introduction: Basics of Digital Communication Systems	6–24
2.1	Gaussian Random Variable	6
2.2	BER Performance of Communication Systems in an AWGN Channel	8
2.2.1	BER for BPSK in AWGN	8
	<i>Example 2.1</i>	11
	<i>Example 2.2</i>	11
2.3	SER and BER for QPSK in AWGN	11
2.4	BER for M -ary PAM	12
2.5	SER for M -QAM	15
2.6	BER for M -ary PSK	17
2.7	Binary Signal Vector Detection Problem	20
2.7.1	An Alternative Approach for M -PSK	23
	<i>Problems</i>	24
Chapter 3	Principles of Wireless Communications	25–82
3.1	The Wireless Communication Environment	25
3.2	Modelling of Wireless Systems	26
	<i>Example 3.1</i>	30
3.3	System Model for Narrowband Signals	30
	<i>Example 3.2</i>	31
3.4	Rayleigh Fading Wireless Channel	32
	<i>Example 3.3</i>	34
	<i>Example 3.4</i>	36

3.4.1	Baseband Model of a Wireless System	37
3.5	BER Performance of Wireless Systems	38
3.5.1	SNR in a Wireless System	38
3.5.2	BER in Wireless Communication Systems	39
	<i>Example 3.5</i>	41
3.5.3	Rayleigh BER at High SNR	42
	<i>Example 3.6</i>	43
3.6	Intuition for BER in a Fading Channel	44
3.6.1	A Simpler Derivation of Approximate Rayleigh BER	45
3.7	Channel Estimation in Wireless Systems	46
	<i>Example 3.7</i>	49
3.8	Diversity in Wireless Communications	50
3.9	Multiple Receive Antenna System Model	51
3.10	Symbol Detection in Multiple Antenna Systems	54
	<i>Example 3.8</i>	57
	<i>Example 3.9</i>	59
3.11	BER in Multi-Antenna Wireless Systems	60
	<i>Example 3.10</i>	61
	<i>Example 3.11</i>	63
3.11.1	A Simpler Derivation of Approximate Multi-Antenna BER	64
3.11.2	Intuition for Diversity	65
	<i>Example 3.12</i>	67
	<i>Example 3.13</i>	68
3.11.3	Channel Estimation for Multi-Antenna Systems	68
	<i>Example 3.14</i>	70
3.12	Diversity Order	71
	<i>Problems</i>	72

Chapter 4 The Wireless Channel

83–118

4.1	Basics of Wireless Channel Modelling	83
4.1.1	Maximum Delay Spread σ_{τ}^{\max}	85
	<i>Example 4.1</i>	87
4.1.2	RMS Delay Spread $\sigma_{\tau}^{\text{RMS}}$	87
	<i>Example 4.2</i>	89
4.1.3	RMS Delay Based on Average Power Profile	91
	<i>Example 4.3</i>	92

4.2	Average Delay Spread in Outdoor Cellular Channels	94
4.3	Coherence Bandwidth in Wireless Communications	95
4.4	Relation Between ISI and Coherence Bandwidth	101
	<i>Example 4.4</i>	104
4.5	Doppler Fading in Wireless Systems	104
	4.5.1 Doppler Shift Computation	105
	<i>Example 4.5</i>	106
4.6	Doppler Impact on a Wireless Channel	106
4.7	Coherence Time of the Wireless Channel	108
	<i>Example 4.6</i>	109
4.8	Jakes Model for Wireless Channel Correlation	110
4.9	Implications of Coherence Time	113
	<i>Problems</i>	115
Chapter 5	Code Division for Multiple Access (CDMA)	119–164
5.1	Introduction to CDMA	119
5.2	Basic CDMA Mechanism	121
5.3	Fundamentals of CDMA Codes	122
5.4	Spreading Codes based on Pseudo-Noise (PN) Sequences	125
	5.4.1 Properties of PN Sequences	127
5.5	Correlation Properties of Random CDMA Spreading Sequences	130
5.6	Multi-User CDMA	133
5.7	Advantages of CDMA	137
	5.7.1 Advantage 1: Jammer Margin	138
	5.7.2 Advantage 2: Graceful Degradation	139
	5.7.3 Advantage 3: Universal Frequency Reuse	140
	5.7.4 Multipath Diversity and Rake Receiver	142
5.8	CDMA Near–Far Problem and Power Control	146
5.9	Performance of CDMA Downlink Scenario with Multiple Users	147
5.10	Performance of CDMA Uplink Scenario with Multiple Users	154
5.11	Asynchronous CDMA	155
	<i>Problems</i>	158
Chapter 6	Multiple-Input Multiple-Output Wireless Communications	165–229
6.1	Introduction to MIMO Wireless Communications	165
6.2	MIMO System Model	166

6.3	MIMO Zero-Forcing (ZF) Receiver	170
6.3.1	Properties of the Zero-Forcing Receiver Matrix F_{ZF}	173
6.3.2	Principle of Orthogonality Interpretation of ZF Receiver	174
	<i>Example 6.1</i>	176
6.4	MIMO MMSE Receiver	179
6.4.1	Robustness of MMSE to Noise Amplification	183
6.4.2	Low and High SNR Properties of the MMSE Receiver	184
6.5	Singular Value Decomposition (SVD) of the MIMO Channel	185
6.5.1	Examples of Singular Value Decomposition	186
	<i>Example 6.2</i>	186
	<i>Example 6.3</i>	187
	<i>Example 6.4</i>	188
6.6	Singular Value Decomposition and MIMO Capacity	189
6.6.1	Optimal MIMO Capacity	192
	<i>Example 6.5</i>	194
6.7	Asymptotic MIMO Capacity	198
6.8	Alamouti and Space-Time Codes	201
6.8.1	Alamouti Code: Procedure	203
	<i>Example 6.6</i>	207
6.9	Another OSTBC Example	209
6.10	Nonlinear MIMO Receiver: V-BLAST	212
	<i>Example 6.7</i>	215
6.11	MIMO Beamforming	216
	<i>Problems</i>	219
Chapter 7	Orthogonal Frequency-Division Multiplexing	230–266
7.1	Introduction	230
7.2	Motivation and Multicarrier Basics	230
7.2.1	Multicarrier Transmission	232
7.2.2	Cyclic Prefix in OFDM	236
7.2.3	Impact of Cyclic Prefix on Data Rate	241
7.3	OFDM Example	243
7.4	Bit-Error Rate (BER) for OFDM	245
7.5	MIMO-OFDM	247

7.6	Effect of Frequency Offset in OFDM	250
	<i>Example 7.1</i>	254
7.7	OFDM – Peak-to-Average Power Ratio (PAPR)	255
7.8	SC-FDMA	260
	7.8.1 SC-FDMA Receiver	261
	7.8.2 Subcarrier Mapping in SC-FDMA	261
	<i>Problems</i>	262

Chapter 8 Wireless-System Planning **267–293**

8.1	Introduction	267
8.2	Free Space Propagation Model	268
8.3	Ground-Reflection Scenario	269
8.4	Okumura Model	273
	<i>Example 8.1</i>	275
8.5	Hata Model	276
	<i>Example 8.2</i>	277
8.6	Log-Normal Shadowing	277
	<i>Example 8.3</i>	278
8.7	Receiver-Noise Computation	279
	<i>Example 8.4</i>	280
8.8	Link-Budget Analysis	280
	<i>Example 8.5</i>	282
8.9	Teletraffic Theory	283
8.10	Teletraffic System Model	286
8.11	Steady-State Analysis	286
	<i>Example 8.6</i>	289
	<i>Example 8.7</i>	290
	<i>Problems</i>	291

Preface

Introduction to the Course

The focus of this book is the area of wireless communications, which has witnessed revolutionary developments in the last decade. While previously there existed only 2G GSM-based communication systems, which supported a data rate of around 10 kbps, several innovative and cutting-edge wireless technologies have been developed in the last ten years. These advances have led subsequently to the proposal and implementation of 3G and 4G wireless technologies such as HSDPA, LTE, and WiMAX, which can support data rates in excess of 100 Mbps. Further, futuristic wireless networks can be employed not only for voice communication, but also for multimedia-based broadband communication such as video conferencing, video calling, etc. Starting from the fundamentals, this book will systematically elaborate on the latest techniques and tools in wireless practice and research.

Objective of this Book

This book is designed to help readers get an in-depth grasp of the fundamentals of 3G and 4G advanced wireless techniques, and gain a better understanding of modern and futuristic wireless networks. While the potential benefits of such technologies are promising, there are numerous challenges in the design and implementation of such wireless systems. The basic objective of this book is to provide a comprehensive exposure to the fast-evolving high-tech field of wireless communications and latest technologies such as CDMA, OFDM, and MIMO, which form the bedrock of 3G/4G wireless networks.

It has also been observed that there is a significant gap in the understanding of students around the world regarding wireless technologies. A few high-level texts do address this area, but the presentation is comprehensible only to advanced professionals in the field. Even then, these texts do not address the needs of the typical student who is beginning to explore this area since such books do not deal with the fundamentals thoroughly. This book is, therefore, specifically designed for a student audience with more emphasis on the fundamentals. Hence, it aims to describe to the readers, in a lucid fashion, several concepts of wireless communications, without any assumptions regarding the prerequisites. In a nutshell, the book aims to introduce the concepts with significant emphasis on the fundamentals.

About the Book

Wireless telecommunications is a key technology sector with tremendous opportunities for growth and development around the world. Recent years have seen an explosion in terms of the available wireless technologies such as mobile cellular networks for voice and packet data,

wireless local area networks, Bluetooth, and so on. Yet, the wireless revolution is very nascent and the 21st century is going to see tremendous diversification of wireless applications in 3G and 4G cellular networks such as rich multimedia-integrated voice-video communication, video-conferencing-based interactive services, multiuser gaming, and strategic surveillance for defence. The book comprehensively covers the fundamental technological advances that have led to progress in the area of wireless communication systems in recent years.

Target Audience

Apart from postgraduate and undergraduate students, this book will be useful to practicing engineers, managers, scientists, faculty members, teachers, and research scholars.

Roadmap of Various Target Courses

Principles of Modern Wireless Communication Systems can be used for various courses as follows:

An advanced undergraduate course on digital communications can incorporate Chapter 2 on digital communication systems, followed by chapters 3, 4 on modelling and performance of digital communication over fading channels. This can be followed by diversity, a brief introduction to CDMA in Chapter 5, and a round-up with wireless-system planning aspects in Chapter 8.

A specialized graduate course on wireless communication can assume the background in Chapter 1 and directly start with fading channels; then rigorously cover diversity and wireless-channel modelling in chapters 3, 4, followed by elements of CDMA, MIMO, and OFDM wireless systems. For the graduate course, the material in Chapter 8 can be optional since this can be assumed to be covered in a semi-advanced course on digital communications. Finally, a short course spanning a few days of intensive teaching can be readily organized by utilizing some elements of chapters 3, 4 and introductory portions of chapters 5, 6, 7 on CDMA, MIMO, and OFDM respectively.

Salient Features

- Strong emphasis on ad-hoc networks and new trends in mobile/wireless communication
- Introduces 3G/4G standards such as HSDPA, LTE, WiMAX to help students understand practical aspects
- Demonstrates a deep theoretical understanding of network analysis along with its real-world applications
- Detailed description of radio propagation over wireless channel and its limitations
- Problem-solving-based approach to enhance understanding
- Blend of analytical and simulation-based problems and examples for better understanding of concepts

- Pedagogy includes
 - Over 90 illustrations
 - Over 34 Solved Examples
 - Over 103 Practice Questions

Organization of the Book

The book is organized into various chapters, each focusing on a unique technology aspect of wireless communications, and aims to cover comprehensively several aspects at the core of 3G/4G wireless technologies.

Chapter 1 introduces the readers to a basic timeline of the progress of wireless technologies starting from 2G, i.e., 2nd Generation, through 3G, i.e., 3rd Generation to the current, i.e., 4th Generation, or 4G wireless technologies.

Chapter 2 familiarizes the reader with the key concepts of digital communication systems, an understanding of which is required to comprehend the advanced concepts introduced in the context of wireless communications in later chapters. This also serves to make the book self-sufficient and refresh the concepts for readers of the book.

This is followed by **Chapter 3** which focuses on the key principles of wireless communications. This chapter describes the fundamental distinguishing aspects of the wireless system, beginning from a model of the fading channel to characterizing the bit-error-rate performance in wireless communication systems. Further, the key principle of diversity, which is of fundamental importance in understanding the performance and motivation of various recent technologies that enhance the reliability of modern wireless communication systems, is described in this chapter, along with an elaborate analytical treatment.

The subsequent chapter, **Chapter 4**, on wireless-channel modelling, describes the framework to model the wireless channel and describes concepts such as delay spread and Doppler—fundamental to understanding the defining characteristics and traits of the wireless channel. This chapter also gives valuable practical insights into the design of 3G/4G wireless communication systems and an intuitive understanding of the various physical properties and specifications of current systems.

These key chapters are then followed by dedicated chapters focusing on various latest wireless technologies.

Chapter 5 on Code Division for Multiple Access (CDMA) provides a detailed introduction to the concept and analysis of CDMA-based wireless networks. CDMA, a cutting-edge wireless technology, is used in a variety of 3G wireless standards such as WCDMA, HSDPA, CDMA 2000, 1xEVDO, etc. Thus, it is the key to understanding various 3G technologies.

Multiple-Input Multiple-Output (MIMO) is another major technology, which is the focus of **Chapter 6**. This is described and the pertinent analysis is presented in significant detail. The

reader is comprehensively exposed to various topics such as linear receivers (zero-forcing, minimum mean-squared error), singular-value decomposition, optimal power allocation, non-linear receivers (V-BLAST), beamforming, etc.

Chapter 7 on Orthogonal Frequency Division Multiplexing (OFDM) rounds up this discussion on key technologies. This is one of the most important chapters for a good understanding of modern wireless systems since most 4G technologies, such as LTE, LTE-A, WiMAX, etc., are based on OFDM. Also, other techniques such as SC-FDMA and MIMO-OFDM are described along with an in-depth analysis of various allied aspects.

The final chapter, **Chapter 8**, describes various aspects of wireless-system planning such as large-scale wireless-propagation models, wireless shadowing, link-budget analysis, and also teletraffic modelling and trunking theory.

The approach of this book is based on building up the concepts from its very fundamentals. Therefore, since no prerequisites are assumed, it addresses the needs of students from a variety of backgrounds with various degrees of prior knowledge in this area, ranging from novice readers to professionals with several years of erstwhile experience. Also, it has a collection of analytical problems, combined with hands-on simulation-based examples and problems for the students to gain a thorough understanding of the subject. Further, this book not only considers these technologies individually, but also addresses these from a holistic perspective of how such things perform in a practical wireless setting. For instance, it takes up issues such as the expected throughput and power levels, the number of subscribers they are intended to support, network capacity, performance, and other topics.

Web Supplements

The Solution Manual for instructors can be accessed at
<https://www.mhhe.com/jagannatham/wc1>

Video lectures for the NPTEL (National Program on Technology Enhanced Learning) Course on Advanced 3G & 4G Wireless Mobile Communications can be accessed by scanning the QR code given here
or

visit <https://www.youtube.com/playlist?list=PLbMVogVj5nJSi8FUsvglRxLtNITN9y4nx>



Acknowledgements

I would like to thank all members of the Multimedia Wireless Networks (MWN) lab in the Electrical Engineering Department at IIT Kanpur, particularly all the PhD and MTech students who have been a part of the lab over the years and whose researches have played a pivotal role in shaping this book. My heartfelt gratitude to the faculty members of the Electrical Engineering Department at IIT Kanpur for their valuable research collaborations and discussions in this area. I appreciate the efforts of the following reviewers for going through the draft and suggesting their inputs.

Sanjeev Jain	<i>Government Engineering College, Bikaner, Rajasthan</i>
Ranjan Mishra	<i>University of Petroleum and Energy Studies, Dehradun, Uttarakhand</i>
Aniruddha Chandra, Sanjay Dhar Roy, Sumit Kundu	<i>National Institute of Technology (NIT), Durgapur, West Bengal</i>
Preetida Vinayakray Jani, Vijay Kumar Chakka	<i>Dhirubhai Ambani Institute of Information and Communication Technology (DAIICT), Gandhinagar, Gujarat</i>
N Shah	<i>Sardar Vallabhbhai National Institute of Technology (SVNIT), Surat, Gujarat</i>
Radhika D Joshi	<i>College of Engineering, Pune, Maharashtra</i>
Deivalakshmi, D Sriram Kumar	<i>National Institute of Technology (NIT) Tiruchirappalli, Tamil Nadu</i>
G Sivaradje	<i>Pondicherry Engineering College, Puducherry</i>
T Rama Rao	<i>SRM University, Tamil Nadu</i>
T J Jeyaprabha	<i>Sri Venkateswara College of Engineering, Pennalur, Tamil Nadu</i>
N Shekar V Shet	<i>National Institute of Technology (NIT) Karnataka, Surathkal, Karnataka</i>

Finally, I would like to express gratitude to my family for supporting me throughout this endeavour and bearing with my constant preoccupation during this period.

ADITYA K JAGANNATHAM

Publisher's Note

McGraw Hill Education (India) invites suggestions and comments from you, all of which can be sent to support.india@mheducation.com (kindly mention the title and author name in the subject line).

Piracy-related issues may also be reported.

Introduction to 3G/4G Wireless Communications

1.1 | Introduction

Wireless communications has witnessed revolutionary advancements in the recent decades, which has changed the face of modern telecommunications. Starting from its modest beginning limited to a few hundreds of users initially, wireless communication is now accessible to a dominant fraction of the global population. This has ushered in a radical new era of communication and connectivity. The *Global System for Mobile (GSM)* cellular standard, which was formalized in 1992, has been rapidly adopted by billions of cellular users for voice communication. The advent of the Internet and packet-based data networks has ushered an ever-increasing demand for ubiquitous data access over these wireless networks. This has led to a progressive advancement of wireless communications from traditional voice-based networks to Internet, multimedia, and video-service networks. In this process, successive generations of wireless standards have evolved to support the rich high-data-rate wireless ecosystem, which basically comprise the third and fourth generations of evolution of radio communications, abbreviated as 3G and 4G respectively. Below we give details of the family of salient wireless standards belonging to each generation of the wireless revolution.

1.2 | 2G Wireless Standards

The family of 2G wireless standards were initially proposed to provide basic wireless voice communication facility to users with mobile cellular devices. Further, these comprised the first set of fully digital wireless communication devices compared to 1G systems, which were analog in nature. The dominant 2G standard, GSM, was initially proposed with an aim of

developing a multi-country joint standard in an effort to unify the mobile communication infrastructure across the globe, thus providing better access and facilities. The broad set of such standards and their data rates are given in Table 1.1.

Table 1.1 *Family of 2G wireless cellular standards*

Generation	Standard	Data Rate
2G	GSM	10 kbps
2G	IS-95 (CDMA)	10 kbps
2.5G	GPRS	50 kbps
2.5G	EDGE	200 kbps

Hence, while GSM and IS-95 are based on code division for multiple access (CDMA) are primarily based on voice communication rates of around 10 kbps, the later add-on standards of *General Packet Radio Service (GPRS)* and enhanced data for GSM evolution (*EDGE*) were proposed with an idea of increasing the data rates over cellular networks to provide low-speed data access such as Internet, e-mail, etc, to users with mobile devices. As given above, the data rates supported by such nascent data access standards was in the range of 100 kbps. The increasing demand for higher data rates over mobile devices led to the development of the 3G cellular standards described below.

1.3 | 3G Wireless Standards

The third generation, or 3G wireless standards, were proposed around the year 2000 and primarily based on CDMA technology for multiple access because of the superior properties of CDMA compared to the other access technologies such as *Time Division for Multiple Access (TDMA)* and *Frequency Division for Multiple Access (FDMA)*. Also, 3G standards are termed *wideband wireless technologies* as they employ spectral bandwidth generally in excess of 5 MHz. The list of 3G standards and the associated data rates is given below.

The 3G standard of wideband code division for multiple access (WCDMA) is also sometimes abbreviated as the *Universal Mobile Telecommunications System (UMTS)*. Another comparable 3G standard also based on CDMA is the CDMA 2000 standard, primarily

employed in North America, Japan, and some other countries. Both are capable of data rates around 300 kbps necessary to support low-rate data access over wireless networks. The progressive demand for higher data rate led to the addition of High-Speed Downlink Packet Access (HSDPA) and High Speed Uplink Packet Access (HSUPA), additions to the WCDMA standard. These enhanced the capabilities of the WCDMA suite of 3G standards to the range of 5–30 Mbps, capable of providing services similar to those available on the Digital Subscriber Line (DSL) and Asymmetric Digital Subscriber Line (ADSL) available on the wired network infrastructure. Further, the CDMA 2000 suite was also expanded to include similarly the 1x Evolution Data Optimized (1xEVDO) standard and its subsequent revisions titled simply rev. A and rev. B to enhance the data rates to close to 30 Mbps. Thus, the 3G group of cellular services based on the above set of standards can support data rates in excess of 10 Mbps, making it possible to transmit high-data-rate multimedia and video content to mobile devices. These rates are expected to further increase manifold in 4G cellular networks.

Table 1.2 Family of 3G wireless cellular standards

Generation	Standard	Data Rate
3G	WCDMA/UMTS	384 kbps
3G	CDMA 2000	384 kbps
3.5G	HSDPA/HSUPA	5–30 mbps
3.5G	1xEVDO-Rev. A,B	5–30 mbps

1.4 | 4G Wireless Standards

The set of 4G wireless standards is based on the revolutionary new technology of *Orthogonal Frequency Division Multiplexing (OFDM)*. The multiple access technology based on OFDM is termed *Orthogonal Frequency Division for Multiple Access (OFDMA)*. Also, another breakthrough technology employed in 4G wireless systems is termed *Multiple-Input Multiple-Output (MIMO)*, which basically refers to employing multiple antennas at the transmitter and receiver in such systems. Thus, these radical advancements help 4G wireless systems achieve data rates in excess of 100 Mbps. The specific standards and associated rates are listed in Table 1.3.

Long-Term Evolution (LTE) and LTE Advanced are the standards developed by the 3rd Generation Partnership Project (3GPP) standardization body while the *Worldwide Interoperability for Microwave Access (WiMAX)* is under the purview of the WiMAX forum. Currently, 4G devices and networks are being tested and partially implemented in several parts of the world.

Table 1.3 Family of 4G wireless cellular standards

Generation	Standard	Data Rate
4G	LTE	100–200 Mbps
4G	WiMAX	100 Mbps
4G	LTE Advanced	> 1 Gbps

1.5 | Overview of Cellular Service Progression

As the data rates have progressively increased in successive generations of cellular networks, the nature of applications and services offered by such networks have diversified and grown richer. A brief summary of typical services in various cellular networks is given in Table 1.4.

Table 1.4 Services and features of different generations of cellular networks

Generation	Rate	Applications
2.0–2.75G	10–100 kbps	Voice, Low Rate Data
3.0–3.5G	300 kbps - 30 mbps	Voice, Data, Video Calling, Video Conferencing
4G	100–200 Mbps	Online Gaming, HDTV

Note that each generation in the above table offers all the services of the previous generations in addition to the newer services offered in the present generation. *High-Definition*

Television (HDTV) streaming applications in 4G networks typically require a data rate of 10 Mbps per stream.

PROBLEMS

1. Complete the statements below.

- (a) An example of a 1st generation wireless cellular standard is _____.
- (b) GSM has a per-user raw-data rate of _____.
- (c) The technical name for the CDMAOne standard is _____.
- (d) The acronym UMTS stands for _____.
- (e) HSDPA included in the 3GPP Release 5 has a peak data rate of _____.
- (f) The multiple access technology used in LTE is _____.
- (g) 802.11b operates in the frequency band _____.
- (h) One wireless standard that uses MIMO is _____.
- (i) The acronym GMSK stands for _____.
- (j) AFH-SS used in Bluetooth (IEEE 802.15.1-2005) PHY stands for _____.

2. Fill in the blanks below.

- (a) The downlink data rate of LTE is roughly _____.
- (b) 3G cellular uses CDMA for multiple access while 4G uses _____.

Introduction: Basics of Digital Communication Systems

2.1 | Gaussian Random Variable

Since we are going to deal with Gaussian random variables frequently in this textbook during the course of learning about modern wireless communication systems, it is essential to thoroughly understand the properties of Gaussian random variables. Consider a Gaussian random variable of mean μ and variance σ^2 . This is represented using the notation $\mathcal{N}(\mu, \sigma^2)$. The probability density of such a Gaussian random variable, denoted by $f_X(x)$, is given as

$$f_X(x) = \frac{1}{\sqrt{2\pi\sigma^2}} e^{-\frac{(x-\mu)^2}{2\sigma^2}} \quad (2.1)$$

The probability density function above is not to be confused with a probability. The probability density function $f_X(x)$ is to be interpreted as follows.

Given an infinitesimally small interval of width Δx around x , i.e., the interval $\left[x - \frac{\Delta x}{2}, x + \frac{\Delta x}{2}\right]$, the probability that the random variable X takes values inside this interval is given as $f_X(x) \Delta x$. Further, a Gaussian random variable with mean equal to zero, i.e., $\mu = 0$, and unit variance, i.e., $\sigma^2 = 1$, is known as a *standard Gaussian random variable*. This is represented by the notation $\mathcal{N}(0, 1)$ and has the probability density function

$$f_X(x) = \frac{1}{\sqrt{2\pi}} e^{-\frac{x^2}{2}} \quad (2.2)$$

Of particular interest is the cumulative distribution function of the standard Gaussian random variable, i.e., the function denoted by $Q(t)$, and defined as $Q(t) = \Pr\{X \geq t\}$, which can

be obtained by evaluating the integral

$$Q(t) = \int_t^{\infty} \frac{1}{\sqrt{2\pi}} e^{-\frac{x^2}{2}} dx. \quad (2.3)$$

Also, another useful property of Gaussian random variables is that the linear combination of a set of random variables yields a Gaussian random variable. Consider N independent zero-mean Gaussian random variables X_1, X_2, \dots, X_N with σ_i^2 denoting the variance of X_i . Therefore, each X_i can be represented as $\mathcal{N}(0, \sigma_i^2)$. Observe that $E\{X_i X_j\} = E\{X_i\} E\{X_j\} = 0$, when $i \neq j$, since the random variables X_i are independent. Let the random variable Y be obtained by a linear combination of the above random variables as

$$Y = a_1 X_1 + a_2 X_2 + \dots + a_N X_N = \sum_{i=1}^N a_i X_i,$$

where a_1, a_2, \dots, a_N are the constant coefficients of combination. The random variable Y follows a Gaussian distribution with mean

$$\begin{aligned} E\{Y\} &= E\left\{\sum_{i=1}^N a_i X_i\right\} \\ &= \sum_{i=1}^N a_i E\{X_i\} = 0. \end{aligned}$$

Further, the variance of Y is given as

$$\begin{aligned} E\{Y^2\} &= E\left\{\left(\sum_{i=1}^N a_i X_i\right)^2\right\}, \\ &= E\left\{\left(\sum_{i=1}^N a_i X_i\right)\left(\sum_{j=1}^N a_j X_j\right)\right\} \\ &= E\left\{\sum_{i=1}^N \sum_{j=1}^N a_i a_j X_i X_j\right\} \\ &= \sum_{i=1}^N \sum_{j=1}^N E\{a_i a_j X_i X_j\} \\ &= \sum_{i=1}^N a_i^2 \sigma_i^2 \end{aligned}$$

where the last step follows from the property already described above, i.e., $E\{X_i X_j\} = E\{X_i\} E\{X_j\} = 0$, when $i \neq j$. Thus, Y can be represented as $\mathcal{N}\left(0, \sum_{i=1}^N a_i^2 \sigma_i^2\right)$.

2.2 BER Performance of Communication Systems in an AWGN Channel

The Bit Error Rate (BER) is the most widely used metric to characterize the performance of digital communication systems. Simply stated, it is the average rate of erroneously decoding the transmitted information bits at the communication receiver. For instance, if the symbol constellation is Binary Phase-Shift Keying (BPSK) of average symbol power P , the transmitted symbol levels are given as $+\sqrt{P}$, $-\sqrt{P}$ for the information symbols 1, 0 respectively. In the above BPSK example, bit error would refer to decoding a transmitted $+\sqrt{P}$ (corresponding to the information bit 1) erroneously as the 0 bit and vice versa. This corruption of the detected information symbol stream arises centrally due to the presence of the white Gaussian noise at the receiver. Such a channel is also termed an *Additive White Gaussian Noise (AWGN)* channel and is a good model for wireline channels, i.e., with a wire channel such as a telephone line between the transmitter and the receiver. The equivalent analysis for wireless channels will be dealt subsequent chapters. On the upcoming section, we start with the BER characterization of BPSK transmission across an AWGN channel.

2.2.1 BER for BPSK in AWGN

As stated in the example in the above section, consider the transmission of the BPSK symbols $+\sqrt{P}$, $-\sqrt{P}$ to denote information bits 1, 0, respectively. The system model, as described above, is given as

$$y(k) = x(k) + n(k) \quad (2.4)$$

The symbol $y(k)$ is observed at the receiver in the presence of noise $n(k)$, and one has to make a decision $x_d(k)$ on whether the transmitted information bit was 1 or 0 [i.e., whether $x(k)$ was $+\sqrt{P}$ or $-\sqrt{P}$]. Since the symbol levels $+\sqrt{P}$, $-\sqrt{P}$ are symmetric about 0, one simple symbol detector for the above system that estimates the transmitted symbol $x(k)$ could

be to decide

$$x_d(k) = \begin{cases} 1, & \text{if } y(k) > 0 \\ 0, & \text{if } y(k) < 0 \end{cases}$$

A detection error occurs in the above system when $x_d(k) \neq x(k)$, or in other words, $x_d(k) = 1$, when $x(k) = 0$ and vice versa. Consider the transmission of the level $-\sqrt{P}$ corresponding to the bit 0. By the above reasoning, a detection error occurs if $y(k) < 0$, which can be restated using the system model as

$$-\sqrt{P} + n(k) > 0 \Rightarrow n(k) > \sqrt{P}$$

Since $n(k)$ is the Gaussian noise with zero-mean and variance σ^2 , the chance of the above bit-error event depends on the probability that the noise level $n(k)$ exceeds the signal level \sqrt{P} . This probability is simply given by integrating the Gaussian density function as

$$P(n(k) > \sqrt{P}) = \frac{1}{\sqrt{2\pi\sigma^2}} \int_{\sqrt{P}}^{\infty} e^{-\frac{t^2}{2\sigma^2}} dt = \frac{1}{\sqrt{2\pi}} \int_{\sqrt{\frac{P}{\sigma^2}}}^{\infty} e^{-\frac{r^2}{2}} dr \quad (2.5)$$

The quantity on the right is given by the well-known Gaussian $Q(\cdot)$ function introduced in Section 2.1. This function is defined as

$$Q(x) = \frac{1}{\sqrt{2\pi}} \int_x^{\infty} e^{-\frac{r^2}{2}} dr$$

Hence, finally, the probability of bit-error, or the BER for the above wireline channel can be derived by expressing the probability in Eq. (2.5) in terms of the $Q(\cdot)$ function as

$$P(n(k) > \sqrt{P}) = Q\left(\sqrt{\frac{P}{\sigma^2}}\right) = Q(\sqrt{\text{SNR}}), \quad (2.6)$$

where the quantity $\text{SNR} = \frac{P}{\sigma^2}$ denotes the signal-to-noise power ratio of the above wireline communication system. Also, the SNR of a system is often expressed in dB as

$$\text{SNR (dB)} = 10 \log_{10} \left(\frac{P}{\sigma^2} \right)$$

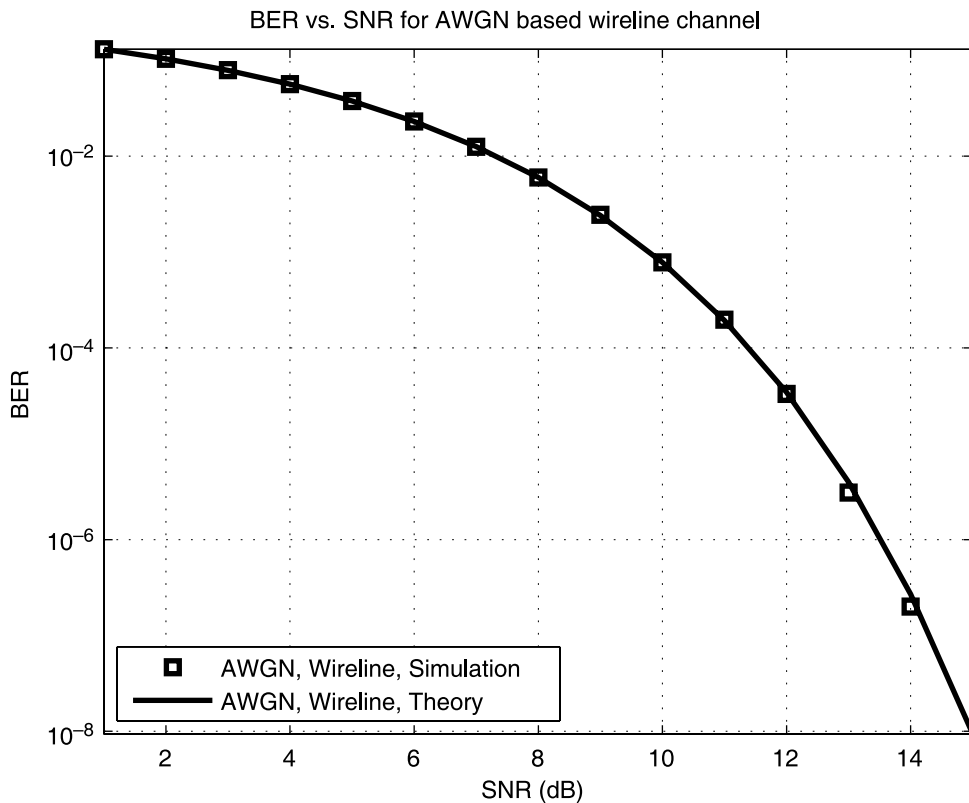


Figure 2.1 BER of a wireline or AWGN channel based communication system. The plot corresponding to 'theory' is obtained from the analytical expression in Eq. (2.6). Observe that the curves obtained from the theory and simulation coincide accurately.

The BER vs SNR for the above wireline system is plotted vs SNR(dB) in Figure 2.1. The Gaussian Q function satisfies the property that $Q(x) \leq \frac{1}{2}e^{-\frac{x^2}{2}}$. Hence, the BER of the wireline channel decreases as

$$Q(\sqrt{\text{SNR}}) \leq \frac{1}{2}e^{-\frac{\text{SNR}}{2}} \quad (2.7)$$

Thus, it has a *faster* exponential rate of decrease with respect to SNR. As can be seen in Figure 2.1, on a wireline channel, one can obtain a BER as low as 10^{-6} at an SNR equal to 13.54 dB. The examples given clearly illustrate the point.

EXAMPLE 2.1

What is the BER of BPSK communication over an AWGN communication channel at $\text{SNR}_{\text{dB}} = 10$ dB?

Solution: The signal-to-noise power ratio in dB is given as $\text{SNR}_{\text{dB}} = 10 \log_{10} (\text{SNR})$. Hence, given $\text{SNR}_{\text{dB}} = 10$ dB, it is easy to see that the corresponding $\text{SNR} = 10^{(\text{SNR}_{\text{dB}}/10)} = 10$. Hence, the bit-error rate for the wireline AWGN channel is given as $Q(\sqrt{\text{SNR}}) = Q(\sqrt{10}) = 7.82 \times 10^{-4}$. This basically implies that in a block of a million, i.e., 10^6 bits, on an average, $7.82 \times 10^{-4} \times 10^6 = 782$ bits are received in error.

EXAMPLE 2.2

Compute the SNR_{dB} required for a probability of bit error, i.e., $\text{BER} = 10^{-6}$ over an AWGN channel.

Solution: This can be computed as follows. From the above discussion, BER over the wireline channel equals $Q(\sqrt{\text{SNR}})$. Hence, for a BER of 10^{-6} , we have $Q(\sqrt{\text{SNR}}) = 10^{-6}$. Thus, the SNR required is

$$\text{SNR} = (Q^{-1}(10^{-6}))^2 = 4.75^2 = 22.60$$

Hence, the SNR in dB is given as, $\text{SNR}_{\text{dB}} = 10 \log_{10}(22.6) = 13.6$ dB.

2.3 | SER and BER for QPSK in AWGN

In *Quadrature Phase Shift Keying (QPSK)*, we consider the complex constellation symbols given as $\pm\sqrt{\frac{P}{2}} \pm j\sqrt{\frac{P}{2}}$. Thus, the total power symbol can be seen to be $\left(\sqrt{\frac{P}{2}}\right)^2 + \left(\sqrt{\frac{P}{2}}\right)^2 = P$, which is constant and equal to that of the BPSK system introduced above. The real and imaginary parts of the constellation symbol denote the in-phase and quadrature symbol components of the complex constellation symbol. Further, we consider

the noise also to be complex Gaussian in nature given as $n(k) = n_I(k) + jn_Q(k)$, with $n_I(k)$, $n_Q(k)$ denoting the in-phase and quadrature Gaussian noise components. Further, the total noise power is $E\{|n(k)|^2\} = \sigma^2$. The power of the in-phase and quadrature noise components is each $\frac{\sigma^2}{2}$, i.e., $E\{|n_I(k)|^2\} = E\{|n_Q(k)|^2\} = \frac{\sigma^2}{2}$. Further, the real and complex noise components are also *uncorrelated*, which implies *independence* since $n_I(k)$, $n_Q(k)$ are Gaussian in nature. Such a noise process is also termed *zero-mean circularly symmetric complex Gaussian noise*.

Thus, in the above QPSK system, we have the symbol and noise power given respectively as $\frac{P}{2}$, $\frac{\sigma^2}{2}$ for both the in-phase and quadrature noise components. Thus, the SNR remains unchanged and is equal to $\frac{P/2}{\sigma^2/2} = \frac{P}{\sigma^2}$. Therefore, the bit-error rate of each channel of QPSK is identical to that of BPSK, and is given as

$$P_e = Q\left(\sqrt{\text{SNR}}\right) \quad (2.8)$$

Further, the probability of symbol error for a QPSK system can be derived as follows. The QPSK symbol is in error if either of the bits are in error. The probability that each bit is received correctly is $1 - P_e$. Therefore, the probability that both the symbols are received without error is $(1 - P_e)^2$. Therefore, the net symbol error rate, i.e., the probability that one or both bits are in error, is given as

$$P_s = 1 - (1 - P_e)^2 = 2P_e - P_e^2 \approx 2P_e$$

since P_e is very small, $P_e^2 \ll P_e$ at high SNR. Thus, at high SNR, the net symbol error rate of the QPSK system is approximately twice the bit error rate.

2.4 | BER for M -ary PAM

We now derive the BER for an M -PAM digital communication system. Let the i^{th} symbol in the constellation be given as $s_i = \pm(2i + 1)\Delta$, where $0 \leq i \leq M - 1$. This constellation is pictorially shown in Figure 2.2. This quantity M can also be related to the number of bits b per symbol as follows. Since $b = \log_2(2M)$, it follows that $M = 2^{b-1}$. For example, consider $b = 3$, which corresponds to 8 PAM, i.e., 3 bits per symbol. The amplitude levels corresponding to this are given as $\pm\Delta$, $\pm3\Delta$, $\pm5\Delta$, $\pm7\Delta$. The average symbol power P of this constellation

is given as

$$\begin{aligned}
 P &= \frac{1}{M} \sum_{k=0}^{M-1} (2k+1)^2 \Delta^2 \\
 &= \frac{\Delta^2}{M} \sum_{k=0}^{M-1} (4k^2 + 4k + 1) \\
 &= \frac{\Delta^2}{M} \left(M + 4 \times \frac{M(M-1)}{2} + 4 \times \frac{(M)(M-1)(2M-1)}{6} \right) \\
 &= \frac{\Delta^2}{M} \left(M + 2M^2 - 2M + \frac{2}{3} (M^2 - M)(2M-1) \right) \\
 &= \frac{\Delta^2}{3M} (3(2M^2 - M) + 2(2M^3 - 3M^2 + M)) \\
 &= \frac{\Delta^2}{3M} (6M^2 - 3M + 4M^3 - 6M^2 + 2M) \\
 &= \frac{\Delta^2}{3M} (4M^3 - M) = \frac{\Delta^2}{3} (4M^2 - 1) \\
 &= \frac{\Delta^2}{3} (2^{2b} - 1) \tag{2.9}
 \end{aligned}$$

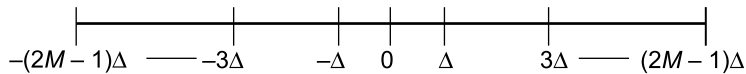


Figure 2.2 *M*-ary PAM constellation

Therefore, the distance between the constellation points Δ is given in terms of P as $\Delta = \sqrt{\frac{3P}{(4M^2-1)}}$. The average probability of error can now be found as follows. Observe from Figure 2.2 that there are basically two kinds of symbols. For the $M-2$ points in the middle, which have one constellation point on either side, error occurs if the noise w of variance σ^2 is either greater than Δ or less than $-\Delta$.

Therefore, the probability of error P_e^i for an interior point is computed as

$$\begin{aligned} P_e^i &= \Pr(w \geq \Delta) + \Pr(w \leq -\Delta) \\ &= \Pr\left(\frac{w}{\sigma} \geq \frac{\Delta}{\sigma}\right) + \Pr\left(\frac{w}{\sigma} \leq -\frac{\Delta}{\sigma}\right) \end{aligned}$$

Observe that since w is a zero-mean Gaussian random variable of variance σ^2 , the quantity (w/σ) is a zero-mean random variable of variance $\mathbb{E}\left\{\left(\frac{w}{\sigma}\right)^2\right\} = \frac{\mathbb{E}\{w^2\}}{\sigma^2} = 1$. The *tail* probability corresponding to a standard Gaussian random variable X of zero-mean and unit variance is defined as

$$\Pr(X \geq x) = Q(x)$$

where $Q(x)$ is also termed the Gaussian Q function. Further, observe that since X is zero-mean and symmetric, it follows that the $\Pr(X \geq x) = \Pr(X \leq -x)$. Employing the above properties, the expression for P_e^i above can be simplified as

$$P_e^i = Q\left(\frac{\Delta}{\sigma}\right) + Q\left(\frac{\Delta}{\sigma}\right) = 2Q\left(\frac{\Delta}{\sigma}\right) \quad (2.10)$$

Now, consider the two symbols at either end. For the leftmost symbols, i.e., $-(2M-1)\Delta$, error occurs if the noise w of variance σ^2 is greater than Δ , while for the rightmost symbol, i.e., $(2M-1)\Delta$, error occurs if the noise w of variance σ^2 is lesser than $-\Delta$. Each of these probabilities is given as

$$\begin{aligned} P_e^i &= \Pr(w \geq \Delta) = \Pr(w \leq -\Delta) \\ &= \Pr\left(\frac{w}{\sigma} \geq \frac{\Delta}{\sigma}\right) \\ &= Q\left(\frac{\Delta}{\sigma}\right) \end{aligned} \quad (2.11)$$

The average probability of error P_e can be expressed as

$$P_e = \sum_i p(e|s_i) \times p(s_i)$$

where $p(s_i)$ is the probability of transmission of the symbol s_i , and $p(e|s_i)$ is the probability of error given s_i is transmitted. Considering a simplistic scenario, we assume that all symbols

s_i are equiprobably, i.e., $p(s_i) = \frac{1}{2M}$, which is frequently the case in practice. Therefore, substituting the various expressions derived for $P(e|s_i)$ derived in (2.10), (2.11) in the expression for P_e above, the resulting expression for P_e can be simplified as

$$\begin{aligned} P_e &= \frac{2(M-1)}{2M} 2Q\left(\frac{\Delta}{\sigma}\right) + \frac{2}{2M} Q\left(\frac{\Delta}{\sigma}\right) \\ &= 2\left(1 - \frac{1}{2M}\right) Q\left(\frac{\Delta}{\sigma}\right). \end{aligned}$$

Substituting the expression for Δ in terms of the average symbol power P from Eq. (2.9) yields the final expression for the symbol error rate of M -PAM as

$$P_e = 2\left(1 - \frac{1}{2M}\right) Q\left(\sqrt{\frac{3P}{(4M^2 - 1)\sigma^2}}\right) \quad (2.12)$$

2.5 | SER for M -QAM

Consider now an M -ary QAM constellation in which each symbol $s_{k,l}$ is described as $s_{k,l} = \pm(2k+1)\Delta \pm (2l+1)\Delta$, where $k, l \in \{0, 1, \dots, M-1\}$. This constellation is pictorially shown in Figure 2.3. Thus, it can be seen that M -QAM constellation is given as the combination of two M -PAM constellations on the x - and y -axes, representing the in-phase and quadrature components of the communication signal. Therefore, considering total average power of P , the average power of each of the constituent PAM constellations is given as $\frac{P}{2}$. Further, considering total noise variance σ^2 , the noise power of each of the in-phase and quadrature components can be obtained as $\frac{\sigma^2}{2}$. Thus, the symbol error rate of each of the individual PAM constellations in the QAM constellation is given from Eq. (2.12) as,

$$\begin{aligned} P_{e,\text{PAM}} &= 2\left(1 - \frac{1}{2M}\right) Q\left(\sqrt{\frac{3\frac{P}{2}}{(4M^2 - 1)\frac{\sigma^2}{2}}}\right) \\ &= 2\left(1 - \frac{1}{2M}\right) Q\left(\sqrt{\frac{3P}{(4M^2 - 1)\sigma^2}}\right) \end{aligned} \quad (2.13)$$

Thus, the symbol error rate of each of the in-phase and quadrature components is identical to that for the M -ary PAM constellation, given in Eq. (2.12). Further, a symbol in the QAM constellation is in error if either of the constituent PAM symbols is in error. This overall

probability of symbol error for the QAM constellation can be calculated as follows. The probability that the constituent PAM symbol decoded correctly is given as $1 - P_{e,\text{PAM}}$. Further, considering the in-phase and quadrature noise components to be independent, the probability that both the constituent PAM symbols are decoded correctly is given as $(1 - P_{e,\text{PAM}})^2$. Therefore, the net probability that at least one of the PAM symbols is in error, in which case the QAM symbol is decoded in error, is given as

$$\begin{aligned}
 P_{e,\text{QAM}} &= (1 - P_{e,\text{PAM}})^2 \\
 &= 2P_{e,\text{PAM}} - P_{e,\text{PAM}}^2 \\
 &\approx 2P_{e,\text{PAM}}
 \end{aligned}
 \tag{2.14}$$

where the last approximate above follows from the fact that at high SNR, $P_{e,\text{PAM}}$ is very small. Therefore, $P_{e,\text{PAM}}^2$ is negligible in comparison to $P_{e,\text{PAM}}$. Thus, it can be seen that the SER of the M -QAM constellation is twice that of the M -PAM constellation for a given average symbol power \mathcal{E}_s .

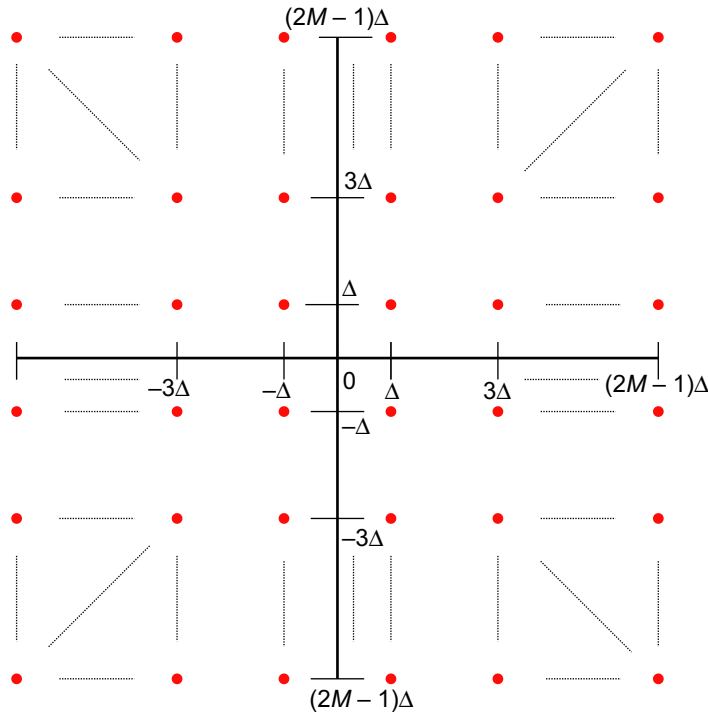


Figure 2.3 M -ary QAM constellation

2.6 | BER for M -ary PSK

The k^{th} symbol of the M -ary Phase Shift Keying (PSK) constellation can be represented as $[\sqrt{P} \cos(\frac{2\pi k}{M}), \sqrt{P} \sin(\frac{2\pi k}{M})]$, for $0 \leq k \leq M - 1$. Thus, these symbols can be visualized as being arranged on the circumference of a circle of radius \sqrt{P} , as shown in Figure 2.4, with an equal phase spacing of $\frac{2\pi}{M}$. The quantity P denotes the symbol energy. We now determine the bit error rate (BER) for M -ary PSK modulation based detection in an additive white Gaussian noise channel. Consider the transmission of the M -PSK symbol corresponding to $k = 0$, i.e., $(\sqrt{E_s}, 0)$. The outputs x, y , corresponding to the in-phase and quadrature components respectively, are given as

$$x = \sqrt{P} + n_I$$

$$y = n_Q$$

Note that n_I, n_Q are Gaussian noise components of mean zero and variance $\tilde{\sigma}^2 = \frac{\sigma^2}{2}$. Therefore, the observation x is Gaussian with mean \sqrt{P} , and the same variance $\tilde{\sigma}^2$. The joint distribution of X, Y is given as

$$\begin{aligned} f_{X,Y}(x, y) &= \frac{1}{2\pi\tilde{\sigma}^2} \exp\left(-\frac{(x - \sqrt{P})^2}{2\tilde{\sigma}^2}\right) \times \exp\left(-\frac{y^2}{2\tilde{\sigma}^2}\right) \\ &= \frac{1}{2\pi\tilde{\sigma}^2} \exp\left(-\frac{x^2 + y^2 - 2\sqrt{P}x + P}{2\tilde{\sigma}^2}\right) \end{aligned} \quad (2.15)$$

Let us now substitute $x = r \cos \theta$, $y = r \sin \theta$, where $0 \leq r \leq \infty$ and $-\pi \leq \theta < 2\pi$. Therefore, the distribution $f_{R,\Theta}(r, \theta)$, in terms of the transformed variables r, θ is given as

$$\begin{aligned} f_{R,\Theta}(r, \theta) &= \frac{1}{2\pi\tilde{\sigma}^2} \exp\left(-\frac{r^2 + P - 2r\sqrt{P}\cos\theta}{2\tilde{\sigma}^2}\right) \times |J_{XY}| \\ &= \frac{r}{2\pi\tilde{\sigma}^2} \exp\left(-\frac{1}{2} \frac{r^2 + P - 2r\sqrt{P}\cos\theta}{\tilde{\sigma}^2}\right) \end{aligned} \quad (2.16)$$

where $|J_{XY}| = r$ is the Jacobian determinant corresponding to the above transformation of random variables. We now integrate over the random variable r to find the distribution with

respect to θ . This can be written as

$$\begin{aligned} f_{\Theta}(\theta) &= \int_0^{\infty} f_{R,\Theta}(r, \theta) dr \\ &= \int_0^{\infty} \frac{r}{2\pi\tilde{\sigma}^2} \exp\left(-\frac{1}{2} \frac{r^2 + P - 2r\sqrt{P}\cos\theta}{\tilde{\sigma}^2}\right) dr \end{aligned}$$

Substitute now $v = \frac{r}{\tilde{\sigma}}$. Therefore, $dr = \tilde{\sigma} dv$. The integral above is transformed as

$$\begin{aligned} f_{\Theta}(\theta) &= \int_0^{\infty} \frac{\tilde{\sigma}v}{2\pi\tilde{\sigma}^2} \exp\left(-\frac{1}{2}(v^2 + \gamma_s - 2\sqrt{\gamma_s}v\cos\theta)\right) \tilde{\sigma}dv \\ &= \int_0^{\infty} \frac{\tilde{\sigma}^2v}{2\pi\tilde{\sigma}^2} \exp\left(-\frac{1}{2}(v - \sqrt{\gamma_s}\cos\theta)^2 - \frac{1}{2}\gamma_s\sin^2\theta\right) \\ &= \frac{1}{2\pi} \exp\left(-\frac{1}{2}\gamma_s\sin^2\theta\right) \int_0^{\infty} v \exp\left(-\frac{1}{2}(v - \sqrt{\gamma_s}\cos\theta)^2\right) dv \end{aligned}$$

where $\gamma_s = \frac{P}{\tilde{\sigma}^2} = 2 \text{ SNR}$. We now employ the substitution $v - \sqrt{\gamma_s}\cos\theta = t$.

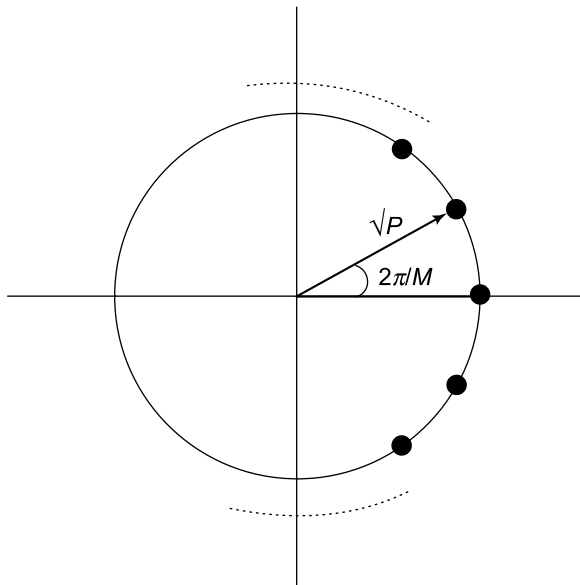


Figure 2.4 *M*-ary PSK constellation

The above expression for $f_{\Theta}(\theta)$ can now be simplified as

$$f_{\Theta}(\theta) = \frac{1}{2\pi} \exp\left(-\frac{1}{2}\gamma_s \sin^2 \theta\right) \int_{-\sqrt{2\gamma_s} \cos \theta}^{\infty} (t + \sqrt{\gamma_s} \cos \theta) e^{-\frac{t^2}{2}} dt$$

As the average symbol SNR $\gamma_s \rightarrow \infty$, the above integral can be approximated as

$$\begin{aligned} f_{\Theta}(\theta) &\approx \frac{1}{2\pi} \exp\left(-\frac{1}{2}\gamma_s \sin^2 \theta\right) \int_{-\sqrt{\gamma_s} \cos \theta}^{\infty} \sqrt{2\gamma_s} \cos \theta e^{-\frac{t^2}{2}} dt \\ &= \frac{\sqrt{\gamma_s}}{\sqrt{2\pi}} \cos \theta e^{-\frac{1}{2}\gamma_s \sin^2 \theta} \end{aligned}$$

It can now also be seen that the decision at the receiver is correct if the phase θ is between the limits $-\frac{\pi}{M} \leq \theta \leq \frac{\pi}{M}$ and in error otherwise. Therefore, the probability of correct decision P_c can be expressed as

$$P_c = \int_{-\frac{\pi}{M}}^{\frac{\pi}{M}} \sqrt{\frac{\gamma_s}{2\pi}} \cos \theta e^{-\frac{1}{2}\gamma_s \sin^2 \theta} d\theta$$

We now use the substitution $\gamma_s \sin^2 \theta = t^2$, and $\sqrt{\gamma_s} \cos \theta d\theta = dt$. The integral for P_c above can be transformed employing this substitution as

$$P_c = \sqrt{\frac{1}{2\pi}} \int_{-\sqrt{\gamma_s} \sin(\frac{\pi}{M})}^{\sqrt{\gamma_s} \sin(\frac{\pi}{M})} \frac{1}{\sqrt{2}} e^{-\frac{t^2}{2}}, dt \quad (2.17)$$

The probability of error $P_e = 1 - P_c$ can, therefore, be simplified as,

$$\begin{aligned} P_e &= 1 - P_c \\ &= 1 - \sqrt{\frac{1}{2\pi}} \int_{-\sqrt{\gamma_s} \sin(\frac{\pi}{M})}^{\sqrt{\gamma_s} \sin(\frac{\pi}{M})} e^{-\frac{t^2}{2}}, dt \\ &= \sqrt{\frac{1}{2\pi}} \int_{-\infty}^{-\sqrt{\gamma_s} \sin(\frac{\pi}{M})} e^{-\frac{t^2}{2}}, dt + \sqrt{\frac{1}{2\pi}} \int_{\sqrt{\gamma_s} \sin(\frac{\pi}{M})}^{\infty} e^{-\frac{t^2}{2}}, dt \\ &= 2Q\left(\sqrt{\gamma_s} \sin\left(\frac{\pi}{M}\right)\right) = 2Q\left(\sqrt{2 \text{SNR}} \sin\left(\frac{\pi}{M}\right)\right) \end{aligned} \quad (2.18)$$

2.7 | Binary Signal Vector Detection Problem

A very useful and insightful detection problem in the context of a digital communication systems is given by the *Binary Signal Vector Detection Problem*. The problem can be stated as follows. Consider the transmission of L symbols u_1, u_2, \dots, u_L across an AWGN channel, with y_1, y_2, \dots, y_L denoting the corresponding observations at the receiver. This system can be analytically modelled as

$$y_1 = u_1 + w_1$$

$$y_2 = u_2 + w_2$$

$$\vdots$$

$$y_L = u_L + w_L$$

where w_1, w_2, \dots, w_L denote the i.i.d. AWGN samples of zero-mean and variance $\sigma^2 = \sqrt{\frac{N_0}{2}}$. This can be represented using vectors as

$$\underbrace{\begin{bmatrix} y_1 \\ y_2 \\ \vdots \\ y_L \end{bmatrix}}_{\mathbf{y}} = \underbrace{\begin{bmatrix} u_1 \\ u_2 \\ \vdots \\ u_L \end{bmatrix}}_{\mathbf{u}} + \underbrace{\begin{bmatrix} w_1 \\ w_2 \\ \vdots \\ w_L \end{bmatrix}}_{\mathbf{w}}$$

Let \mathbf{u}_A and \mathbf{u}_B represent two possible transmit vectors. For example, in a simple repetition-code-based BPSK communication system, one can have $\mathbf{u}_A = [\sqrt{P}, \sqrt{P}, \dots, \sqrt{P}]$ and $\mathbf{u}_B = [-\sqrt{P}, -\sqrt{P}, \dots, -\sqrt{P}]$. Thus, at the receiver, one has to decide between the two vectors $\mathbf{u}_A, \mathbf{u}_B$ given the observation vector \mathbf{y} . Consider now the transmission of the vector \mathbf{u}_A . The optimal detector and the probability of error can be found for this system as follows. The vectors $\mathbf{u}_A, \mathbf{u}_B$ lie in an L -dimensional space. Figure 2.5 schematically shows the possible transmit vectors $\mathbf{u}_A, \mathbf{u}_B$ of the signal constellation along with the plane *perpendicularly bisecting* the line between \mathbf{u}_A and \mathbf{u}_B . It can now be seen that the optimal detector should decide \mathbf{u}_A if the observed vector \mathbf{y} lies on the side of this bisecting plane containing \mathbf{u}_A and as \mathbf{u}_B otherwise. Therefore, when \mathbf{u}_A is transmitted, an error occurs if the received vector \mathbf{y} is on the side containing \mathbf{u}_B as shown in Figure 2.5. This implies that its dot product with $\mathbf{u}_B - \mathbf{u}_A$ is greater than or equal to zero, since the dot product depends on the cosine of the

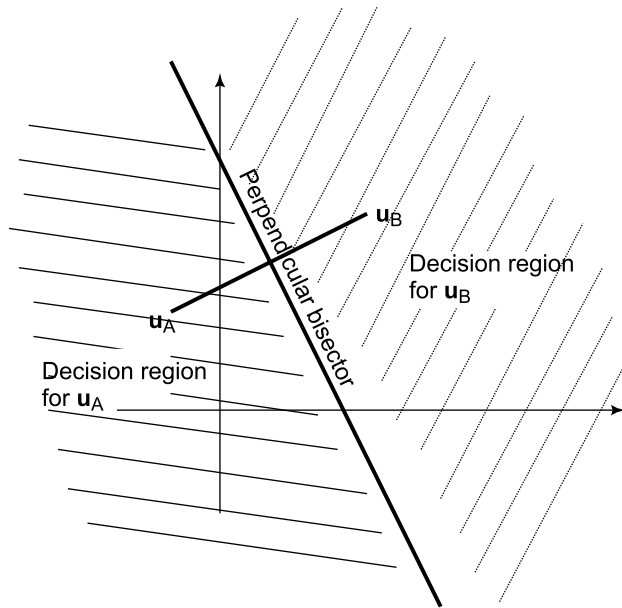


Figure 2.5 Binary signal vector detection

angle θ between \mathbf{y} and $\mathbf{u}_B - \mathbf{u}_A$. Hence, an error occurs if

$$\begin{aligned} \left(\mathbf{y} - \frac{\mathbf{u}_A + \mathbf{u}_B}{2} \right)^T (\mathbf{u}_B - \mathbf{u}_A) &\geq 0 \\ \Rightarrow \mathbf{y}^T (\mathbf{u}_B - \mathbf{u}_A) &\geq \frac{1}{2} (\mathbf{u}_B + \mathbf{u}_A)^T (\mathbf{u}_B - \mathbf{u}_A) \end{aligned}$$

Since \mathbf{u}_A is transmitted, we have $\mathbf{y} = \mathbf{u}_A + \mathbf{w}$. Substituting this above, we have, error if,

$$\begin{aligned} (\mathbf{u}_A + \mathbf{w})^T (\mathbf{u}_B - \mathbf{u}_A) &= \frac{1}{2} (\mathbf{u}_B + \mathbf{u}_A)^T (\mathbf{u}_B - \mathbf{u}_A) \\ \Rightarrow \underbrace{\mathbf{w}^T (\mathbf{u}_B - \mathbf{u}_A)}_{\tilde{w}} &\geq \frac{1}{2} (\mathbf{u}_B - \mathbf{u}_A)^T (\mathbf{u}_B - \mathbf{u}_A) \\ &= \frac{1}{2} \|\mathbf{u}_B - \mathbf{u}_A\|^2 \end{aligned} \quad (2.19)$$

Consider now $\tilde{w} = \mathbf{w}^T (\mathbf{u}_B - \mathbf{u}_A)$. Since each element of \mathbf{w} is i.i.d. Gaussian of mean zero and variance σ^2 , we can deduce that \tilde{w} is Gaussian since it is obtained as a linear combination of several Gaussian noise samples. Further, the expected value of \tilde{w} is given as $E\{\tilde{w}\} = E\{\mathbf{w}^T (\mathbf{u}_B - \mathbf{u}_A)\} = 0$, since each element of \mathbf{w} is zero mean. Also, the variance

of \tilde{w} can be obtained as

$$\begin{aligned}
 \underbrace{\mathbb{E}\{\tilde{w}^2\}}_{\tilde{\sigma}^2} &= \mathbb{E}\{\tilde{w}^T \tilde{w}\} \\
 &= \mathbb{E}\left\{(\mathbf{u}_B - \mathbf{u}_A)^T \mathbf{w} \mathbf{w}^T (\mathbf{u}_B - \mathbf{u}_A)\right\} \\
 &= (\mathbf{u}_B - \mathbf{u}_A)^T \mathbb{E}\{\mathbf{w} \mathbf{w}^T\} (\mathbf{u}_B - \mathbf{u}_A) \\
 &= (\mathbf{u}_B - \mathbf{u}_A)^T \sigma^2 \mathbf{I}_L (\mathbf{u}_B - \mathbf{u}_A) \\
 &= \sigma^2 \|\mathbf{u}_B - \mathbf{u}_A\|^2
 \end{aligned} \tag{2.20}$$

Thus, we have \tilde{w} is Gaussian with mean zero and variance $\tilde{\sigma}^2 = \sigma^2 \|\mathbf{u}_B - \mathbf{u}_A\|^2$ or, in other words, $\mathcal{N}\left(0, \sigma^2 \|\mathbf{u}_B - \mathbf{u}_A\|^2\right)$. Therefore, the probability of error is given from Eq. (2.19) as

$$\begin{aligned}
 P_e &= \Pr\left(\tilde{w} \geq \frac{1}{2} \|\mathbf{u}_B - \mathbf{u}_A\|^2\right) \\
 &= \Pr\left(\frac{\tilde{w}}{\tilde{\sigma}} \geq \frac{1}{2} \frac{\|\mathbf{u}_B - \mathbf{u}_A\|^2}{\tilde{\sigma}}\right) \\
 &= Q\left(\frac{\|\mathbf{u}_B - \mathbf{u}_A\|^2}{2\tilde{\sigma}}\right) \\
 &= Q\left(\frac{\|\mathbf{u}_B - \mathbf{u}_A\|}{2\tilde{\sigma}}\right)
 \end{aligned}$$

where the last equation above has been simplified by substituting the expression for $\tilde{\sigma}^2$ from Eq. (2.20). This yields a very interesting result. Observe that the probability of error depends only on the *distance* $\|\mathbf{u}_B - \mathbf{u}_A\|$ between the vectors \mathbf{u}_B and \mathbf{u}_A . In fact, the above probability of error P_e can be written as,

$$P_e = Q\left(\frac{d(\mathbf{u}_A, \mathbf{u}_B)}{2\sigma}\right)$$

where $d(\mathbf{u}_A, \mathbf{u}_B) = \|\mathbf{u}_B - \mathbf{u}_A\|$ denotes the distance between \mathbf{u}_A , \mathbf{u}_B . This is an interesting property of signal detection in AWGN which will be employed in the later chapters in the textbook. Further, for a complex signal constellation, the same relation above can be used by replacing σ by $\tilde{\sigma} = \frac{\sigma}{\sqrt{2}}$.

2.7.1 An Alternative Approach for M -PSK

A simpler alternative approach to compute the probability of error for the M -PSK constellation above is as follows. At high SNR, the symbol corresponding to $k = 0$ is confused only with its nearest neighbours, i.e., symbols corresponding to $k = 1$, $k = M - 1$. The distance d between the nearest neighbors in this M -PSK constellation is

$$d = 2\sqrt{P} \sin\left(\frac{\pi}{M}\right)$$

as shown in Figure 2.6. Therefore, the probability of confusion between the neighbours $k = 0$, $k = 1$ is

$$\begin{aligned} P_{0 \rightarrow 1} &= Q\left(\frac{d}{2\tilde{\sigma}}\right) \\ &= Q\left(\frac{2\sqrt{P}}{2\tilde{\sigma}} \sin\left(\frac{\pi}{M}\right)\right) \\ &= Q\left(\sqrt{\gamma_s} \sin\left(\frac{\pi}{M}\right)\right) \end{aligned} \quad (2.21)$$

This is identical to the confusion probability between the symbols $k = 0$, $k = M - 1$. Therefore, since there are two nearest neighbors for the symbol $k = 0$, employing the union

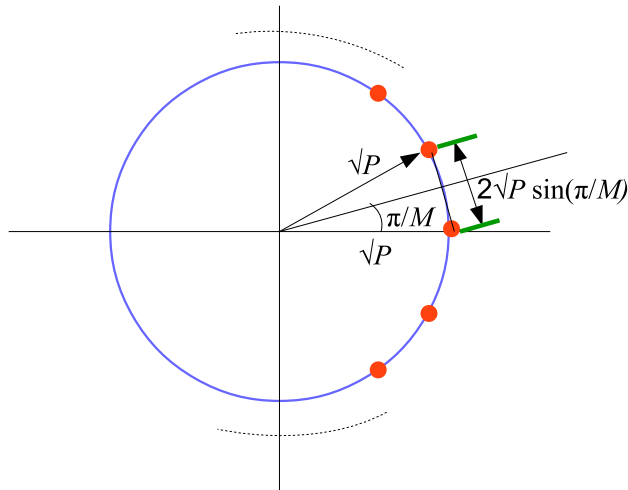


Figure 2.6 M -ary PSK constellation with distance between nearest neighbours

bound, the probability of error P_e can be approximated as

$$\begin{aligned} P_e &\approx P_{0 \rightarrow 1} + P_{0 \rightarrow M-1}, \\ &= 2Q\left(\sqrt{\gamma_s} \sin\left(\frac{\pi}{M}\right)\right) = 2Q\left(\sqrt{2 \text{SNR}} \sin\left(\frac{\pi}{M}\right)\right) \end{aligned} \quad (2.22)$$

which is identical to the expression derived above in Eq. (2.18) for the BER of M -PSK modulation.

PROBLEMS

1. The signal constellation for M -ary PAM is of the form $\pm(2k+1)\Delta$, for $0 \leq k \leq \frac{M}{2} - 1$, where M is an even number. Consider $M = 8$ and assume equal probability for transmission of each symbol to answer the questions that follow.
 - (a) Express the average symbol power \bar{P} for the 8-ary PAM constellation above as a function of Δ .
 - (b) Find the expression for the symbol error rate over an AWGN channel for the 8-ary constellation above as a function of the average symbol power \bar{P} and noise power σ^2 .
 - (c) Find the average power \bar{P} required to achieve probability of symbol error 10^{-6} in an AWGN channel with noise power $\sigma^2 = -3$ dB.
2. Compute the dB transmit SNR required to achieve $P_e = 5 \times 10^{-4}$ for 8-PSK in an AWGN channel.
3. Consider detecting the transmit vector \mathbf{u} equally likely to be $\mathbf{u}_A = \sqrt{P}[1, 1, 1, 1,]^T$ or $\mathbf{u}_B = \sqrt{P}[1, -1, 1, -1]^T$, where $P = 15$ dB. The received vector is

$$\mathbf{y} = \mathbf{u} + \mathbf{w}$$

and $\mathbf{w} \sim \mathcal{N}(0, 2\mathbf{I})$. Derive the average probability of error for this system.

Principles of Wireless Communications

3.1 | The Wireless Communication Environment

In conventional wireline communication systems, there is a single signal-propagation path between the transmitter and the receiver, which is constrained by the propagation medium such as a coaxial cable or a twisted pair. However, in wireless systems, the signal can reach the receiver via direct, reflected, and scattered paths as shown in Figure 3.1. As a result, at the receiver, there is a superposition of multiple copies of the transmitted signal. These signal copies experience different attenuations, delays, and phase shifts arising from the varied propagation distances and properties of the scattering media. Hence, at the wireless receiver, there is interference of signals received from these multiple propagation paths, which is termed *multipath interference*.

The multipath interference, in turn, results in an amplification or attenuation of the net received signal power observed at the receiver, and this variation in the received signal strength arising from the multipath propagation phenomenon is termed *multipath fading* or simply *fading*. Strong destructive interference at the receiver is referred to as a *deep fade*, and such a condition may result in temporary failure of communication due to a severe drop in the SNR at the receiver. This phenomenon of fading is the *critical difference* between the wireline and wireless communication systems, which causes a radical paradigm shift in the nature of wireless communications, necessitating the development of a fundamentally novel approach to design wireless systems.

One of the main objectives, therefore, in wireless-system design, is to develop schemes to **combat fading** and ensure reliability of signal reception in wireless communication systems.

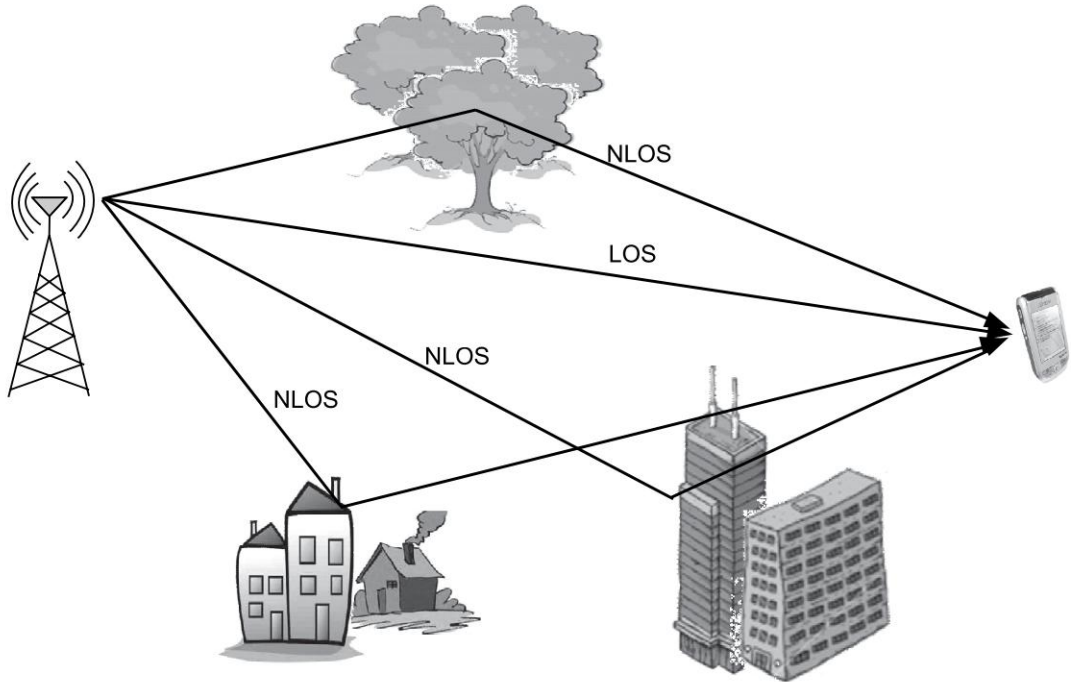


Figure 3.1 Schematic of the wireless-propagation environment

3.2 | Modelling of Wireless Systems

To gain a better understanding of the nature of the wireless environment and quantitatively analyze the performance of wireless communication systems, one needs to develop accurate analytical models to characterize them. In this section, we introduce the basic theory that deals with the analytical tools and techniques used extensively to model and assess wireless systems. In subsequent parts of the book, we build extensively on this theoretical framework to quantify the performance of various wireless communication schemes and systems. Let us start by considering the transmitted passband wireless signal $s(t)$, which is transmitted across

a wireless channel. Such a passband signal can be described analytically as,

$$s(t) = \text{Re} \left\{ s_b(t) e^{j2\pi f_c t} \right\} \quad (3.1)$$

The quantity $s_b(t)$ is the complex baseband representation of the transmitted signal and f_c is simply the carrier frequency employed for transmission. Next, we need an analytical model for the wireless communication channel. To make things simple, we will assume initially that the wireless channel is time invariant. Let us consider a channel with L multipath components. Observe that each path of the wireless channel basically has two characteristic properties. Firstly, it delays the signal because of the propagation distance. Secondly, there is an attenuation of the signal arising because of the scattering effect. Let the signal attenuation and delay of the i^{th} channel be denoted by the quantities a_i, τ_i respectively. Recall from your knowledge of Linear Time Invariant (LTI) systems that the impulse response of an LTI system which attenuates a signal by a_i and delays it by τ_i is given as

$$h_i(\tau) = a_i \delta(\tau - \tau_i)$$

Hence, the above equation gives the impulse response of a single path of a wireless communication system. Further, observe that the wireless channel represents a linear input–output system, since the signal observed at the receiver is the sum of the different multipath signal copies impinging on the receive antenna. Therefore, a typical Channel Impulse Response (CIR) of a multipath-scattering based wireless channel is given by the sum of the above impulse responses corresponding to the individual model,

$$h(\tau) = \sum_{i=0}^{L-1} a_i \delta(\tau - \tau_i) \quad (3.2)$$

The above impulse response is also termed the *tapped delay-line* model because of the nature of the arrival of several progressively delayed components of the signal. It can be observed that the above wireless channel model consists of L propagation paths arising from the several reflection and scattering multipath *Non-Line-Of-Sight (NLOS)* components. One of the multipath components can also be a direct *Line-Of-Sight (LOS)* component. Each such i^{th} path is characterized by two parameters, which are,

1. The attenuation factor a_i
2. The path delay τ_i

Since the above wireless is a linear time-invariant (LTI) system, the received signal $y(t)$ can be expressed as the convolution of the transmitted signal $s(t)$ with the CIR $h(t)$. Therefore, the received wireless signal $y(t)$ is given as

$$y(t) = s(t) * h(t) = \int_{-\infty}^{\infty} h(\tau) s(t - \tau) d\tau$$

By inserting the expression for the tapped delay-line channel in Eq. (3.2) in the above convolution, the expression for the received wireless signal $y(t)$ across this tapped delay-line channel can be derived as

$$y(t) = \sum_{i=0}^{L-1} a_i \int_{-\infty}^{\infty} \delta(\tau - \tau_i) s(t - \tau) d\tau = \sum_{i=0}^{L-1} a_i s(t - \tau_i)$$

Further, this expression for the received signal can be written in terms of the transmitted baseband signal $s_b(t)$ by substituting the relation between $s(t)$ and $s_b(t)$ in Eq. (3.1) in the above expression and simplifying it as

$$\begin{aligned} y(t) &= \text{Re} \left\{ \sum_{i=0}^{L-1} a_i s_b(t - \tau_i) e^{j2\pi f_c(t - \tau_i)} \right\} \\ &= \text{Re} \left\{ \underbrace{\left(\sum_{i=0}^{L-1} a_i e^{-j2\pi f_c \tau_i} s_b(t - \tau_i) \right)}_{y_b(t)} e^{j2\pi f_c t} \right\} \end{aligned}$$

From the above expression, it can readily be seen that $y_b(t)$, the complex baseband signal equivalent of the received signal $y(t)$, is simply given as

$$y_b(t) = \sum_{i=0}^{L-1} a_i e^{-j2\pi f_c \tau_i} s_b(t - \tau_i) \quad (3.3)$$

Notice that in addition to the attenuation and delay parameters in the passband channel model described earlier, the baseband system model consists of the addition *phase* $e^{-j2\pi f_c \tau_i}$ parameter. This basically arises because of the path delay of the carrier signal $e^{j2\pi f_c t}$ corresponding to the i^{th} path. On close observation of the above expression, one can readily

see that the received baseband signal consists of multiple delayed copies $s_b(t - \tau_i)$ of the transmitted signal $s_b(t)$. Each such i^{th} signal copy arising from the i^{th} multipath component is associated with the following three parameters.

1. The attenuation factor a_i
2. The path delay τ_i
3. The phase factor $e^{-j2\pi f_c \tau_i}$

The different signal copies for a typical baseband BPSK information signal $s_b(t)$ is shown in Figure 3.2. The quantity T denotes the symbol time, while T_m , which is the *delay* between the first and last arriving copies of the signal, is termed the *delay spread*. This is an important parameter of the wireless channel and will be explored in detail in the next chapter. For the purpose of the discussion below and in the rest of the chapter we will assume a narrowband channel, i.e., one in which $T_m \ll T$. The above signal model will be further simplified in the following sections to yield meaningful insights into the performance of wireless communication systems.

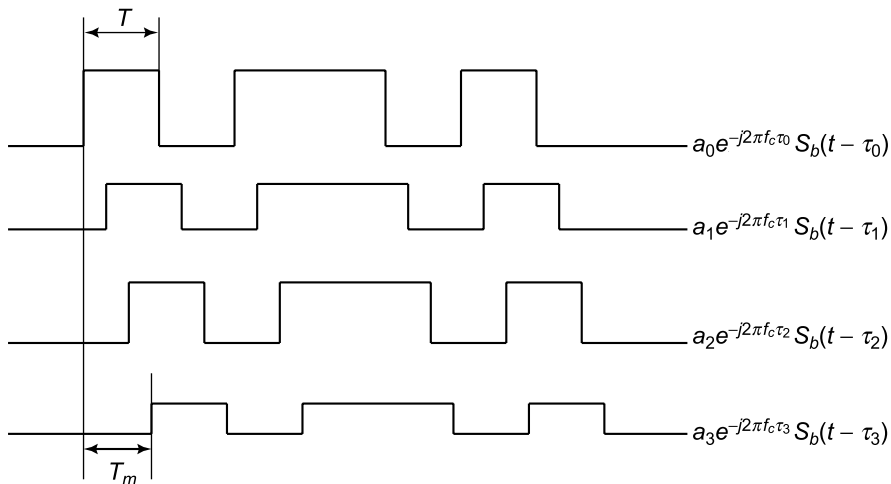


Figure 3.2 *Multipath signal components at the receiver*

EXAMPLE 3.1

Consider a wireless signal with a carrier frequency of $f_c = 850$ MHz, which is transmitted over a wireless channel that results in $L = 4$ multipath components at delays of 201, 513, 819, 1223 ns and corresponding to received signal amplitudes of 1, 0.6, 0.3, 0.2 respectively. Derive the expression for the received baseband signal $y_b(t)$ if the transmitted baseband signal is $s_b(t)$.

Solution: As given in the expression for the received baseband signal in Eq. (3.3), we need to compute the factors $a_i e^{-j2\pi f_c \tau_i}$ for $i = 0, 1, 2, 3$ to derive the expression for the received baseband signal $y_b(t)$. Accordingly, the factor $a_0 e^{-j2\pi f_c \tau_0}$ is given as

$$\begin{aligned} a_0 e^{-j2\pi f_c \tau_0} &= 1 \times e^{-j2\pi 850 \times 10^6 \times 201 \times 10^{-9}} \\ &= 0.59 + j0.81 \end{aligned}$$

Similarly, the other factors for $i = 1, 2, 3$ can be computed as $0.57 - j0.19$, $0.18 - j0.24$, $-0.19 + j0.06$ respectively. Hence, the receive baseband signal is, therefore, given as

$$\begin{aligned} y_b(t) &= (0.59 + j0.81) s_b(t) + (0.57 - j0.19) s_b(t - 201 \times 10^{-9}) \\ &\quad + (0.18 - j0.24) s_b(t - 513 \times 10^{-9}) + (-0.19 + j0.06) s_b(t - 1223 \times 10^{-9}) \end{aligned}$$

Thus, the receiver sees $L = 4$ signal copies $s_b(t - \tau_i)$, each delayed by τ_i , attenuated and phase shifted by $a_i e^{-j2\pi f_c \tau_i}$.

3.3 | System Model for Narrowband Signals

A fairly simplistic approximation of the above baseband system model can be arrived at by employing the narrowband signal approximation, which can be stated as follows. For a sufficiently narrowband signal $s_b(t)$, the different delayed components $s_b(t - \tau_i)$ are approximately equal to each other, i.e., $s_b(t - \tau_i) \approx s_b(t)$ (It will be shown in subsequent chapters that such a wireless channel is also known as a *flat-fading* wireless channel). Hence, for a narrowband transmit signal $s_b(t)$, the expression for the received baseband signal $y_b(t)$

can be further simplified as

$$y_b(t) = \underbrace{\left(\sum_{i=0}^{L-1} a_i e^{-j2\pi f_c \tau_i} \right)}_{ae^{j\phi}} s_b(t) = h s_b(t) \quad (3.4)$$

where $h = ae^{j\phi} = \sum_{i=0}^{L-1} a_i e^{-j2\pi f_c \tau_i}$ is termed the *complex fading channel coefficient*. Hence, the output baseband signal $y_b(t)$ is related to the input baseband signal $s_b(t)$ by a complex attenuation factor $ae^{j\phi}$. The fading nature of the wireless channel can now be readily observed from the above expression. The signal power at the receiver critically depends on the magnitude of the overall attenuation factor $ae^{j\phi}$. For instance, consider a two-component multipath channel with identical magnitude and exactly out-of-phase components, i.e., $a_0 = a_1$ and $e^{-j2\pi f_c \tau_0} = -e^{-j2\pi f_c \tau_1}$. In this extreme case, the received signal $y_b(t) = 0$, resulting in 0 (i.e., $-\infty$ dB) received signal power and the channel is in a deep fade. Thus, the fortunes of the signal processor at the receiver are hinged on this erratic factor $ae^{j\phi}$, which is also termed the complex baseband *fading coefficient* or simply, the *fading coefficient*.

Further, regarding the narrowband approximation, it is instructive to note that the narrowband approximation does NOT hold in a wideband system such as a CDMA-based one. Moreover, the narrowband assumption essentially implies that the carrier phase is sensitive to the delay spread while the baseband signal is not. This is essentially a rehashing of one of the most common assumptions in communication systems, which states that “*the bandwidth of the transmitted signal is usually orders of magnitude smaller than the carrier frequency f_c* ”. Next, we initiate a statistical characterization of the fading coefficient.

EXAMPLE 3.2

For the wireless channel given in Example 3.1, derive the corresponding received signal with the narrowband assumption.

Solution: As given in Eq. (3.4), the received signal with the narrowband assumption is given as

$$\begin{aligned} y(t) &= \left(\sum_{i=0}^3 a_i e^{-j2\pi f_c \tau_i} \right) s_b(t) \\ &= (1.14 + j0.44) s_b(t) \end{aligned}$$

Thus, the net received baseband signal in this case can be expressed as $y_b(t) = h s_b(t)$, where h the channel coefficient is $h = 1.14 + j0.44$.

3.4 Rayleigh Fading Wireless Channel

The complex fading coefficient h can be expressed in terms of its real and imaginary components as,

$$h = a e^{j\phi} = \sum_{i=0}^{L-1} (x_i + j y_i) = X + j Y$$

Thus, X, Y , which are the real and imaginary components of the fading coefficient $a e^{j\phi}$, are derived from the summation of a large number of random multipath components x_i, y_i , especially in a rich urban setting which allows for a large number of scatterers. Hence, it is reasonable to assume that X, Y are random in nature. Further, a simplistic model for the statistical characterization of X, Y would be to assume that they are *Gaussian* and un-correlated. The assumption of Gaussianity is lent support by the *central limit theorem*, which in simple terms states that a normalized random variable derived from the sum of a large number of independent identically distributed random components, converges to a Gaussian random variable.

The above assumption is valid as $L \rightarrow \infty$, i.e., the number of multipath components is fairly large. Hence, X, Y are distributed as $\mathcal{N}(0, \frac{1}{2})$ (assuming zero-mean and variance $\frac{1}{2}$). Further, since X, Y are Gaussian in nature and un-correlated, it directly follows that they are *independent*. The joint distribution of X, Y is given by the standard multivariate Gaussian as

$$f_{X,Y}(x, y) = \frac{1}{\pi} e^{-(x^2 + y^2)}$$

One can now derive the statistics of the fading coefficient $a e^{j\phi}$ in terms of its amplitude and phase factors a, ϕ . It can be seen through elementary trigonometric properties that

$$x = a \cos \phi, \quad y = a \sin \phi$$

The joint distribution $f_{A,\Phi}(a, \phi)$ can be derived from $f_{X,Y}(x, y)$ using the relation for multivariate PDF transformation as

$$f_{A,\Phi}(a, \phi) = \frac{1}{\pi} e^{-a^2} J_{X,Y}$$

where we have used the property that $x^2 + y^2 = a^2$ in the above expression. The quantity $J_{X,Y}$ is termed the Jacobian of X, Y and is given by the expression

$$J_{X,Y} = \left| \begin{bmatrix} \cos \phi & \sin \phi \\ -a \sin \phi & a \cos \phi \end{bmatrix} \right| = a$$

where $|\mathbf{A}|$ denotes the determinant of the matrix \mathbf{A} . Substituting the Jacobian in the expression for multivariate PDF transformation above, the joint PDF with respect to the random variables A, Φ can be derived as

$$f_{A,\Phi}(a, \phi) = \frac{a}{\pi} e^{-a^2}$$

The marginal distributions f_A, f_Φ with respect to the amplitude and phase factor random variables A, Φ can be readily derived from the above joint distribution as

$$f_A(a) = \int_{-\pi}^{\pi} f_{A,\Phi}(a, \phi) d\phi = 2ae^{-a^2}, 0 \leq a \leq \infty$$

$$f_\Phi(\phi) = \int_0^{\infty} f_{A,\Phi}(a, \phi) da = \frac{1}{2\pi} e^{-a^2} \Big|_0^{\infty} = \frac{1}{2\pi}, -\pi < \phi \leq \pi$$

We have now derived one of the most popular and frequently employed models for the wireless channel, termed a *Rayleigh fading* wireless channel. This nomenclature arises from the distribution f_A of the amplitude factor a , which is the well known Rayleigh density, shown in Figure 3.3. Observe that the average power in the amplitude a of the Rayleigh fading channel coefficient h is given as

$$\mathbb{E} \{ |h|^2 \} = \mathbb{E} \{ a^2 \} = \mathbb{E} \{ X^2 + Y^2 \} = 1$$

Further, it is important to note that although strictly speaking, the term Rayleigh refers to the distribution of the amplitude factor, the Rayleigh fading wireless channel characterizes both

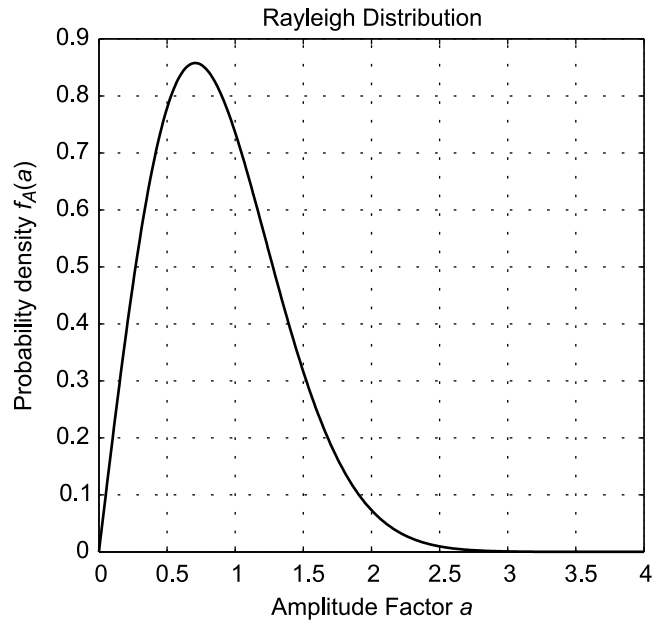


Figure 3.3 Rayleigh density for amplitude factor a

the amplitude factor as a Rayleigh fading random variable and the phase factor as uniformly distributed in $(-\pi, \pi)$. Finally, it can be readily seen that the joint distribution $f_{A,\Phi}(a, \phi)$ is related to the marginals $f_A(a)$, $f_\Phi(\phi)$ as,

$$f_{A,\Phi}(a, \phi) = f_A(a) f_\Phi(\phi)$$

essentially implying that the random variables A , Φ are *independent*. This is a fairly important result since it suggests that the random varying nature of the phase factor of the arriving signal is independent of that of the amplitude, i.e., for a given amplitude a , all phase factors in $(-\pi, \pi)$ are equiprobable. Figure 3.4 shows a scatter plot of the real and imaginary components of 10000 randomly generated samples of the Rayleigh fading coefficient. From the circular symmetry of the plot, it can be readily seen that the phase of the Rayleigh coefficient is distributed uniformly in $(-\pi, \pi)$.

EXAMPLE 3.3

Derive the probability density function of the channel power gain $g = a^2$, where a , as defined above, is the magnitude of the Rayleigh fading channel with $E\{a^2\} = 1$.

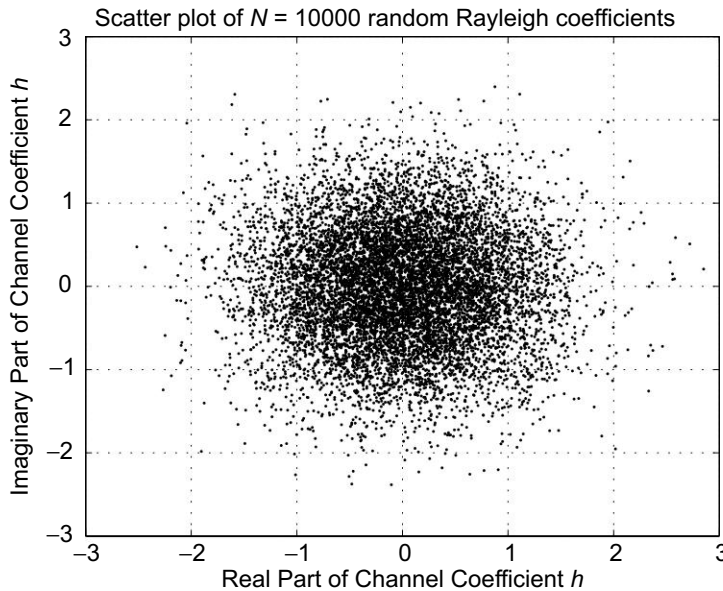


Figure 3.4 Scatter plot of the Rayleigh fading channel coefficient h

Solution: In the discussion above, we have demonstrated that the pdf of the magnitude of the channel coefficient a , where $E\{a^2\} = 1$, is given by the Rayleigh distribution as

$$f_A(a) = 2ae^{-a^2}, \quad a \geq 0$$

Define the function w as $g = w(a) = a^2$. Then, from the standard result of the probability density of a function of a random variable, the distribution of g is given by the pdf transformation

$$f_G(g) = \frac{f_A(w^{-1}(g))}{\left. \frac{dg}{da} \right|_{w^{-1}(g)}}$$

Observe that since $g = w(a) = a^2$, we have $w^{-1}(g) = a = \sqrt{g}$. Hence, the above expression can be simplified as

$$f_G(g) = \frac{f_A(\sqrt{g})}{2\sqrt{g}} = \frac{2\sqrt{g}e^{-g}}{2\sqrt{g}} = e^{-g}$$

Thus, the expression for the power gain of the wireless channel has a rather simple expression given as $f_G(g) = e^{-g}$. However, it should be kept in mind that this is valid only for the case

$E\{a^2\} = E\{g\} = 1$. Further, one can confirm that $E\{g\} = 1$ as

$$E\{g\} = \int_0^{\infty} e^{-g} = -e^{-g} \Big|_0^{\infty} = 1$$

EXAMPLE 3.4

In the wireless Rayleigh fading channel described above, consider a transmit power P_t (dB) = 20 dB. What is the probability that the power at the receiver is greater than P_r (dB) = 10 dB ?

Solution: First, let us begin by computing the appropriate linear power values for the above given dB values. P_t (dB) = $10 \log_{10}(P_t)$. Hence, the linear transmit power P_t is given as $P_t = 10^{P_t(\text{dB})/10} = 10^2 = 100$. Similarly, the linear receiver power corresponding to P_r (dB) = 10 dB is given as $P_r = 10^1 = 10$. Also, observe that given a power gain g , the received power is simply $P_r = gP_t$. Hence, for a received power $P_r > 10$, it naturally implies that

$$\begin{aligned} gP_t &> 10 \\ \Rightarrow g &> \frac{10}{P_t} = \frac{10}{100} \\ &= \frac{1}{10} \end{aligned}$$

Thus, the probability that the received power is greater than 10 essentially corresponds to the probability that the random power gain g of the Rayleigh fading wireless channel is greater than $\frac{1}{10}$. This probability can be readily computed as

$$\begin{aligned} \Pr\left(g > \frac{1}{10}\right) &= \int_{\frac{1}{10}}^{\infty} f_G(g) dg \\ &= \int_{\frac{1}{10}}^{\infty} e^{-g} dg \\ &= -e^{-g} \Big|_{\frac{1}{10}}^{\infty} \\ &= e^{-\frac{1}{10}} \\ &= 0.90 \end{aligned}$$

3.4.1 Baseband Model of a Wireless System

The baseband digital wireless communication system model for the above Rayleigh fading channel can be now readily derived as follows. Let $x(k), y(k)$ be the k^{th} transmitted and received symbols respectively and h denote the Rayleigh fading channel coefficient. The baseband system model for symbol detection in this channel is given as

$$y(k) = hx(k) + n(k) \quad (3.5)$$

where $n(k)$ is the additive white Gaussian noise (AWGN). Without loss of generality, one can assume that the AWGN is of unit power, i.e., $E \{ |n(k)|^2 \} = 1$ (for if this does not hold then the whole system can be scaled by a constant scaling factor without affecting the performance, since the SNR is invariant under scaling by a constant factor).

In particular, the information symbols $x(k)$ are derived from a digital modulation constellation such as BPSK, QPSK, etc. For instance, if the symbol constellation is BPSK of average symbol power P , the transmitted symbol levels are given as $+\sqrt{P}, -\sqrt{P}$ for the information symbols 1, 0 respectively. Finally, one can derive the standard nonfading model for the conventional wireline systems as

$$y(k) = x(k) + n(k) \quad (3.6)$$

where the Rayleigh fading factor a has simply been replaced by the constant 1 in the previous system model, which is essentially due to the fact there is no multipath fading phenomenon in a wireline system.

Important Note: Even though both the above system models employ AWGN frequently, the wireless channel is referred to as a Rayleigh channel (or more appropriately, a Rayleigh fading wireless channel) and the wireline channel as an AWGN channel, simply because of established conventions in literature. We will follow the same convention and refer to the wireline system model in Eq. (3.6) as an AWGN channel.

3.5 | BER Performance of Wireless Systems

The bit-error rate (BER) is the most widely used metric to characterize the performance of digital communication systems. Simply stated, it is the average rate of erroneously decoding the transmitted information bits at the communication receiver. For instance, in the above BPSK example, it would refer to decoding a transmitted $+\sqrt{P}$ (corresponding to the information bit 1) erroneously as the 0 bit and vice versa. The BER characterization of the conventional wireline (or AWGN) channel described above in Eq. (3.6) has already been derived in previous chapters. How does the BER performance of the conventional wireline communication systems compare with that of a typical wireless communication system? This is the question we answer in the next section.

3.5.1 SNR in a Wireless System

Similar to the wireline or the simple nonfading AWGN channel described previously, consider the transmission of the BPSK symbols $x(k) = \pm\sqrt{P}$ across a Rayleigh fading wireless channel. Recall from Eq. (3.5) above that the baseband Rayleigh wireless system can be modelled as

$$y(k) = hx(k) + n(k)$$

Observe that the critical difference between the above wireless channel and the wireline channel is the multiplicative fading coefficient h , due to which the received baseband signal is $hx(k)$. Therefore, the received signal power in the wireless channel is given as

$$\mathbb{E} \left\{ |hx(k)|^2 \right\} = |h|^2 \mathbb{E} \left\{ |x(k)|^2 \right\} = |h|^2 P = a^2 P \quad (3.7)$$

where $\|h\|^2 = a^2$ since $h = ae^{j\phi}$. This clearly illustrates the fact that the received power at the wireless receiver depends on the amplitude a of the random channel fading coefficient h . Further, we will term this SNR at the receiver, as a function of the fading amplitude a as the instantaneous SNR, i.e.,

$$\text{Instantaneous SNR} = a^2 \frac{P}{\sigma_n^2}$$

Further, notice that the average SNR in such a wireless system can be obtained as

$$\text{Average SNR} = \mathbb{E} \left\{ a^2 \frac{P}{\sigma_n^2} \right\} = \mathbb{E} \{ a^2 \} \frac{P}{\sigma_n^2} = \frac{P}{\sigma_n^2}$$

since $\mathbb{E} \{ a^2 \} = \mathbb{E} \{ |h|^2 \} = 1$ as demonstrated in Section 3.4. Thus, the average SNR of this wireless system is equal to $\frac{P}{\sigma_n^2}$, which we will refer to simply as SNR in the subsequent discussion to avoid confusion with the instantaneous SNR. Further, it can also be seen that since the average SNR of the wireless system is $\frac{P}{\sigma_n^2}$, which is equal to that of the wireline AWGN channel, it makes possible a fair comparison between these systems.

3.5.2 BER in Wireless Communication Systems

Hence, applying the result developed above for the wireline channel, the instantaneous BER (a) for a particular value of the amplitude a of the Rayleigh fading channel coefficient h is given by the standard Gaussian Q function as

$$\begin{aligned} \text{BER}(a) &= Q \left(\sqrt{\frac{a^2 P}{\sigma_n^2}} \right) = Q \left(a \sqrt{\frac{P}{\sigma_n^2}} \right) \\ &= \frac{1}{\sqrt{2\pi}} \int_{a\sqrt{\frac{P}{\sigma_n^2}}}^{\infty} e^{-x^2/2} dx = \frac{1}{\sqrt{2\pi}} \int_{a\sqrt{\mu}}^{\infty} e^{-x^2/2} dx \end{aligned} \quad (3.8)$$

where the quantity μ has been defined as the SNR, i.e., $\mu = \frac{P}{\sigma_n^2}$ to simplify the notation. Substituting $\frac{x}{a\sqrt{\mu}} = t$, the above integral can be simplified using standard calculus as

$$\text{BER}(a) = \int_1^{\infty} e^{-\mu a^2 t^2/2} a\sqrt{\mu} dt$$

Observe that the above expression for BER in the wireless channel depends on the *instantaneous* amplitude a of the fading coefficient, which is a random quantity. Thus, the above BER itself is random in nature, i.e., it is low for high values of a and vice versa. Therefore, to get a fair idea of the BER in such a system, one has to consider the average of all such observed BERs, which is obtained by averaging the above function $\text{BER}(a)$ over the distribution of the amplitude given as $f_A(a) = 2ae^{-a^2}$. The average BER in a Rayleigh fading channel, denoted by $\text{BER}_{\text{Rayleigh}}$ is given by averaging the above BER over the Rayleigh distribution $f_A(a) = 2ae^{-a^2}$ as

$$\begin{aligned}
\text{BER}_{\text{Rayleigh}} &= \int_0^{\infty} \text{BER}(a) 2ae^{-a^2} da \\
&= \frac{1}{\sqrt{2\pi}} \int_0^{\infty} \left(\int_1^{\infty} e^{-\mu a^2 t^2 / 2} a \sqrt{\mu} \right) 2ae^{-a^2} dt da \\
&= \frac{\sqrt{\mu}}{\sqrt{2\pi}} \int_0^{\infty} \int_1^{\infty} 2a^2 e^{-a^2 \frac{2+\mu t^2}{2}} dt da
\end{aligned}$$

The order of integration in the above integral can be interchanged to simplify the expression as

$$\begin{aligned}
\text{BER}_{\text{Rayleigh}} &= \frac{\sqrt{\mu}}{\sqrt{2\pi}} \int_1^{\infty} \int_0^{\infty} 2a^2 e^{-a^2 \frac{2+\mu t^2}{2}} da dt \\
&= \sqrt{\mu} \int_1^{\infty} \left(\frac{1}{\sqrt{2\pi}} \int_0^{\infty} 2a^2 e^{-\frac{a^2}{2\gamma^2}} da \right) dt
\end{aligned}$$

where we have defined γ as $\gamma = \sqrt{\frac{1}{2+\mu t^2}}$ for convenience. Now, employing the property,

$$\frac{1}{\sqrt{2\pi}} \int_0^{\infty} 2a^2 e^{-\frac{a^2}{2\gamma^2}} da = \gamma^3$$

which is proved in Example 3.5, the above expression for $\text{BER}_{\text{Rayleigh}}$ can be further simplified by recasting it as

$$\text{BER}_{\text{Rayleigh}} = \sqrt{\mu} \int_1^{\infty} \gamma^3 dh = \sqrt{\mu} \int_1^{\infty} \left(\frac{1}{2 + \mu t^2} \right)^{3/2} dt$$

We now employ the following reparameterization of t in terms of θ to simplify the above expression as

$$t = \sqrt{\frac{2}{\mu}} \tan \theta, \quad dt = \sqrt{\frac{2}{\mu}} \sec^2 \theta d\theta$$

Using this reparameterization, the $\text{BER}_{\text{Rayleigh}}$ expression can be readily recast to a more tractable standard integral of trigonometric functions as

$$\begin{aligned}
\text{BER}_{\text{Rayleigh}} &= \sqrt{\mu} \int_{\tan^{-1} \sqrt{\frac{\mu}{2}}}^{\pi/2} \frac{1}{2^{3/2}} \frac{1}{\sec^3 \theta} \sec^2 \theta \sqrt{\frac{2}{\mu}} d\theta \\
&= \frac{1}{2} \int_{\tan^{-1} \sqrt{\frac{\mu}{2}}}^{\pi/2} \cos \theta d\theta \\
&= \frac{1}{2} \sin \theta \Big|_{\tan^{-1} \sqrt{\frac{\mu}{2}}}^{\pi/2} \\
&= \frac{1}{2} \left(\sin \frac{\pi}{2} - \sin \left(\tan^{-1} \sqrt{\frac{\mu}{2}} \right) \right)
\end{aligned}$$

Hence, the final expression for $\text{BER}_{\text{Rayleigh}}$, the average bit-error rate for a Rayleigh fading wireless channel, can be derived in terms of the baseband SNR of the communication system as

$$\text{BER}_{\text{Rayleigh}} = \frac{1}{2} \left(1 - \frac{\sqrt{\frac{\mu}{2}}}{\sqrt{1 + \frac{\mu}{2}}} \right) = \frac{1}{2} \left(1 - \sqrt{\frac{\text{SNR}}{2 + \text{SNR}}} \right) \quad (3.9)$$

In the next example, we illustrate an application of this result.

EXAMPLE 3.5

Compare the BER for BPSK transmission at $\text{SNR}_{\text{dB}} = 10$ dB over a Rayleigh fading wireless channel with that of the wireline AWGN channel.

Solution: The $\text{SNR}_{\text{dB}} = 10$ dB corresponds to $\text{SNR} = 10$. Hence, from the above discussion,

$$\text{BER}_{\text{Rayleigh}} = \frac{1}{2} \left(1 - \sqrt{\frac{\text{SNR}}{2 + \text{SNR}}} \right) = \frac{1}{2} \left(1 - \sqrt{\frac{10}{12}} \right) = 4.4 \times 10^{-2}$$

Comparing this with the corresponding BER for the wireline channel derived previously, it can be seen that the BER for the fading wireless channel is approximately 100 times higher compared to the wireline channel. This illustrates the serious challenge in achieving reliable communication over wireless communication systems. This stark difference in the BER of communication over these channels can be visually seen in Figure 3.5. The reason for this can

be better understood from the following section on the high SNR behaviour of the bit-error rate of the wireless channel.

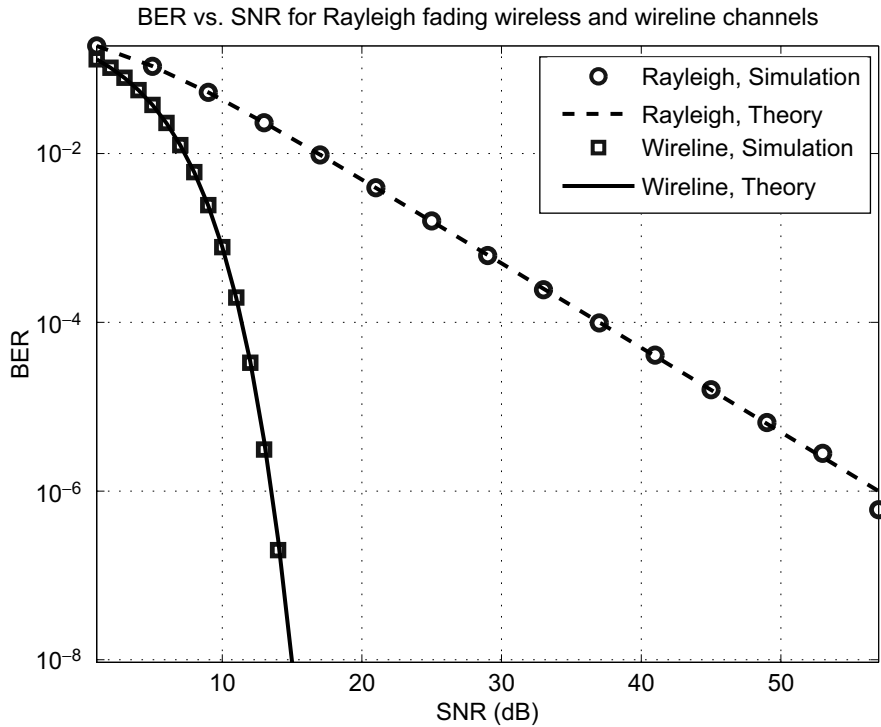


Figure 3.5 BER of BPSK detection over a Rayleigh fading wireless channel. The term ‘theory’ in the legend refers to the theoretical value of BER obtained from the expression in Eq. (3.9)

3.5.3 Rayleigh BER at High SNR

It is instructive to study the behaviour of the above Rayleigh BER under high SNR conditions. As system SNR $\rightarrow \infty$, the BER expression in Eq. (3.9) can be simplified as

$$\begin{aligned}
\text{BER}_{\text{Rayleigh}} &= \frac{1}{2} \left(1 - \sqrt{\frac{\text{SNR}}{2 + \text{SNR}}} \right) = \frac{1}{2} \left(1 - \frac{1}{\sqrt{1 + \frac{2}{\text{SNR}}}} \right) \\
&\approx \frac{1}{2} \left[1 - \left(1 - \frac{1}{2} \left(\frac{2}{\text{SNR}} \right) \right) \right] \\
&= \frac{1}{2 \text{SNR}} \tag{3.10}
\end{aligned}$$

Thus, surprisingly, at high SNR, the BER of a wireless fading channel decreases at a very slow rate of $\frac{1}{\text{SNR}}$ compared to that of a wireline channel with decreases exponentially as $e^{-\frac{\text{SNR}}{2}}$ as illustrated previously. Thus, this naturally results in a very high BER for the wireless communication system. This concept is more lucid from Example 3.6.

EXAMPLE 3.6

Compute the SNR_{dB} required to achieve a bit-error rate of 10^{-6} over a Rayleigh fading wireless channel.

Solution: To compute this, one can use the high SNR approximation for the wireless BER in Section 3.5.3. We, therefore, have,

$$\frac{1}{2 \text{SNR}} \approx 10^{-6} \Rightarrow \text{SNR} = \frac{1}{2} \times 10^6$$

Converting the above SNR to the dB scale, we have the required $\text{SNR}_{\text{dB}} = 57$ dB. Comparing the above SNR with that required to achieve a similar BER of 10^{-6} over the wireline channel, one can readily observe that the SNR required for a Rayleigh fading wireless channel is approximately $57 - 13 = 44$ dB higher. Thus, the SNR required for the Rayleigh wireless channel is significantly higher compared to that required for a wireline channel. The same is confirmed from Figure 3.5, which compares the BER for the wireline AWGN and Rayleigh fading wireless channel. It can be seen therein that for a given SNR, the BER of a Rayleigh fading wireless link is significantly higher compared to that of the conventional wireline channel.

3.6 Intuition for BER in a Fading Channel

Consider again the baseband wireless system model described as

$$y(k) = \underbrace{hx(k)}_{\text{signal}} + \underbrace{n(k)}_{\text{noise}}$$

Recall that the signal power in the above system is $|h|^2 P$, while the noise power is σ_n^2 . Due to the random nature of the fading coefficient h , the received signal power $|h|^2 P$ is variable. In the adverse scenario that the received signal power $|h|^2 P$ is lower than the noise power, i.e., $|h|^2 P = a^2 P < \sigma_n^2$, the BER of the system will be significantly high. Such a system can be considered to be in a **deep** fade, i.e.,

$$\begin{aligned} \text{Deep fade} &\Rightarrow a^2 P < \sigma_n^2 \\ &\Rightarrow a < \sqrt{\frac{\sigma_n^2}{P}} = \frac{1}{\sqrt{\text{SNR}}} \end{aligned}$$

One can compute the probability of this deep fade event as follows.

$$\begin{aligned} P_{\text{Deep fade}} &= P\left(a < \frac{1}{\sqrt{\text{SNR}}}\right) \\ &= \int_0^{\frac{1}{\sqrt{\text{SNR}}}} f_a(a) da \\ &= \int_0^{\frac{1}{\sqrt{\text{SNR}}}} 2ae^{-a^2} da \end{aligned}$$

At high SNR, $\frac{1}{\sqrt{\text{SNR}}} \approx 0$. Hence, the quantity $e^{-a^2} \approx 1$. Employing this approximation, the

above integral can be readily simplified as

$$\begin{aligned} P_{\text{Deep fade}} &\approx \int_0^{\frac{1}{\sqrt{\text{SNR}}}} 2a \, da \\ &= a^2 \Big|_0^{\frac{1}{\sqrt{\text{SNR}}}} \\ &= \frac{1}{\text{SNR}} \end{aligned}$$

Therefore, the probability that the system is in a deep fade is $\frac{1}{\text{SNR}}$, which is proportional to the BER for the fading wireless channel, i.e., $\frac{1}{2\text{SNR}}$. This remarkable observation essentially implies that the significant adversity for communication across a wireless channel is the random variation in the received signal power due to the fading process. The BER is basically the probability that the system is in a deep fade, implying that whenever the system is in a deep fade, which occurs with probability of $\frac{1}{\text{SNR}}$, the entire stream of bits is received with an extremely high percentage (roughly 50% as shown by the factor of $\frac{1}{2}$ in BER) of bit errors. Hence, it is extremely critical to combat these ill effects of fading over the wireless channel.

Thus, it can be readily seen from the above examples that the fading nature of the wireless channel results in an extremely high BER and poor quality of communication. Lowering the BER and enhancing the reliability of data transmission over the fading wireless channel is the central focus of our study in wireless communications. In this context, the topic discussed next, i.e., **diversity**, plays a fundamental role of overcoming the ill effects of the fading wireless channel and forms the bedrock of techniques designed to achieve high data rates in the wireless system.

3.6.1 A Simpler Derivation of Approximate Rayleigh BER

A simple derivation compared to the elaborate one in Section 3.5.2 for the approximate BER over a Rayleigh fading wireless channel is given below. Towards this end, one can employ the Chernoff bound for the Gaussian $Q(x)$ function, which states

$$Q(x) \leq \frac{1}{2} e^{-\frac{1}{2}x^2}$$

The student is guided towards a proof of the above result in Problem 4 of Section 3.12. Using this result, the instantaneous BER of the wireless channel from Eq. (3.8) can be upper bounded

as

$$\text{BER}(a) = Q\left(\sqrt{a^2 \text{SNR}}\right) \leq \frac{1}{2} e^{-\frac{1}{2} a^2 \text{SNR}}$$

Averaging the above quantity over the Rayleigh distribution $f_A(a)$ of the Rayleigh wireless channel, the average BER for the Rayleigh fading wireless channel can be upper bounded as

$$\begin{aligned} \text{BER}_{\text{Rayleigh}} &\leq \int_0^\infty \frac{1}{2} e^{-\frac{1}{2} a^2 \text{SNR}} 2a e^{-a^2} da \\ &= \frac{1}{2} \int_0^\infty 2a e^{-a^2 \left(1 + \frac{\text{SNR}}{2}\right)} da \\ &= -\frac{1}{2} \frac{1}{1 + \frac{\text{SNR}}{2}} e^{-a^2 \left(1 + \frac{\text{SNR}}{2}\right)} \Big|_0^\infty \\ \Rightarrow \text{BER}_{\text{Rayleigh}} &\leq \frac{1}{2 + \text{SNR}} \end{aligned} \quad (3.11)$$

As can be readily observed, the above bound for the probability of bit error for BPSK is similar to the high SNR approximation of the BER derived in Eq. (3.10). In fact, at very high SNR, i.e., as $\text{SNR} \rightarrow \infty$, the above bound can be simplified as $\frac{1}{\text{SNR}}$, which is similar to the one in Eq. (3.10) in that the bit-error rate decreases at the rate of $\frac{1}{\text{SNR}}$.

3.7 | Channel Estimation in Wireless Systems

Consider again the wireless channel model given as

$$y(k) = hx(k) + n(k)$$

where h is the flat-fading channel coefficient. The estimate $\hat{x}(k)$ of the symbol $x(k)$ can then be recovered from $y(k)$ simply as $\hat{x}(k) = \frac{1}{h} y(k)$. This is termed the *zero-forcing* receiver in wireless system. It can be seen now that in order to detect the transmitted symbol $x(k)$ at the receiver, one needs to know the channel coefficient h . The process of computing this channel coefficient h at the wireless receiver is termed *channel estimation* and is an important procedure in every wireless communication system. A popular scheme for estimating the wireless channel is through the transmission of *pilot* or *training* symbols. Pilot symbols are

a predetermined fixed set of symbols which are transmitted over the wireless channel. This set of symbols is known to the wireless receiver as it is programmed beforehand. The receiver observes the outputs corresponding to the transmitted pilot symbols and with knowledge of the transmitted pilot symbols, proceeds to estimate the unknown fading channel coefficient. This procedure for pilot-based channel estimation is described below.

Consider the transmission of $L^{(p)}$ pilot symbols $x^{(p)}(1), x^{(p)}(2), \dots, x^{(p)}(L^{(p)})$ for the purpose of channel estimation. Let the corresponding received outputs be $y^{(p)}(1), y^{(p)}(2), \dots, y^{(p)}(L^{(p)})$, i.e., each $y^{(p)}(k)$, $1 \leq k \leq L^{(p)}$ is the output corresponding to the transmitted pilot symbol $x^{(p)}(k)$. The model for these received pilot symbols is given as

$$y^{(p)}(k) = hx^{(p)}(k) + n(k)$$

To simplify the derivation below, let us assume for the moment that all the quantities $y^{(p)}(k)$, $x^{(p)}(k)$, $n(k)$ and the channel coefficient h are real. Due to the presence of noise $n(k)$ in the above system, it is clear that $y(k) \neq hx(k)$ for any k . Thus, one has to determine an estimate of h from the noisy observation samples $y(k)$. Intuitively then, a reasonable estimate \hat{h} of h can be derived as a minimizer of the cost function

$$\begin{aligned} \hat{h} &= \arg \min_h \left\{ \left(y^{(p)}(1) - hx^{(p)}(1) \right)^2 + \left(y^{(p)}(2) - hx^{(p)}(2) \right)^2 \right. \\ &\quad \left. + \dots + \left(y^{(p)}(L^{(p)}) - hx^{(p)}(L^{(p)}) \right)^2 \right\} \\ &= \underbrace{\sum_{k=1}^{L^{(p)}} \left(y^{(p)}(k) - hx^{(p)}(k) \right)^2}_{\xi(h)} \end{aligned}$$

The above minimization aims to find the best estimate of h which corresponds to the lowest observation error $\xi(h)$ and is, hence, termed the *least-squares* estimate. Naturally, the convenient way to minimize the error function $\xi(h)$ above is to differentiate it and set it equal

to zero. This procedure yields

$$\begin{aligned}
 \frac{d\xi(h)}{dh} &= \sum_{k=1}^L 2 \left(y^{(p)}(k) - hx^{(p)}(k) \right) \left(x^{(p)}(k) \right) \\
 0 &= \sum_{k=1}^L x^{(p)}(k) \left(y^{(p)}(k) - \hat{h}x^{(p)}(k) \right) \\
 \Rightarrow \hat{h} &= \frac{\sum_{k=1}^L y^{(p)}(k) x^{(p)}(k)}{\sum_{k=1}^L \left(x^{(p)}(k) \right)^2} \tag{3.12}
 \end{aligned}$$

Thus, one can compute the channel estimate \hat{h} of the fading channel coefficient h . Let us now derive a more elegant matrix-based framework to derive the result above. The vector model for the pilot-symbol transmission reception is given as

$$\underbrace{\begin{bmatrix} y^{(p)}(1) \\ y^{(p)}(2) \\ \vdots \\ y^{(p)}(L^{(p)}) \end{bmatrix}}_{\mathbf{y}^{(p)}} = h \underbrace{\begin{bmatrix} x^{(p)}(1) \\ x^{(p)}(2) \\ \vdots \\ x^{(p)}(L^{(p)}) \end{bmatrix}}_{\mathbf{x}^{(p)}} + \underbrace{\begin{bmatrix} n(1) \\ n(2) \\ \vdots \\ n(L^{(p)}) \end{bmatrix}}_{\mathbf{n}}$$

Hence, the vector model for the above system can be comprehensively given as

$$\mathbf{y}^{(p)} = h\mathbf{x}^{(p)} + \mathbf{n}$$

where $\mathbf{y}^{(p)}$, $\mathbf{x}^{(p)}$, \mathbf{n} are $L^{(p)}$ dimensional vectors. The least-squares estimate of the channel coefficient h given as

$$\begin{aligned}
 \hat{h} &= \arg \min_h \left\| \mathbf{y}^{(p)} - h\mathbf{x}^{(p)} \right\|^2 \\
 &= \arg \min_h \left\{ \left(\mathbf{y}^{(p)} - h\mathbf{x}^{(p)} \right)^T \left(\mathbf{y}^{(p)} - h\mathbf{x}^{(p)} \right) \right\} \\
 &= \arg \min_h \left\{ \underbrace{\left(\mathbf{y}^{(p)} \right)^T \mathbf{y}^{(p)} - 2 \left(\left(\mathbf{x}^{(p)} \right)^T \mathbf{y}^{(p)} \right) h + \left(\left(\mathbf{x}^{(p)} \right)^T \mathbf{x}^{(p)} \right) h^2}_{\xi(h)} \right\}
 \end{aligned}$$

As illustrated previously, to minimize the observation error, one can now differentiate the above cost function $\xi(h)$ and set it equal to zero, to compute the estimate \hat{h} as

$$\begin{aligned}\frac{d\xi(h)}{dh} &= -2 \left(\left(\mathbf{x}^{(p)} \right)^T \mathbf{y}^{(p)} \right) + 2 \left(\left(\mathbf{x}^{(p)} \right)^T \mathbf{x}^{(p)} \right) \hat{h} \\ \Rightarrow 0 &= -2 \left(\left(\mathbf{x}^{(p)} \right)^T \mathbf{y}^{(p)} \right) + 2 \left(\left(\mathbf{x}^{(p)} \right)^T \mathbf{x}^{(p)} \right) \hat{h} \\ \hat{h} &= \frac{\left(\mathbf{x}^{(p)} \right)^T \mathbf{y}^{(p)}}{\left(\mathbf{x}^{(p)} \right)^T \mathbf{x}^{(p)}} \\ &= \frac{\sum_{k=1}^L y^{(p)}(k) x^{(p)}(k)}{\sum_{k=1}^L \left(x^{(p)}(k) \right)^2}\end{aligned}$$

which is identical to the expression derived above in Eq. (3.12). Further, one can now easily derive the expression for the channel estimation for complex numbers $h, x^{(p)}(k), y^{(p)}(k)$ by simply replacing the transpose operator above with the Hermitian operator. Hence, the general expression for the channel estimate \hat{h} when the various quantities are complex numbers is given as

$$\hat{h} = \frac{\left(\mathbf{x}^{(p)} \right)^H \mathbf{y}^{(p)}}{\left(\mathbf{x}^{(p)} \right)^H \mathbf{x}^{(p)}} = \frac{\left(\mathbf{x}^{(p)} \right)^H \mathbf{y}^{(p)}}{\left\| \mathbf{x}^{(p)} \right\|^2} \quad (3.13)$$

EXAMPLE 3.7

Below are the vectors $\mathbf{x}^{(p)}, \mathbf{y}^{(p)}$ corresponding to the transmitted pilot symbols and received outputs respectively across the standard Rayleigh fading wireless channel (Single Rx/Tx antenna) as per the channel estimation model discussed above.

$$\mathbf{y}^{(p)} = \begin{bmatrix} -0.7850 + j0.3631 \\ 0.4072 + j0.7757 \\ 0.8004 - j0.4359 \\ 0.4464 + j0.8222 \end{bmatrix}, \quad \mathbf{x}^{(p)} = \frac{1}{\sqrt{2}} \begin{bmatrix} -1 + j \\ 1 + j \\ 1 - j \\ 1 + j \end{bmatrix}$$

Given that the noise is AWGN, what is the estimate of the fading channel coefficient h ?

Solution: As can be observed, the number of pilot symbols $L^{(p)} = 4$. Further, pilot symbols and received outputs are complex in nature, corresponding to a complex baseband representation of the wireless communication system. The estimate \hat{h} of the channel coefficient can be computed using Eq. (3.13) above. The quantity $(\mathbf{x}^{(p)})^H \mathbf{x}^{(p)}$ can be simplified as

$$\begin{aligned} (\mathbf{x}^{(p)})^H \mathbf{x}^{(p)} &= \|\mathbf{x}^{(p)}\|^2 \\ &= \frac{1}{2} \{ |-1 + j|^2 + |1 + j|^2 + |1 - j|^2 + |1 + j|^2 \} \\ &= 4 \end{aligned}$$

Also, the numerator quantity $(\mathbf{x}^{(p)})^H \mathbf{y}^{(p)}$ can be computed as

$$(\mathbf{x}^{(p)})^H \mathbf{y}^{(p)} = 3.4195 + j1.0824$$

Hence, the channel estimate is given as

$$\hat{h} = \frac{3.4195 + j1.0824}{4} = 0.8549 + j0.2706$$

3.8 Diversity in Wireless Communications

The theory of *diversity* lies at the heart of all modern wireless communication theory and technologies. It is by far the best tool available to combat the effects of multipath fading in a wireless channel and thereby ensure reliable communication. As seen in the previous chapter, the probability of bit-error (BER) in a typical wireless fading channel for BPSK transmission at a reasonably high SNR of 13–14 dB can be as high as 10^{-1} , thus raising the spectre of an extremely error-prone communication system. Diversity techniques can be employed in such scenarios to substantially improve the reliability of wireless communication, while reducing the BER as will be elaborated in the sections below.

Diversity is based on the simple fact that *independent* wireless channels experience randomly independent levels of fading. Hence, the probability that multiple independent wireless channels are simultaneously in a deep fade is drastically lower compared to that of a single fading channel. One can, therefore, significantly improve the reliability of symbol detection by simultaneously transmitting multiple versions of the same information signal over a set of independent fading channels.

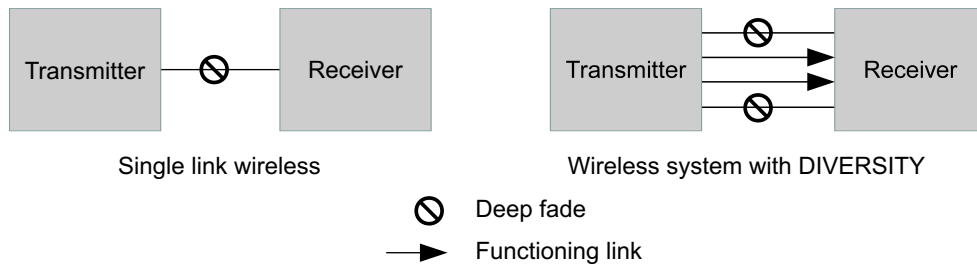


Figure 3.6 Schematic of diversity-based wireless system

At the receiver, these signals can then be judiciously combined using appropriate schemes to maximize the reliability of symbol detection. This key principle behind diversity is schematically represented in Figure 3.6. Observe that the wireless system on the left fails because of the single link in deep fade. However, the diversity-based system, which operates on four parallel links in the above example, is able to operate even with two links in a deep fade. Hence, the philosophy of diversity can, therefore, be stated concisely as

“transmission of multiple copies of the information signal over independent channels, thereby substantially reducing the chance of information loss due to the erratic nature of the wireless channels which causes any one or a subset of these channels to be in a deep fade”.

A typical example of such a diversity-based system is the multiple receive antenna wireless system, also termed the Single-Input Multiple-Output (SIMO) wireless system, schematically shown in Figure 3.7. The single transmit antenna in this system is denoted by Tx #1, while the L receive antennas are denoted by Rx # i , $0 \leq i \leq L$. In this system, there is a wireless link between the transmit antenna and each of the receive antennas, thus accounting for a total of L links between the transmitter and receiver. Hence, naturally, such a system is a diversity-based wireless system. In the next section, we describe in detail the functioning of such a multi-antenna system and analyze its performance in the context of diversity.

3.9 | Multiple Receive Antenna System Model

We start the diversity analysis of the multi-antenna system by initially developing an analytical model for the system illustrated in Figure 3.7.

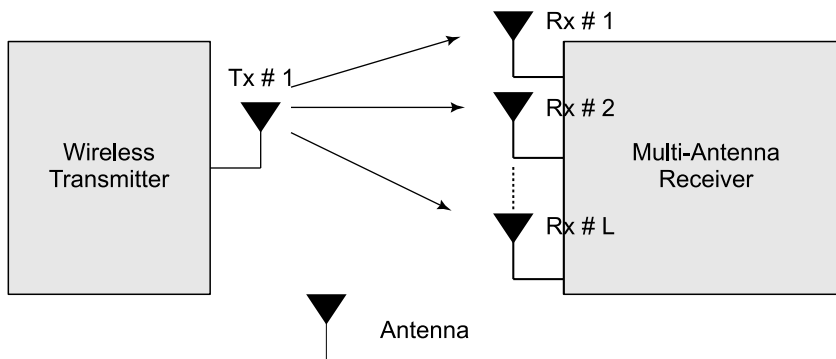


Figure 3.7 Schematic of multiple receive antenna wireless system

Consider the transmission of a BPSK data symbol $x(k)$ at the time instant k from the single transmit antenna, i.e., Tx #1. If each symbol is of average power P , it naturally follows that $x(k) = \pm\sqrt{P}$, where a transmission of $+\sqrt{P}$, $-\sqrt{P}$ corresponds to the information bits 1, 0 respectively. Since there are L receive antennas, there is correspondingly a wireless channel between the transmit antenna and each receive antenna, i.e., L channels in total over which the signal is received at the receiver. Let the channel coefficient between the transmit antenna and the i^{th} receive antenna be denoted by h_i , which is the complex Rayleigh fading coefficient. Hence, $y_i(k)$, the signal at the receiver over the i^{th} antenna can be expressed as

$$y_i(k) = h_i x(k) + n_i(k)$$

where $n_i(k)$ is the additive white Gaussian noise of variance, i.e., power σ_n^2 at the i^{th} receive antenna. Hence, the complete set of signals received at the receiver over the L antennas can be represented conveniently in vector form as

$$\begin{bmatrix} y_1(k) \\ y_2(k) \\ \vdots \\ y_L(k) \end{bmatrix} = \begin{bmatrix} h_1 \\ h_2 \\ \vdots \\ h_L \end{bmatrix} x(k) + \begin{bmatrix} n_1(k) \\ n_2(k) \\ \vdots \\ n_L(k) \end{bmatrix} \quad (3.14)$$

One can now use the following vector notation to elegantly capture the multi-antenna receiver wireless communication system.

$$\mathbf{y}(k) = \begin{bmatrix} y_1(k) \\ y_2(k) \\ \vdots \\ y_L(k) \end{bmatrix}, \quad \mathbf{h} = \begin{bmatrix} h_1 \\ h_2 \\ \vdots \\ h_L \end{bmatrix}, \quad \mathbf{n}(k) = \begin{bmatrix} n_1(k) \\ n_2(k) \\ \vdots \\ n_L(k) \end{bmatrix} \quad (3.15)$$

Basically, the vector quantities $\mathbf{y}(k)$, \mathbf{h} , $\mathbf{n}(k)$ denote the L -dimensional received signal, multiple antenna channel and receiver noise samples respectively. Thus, one can compactly represent the multiple-antenna wireless system model as

$$\mathbf{y}(k) = \mathbf{h}x(k) + \mathbf{n}(k)$$

In the rest of the book, we use the notation $\mathbf{y} \in \mathbb{C}^{L \times 1}$ to denote the fact the \mathbf{y} is an L -dimensional vector with complex entries. Similarly, we have, $\mathbf{h}, \mathbf{n}(k) \in \mathbb{C}^{n \times 1}$. Finally, note that we employ boldfaced small letters such as $\mathbf{a}, \mathbf{b}, \mathbf{n}$, etc., to represent vectors. In addition, we make the reasonable assumption that these noise samples across the different antennas are independent, i.e., $E\{n_i(k)n_j(k)\} = 0$ for $i \neq j$. This can also be represented using the *covariance* matrix \mathbf{R}_n of the noise vector $\mathbf{n}(k)$ defined as

$$\begin{aligned} \mathbf{R}_n &= E\{\mathbf{n}(k)\mathbf{n}^H(k)\} \\ &= E\left\{ \begin{bmatrix} n_1(k) \\ n_2(k) \\ \vdots \\ n_L(k) \end{bmatrix} \begin{bmatrix} n_1^*(k) & n_2^*(k) & \dots & n_L^*(k) \end{bmatrix} \right\} \\ &= \begin{bmatrix} E\{|n_1(k)|^2\} & E\{n_1(k)n_2^*(k)\} & \dots & E\{n_1(k)n_L^*(k)\} \\ E\{n_2(k)n_1^*(k)\} & E\{|n_2(k)|^2\} & \dots & E\{n_2(k)n_L^*(k)\} \\ \vdots & \vdots & \ddots & \vdots \\ E\{n_L(k)n_1^*(k)\} & E\{n_L(k)n_2^*(k)\} & \dots & E\{|n_L(k)|^2\} \end{bmatrix} \end{aligned}$$

$$\begin{aligned}
&= \begin{bmatrix} \sigma_n^2 & 0 & 0 & \dots & 0 \\ 0 & \sigma_n^2 & 0 & \dots & 0 \\ \vdots & \vdots & \vdots & \ddots & \vdots \\ 0 & 0 & 0 & \dots & \sigma_n^2 \end{bmatrix} \\
&= \sigma_n^2 \mathbf{I}_L
\end{aligned}$$

This shows that the noise covariance of the noise vector consisting of IID noise components of power σ_n^2 is given as $\mathbf{R}_n = \sigma_n^2 \mathbf{I}$, i.e., it is proportional to the $L \times L$ identity matrix.

3.10 | Symbol Detection in Multiple Antenna Systems

Consider the signal $y_1(k), y_2(k), \dots, y_L(k)$ received over the L receive antennas at the time instant k . These can now be employed at the receiver for detection of the transmitted symbol $x(k)$. For this purpose, we combine the received signals with complex weights w_1, w_2, \dots, w_L as follows:

$$r(k) = w_1^* y_1 + w_2^* y_2 + \dots + w_L^* y_L$$

where w_i^* denotes the complex conjugate of w_i and $r(k)$ is termed the *decision statistic* that is formed from the received signals. Defining the vector $\mathbf{w} \in \mathbb{C}^{L \times 1}$ as

$$\mathbf{w} = \begin{bmatrix} w_1 \\ w_2 \\ \vdots \\ w_L \end{bmatrix}$$

it can be easily seen that the receiver statistic $r(k)$ can be compactly expressed in vector form as

$$r(k) = \begin{bmatrix} w_1^* & w_2^* & \dots & w_L^* \end{bmatrix} \begin{bmatrix} y_1(k) \\ y_2(k) \\ \vdots \\ y_L(k) \end{bmatrix}$$

$$\begin{aligned}
&= \mathbf{w}^H \mathbf{y}(k), \\
&= \mathbf{w}^H (\mathbf{h}x(k) + \mathbf{n}(k)) \\
&= \underbrace{\mathbf{w}^H \mathbf{h}x(k)}_{\text{Signal}} + \underbrace{\mathbf{w}^H \mathbf{n}(k)}_{\text{Noise}}
\end{aligned}$$

where \mathbf{w}^H represents the *Hermitian transpose* of the vector \mathbf{w} . The weight vector \mathbf{w} is also termed the receive *beamformer* at the wireless receiver. As given above, the signal and noise components of the received statistic are given as $\mathbf{w}^H \mathbf{h}x(k)$ and $\mathbf{w}^H \mathbf{n}(k)$ respectively. Hence, the signal power is given as

$$\text{Signal power} = \mathbb{E} \left\{ \left| \mathbf{w}^H \mathbf{h}x(k) \right|^2 \right\} = \left| \mathbf{w}^H \mathbf{h} \right|^2 \mathbb{E} \left\{ (x(k))^2 \right\} = \left| \mathbf{w}^H \mathbf{h} \right|^2 P$$

Next, we need to compute the noise power to characterize the signal-to-noise power ratio of the receiver statistic. This is computed as follows.

$$\begin{aligned}
\text{Noise power} &= \mathbb{E} \left\{ \left| \mathbf{w}^H \mathbf{n}(k) \right|^2 \right\} = \mathbb{E} \left\{ \left| \sum_{i=1}^L w_i^* n_i \right|^2 \right\} \\
&= \mathbb{E} \left\{ \left(\sum_{i=1}^L w_i^* n_i \right) \left(\sum_{j=1}^L w_j^* n_j \right)^* \right\} \\
&= \mathbb{E} \left\{ \sum_{i=1}^L \sum_{j=1}^L w_i w_j^* n_i n_j^* \right\} = \sum_{i=1}^L \sum_{j=1}^L w_i w_j^* \mathbb{E} \{ n_i n_j^* \}
\end{aligned}$$

Recall now that the noise samples $n_1(k), n_2(k), \dots, n_L(k)$ are independent with noise power σ_n^2 . Hence, we have $\mathbb{E} \{ n_i(k) n_j^*(k) \} = \delta(i-j) \sigma_n^2$, i.e., $\mathbb{E} \{ n_i(k) n_j^*(k) \} = \sigma_n^2$ only if $i = j$ and 0 if $i \neq j$. The noise power can, therefore, be simplified as

$$\begin{aligned}
\text{Noise power} &= \sum_{i=1}^L \sum_{j=1}^L \delta(i-j) w_i w_j^* \sigma_n^2 = \sum_{i=1}^L w_i w_i^* \sigma_n^2 \\
&= \sigma_n^2 \sum_{i=1}^L |w_i|^2 = \sigma_n^2 \|\mathbf{w}\|^2 \\
&= \sigma_n^2 \mathbf{w}^H \mathbf{w}
\end{aligned}$$

The above can also be derived conveniently using the noise-covariance matrix \mathbf{R}_n defined above as

$$\begin{aligned} \text{Noise power} &= \mathbb{E} \left\{ \left| \mathbf{w}^H \mathbf{n}(k) \right|^2 \right\} = \mathbb{E} \left\{ (\mathbf{w}^H \mathbf{n}(k)) (\mathbf{w}^H \mathbf{n}(k))^H \right\} \\ &= \mathbb{E} \left\{ \mathbf{w}^H \mathbf{n}(k) \mathbf{n}^H(k) \mathbf{w} \right\} = \mathbf{w}^H \mathbb{E} \left\{ \mathbf{n}(k) \mathbf{n}^H(k) \right\} \mathbf{w} \\ &= \mathbf{w}^H \mathbf{R}_n \mathbf{w} = \mathbf{w}^H \sigma_n^2 \mathbf{I} \mathbf{w} \\ &= \sigma_n^2 \mathbf{w}^H \mathbf{w} = \sigma_n^2 \|\mathbf{w}\|^2 \end{aligned}$$

Hence, the noise power at the output corresponding to the receive beamformer \mathbf{w} is equal to $\sigma_n^2 \|\mathbf{w}\|^2$. Therefore, the signal-to-noise power ratio at the output of the beamformer is given as

$$\text{SNR}(\mathbf{w}) = \frac{|\mathbf{w}^H \mathbf{h}|^2 P}{\mathbf{w}^H \mathbf{w} \sigma_n^2} = \left(\frac{P}{\sigma_n^2} \right) \frac{|\mathbf{w}^H \mathbf{h}|^2}{\mathbf{w}^H \mathbf{w}}$$

We wish to now find the *optimum* beamformer \mathbf{w} such that the output SNR is maximized. Firstly, observe that scaling the beamformer \mathbf{w} by a constant C leaves the SNR unchanged. This can be observed by substituting $\tilde{\mathbf{w}} = C\mathbf{w}$ in the above expression. One can see,

$$\begin{aligned} \text{SNR}(\tilde{\mathbf{w}}) &= \left(\frac{P}{\sigma_n^2} \right) \frac{|\tilde{\mathbf{w}}^H \mathbf{h}|^2}{\tilde{\mathbf{w}}^H \tilde{\mathbf{w}}} = \left(\frac{P}{\sigma_n^2} \right) \frac{|(C\mathbf{w})^H \mathbf{h}|^2}{(C\mathbf{w})^H (C\mathbf{w})} \\ &= \left(\frac{P}{\sigma_n^2} \right) \frac{|C|^2 |\mathbf{w}^H \mathbf{h}|^2}{|C|^2 \mathbf{w}^H \mathbf{w}} = \left(\frac{P}{\sigma_n^2} \right) \frac{|\mathbf{w}^H \mathbf{h}|^2}{\mathbf{w}^H \mathbf{w}} \end{aligned}$$

Hence, to fix the scale of the beamformer \mathbf{w} , one can restrict the choice of beamformers such that $\|\mathbf{w}\|^2 = 1$. The optimal SNR maximizing beamformer computation, therefore, reduces to,

$$\max. \left(\frac{P}{\sigma_n^2} \right) |\mathbf{w}^H \mathbf{h}|^2 \text{ s.t. } \|\mathbf{w}\|^2 = 1$$

where "s.t." is the acronym for *subject to* and denotes the constraint for the optimization problem. Observe that from the standard *Cauchy-Schwarz* inequality, we have $|\mathbf{w}^H \mathbf{h}|^2 \leq \|\mathbf{w}\|^2 \|\mathbf{h}\|^2 = \|\mathbf{h}\|^2$, with equality only if $\mathbf{w} = \frac{1}{\|\mathbf{h}\|} \mathbf{h}$. This is more intuitively illustrated in Example 3.8. Further, the maximum SNR is given as

$$\text{SNR}_{\max} = \text{SNR} \left(\frac{1}{\|\mathbf{h}\|} \mathbf{h} \right) = \left(\frac{P}{\sigma_n^2} \right) \left| \frac{1}{\|\mathbf{h}\|} \mathbf{h}^H \mathbf{h} \right|^2 = \left(\frac{P}{\sigma_n^2} \right) \|\mathbf{h}\|^2$$

The optimal beamformer $\mathbf{w}_{\text{opt}} = \frac{1}{\|\mathbf{h}\|} \mathbf{h}$ is termed the *Maximal Ratio Combiner (MRC)* and this beamforming technique is termed *maximal ratio combining*. The beamforming step is a key step to achieving high SNR over a multi-antenna wireless link.

Observe that the MRC beamformer $\mathbf{w}_{\text{opt}} = C\mathbf{h}$, where the constant of proportionality $C = \frac{1}{\|\mathbf{h}\|}$. Hence, this is a vector **matched** to the direction of \mathbf{h} , similar to the concept of a matched filter in the receiver of a digital communication system. In fact, one can term the MRC beamformer as a **spatially** matched filter.

EXAMPLE 3.8

Given the multi-antenna wireless channel \mathbf{h} , prove that of all the beamformers \mathbf{w} such that $\|\mathbf{w}\| = 1$, the one that maximizes $|\mathbf{w}^H \mathbf{h}|$ is $\mathbf{w} = \frac{\mathbf{h}}{\|\mathbf{h}\|}$.

Solution: Consider any beamformer \mathbf{w} . Since any two vectors uniquely define a plane, consider the plane formed by the vectors \mathbf{w} , \mathbf{h} . From a basic undergraduate level knowledge of the properties of vectors, it is clear that any vector \mathbf{w} can be decomposed as the linear combination of \mathbf{u}_h , \mathbf{v}_h , which are unit vectors along the direction of \mathbf{h} and perpendicular to \mathbf{h} . This is illustrated graphically in Figure 3.8. Also note that the unit vector in the direction of \mathbf{h} is $\mathbf{u} = \frac{\mathbf{h}}{\|\mathbf{h}\|}$. Thus, let this linear combination be described as

$$\mathbf{w} = \alpha \mathbf{u}_h + \beta \mathbf{v}_h$$

where α , β are the coefficients of linear combination. Observe further that since \mathbf{u}_h , \mathbf{v}_h are perpendicular. Hence, $\|\mathbf{w}\|^2 = |\alpha|^2 + |\beta|^2$. Further, since $\|\mathbf{w}\|^2 = 1$, we have

$$|\alpha|^2 + |\beta|^2 = 1$$

$$\Rightarrow |\alpha|^2 \leq 1$$

The expression for $\mathbf{w}^H \mathbf{h}$ can now be simplified as

$$\mathbf{w}^H \mathbf{h} = (\alpha \mathbf{u}_h + \beta \mathbf{v}_h)^H \mathbf{h}$$

$$\begin{aligned}
&= \alpha^* (\mathbf{u}_h)^H \mathbf{h} + \beta^* (\mathbf{v}_h)^H \mathbf{h} \\
&= \alpha^* (\mathbf{u}_h)^H \mathbf{h} + 0 \\
&= \alpha^* \|\mathbf{h}\|
\end{aligned}$$

where we have used the fact that $\mathbf{v}_h^H \mathbf{h} = 0$, since \mathbf{v}_h is perpendicular to \mathbf{h} . Also, $(\mathbf{u}_h)^H \mathbf{h} = \frac{\mathbf{h}^H \mathbf{h}}{\|\mathbf{h}\|} = \|\mathbf{h}\|$. Therefore, $|\mathbf{w}^H \mathbf{h}|^2$ is given as

$$\begin{aligned}
|\mathbf{w}^H \mathbf{h}|^2 &= |\alpha^* \|\mathbf{h}\||^2 \\
&= |\alpha|^2 \|\mathbf{h}\|^2 \\
&\leq \|\mathbf{h}\|^2
\end{aligned}$$

where the last inequality follows from the fact derived above that $|\alpha|^2 \leq 1$. Thus the maximum value above occurs for $\alpha = 1$, which implies that $\beta = 0$, since $|\alpha|^2 + |\beta|^2 = 1$. Thus, the beamformer that maximizes $|\mathbf{w}^H \mathbf{h}|$, in turn maximizing the receive SNR is given as

$$\mathbf{w} = \mathbf{u}_h = \frac{1}{\|\mathbf{h}\|} \mathbf{h}$$

proving the desired result.

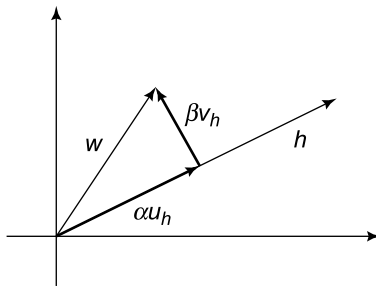


Figure 3.8 Plane containing \mathbf{w} the beamformer and \mathbf{h} , the multi-antenna channel

EXAMPLE 3.9

Maximum Ratio Combining Consider an $L = 2$ receive antenna wireless channel with complex fading channel coefficients $h_1 = \frac{1}{\sqrt{2}} + \frac{1}{\sqrt{2}}j$, $h_2 = \frac{1}{\sqrt{2}} - \frac{1}{\sqrt{2}}j$. Describe the system model for the multi-antenna channel and derive the SNR with MRC.

Solution: Given the channel coefficients h_1, h_2 , the system model for the received outputs y_1, y_2 at the two receive antennas is given as

$$\begin{bmatrix} y_1(k) \\ y_2(k) \end{bmatrix} = \underbrace{\begin{bmatrix} \frac{1}{\sqrt{2}} + \frac{1}{\sqrt{2}}j \\ \frac{1}{\sqrt{2}} - \frac{1}{\sqrt{2}}j \end{bmatrix}}_{\mathbf{h}} x(k) + \begin{bmatrix} n_1(k) \\ n_2(k) \end{bmatrix}$$

Observe that $|h_1| = |h_2| = \sqrt{\left(\frac{1}{\sqrt{2}}\right)^2 + \left(\frac{1}{\sqrt{2}}\right)^2} = 1$. Hence, we have, $\|\mathbf{h}\| = \sqrt{|h_1|^2 + |h_2|^2} = \sqrt{2}$. Hence, the SNR maximizing maximum ratio beamformer for the above system is given as

$$\mathbf{w} = \frac{1}{\|\mathbf{h}\|} = \frac{1}{\sqrt{2}} \begin{bmatrix} \frac{1}{\sqrt{2}} + \frac{1}{\sqrt{2}}j \\ \frac{1}{\sqrt{2}} - \frac{1}{\sqrt{2}}j \end{bmatrix} = \begin{bmatrix} \frac{1}{2} + \frac{1}{2}j \\ \frac{1}{2} - \frac{1}{2}j \end{bmatrix}$$

Therefore, $\mathbf{w}^H = \left[\frac{1}{2} - \frac{1}{2}j, \frac{1}{2} + \frac{1}{2}j\right]$. The receiver statistic $r(k)$ computed at the receiver is, therefore, given as

$$\begin{aligned} r(k) &= \mathbf{w}^H \mathbf{y} = \left[\left(\frac{1}{2} - \frac{1}{2}j\right), \left(\frac{1}{2} + \frac{1}{2}j\right) \right] \begin{bmatrix} y_1(k) \\ y_2(k) \end{bmatrix} \\ &= \left(\frac{1}{2} - \frac{1}{2}j\right) y_1 + \left(\frac{1}{2} + \frac{1}{2}j\right) y_2 \end{aligned}$$

Finally, since $\|\mathbf{h}\|^2 = 2$, the SNR after MRC is given as $\text{SNR}_{\text{MRC}} = \|\mathbf{h}\|^2 \frac{P}{\sigma_n^2} = 2 \frac{P}{\sigma_n^2}$.

3.11 | BER in Multi-Antenna Wireless Systems

Continuing the above discussion, let the quantity g denote the channel power gain, i.e.,

$$g = \|\mathbf{h}\|^2 = |h_1|^2 + |h_2|^2 + \dots + |h_L|^2 \quad (3.16)$$

As seen above, the SNR after MRC is given as $\text{SNR}_{\text{MRC}} = \|\mathbf{h}\|^2 \frac{P}{\sigma_n^2} = g \frac{P}{\sigma_n^2}$. It can be demonstrated that the quantity g is a chi-squared random variable with $2L$ degrees of freedom and probability density given as

$$f_G(g) = \frac{1}{(L-1)!} g^{L-1} e^{-g}$$

Hence, the instantaneous bit-error rate of this multi-antenna wireless channel is given as $\text{BER} = Q\left(\sqrt{g \frac{P}{\sigma_n^2}}\right)$. The average bit-error rate can then be obtained by averaging over the distribution of the channel coefficient $f_G(g)$ as

$$\text{BER}_{\text{Multi-Antenna}} = \int_0^\infty Q\left(\sqrt{g \frac{P}{\sigma_n^2}}\right) f_G(g) dg$$

Since the exact computation of the above expression for BER is quite complex, we will skip it here. The final expression for the BER of this multi-antenna wireless system with MRC combining is given as

$$\text{BER}_{\text{Multi-Antenna}} = \left(\frac{1-\lambda}{2}\right)^L \sum_{l=0}^{L-1} {}^{L+l-1}C_l \left(\frac{1+\lambda}{2}\right)^l \quad (3.17)$$

where the quantity λ is defined as $\lambda = \sqrt{\frac{\text{SNR}}{2+\text{SNR}}}$, with SNR denoting the average receiver SNR for each link given by $\frac{P}{\sigma_n^2}$ and ${}^n C_k = \frac{n!}{k!(n-k)!}$. Notice that for $L = 1$, i.e., the case with a single receive antenna, the above expression reduces to

$$\begin{aligned} \text{BER} &= \left(\frac{1-\lambda}{2}\right)^1 \sum_{l=0}^0 {}^0 C_l \left(\frac{1+\lambda}{2}\right)^l = \frac{1}{2}(1-\lambda) \\ &= \frac{1}{2} \left(1 - \sqrt{\frac{\text{SNR}}{2+\text{SNR}}}\right) \end{aligned}$$

which is the exact same expression that has been derived for the Rayleigh fading wireless channel with a single receive antenna in Eq. (3.9). It has already been noted in Eq. (3.10) that at high SNR $\frac{1}{2}(1 - \lambda) \approx \frac{1}{2} \frac{1}{\text{SNR}}$. Further, the quantity $\frac{1}{2}(1 + \lambda)$ can be simplified at high SNR as

$$\begin{aligned} \frac{1}{2}(1 + \lambda) &= \frac{1}{2} \left(1 + \sqrt{\frac{\text{SNR}}{2 + \text{SNR}}} \right) = \frac{1}{2} \left(1 + \frac{1}{\left(1 + \frac{2}{\text{SNR}}\right)^{\frac{1}{2}}} \right) \\ &\approx \frac{1}{2} \left(1 + \left(1 - \frac{1}{2} \frac{2}{\text{SNR}} \right) \right) = \frac{1}{2} \left(2 - \frac{1}{\text{SNR}} \right) \\ &\approx \frac{1}{2} \cdot 2 = 1 \end{aligned}$$

The above simplifications imply that at high SNR, the BER in a multi-antenna wireless system can be simplified as

$$\begin{aligned} \text{BER}_{\text{Multi-Antenna}} &= \left(\frac{1 - \lambda}{2} \right)^L \sum_{l=0}^{L-1} {}^{L+l-1}C_l \left(\frac{1 + \lambda}{2} \right)^l \\ &= \left(\frac{1}{2 \text{SNR}} \right)^L \sum_{l=0}^{L-1} {}^{L+l-1}C_l \\ &= {}^{2L-1}C_L \left(\frac{1}{2} \right)^L \left(\frac{1}{\text{SNR}} \right)^L \end{aligned} \quad (3.18)$$

Recall from the expression (3.10) that the BER for a single-antenna Rayleigh fading wireless channel decreases at a very slow rate of $\frac{1}{\text{SNR}}$. As the above expression shows, the BER in a multi-antenna channel decreases at a much faster rate of $\left(\frac{1}{\text{SNR}}\right)^L$. The following example illustrates this point much more clearly.

EXAMPLE 3.10

Compute the BER for BPSK communication over a multi-antenna fading wireless channel with $L = 4$ receive antennas at an SNR of 20 dB.

Solution: Given SNR (dB) = 20 dB, the corresponding linear SNR is given as $\text{SNR} = 10^2 = 100$. The parameter λ can, therefore, be computed as

$$\lambda = \sqrt{\frac{\text{SNR}}{2 + \text{SNR}}} = \sqrt{\frac{100}{102}} = 0.9901$$

Hence, the quantities $\frac{1}{2}(1 - \lambda)$ and $\frac{1}{2}(1 + \lambda)$ are given as 0.0049 and 0.9951 respectively. Hence, the BER for the above multichannel system is given from the expression (3.17) as

$$\begin{aligned} \text{BER} &= (0.0049)^4 \left({}^3C_0 (0.9951)^0 + {}^4C_1 (0.9951)^1 + {}^5C_2 (0.9951)^2 + {}^6C_3 (0.9951)^3 \right) \\ &= 2.037 \times 10^{-8} \end{aligned}$$

In comparison, observe that the corresponding BER at SNR = 20 dB for the conventional wireline AWGN channel is $Q(\sqrt{\text{SNR}}) = Q(10) = 7.62 \times 10^{-24}$ and that of the single receive antenna Rayleigh fading wireless link is $\frac{1}{2} \left(1 - \sqrt{\frac{\text{SNR}}{2 + \text{SNR}}} \right) = 4.9 \times 10^{-3}$. Hence, the BER for the multi-antenna system is worse than that of a wireline channel, but significantly better than that of the single antenna wireless channel.

EXAMPLE 3.11

Consider a multi-antenna system with $L = 2$ receive antennas. What is the approximate SNR required to achieve a BER of 10^{-6} in this wireless system?

Solution: From the high SNR approximation for the BER in a multi-antenna wireless system given in Eq. (3.18), to achieve a BER of 10^{-6} in an $L = 2$ antenna system, we have,

$$\begin{aligned} 10^{-6} &= {}^3C_2 \left(\frac{1}{2} \right)^2 \left(\frac{1}{\text{SNR}} \right)^L = \frac{3}{4} \frac{1}{\text{SNR}^2} \\ \text{SNR} &= \frac{\sqrt{3}}{2} \times 10^3 \end{aligned}$$

$$\text{SNR}_{\text{dB}} = 29.37 \text{ dB}$$

Recall from Example 3.6 that the SNR required to achieve a similar BER across the Rayleigh fading wireless channel is 57 dB. Thus, increasing the number of antennas to $L = 2$ results in a humungous saving of transmit power by approximately $57 \text{ dB} - 29 \text{ dB} = 28 \text{ dB}$. To see this explicitly, let P_i^w , $i = 1, 2$ denote the transmit power required to achieve a BER of 10^{-6} with i receive antennas. Then, from the above analysis, we have

$$10 \log_{10} \left(\frac{P_1^w}{P_2^w} \right) = 28 \text{ dB}$$

$$\Rightarrow \frac{P_2^w}{P_1^w} = 10^{2.8} = 631$$

$$\Rightarrow P_2^w = \frac{P_1^w}{631}$$

Thus, the transmit power required for a similar BER with $L = 2$ transmit antennas is 631 times lower compared to the single-antenna fading-channel scenario.

The BER vs SNR for $L = 1, 2, 4, 8$ receive antenna Rayleigh fading systems, obtained from simulations and the theoretical BER expression in Eq. (3.17), is shown in Figure 3.9. Observe that the BER obtained analytically matches closely with that obtained from simulations. As the number of receive antennas increases significantly, it improves the BER performance of the

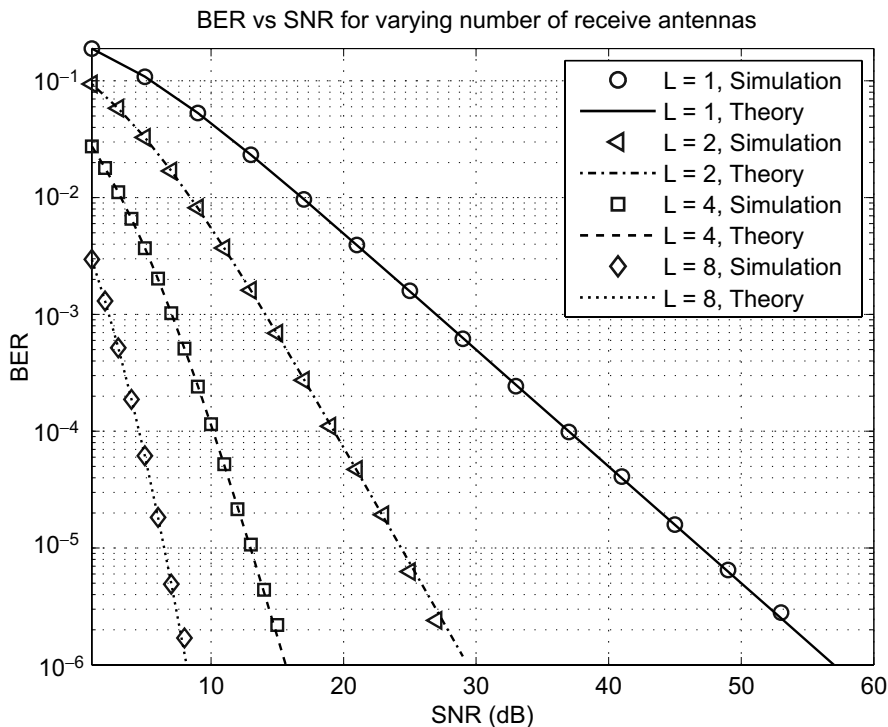


Figure 3.9 BER of multi-antenna Rayleigh channel. The term ‘theory’ in the legend refers to the theoretical value of BER obtained from the expression in Eq. (3.17)

wireless channel. This phenomenon of enhancing the reliability of the wireless communication system through transmission of signal copies over multiple *independently* fading wireless channels is termed *diversity*. In this case, the multiple fading channels correspond to the individual wireless links between the transmit antenna and the multiple receive antennas. This specific realization of diversity is termed *receive diversity* or also *spatial diversity* since it is arising due to the spatially separated antennas. Receive diversity is an important technique in 3G/4G wireless communication systems and is employed in all key wireless standards such as WCDMA, HSDPA, LTE, WiMAX amongst others.

3.11.1 A Simpler Derivation of Approximate Multi-Antenna BER

Similar to the derivation of the simple bound for the Rayleigh single antenna BER in Section 3.6.1, one can derive a simple bound for the multi-antenna Rayleigh BER as

$$\begin{aligned} \text{BER}_{\text{Multi-Antenna}} &= \int_0^\infty Q\left(\sqrt{g\text{SNR}}\right) f_G(g) dg \\ &\leq \int_0^\infty \frac{1}{2} e^{-\frac{1}{2}g\text{SNR}} f_G(g) dg \end{aligned}$$

Now we point the reader to two observations. Firstly, recall that the gain g of the wireless channel is defined as $g = \sum_{i=1}^L |h_i|^2 = \sum_{i=1}^L a_i^2$, where $a_i = |h_i|$. Secondly, since the fading channels across the antennas in the system are assumed to be independent, the amplitude gains a_i , $1 \leq i \leq L$ are independent Rayleigh distributed. Hence, the probability distribution $f_{A_1, A_2, \dots, A_L}(a_1, a_2, \dots, a_L)$ can be simplified as

$$\begin{aligned} f_{A_1, A_2, \dots, A_L}(a_1, a_2, \dots, a_L) &= f_{A_1}(a_1) \times f_{A_2}(a_2) \times \dots \times f_{A_L}(a_L) \\ &= \prod_{i=1}^L 2a_i e^{-a_i^2} \end{aligned}$$

where in the above simplification, we have used the simple result that the joint density of a group of independent random variables is the product of the individual probability densities.

Employing this result, the above bound for the multi-antenna Rayleigh BER can be simplified as

$$\begin{aligned}
 \text{BER}_{\text{Multi-Antenna}} &\leq \frac{1}{2} \int_{a_1=0}^{\infty} \int_{a_2=0}^{\infty} \dots \int_{a_L=0}^{\infty} e^{-\frac{1}{2}\text{SNR} \sum_{i=1}^L a_i^2} \prod_{i=1}^L 2a_i e^{-a_i^2} da_i \\
 &= \frac{1}{2} \prod_{i=1}^L \int_{a_i=0}^{\infty} e^{-\frac{1}{2}\text{SNR} a_i^2} 2a_i e^{-a_i^2} da_i \\
 &= \frac{1}{2} \prod_{i=1}^L \int_{a_i=0}^{\infty} 2a_i e^{-a_i^2(1+\frac{1}{2}\text{SNR})} da_i \\
 &= \frac{1}{2} \left(\frac{1}{1+\frac{1}{2}\text{SNR}} \right)^L
 \end{aligned}$$

Once again, as $\text{SNR} \rightarrow \infty$, the above bound can be simplified as

$$\text{BER}_{\text{Multi-Antenna}} \leq \frac{2^{L-1}}{\text{SNR}^L}$$

which clearly indicates that the multi-antenna bit-error rate decreases as $\left(\frac{1}{\text{SNR}}\right)^L$.

3.11.2 Intuition for Diversity

How does the increase in number of receive antennas to L lead to a BER decrease at rate $\left(\frac{1}{\text{SNR}}\right)^L$? The following discussion is intended to give the reader the key intuition behind this finding. Consider the multi-antenna wireless system model,

$$\mathbf{y}(k) = \mathbf{h}x(k) + \mathbf{n}(k)$$

As has been derived above, the signal and noise power after MRC beamforming are given as gP , σ_n^2 respectively, where $g = \|\mathbf{h}\|^2$. Similar to the case of a single-antenna fading link, the wireless system is in a deep fade if the signal power is lower than the noise power, i.e.,

$$\begin{aligned}
 gP &< \sigma_n^2 \\
 \Rightarrow g &< \frac{\sigma_n^2}{P} = \frac{1}{\text{SNR}}
 \end{aligned}$$

Further, recall that the gain g is a chi-squared distributed random variable with density function given as $f_G(g) = \frac{g^{L-1}}{(L-1)!}e^{-g}$. Hence, the probability that the multi-antenna system is in a deep fade is given by the probability $P\left(g < \frac{1}{\text{SNR}}\right)$, which is simplified as

$$\begin{aligned} P_{\text{Deep fade}} &= P\left(g < \frac{1}{\text{SNR}}\right) \\ &= \int_0^{\frac{1}{\text{SNR}}} f_G(g) dg = \int_0^{\frac{1}{\text{SNR}}} \frac{g^{L-1}}{(L-1)!} e^{-g} dg \end{aligned}$$

At high SNR, i.e., $\frac{1}{\text{SNR}} \approx 0$, the term $e^{-g} \approx 1$. Hence, the above probability can be simplified as

$$\begin{aligned} P_{\text{Deep fade}} &= \int_0^{\frac{1}{\text{SNR}}} \frac{g^{L-1}}{(L-1)!} dg \\ &= \left. \frac{g^L}{L!} \right|_0^{\frac{1}{\text{SNR}}} \\ &= \frac{1}{L!} \left(\frac{1}{\text{SNR}} \right)^L \end{aligned}$$

Hence, the probability of deep fade in the multi-antenna diversity system essentially decreases at a rate of $\left(\frac{1}{\text{SNR}}\right)^L$, which is significantly lower compared to that of a single-antenna fading Rayleigh wireless channel. This can be better understood as follows. Consider the single-antenna channel. This system is in a deep fade if the only pathway between the transmit and single-receive antenna is in a deep fade. As seen earlier, the probability of this event is $\propto \frac{1}{\text{SNR}}$. On the other hand, in a multi-antenna wireless system, there are L pathways, one between the transmit antenna and each of the individual receive antennas. Hence, if E_i denotes the event that the pathway between the transmit antenna and the i^{th} receive antenna is in a deep fade, we have $P(E_i) \propto \frac{1}{\text{SNR}}$. Further, note that since there are L independent pathways, the overall system is in a deep fade only if *each* of the individual pathways is in a deep fade. Hence, the net probability of deep fade in the multi-antenna system is

$$P_{\text{Deep fade}} = P(E_1 \cap E_2 \cap \dots \cap E_L)$$

Since the channels are assumed to be independently fading, the events E_1, E_2, \dots, E_L are independent. From the principle of probability of independent events which states that

$P(A \cap B) = P(A)P(B)$. If A, B are independent, we have

$$\begin{aligned} P_{\text{Deep fade}} &= P(E_1 \cap E_2 \cap \dots \cap E_L) \\ &= P(E_1) \times P(E_2) \times \dots \times P(E_L) \\ &\propto \frac{1}{\text{SNR}} \times \frac{1}{\text{SNR}} \times \dots \times \frac{1}{\text{SNR}} \\ &\propto \left(\frac{1}{\text{SNR}}\right)^L. \end{aligned}$$

The probability of deep fade of the system comprising these L independently fading channels decreases at a rate of $\left(\frac{1}{\text{SNR}}\right)^L$. Thus, *independence* of the fading channels is a key assumptions in achieving diversity in this multi-antenna systems. Finally, as described previously, diversity is achieved by transmission of signal copies through parallel independent fading channels, thus reducing the probability of deep fade, since the probability that all the L independent signal pathways are simultaneously in a deep fade is significantly lower compared to a single-pathway wireless system.

For the independent fading assumption to be valid in multi-antenna systems such as the one illustrated above, one needs the antennas to be separated by an appropriately large spacing. A popular rule-of-thumb for the minimum required antenna spacing is given as $\frac{\lambda}{2}$, where λ is the wavelength of the radio wave and is given as $\lambda = \frac{c}{f_c}$, the quantity f_c denoting the carrier frequency and $c = 3 \times 10^8 \text{ms}^{-1}$ denotes the velocity of an electromagnetic wave in free space.

EXAMPLE 3.12

Consider a GSM system operating at a carrier frequency of $f_c = 900$ MHz. Compute the minimum spacing required between the antennas for independently fading channels.

Solution: Given $f_{\text{GSM}} = 900$ MHz, the wavelength λ_{GSM} is given as

$$\lambda_{\text{GSM}} = \frac{c}{f_{\text{GSM}}} = \frac{3 \times 10^8}{900 \times 10^6} = 0.3333 \text{ m} = 33.33 \text{ cm}$$

Hence, the minimum required spacing for the GSM system is given as $\frac{1}{2}\lambda_{\text{GSM}} = 16.66$ cm. Notice that this is slightly larger compared to the dimensions of most modern cellular phones. Therefore, implementing multi-antenna systems on current GSM cellphones is intuitively not expected to yield a significant advantage due to the correlated nature of the fading channels.

However, it can still be implemented in larger devices such as notebook computers for broadband wireless data access.

EXAMPLE 3.13

Compute the minimum spacing required between the antennas for independently fading channels in a 4G system operating at a typical carrier frequency of $f_c = 2.3$ GHz.

Solution: The wavelength λ corresponding to $f_c = 2.3$ GHz can be computed similar to the above as $\lambda = \frac{c}{f_c} = 13.04$ cm. Hence, the required antenna spacing is $\frac{\lambda}{2} = 6.04$ cm. Notice that this is in the range of the dimension of typical modern cellular phones. Thus, one implementing multi-antenna systems in 4G devices potentially yields benefits of enhanced performance due to diversity.

3.11.3 Channel Estimation for Multi-Antenna Systems

As given in Section 3.3, channel estimation for multi-antenna wireless systems can be carried out similarly. Consider the transmission of $L^{(p)}$ pilot symbols $x^{(p)}(1), x^{(p)}(2), \dots, x^{(p)}(L^{(p)})$. Let $y_j^{(p)}(i)$ denote the i^{th} transmitted pilot symbol, $1 \leq i \leq L^{(p)}$ at the j^{th} antenna. The vector model for the same can be represented as

$$\underbrace{\begin{bmatrix} y_j^{(p)}(1) \\ y_j^{(p)}(2) \\ \vdots \\ y_j^{(p)}(L^{(p)}) \end{bmatrix}}_{\mathbf{y}_j^{(p)}} = \underbrace{\begin{bmatrix} x^{(p)}(1) \\ x^{(p)}(2) \\ \vdots \\ x^{(p)}(L^{(p)}) \end{bmatrix}}_{\mathbf{x}^{(p)}} h_j + \underbrace{\begin{bmatrix} n_j(1) \\ n_j(2) \\ \vdots \\ n_j(L^{(p)}) \end{bmatrix}}_{\mathbf{n}_j}$$

Observe that the above model is different from the one described in Eq. (3.14), which corresponds to the different outputs at the received antennas at a given instant of time. The above model corresponds to the outputs at different instances of time at the j^{th} antenna, $1 \leq j \leq L$, where L is the number of antennas. This is naturally the case since we would like to estimate the channel between the transmit antenna, the j^{th} receive antenna. Hence, similar

to Eq. (3.13), the estimate of channel coefficient h_j is given as,

$$\hat{h}_j = \frac{(\mathbf{x}^{(p)})^H \mathbf{y}_j^{(p)}}{(\mathbf{x}^{(p)})^H \mathbf{x}^{(p)}} = \frac{(\mathbf{x}^{(p)})^H \mathbf{y}_j^{(p)}}{\|\mathbf{x}^{(p)}\|^2} \quad (3.19)$$

Finally, putting all the estimated channel coefficients \hat{h}_j together for $1 \leq j \leq L$, the estimate $\hat{\mathbf{h}}$ of the multi-antenna channel vector is given as

$$\hat{\mathbf{h}} = \begin{bmatrix} \hat{h}_1 \\ \hat{h}_2 \\ \vdots \\ \hat{h}_L \end{bmatrix} \quad (3.20)$$

Another alternative concise formula to compute the multi-antenna channel estimate can be derived as follows. Let the input-output system model for the received pilot symbol vectors be given as

$$\underbrace{\begin{bmatrix} y_1^{(p)}(k) \\ y_2^{(p)}(k) \\ \vdots \\ y_L^{(p)}(k) \end{bmatrix}}_{\mathbf{y}^{(p)}(k)} = \underbrace{\begin{bmatrix} h_1 \\ h_2 \\ \vdots \\ h_L \end{bmatrix}}_{\mathbf{h}} x^{(p)}(k) + \underbrace{\begin{bmatrix} n_1(k) \\ n_2(k) \\ \vdots \\ n_L(k) \end{bmatrix}}_{\mathbf{n}(k)} \quad (3.21)$$

The net system model corresponding to the transmission of $L^{(p)}$ pilot symbols can be compactly represented in matrix notation as

$$\underbrace{\begin{bmatrix} \mathbf{y}^{(p)}(1) \\ \mathbf{y}^{(p)}(2) \\ \vdots \\ \mathbf{y}^{(p)}(L^{(p)}) \end{bmatrix}}_{\mathbf{Y}^{(p)}} = \mathbf{h} \underbrace{\begin{bmatrix} x^{(p)}(1) \\ x^{(p)}(2) \\ \vdots \\ x^{(p)}(L^{(p)}) \end{bmatrix}}_{\mathbf{x}^{(p)}} + \underbrace{\begin{bmatrix} \mathbf{n}(1) \\ \mathbf{n}(2) \\ \vdots \\ \mathbf{n}(L^{(p)}) \end{bmatrix}}_{\mathbf{N}^{(p)}} \quad (3.22)$$

where $\mathbf{Y}^{(p)}$ is the $L \times L^{(p)}$ matrix of received pilot vectors, $\mathbf{x}^{(p)}$ is the $1 \times L^{(p)}$ row vector of transmitted pilot symbols. Thus, the net aggregated system model for channel estimation is

$$\mathbf{Y}^{(p)} = \mathbf{h}\mathbf{x}^{(p)} + \mathbf{N}^{(p)}$$

Hence, proceeding similar to the case of a single-antenna channel, the least-squares estimate of the channel vector \mathbf{h} is given as

$$\hat{\mathbf{h}} = \frac{1}{\|\mathbf{x}^{(p)}\|^2} \mathbf{Y}^{(p)} \left(\mathbf{x}^{(p)} \right)^H \quad (3.23)$$

The estimate of the channel coefficient \hat{h}_j from the above formula can be seen to be exactly identical to the one obtained from Eq. (3.19).

EXAMPLE 3.14

Consider the estimation of the wireless channel coefficient vector of an $L = 2$ receive antenna system, with a pilot sequence consisting of $L^{(p)} = 4$ symbols. The transmitted pilot symbols are, $x^{(p)}(1) = \frac{1}{\sqrt{2}}(-1 + j)$, $x^{(p)}(2) = \frac{1}{\sqrt{2}}(-1 - j)$, $x^{(p)}(3) = \frac{1}{\sqrt{2}}(1 + j)$ and $x^{(p)}(4) = \frac{1}{\sqrt{2}}(1 - j)$. Let the corresponding received output pilot symbol vectors be given as

$$\mathbf{y}^{(p)}(1) = \begin{bmatrix} 0.3775 - 0.8344i \\ -0.5605 - 0.4712i \end{bmatrix}, \mathbf{y}^{(p)}(2) = \begin{bmatrix} 0.7153 + 0.2142i \\ 0.4815 - 0.6657i \end{bmatrix}$$

$$\mathbf{y}^{(p)}(3) = \begin{bmatrix} -0.8959 - 0.3688i \\ -0.3678 + 0.6011i \end{bmatrix}, \mathbf{y}^{(p)}(4) = \begin{bmatrix} -0.3118 + 0.8083i \\ 0.6195 + 0.5202i \end{bmatrix}$$

Hence, as described in the section above for estimation of multiple-receive antenna channels, the relevant row vector of pilot symbols $\mathbf{x}^{(p)}$ is given as

$$\mathbf{x}^{(p)} = \frac{1}{\sqrt{2}} [-1 + j, -1 - j, 1 + j, 1 - j]$$

while the matrix of output symbols $\mathbf{Y}^{(p)}$ is,

$$\mathbf{Y}^{(p)} = \begin{bmatrix} 0.3775 - j0.8344 & 0.7153 + j0.2142 & -0.8959 - j0.3688 & -0.3118 + j0.8083 \\ -0.5605 - j0.4712 & 0.4815 - j0.6657 & -0.3678 + j0.6011 & 0.6195 + j0.5202 \end{bmatrix}$$

Finally, from the expression given in Eq. (3.23), the estimate of the channel coefficient vector $\hat{\mathbf{h}}$ can be obtained as

$$\hat{\mathbf{h}} = \frac{1}{\|\mathbf{x}^{(p)}\|^2} \mathbf{Y}^{(p)} (\mathbf{x}^{(p)})^H = \begin{bmatrix} -0.8001 + 0.3503i \\ 0.1071 + 0.7579i \end{bmatrix}$$

3.12 | Diversity Order

A very important concept related to diversity performance of a fading-channel-based wireless communication system is the diversity order of BER decrease with SNR in the system. Let $P_e(\text{SNR})$ give the probability of error as a function of SNR in the system. The diversity order d of the system is defined as

$$d = - \lim_{\text{SNR} \rightarrow \infty} \frac{\log(P_e(\text{SNR}))}{\log(\text{SNR})}$$

The diversity order d is essentially the number of independently fading channels comprising the given system or scheme. For instance, consider the single-antenna Rayleigh fading wireless channel. It has been demonstrated in Eq. (3.10) that the probability of bit-error at high SNR in this system is given as $P_e(\text{SNR}) \approx \frac{1}{2\text{SNR}}$. Hence, the diversity order is given as

$$\begin{aligned} d &= - \lim_{\text{SNR} \rightarrow \infty} \frac{\log\left(\frac{1}{2\text{SNR}}\right)}{\log(\text{SNR})} = - \lim_{\text{SNR} \rightarrow \infty} \left\{ -\frac{\log(2)}{\log(\text{SNR})} - \frac{\log(\text{SNR})}{\log(\text{SNR})} \right\} \\ &= - \underbrace{\lim_{\text{SNR} \rightarrow \infty} \left\{ -\frac{\log(2)}{\log(\text{SNR})} \right\}}_{=0} + 1 = 1 \end{aligned}$$

Consider now an L receive antenna wireless system. It has been shown earlier that the BER of such a system at high SNR is given from Eq. (3.18) as ${}^{2L-1}C_L \left(\frac{1}{2}\right)^L \left(\frac{1}{\text{SNR}}\right)^L$. The diversity

order of this system is, therefore, given as

$$\begin{aligned}
 d &= - \lim_{\text{SNR} \rightarrow \infty} \left\{ \frac{\log \left({}^{2L-1}C_L \left(\frac{1}{2} \right)^L \right)}{\log (\text{SNR})} - \frac{L \log (\text{SNR})}{\log (\text{SNR})} \right\} \\
 &= - \underbrace{\lim_{\text{SNR} \rightarrow \infty} \left\{ \frac{\log \left({}^{2L-1}C_L \left(\frac{1}{2} \right)^L \right)}{\log (\text{SNR})} \right\}}_{=0} + \lim_{\text{SNR} \rightarrow \infty} \left\{ \frac{L \log (\text{SNR})}{\log (\text{SNR})} \right\} \\
 &= L
 \end{aligned}$$

Hence, as expected, the diversity order of the L antenna system is L indicating the presence of L independently fading signal copies. How about the diversity order of a wireline communication system? Recall that the BER for communication over the wireline channel is given as $Q(\text{SNR})$, which can be approximated as $\frac{1}{2}e^{-\frac{1}{2}\text{SNR}}$ at high SNR. The diversity order of this system is, therefore, given as

$$\begin{aligned}
 d &= - \lim_{\text{SNR} \rightarrow \infty} \left\{ \frac{\log \left(\frac{1}{2} e^{-\frac{1}{2}\text{SNR}} \right)}{\log (\text{SNR})} \right\} = - \lim_{\text{SNR} \rightarrow \infty} \left\{ - \frac{\log (2)}{\log (\text{SNR})} - \frac{\frac{1}{2}\text{SNR}}{\log (\text{SNR})} \right\} \\
 &= \frac{1}{2} \lim_{\text{SNR} \rightarrow \infty} \left\{ \frac{\text{SNR}}{\log (\text{SNR})} \right\} \\
 &= \infty
 \end{aligned}$$

where the last equality follows from noting that $\lim_{x \rightarrow \infty} \frac{x}{\log(x)} = \infty$. Thus, the diversity order of the wireline channel is equal to ∞ . What does this intuitively mean? It basically suggests that the wireline AWGN channel can be thought of as comprising of an infinite number of fading links. Hence, the probability that all of them are simultaneously in a deep fade is zero, thus resulting in a perfect system not susceptible to fading. In fact, the standard wireline AWGN channel can be thought of as having a constant fading coefficient $h_{\text{AWGN}} = 1$, which can never result in a deep fade.

PROBLEMS

1. Consider a wireless signal with a carrier frequency of $f_c = 1800$ MHz, which is transmitted over a wireless channel that results in $L = 4$ multipath components at delays of

227, 463, 942, 1783 ns and corresponding to received signal amplitudes of 1, 0.8, 0.6, 0.5 respectively. Derive the expression for the received baseband signal $y_b(t)$ if the transmitted baseband signal is $s_b(t)$. Also, compute the channel coefficient h for this system for the scenario that the signal $s_b(t)$ is narrowband.

2. Consider a Rayleigh fading-channel-based wireless system such that $E\{|h|^2\} = 1$, where h is the flat-fading channel coefficient. If the transmit power P_t (dB) = 25 dB, what is the probability that the receive power is greater than 20 dB? Compute the same for a receive power of 10 dB.
3. Derive the following distributions.
 - (a) The probability density function of the magnitude $|X|$ of a complex circular symmetric Gaussian random variable X with variance σ^2 .
 - (b) Let X_1, X_2, \dots, X_n be n independent random variables each of which has an exponential density with mean μ . Let M be the minimum value of the X_j . Compute the density $f_M(m)$.
4. Employing the inequality $t^2 \geq (t - u)^2 + u^2$, prove that

$$Q(u) \leq \frac{1}{2}e^{-u^2/2}, \text{ for } u > 0$$

where $Q(u)$ is the Gaussian Q function. This is termed the *Chernoff* bound for the Q function.

5. Compute the exact bit-error rates (BER) for BPSK communication over an additive white Gaussian noise (AWGN) channel at SNRs of 15 dB, 40 dB. Also, compute the corresponding approximate BER values employing the Chernoff bound above for the Gaussian $Q(\cdot)$ function.
6. Compute the SNRs in dB required for BERs of 10^{-8} , 10^{-10} for BPSK transmission over an AWGN channel.
7. Compute the exact BERs for BPSK modulation-based communication over a Rayleigh fading wireless channel for SNRs 15 dB, 40 dB and compare these values with the corresponding BER values for the AWGN channel from Problem 5.
8. Compute the SNRs in dB required to achieve BERs 10^{-8} , 10^{-10} over the standard Rayleigh fading wireless channel, i.e., one for which $E\{|h|^2\} = 1$ for BPSK transmission and compare these with those corresponding to the AWGN channel from Problem 6.

9. In this problem, we consider a scenario of Quality of Service (QoS) in wireless communications. A wireless application across the standard Rayleigh fading wireless channel has a maximum tolerable BER of 10^{-4} as the QoS constraint. What is the minimum SNR required to support this application so as to ensure disruption-free service? Also what is the corresponding minimum SNR for a wireline AWGN channel?
10. For the estimation of a single-antenna Rayleigh fading channel, $L^{(p)} = 4$ pilot symbols $x^{(p)}(1) = (-1 + 2j)$, $x^{(p)}(2) = (-2 - j)$, $x^{(p)}(3) = (2 + j)$ and $x^{(p)}(4) = (1 - 2j)$. Let the corresponding received symbols $y^{(p)}(k)$, $1 \leq k \leq 4$ be given as $y^{(p)}(1) = (0.4154 - 1.3305j)$, $y^{(p)}(2) = (1.1974 + 0.5276j)$, $y^{(p)}(3) = (-1.2766 - 0.5172j)$ and $y^{(p)}(4) = (-0.3929 + 1.3551j)$. Compute the estimate of the flat-fading channel coefficient h .
11. Consider an $L = 3$ receive antenna wireless channel with complex fading channel coefficients $h_1 = 1 + 2j$, $h_2 = 1 + j$, $h_3 = 2 - j$. Describe the system model for the multi-antenna channel and derive the SNR with MRC.
12. Consider an $L = 2$ multi-antenna Rayleigh fading-channel-based wireless system. If the transmit power P_t (dB) = 25 dB, what is the probability that the receive power is greater than 20 dB? Compute the same for a receive power of 10 dB. Repeat this for an $L = 3$ multi-antenna Rayleigh fading channel.
13. Compute the exact BERs for BPSK modulation-based communication over a $L = 4$ multi-antenna Rayleigh fading wireless channel for SNRs 15 dB, 40 dB and compare these values with the corresponding BER values for the AWGN channel from Problem 5 and single-antenna rayleigh fading channel from Problem 7.
14. Compute the approximate SNRs in dB required to achieve BERs 10^{-8} , 10^{-10} over an $L = 4$ antenna Rayleigh fading wireless channel, i.e., one for which $E\{|h_i|^2\} = 1$, $1 \leq i \leq 4$ for BPSK transmission and compare these with those corresponding to the AWGN channel from Problem 6 and single-antenna Rayleigh fading channel from Problem 8.
15. In Section 3.10, we demonstrated that the diversity order of MRC with L independent Rx antennas is L . Consider a slightly different beamforming vector given as below.

$$\mathbf{w}_e = \begin{bmatrix} \frac{h_1}{|h_1|} \\ \frac{h_2}{|h_2|} \\ \vdots \\ \frac{h_L}{|h_L|} \end{bmatrix}$$

- (a) The above beamforming vector is termed the *equal gain combiner*. Can you explain why?
- (b) Give the expression for $\tilde{\mathbf{w}}_e$, the above beamformer normalized to have unit norm.
- (c) Employing the high SNR argument, derive the diversity order of the above system when the receive beamformer is $\tilde{\mathbf{w}}_e$.
- 16.** Similar to Problem 9, consider a scenario of Quality of Service (QoS) for the $L = 2$ multi-antenna Rayleigh fading wireless channel. A wireless application across the standard Rayleigh fading wireless channel has a maximum tolerable BER of 10^{-4} as the QoS constraint. What is the minimum SNR required to support this application so as to ensure that the BER across *at least* one of the receive antennas is greater than this threshold? Compare this with that of the required SNR for the single-antenna channel from Problem 9.
- 17. Beamforming** Consider the receive (Rx) diversity system described in the class which is given as

$$\mathbf{y}(k) = \mathbf{h}x(k) + \eta(k)$$

where $\mathbf{y}(k)$, \mathbf{h} , $\eta(k)$ are complex L -dimensional vectors and $x(k)$ is the transmitted scalar complex symbol. The signal power is $E\{|x(k)|^2\} = P$ and the noise $\eta(k)$ is AWG with covariance $E\{\eta(k)\eta(k)^H\} = \sigma_n^2\mathbf{I}$. Each entry of \mathbf{h} is IID Rayleigh with $E\{|h_i|^2\} = 1$. Consider an L -dimensional complex receive beamforming vector \mathbf{w} applied at the receiver.

- (a) For a general Rx beamformer \mathbf{w} , elucidate the signal and noise components at the receiver and give the expressions for the signal and noise powers after beamforming.
- (b) Give the step-by-step derivation of the optimal beamformer \mathbf{w}_o that maximizes the SNR at the receiver.
- (c) Consider a system in which the receive symbol vector \mathbf{y} is pre-processed by employing an $L \times L$ complex unitary matrix \mathbf{U} (i.e., $\mathbf{U}\mathbf{U}^H = \mathbf{U}^H\mathbf{U} = \mathbf{I}$) as $\tilde{\mathbf{y}} = \mathbf{U}^H\mathbf{y}$. Give the expression for the receive SNR maximizing optimal beamformer for this Rx symbol vector and justify your answer.
- 18.** Consider a multiple-input single-output (MISO) wireless system. Similar to the SIMO system discussed in Section 3.9, formulate the system model for the received signal at the receiver of an L antenna MISO system, i.e., one which has L transmit antennas and a single receive antenna. Finally, demonstrate that transmitting the same symbol $x(k)$ from all the transmit antennas yields no diversity gain.

19. Consider the estimation of the wireless channel coefficient vector of an $L = 2$ receive antenna system, with a pilot sequence consisting of $L^{(p)} = 4$ symbols. The transmitted pilot symbols are, $x^{(p)}(1) = (-1 + 2j)$, $x^{(p)}(2) = (-2 - j)$, $x^{(p)}(3) = (2 + j)$ and $x^{(p)}(4) = (1 - 2j)$. Let the corresponding received output pilot symbol vectors be given as

$$\mathbf{y}^{(p)}(1) = \begin{bmatrix} -1.3402 + 1.9184i \\ -2.4023 - 0.5275i \end{bmatrix}, \mathbf{y}^{(p)}(2) = \begin{bmatrix} -1.8083 - 1.3305i \\ 0.6931 - 2.4383i \end{bmatrix}$$

$$\mathbf{y}^{(p)}(3) = \begin{bmatrix} 1.8826 + 1.2775i \\ -0.7927 + 2.3148i \end{bmatrix}, \mathbf{y}^{(p)}(4) = \begin{bmatrix} 1.2022 - 1.8984i \\ 2.4589 + 0.5834i \end{bmatrix}$$

Compute the estimate of the channel coefficient vector $\mathbf{h} = [h_1, h_2]^T$.

20. SNR Requirements in Wireless Channels

- (a) Derive the exact dB difference between the SNR required to achieve a $P_e = 10^{-2}$ for BPSK in an AWGN channel and that of a Rayleigh fading wireless channel with no Rx diversity.
- (b) Consider an Rx diversity system with $L = 30$ receive antennas. Let the system be a normalized one in which the average receiver SNR equals the transmit SNR. What does that mean? **Without** using the high SNR P_e approximation (i.e., $\left(\frac{1}{SNR}\right)^L$), but some other **intelligent** approximation, compute the P_e for this system for BPSK transmission at SNR = 3 dB.
- (c) What is the approximate P_e for the same system above, but un-normalized (i.e., $E\{|h_i|^2\} = 1$). Again, do **NOT** use the high SNR approximation of $\left(\frac{1}{SNR}\right)^L$.
21. Consider a scheme that transmits the vector $\mathbf{x} = \mathbf{R}[u_1, u_2]^T$, over two symbol times, where \mathbf{R} is the standard rotation matrix parameterized by $\theta = 30^\circ$ and u_1, u_2 are independent BPSK symbols, each of 15 dB energy. Assume the scenario is fast fading, so that the channel coefficients for these two symbol times are independent. This is an instance of time diversity. Let the noise power be $\sigma_n^2 = \frac{N_0}{2} = 3$ dB. Systematically, derive the probability of error for this system.
22. Consider the use of a differential BPSK scheme for the Rayleigh flat-fading channel in which the transmitted symbol $x(k) = u(k)x(k-1)$, where each $u(k)$ is BPSK ± 1 . Let the initial transmitted symbol $x(0)$ be \sqrt{P} .

- (a) Find a natural noncoherent scheme to detect $u[m]$ based on $y[m-1]$ and $y[m]$, assuming the channel is constant across the two symbol times. Your scheme does not have to be the ML detector.
- (b) Analyze the performance of your detector at high SNR. You may need to make some approximations.
- (c) What is the ideal coherent detector and how does the high SNR performance of your detector compare to that of the coherent detector?
- (d) Does coherent or noncoherent detection affect the diversity order of the system?

23. BER in Fading Channels

- (a) Extend the principle of noncoherent detection proposed for differential BPSK modulated data in Problem 22 to a receiver with L receive antennas, i.e., outline the detector operation and compute the SNR at the output.
- (b) What is the diversity order of this system? Derive an approximate expression for the BER of this system at high SNR (P/σ_n^2). Assume the channels across receive antennas to be independent Rayleigh fading channels of average power unity.
- (c) Compute the approximate BER at SNR = 25 dB with an array of $L = 3$ receive antennas at the receiver.

24. Answer the questions that follow:

- (a) Derive the exact dB difference between the SNR required to achieve $P_e = 5 \times 10^{-3}$ for BPSK in an AWGN channel and that of a Rayleigh fading wireless channel with no Rx diversity.
- (b) Derive the dB difference between the SNR required to achieve $P_e = 5 \times 10^{-3}$ for BPSK in an AWGN channel with 2 Rx antennas and that of a Rayleigh fading wireless channel with 2 Rx antennas. You can use the approximation for BER developed in the class for the diversity system.
- (c) What is the SNR required to achieve $P_e = 5 \times 10^{-3}$ for BPSK in a Rayleigh fading wireless channel with 30 Rx antennas.

25. Diversity Coding Consider a scheme that transmits the vector $\mathbf{x} = \mathbf{R}\mathbf{u}$, over two symbol times, where the vector \mathbf{u} and the matrix \mathbf{R} are

$$\mathbf{u} = \begin{bmatrix} u_1 \\ u_2 \end{bmatrix}, \quad \mathbf{R} = \begin{bmatrix} 1 & \frac{1}{2} \\ 1 & \frac{1}{2} \end{bmatrix}$$

and u_1, u_2 are BPSK symbols, each of power P . Assume the scenario is fast fading, so that the channel coefficients for these two symbol times are independent. This is an instance of time diversity. Let the noise power be σ_n^2 .

(a) Derive the *confusion* probability $P_{\mathbf{x}_A \rightarrow \mathbf{x}_B}$, where $\mathbf{x}_A, \mathbf{x}_B$ are defined as (1.0)

$$\mathbf{x}_A = \begin{bmatrix} \sqrt{P} \\ \sqrt{P} \end{bmatrix}, \quad \mathbf{x}_B = \begin{bmatrix} -\sqrt{P} \\ \sqrt{P} \end{bmatrix}$$

(b) Employing an *appropriate* bound, systematically derive the probability of error for this system.

(c) Compute this probability of error for $P = 30$ dB and $\sigma_n^2 = 3$ dB.

26. The signal constellation for MPSK has $s_{i1} = \sqrt{P} \cos \left[\frac{2\pi(i-1)}{M} \right]$ and $s_{i2} = \sqrt{P} \sin \left[\frac{2\pi(i-1)}{M} \right]$ for $i = 1, \dots, M$. The symbol energy is $E_s = P$ and noise power is σ^2 . Consider $M = 16$ and answer the questions below.

(a) Find the expression for probability of symbol error P_e for this constellation in an AWGN channel as a function of $\text{SNR} = \frac{P}{\sigma^2}$.

(b) Compute the above AWGN P_e for $\text{SNR} = 25$ dB.

(c) Find an expression for the average probability of symbol error $P_{e,R}$ in a Rayleigh fading channel with $E \{ |h|^2 \} = 1$ as a function of SNR .

(d) Compute the above Rayleigh error rate $P_{e,R}$ at $\text{SNR} = 45$ dB.

(e) Derive, as a function of SNR , the average probability of symbol error $P_{e,MRC}$ with 2 receive antennas and MRC combining with each Rayleigh coefficient of average power unity.

(f) Compute the above MRC error rate $P_{e,MRC}$ at $\text{SNR} = 30$ dB.

27. Consider detecting the transmit vector \mathbf{u} equally likely to be $\mathbf{u}_A = \sqrt{P}[1, 1, 1, 1]^T$ or $\mathbf{u}_B = \sqrt{P}[1, -1, 1, -1]^T$, where $P = 40$ dB. The received vector is

$$\mathbf{y} = h\mathbf{u} + \mathbf{w}$$

and $\mathbf{w} \sim \mathcal{N}(0, 2\mathbf{I})$ and h is Rayleigh with $\mathbb{E}\{|h|^2\} = 5$. Derive the average probability of error for this system.

- 28. The Moment-Generating Function (MGF)** for a non-negative random variable γ with pdf $p_\gamma(\gamma)$, $\gamma \geq 0$, is defined as

$$\mathcal{M}_\gamma(s) = \int_0^\infty p_\gamma(\gamma) e^{s\gamma} d\gamma$$

- (a) Demonstrate that the moment-generating function of the Rayleigh random channel with distribution $\frac{1}{\gamma_s} e^{-\frac{\gamma}{\gamma_s}}$ is,

$$\mathcal{M}_\gamma(s) = (1 - s\overline{\gamma_s})^{-1}.$$

- (b) Derive the average BER for BPSK transmission over the Rayleigh channel employing the moment-generating function approach. For this, you can use the alternative definition of the Q-function, $Q(x) = \frac{1}{\pi} \int_0^{\frac{\pi}{2}} \exp\left(-\frac{x^2}{2\sin^2\theta}\right) d\theta$.

- 29.** Consider an $L = 2$ receive antenna system with instantaneous channel coefficients $h_1 = 2 - j$, $h_2 = 1 + 2j$ and BPSK modulation. Answer the questions that follow.

- (a) Assuming optimal combining, compute the transmit SNR required to achieve an **instantaneous** BER of 5×10^{-5} .
- (b) If the fading coefficients are Rayleigh with average power $\mathbb{E}\{|h_i|^2\} = 3$, compute the transmit SNR required to achieve **average** BER 5×10^{-5} with optimal combining.
- (c) Considering the receiver employs sub-optimal average combining, i.e., $\frac{1}{2}(y_1 + y_2)$, compute the transmit SNR required to achieve an **instantaneous** BER of 5×10^{-5} ?
- (d) Considering the receiver employs sub-optimal *mean* combining, i.e., $\frac{1}{2}(y_1 + y_2)$ and that the fading coefficients are Rayleigh with average power $\mathbb{E}\{|h_i|^2\} = 3$, compute the transmit SNR required to achieve an **average** BER of 5×10^{-5} .

- 30.** Compute the dB transmit SNR required to achieve $P_e = 5 \times 10^{-4}$ for 8-PSK in an AWGN channel and for a Rayleigh fading wireless channel with no Rx diversity.

- 31.** Consider a version of the repetition code in which the transmitted symbol is $x(m) = \sqrt{m}u$, where u is the BPSK symbol $\pm\sqrt{P}$ for $1 \leq m \leq L$. The received symbol $y(m) = h(m)x(m) + n(m)$, where $n(m)$ is AWGN of variance σ^2 and $h(m)$ is a Rayleigh fading coefficient. Assume $\mathbb{E}\{|h(m)|^2\} = 1$ and answer the questions that follow.

- (a) If the fading coefficient is constant over the L instants, i.e., $h(m) = h$ for $1 \leq m \leq L$, derive the average BER.
- (b) If the fading coefficients are uncorrelated over the L instants, derive the average BER employing a suitable approximation.
32. The signal constellation for M -ary PAM is of the form $\pm(2k+1)\Delta$, for $0 \leq k \leq \frac{M}{2} - 1$, where M is an even number. Consider $M = 8$ and assume equal probability for transmission of each symbol to answer the questions that follow.
- (a) Express the average symbol power \bar{P} for the 8-ary PAM constellation above as a function of Δ .
- (b) Find the expression for the symbol error rate over an AWGN channel for the 8-ary constellation above as a function of the average symbol power \bar{P} and noise power σ^2 .
- (c) Find the average power \bar{P} required to achieve a probability of symbol error 10^{-6} in an AWGN channel with noise power $\sigma^2 = -3$ dB.
- (d) Find the expression for symbol error rate over a Rayleigh fading channel for the above 8-ary PAM constellation as a function of the average symbol power \bar{P} , average Rayleigh fading channel gain $E\{|h|^2\} = \rho$ and noise power σ^2 .
- (e) Find the average power \bar{P} required to achieve probability of symbol error 10^{-6} over a Rayleigh fading channel with noise power $\sigma^2 = -3$ dB and Rayleigh fading coefficient h with $E\{|h|^2\} = 2$.
33. Consider the multiple antenna system $\bar{y} = \bar{h}x + \bar{n}$, with L receive antennas and **non-identical** independent noise samples n_i with variance $E\{|n_i|^2\} = \sigma_i^2$, $1 \leq i \leq L$. Consider the beamformer \bar{w} and for this problem only to simplify things consider all quantities to be **real**.
- (a) Describe the covariance matrix \mathbf{R} of the noise vector \bar{n} .
- (b) What is the noise power at the output as a function of the beamformer \bar{w} and noise covariance matrix \mathbf{R} ?
- (c) Derive the noise power for the above scenarios as a function of the beamformer entries w_i , $1 \leq i \leq L$ and the various σ_i^2 .
- (d) What happens to the SNR when the beamformer \bar{w} is scaled by a constant K ?
- (e) Formulate the optimization problem to minimize the noise power while constraining the gain of the signal to be unity.
- (f) Formulate the Lagrangian for the above optimization problem.

- (g) Derive the optimal beamformer for the above scenario.
- (h) Compute the SNR for the optimal beamformer derived above.
34. Consider an L receive antenna version of the repetition code in which the transmitted symbol is $x(m) = \sqrt{m}u$, where u is the BPSK symbol $\pm\sqrt{P}$ for $1 \leq m \leq M$. The received symbol $y_l(m) = h_l(m)x(m) + n_l(m)$, where $n_l(m)$ is IID (across antennas and time) AWGN of variance σ^2 and $h_l(m)$ is the Rayleigh fading coefficient for the l^{th} receive antenna, $1 \leq l \leq L$ at the m^{th} time instant. Assume $E\{|h_l(m)|^2\} = 1$ and answer the questions below.
- (a) If the fading coefficient is constant over the M instants and L antennas, i.e., $h_i(m) = h$ for $1 \leq m \leq M, 1 \leq i \leq L$, derive the **exact** average BER.
- (b) If the fading coefficients are uncorrelated over the M time instants but constant across the L antennas, derive the average BER employing a suitable **approximation**.
- (c) If the fading coefficients are constant over the M time instants but uncorrelated across the L antennas, derive the **exact** average BER.
- (d) If the fading coefficients are uncorrelated over the M time instants as well as the L antennas, derive the average BER employing a suitable **approximation**.
35. Consider a single-input multiple-output (SIMO) system with L antennas and channel vector $\mathbf{h} = [h_1, h_2, \dots, h_L]^T$ with channel covariance matrix $\mathbf{R} = E\{\mathbf{h}\mathbf{h}^H\}$ and Rayleigh fading coefficients. Let P denote the transmitted BPSK symbol power and σ^2 denote the noise power at each receive antenna. Further, consider the noise samples across the receive antennas to be i.i.d. zero-mean symmetric complex Gaussian. Answer the questions that follow.
- (a) What is the SNR with maximum ratio combining (MRC) at the receiver?
- (b) Consider the coefficients h_i to be i.i.d. with average power unity. What is the channel covariance matrix \mathbf{R}_{iid} ?
- (c) For the above channel covariance matrix \mathbf{R}_{iid} , derive the probability of deep fade and the associated diversity order with MRC.
- (d) Now consider the case where the channel coefficients h_i are correlated. Let the channel covariance matrix $\mathbf{R}_c = \mathbf{U}\mathbf{\Lambda}\mathbf{U}^H$, where $\mathbf{\Lambda}$ is the diagonal matrix containing the eigenvalues $\lambda_i, 1 \leq i \leq L$. What are the properties \mathbf{U} and λ_i satisfy?
- (e) For the above system with channel covariance matrix \mathbf{R}_c , derive a bound on the probability of deep fade and the associated **maximum** possible diversity order. When is this achieved?

- (f) For channel covariance matrix \mathbf{R}_c , when is the diversity order strictly less than the maximum possible value?
- (g) Consider now a channel covariance matrix $\mathbf{R}_s = \overline{\mathbf{1}}\overline{\mathbf{1}}^T$, where $\overline{\mathbf{1}}$ is the L dimensional column vector of all ones. What is the rank and what are the eigenvalues of this channel covariance matrix?
- (h) What is the probability of deep fade in the system with MRC and channel covariance matrix \mathbf{R}_s ?
- (i) What the BER for BPSK transmission in the system with MRC and channel covariance matrix \mathbf{R}_s ?
- (j) What is the associated diversity order for the system with MRC and channel covariance matrix \mathbf{R}_s ?
- 36.** Consider an $N = 2$ user multi-user system with 2 antennas at the receiver and a single transmit antenna for each of the users. Therefore, the system model is given as $\mathbf{y} = \mathbf{h}_1x_1 + \mathbf{h}_2x_2 + \eta$, where $\mathbf{h}_1 = [1, 2]^T$ and $\mathbf{h}_2 = [2, 1]^T$. Using the concepts illustrated in class, find the optimal beamformer \mathbf{w}_1 to decode the symbol corresponding to the user 1 and derive the instantaneous SNR. Assume η is AWGN with each entry IID of variance σ_n^2 . What is the dB loss of SNR compared to MRC with single user.
- 37.** Consider a $2N$ multiple antenna system. Let us call antennas $2i - 1, 2i$ for $1 \leq i \leq N$ as an antenna pair. For receive processing, we use the following scheme. Out of the N antenna pairs, we choose the antenna pair which yields the maximum MRC gain and use this antenna pair for receive processing. Using a deep-fade argument, derive the diversity order of this scheme.

The Wireless Channel

4.1 Basics of Wireless Channel Modelling

As we had seen in the previous chapter, the fading wireless channel comprises several *multipath* components arising from the presence of multiple *Non-Line-Of-Sight* (NLOS) Signal-propagation paths. These NLOS components arise from the scattering effects of objects in the wireless environment such as buildings, trees, vehicles, water bodies, etc. In this chapter, we aim to develop a systemic framework to study the nature of the wireless channel, especially with respect to key properties such as inter-symbol interference and, time-varying characteristics amongst others.

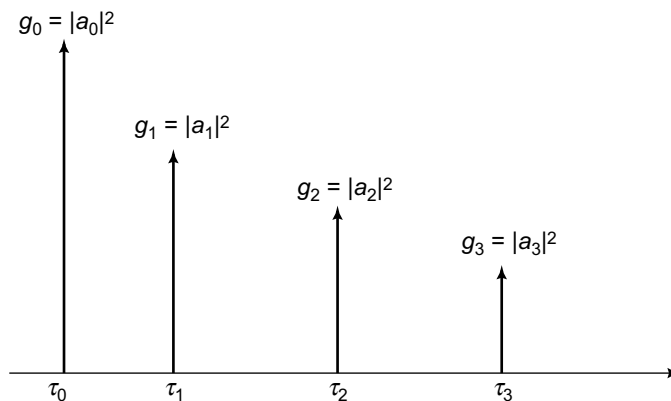


Figure 4.1 Schematic of an $L = 4$ tap wireless channel profile

Recall that the impulse response of the standard multipath wireless channel can be modelled as,

$$h(t) = \sum_{i=0}^{L-1} a_i \delta(t - \tau_i)$$

where each $\delta(t - \tau_i)$ corresponds to delaying the signal by τ_i , and a_i is the attenuation associated with the i^{th} path. The quantity L denotes the number of paths or multipath components. From the above impulse response, one can define the multipath power profile of the multipath channel as

$$\begin{aligned} \phi(t) &= \sum_{i=0}^{L-1} |a_i|^2 \delta(t - \tau_i) \\ &= \sum_{i=0}^{L-1} g_i \delta(t - \tau_i) \end{aligned} \quad (4.1)$$

where $g_i = |a_i|^2$ is the power gain of the i^{th} path. For instance, consider an $L = 4$ path multipath channel. The gains and the corresponding delays of the paths of this multipath channel can be listed as given in Table 4.1, and this is schematically shown in Figure 4.1. Thus, one can readily observe that the total energy corresponding to the transmitted wireless signal is received in increments at the receiver, with a part of it arriving in each multipath component. For instance, power with gain g_0 is received after a delay of τ_0 , while a gain of g_1 is received after a delay τ_1 , and so on, till the last path arriving at a delay of τ_{L-1} delivers power with a gain of g_{L-1} .

Thus, the total power received in a multipath wireless channel occurs over a *spread* of time referred to as the **delay spread**.

This spread of the arriving power at the wireless receiver is schematically shown in Figure 4.2. Observe that this property of the wireless channel is in contrast to that of a wireline channel, in which all the power is received at a single time instant due to the presence of only a single propagation path. The delay spread of a wireless channel is a key parameter that characterizes the nature of the wireless environment and is denoted by the parameter σ_τ . We describe the procedure for computation of the delay-spread parameter σ_τ of a wireless channel next.

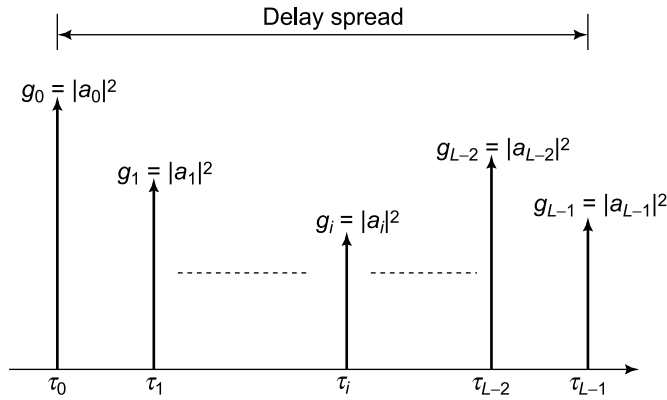


Figure 4.2 Schematic of a typical wireless channel power profile and delay spread

Table 4.1 Path gains and associated delays for an $L = 4$ multipath channel

Gain	Delay
$ a_0 ^2$	τ_0
$ a_1 ^2$	τ_1
$ a_2 ^2$	τ_2
$ a_3 ^2$	τ_3

4.1.1 Maximum Delay Spread σ_τ^{\max}

A framework to quantify the delay spread of a wireless channel is through the maximum delay spread of the channel denoted by σ_τ^{\max} . Consider a wireless channel with L multipath components, with the first path arriving at a delay of τ_0 and the last signal copy arriving at τ_{L-1} . The maximum delay spread is simply defined as

$$\sigma_\tau^{\max} = \tau_{L-1} - \tau_0 \tag{4.2}$$

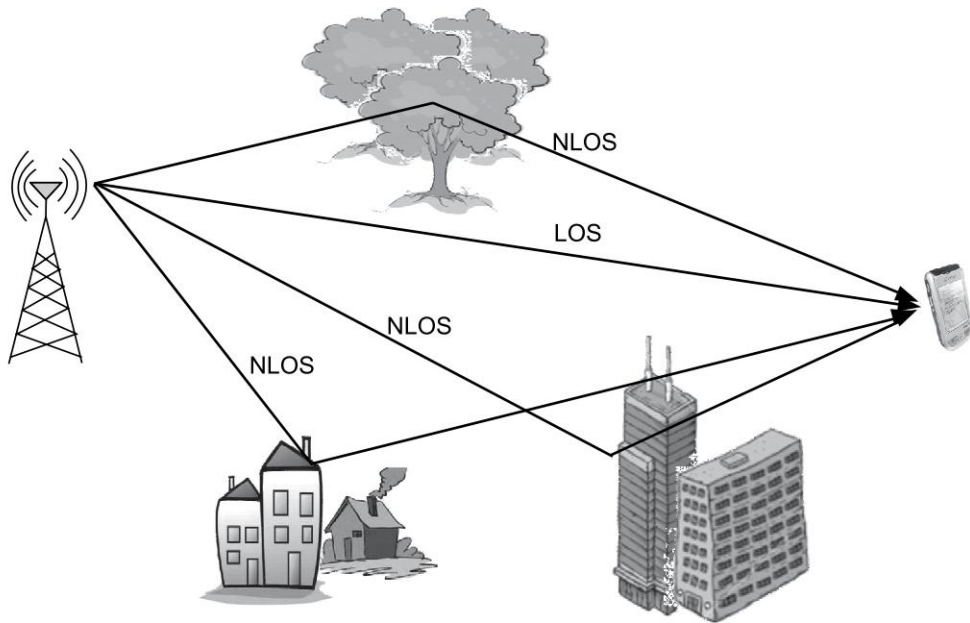


Figure 4.3 *Schematic of the wireless-propagation environment*

or, in other words, the time interval between the arrival of the first and last signal copies at the receiver. This is a simple measure of the spread of the energy in the wireless channel, while effectively capturing the multipath signal arrival. It can be readily seen that a larger value of σ_{τ}^{\max} naturally implies a richer scatter environment and larger differential propagation delays between the paths. Further, observe the key property that the delay spread does NOT depend on the absolute delays τ_0, τ_{L-1} , but the difference $\tau_{L-1} - \tau_0$. Thus, the distance of the mobile-receiver node from the base station has no impact on the delay spread, which leads to a larger propagation delay. For instance, consider a scenario where there is a single propagation path, corresponding to a large delay τ_0 for a mobile at a large distance from the base station. Since there is only a single path in this case, the first and last components correspond to the single component arriving at a delay of τ_0 . Hence, the corresponding delay spread is $\tau_0 - \tau_0 = 0$. Thus, the delay spread indeed depends critically on the presence of multipath components and the richness of the scatter environment, which basically affects the total number of multipath scatter-signal components arriving at the receiver.

EXAMPLE 4.1

Consider an $L = 4$ multipath channel with the delays τ_0, τ_{L-1} corresponding to the first and last arriving paths, given as $\tau_0 = 0 \mu\text{s}$ and $\tau_{L-1} = 5 \mu\text{s}$. Such a wireless-channel power profile is shown schematically in Figure 4.4. What is the maximum delay spread σ_τ^{max} corresponding to this wireless channel?

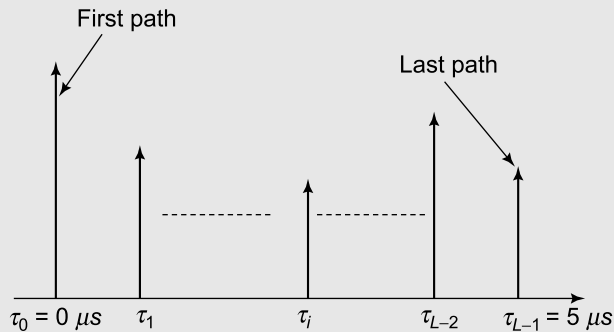


Figure 4.4 Power profile for Example 4.1.

Solution: By a simple application of the result in Eq. (4.2) for L multipath components, it can be seen that the maximum delay spread is

$$\sigma_\tau^{\text{max}} = 5 \mu\text{s} - 0 \mu\text{s} = 5 \mu\text{s}$$

4.1.2 RMS Delay Spread σ_τ^{RMS}

In typical wireless channels, the paths which arrive later are significantly lower in power due to the larger propagation distances and weaker reflections as shown in Figure 4.5. This results in a large value of the maximum delay spread σ_τ^{max} even though several of the later paths comprise weak scatter components with negligible power. Thus, the maximum delay spread metric is not a reliable indicator of the true power spread of the arriving multipath signal components in such scenarios, since it does not weight the delays in proportion to the signal power in the multipath components. For this purpose, the RMS delay spread is a more realistic indicator of the spread of the signal power in the arriving components. Further, since it weights the delays

of the signal components with respect to the power in the arriving paths, it is not susceptible to distortion in scenarios with a large number of trailing weak components, unlike the maximum delay spread.

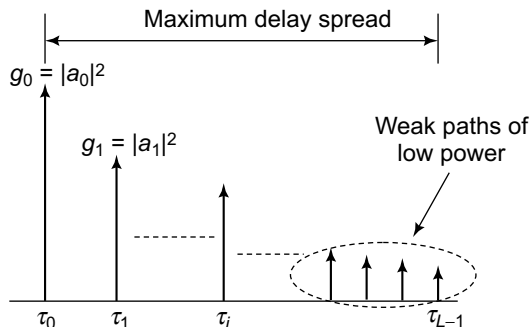


Figure 4.5 Power profile with weak trailing paths of very low power

Consider the power profile comprising of L multipath components defined in Eq. (4.1), with $g_i = |a_i|^2$, $0 \leq i \leq L - 1$ denoting the power gain of each multipath component. We define a new quantity b_i as

$$b_i = \frac{g_i}{g_0 + g_1 + \dots + g_{L-1}},$$

where g_i denotes the total power corresponding to the i^{th} path, while $g_0 + g_1 + \dots + g_{L-1}$ denotes the total power in the multipath power profile. Thus, the ratio b_i denotes the *fraction* of power in the i^{th} multipath component. One can now conveniently employ this quantity b_i proportionally with the multipath delay components. Observe now that the various b_i define a power distribution for the above multipath power profile since each $b_i > 0$ and $b_0 + b_1 + \dots + b_{L-1} = 1$. Therefore, the average delay $\bar{\tau}$ can be computed to the mean of the above power distribution as

$$\begin{aligned} \bar{\tau} &= b_0\tau_0 + b_1\tau_1 + \dots + b_{L-1}\tau_{L-1} = \sum_{i=0}^{L-1} b_i\tau_i \\ &= \sum_{i=0}^{L-1} \frac{g_i}{\sum_{j=0}^{L-1} g_j} \tau_i \\ &= \frac{\sum_{i=0}^{L-1} g_i\tau_i}{\sum_{j=0}^{L-1} g_j} \end{aligned}$$

It can be seen that the average delay $\bar{\tau}$ is obtained by weighing each delay τ in proportion to the fraction of the power b_i . Finally, the RMS delay spread $\sigma_{\tau}^{\text{RMS}}$ can be computed as the *standard deviation* of the power distribution, which is defined as

$$\begin{aligned} (\sigma_{\tau}^{\text{RMS}})^2 &= b_0 (\tau_0 - \bar{\tau})^2 + b_1 (\tau_1 - \bar{\tau})^2 + \dots + b_{L-1} (\tau_{L-1} - \bar{\tau})^2 \\ &= \sum_{i=0}^{L-1} b_i (\tau_i - \bar{\tau})^2 \\ \sigma_{\tau}^{\text{RMS}} &= \sqrt{\frac{\sum_{i=0}^{L-1} g_i (\tau_i - \bar{\tau})^2}{\sum_{i=0}^{L-1} g_i}} \end{aligned} \quad (4.3)$$

$$= \sqrt{\frac{\sum_{i=0}^{L-1} |a_i|^2 (\tau_i - \bar{\tau})^2}{\sum_{i=0}^{L-1} |a_i|^2}} \quad (4.4)$$

Thus, the RMS metric to characterize the delay spread defined above is not sensitive to spurious multipath components of weak signal power since it weights each delay in proportion to its power, thereby automatically suppressing the contribution of weaker paths.

EXAMPLE 4.2

Consider the multipath power profile of a wireless channel shown in Figure 4.6 comprising $L = 4$ multipath components. Compute the RMS delay spread $\sigma_{\tau}^{\text{RMS}}$ for this wireless channel.

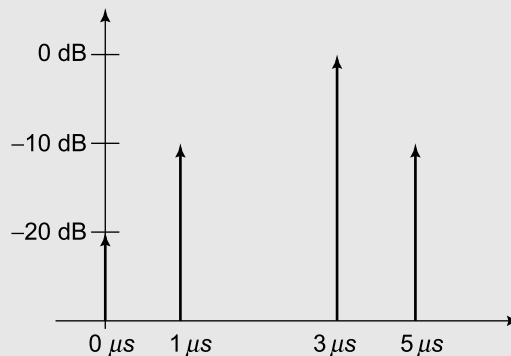


Figure 4.6 Power profile for Example 4.2

Solution: Consider the first path corresponding to $\tau_0 = 0 \mu s$. The power associated with this path is g (dB) = -20 dB. Hence, the linear power can be obtained as

$$\begin{aligned} 10 \log_{10} g_0 &= -20 \text{ dB} \\ \Rightarrow \log_{10} g_0 &= -2 \\ \Rightarrow g_0 &= 10^{-2} = 0.01 \end{aligned}$$

Also, the amplitude a_0 associated with this path can be derived as

$$a_0 = \sqrt{g_0} = 0.1$$

Thus, one can compute the corresponding power g_i and amplitude a_i for each of the $L = 4$ multipath components corresponding to $0 \leq i \leq 3$. These are listed in Table 4.2.

Table 4.2 Table of gains for Example 4.22

τ	dB Gain	g	$a = \sqrt{g}$
$0 \mu s$	-20 dB	0.01	0.1
$1 \mu s$	-10 dB	0.1	0.3162
$3 \mu s$	0 dB	1	1
$5 \mu s$	-10 dB	0.1	0.3162

One can now compute the mean delay $\bar{\tau}$ for this channel as

$$\begin{aligned} \bar{\tau} &= \frac{\sum_{i=1}^{L-1} g_i \tau_i}{\sum_{i=0}^{L-1} g_i} \\ &= \frac{0.01 \times 0 + 0.1 \times 1 + 1 \times 3 + 0.1 \times 5}{0.01 + 0.1 + 1 + 0.1} \mu s \\ &= 2.9752 \mu s \end{aligned}$$

Thus, the mean delay is $\bar{\tau} = 2.9752 \mu s$. Employing the expression in Eq. (4.3), the RMS delay spread can be computed as

$$\begin{aligned}\sigma_{\tau}^{\text{RMS}} &= \frac{0.01 \times (0 - 2.9752)^2 + 0.1 \times (1 - 2.9752)^2 + 1 \times (3 - 2.9752)^2 + 0.1 \times (5 - 2.9752)^2}{0.01 + 0.1 + 1 + 0.1} \\ &= 0.8573 \mu\text{s}\end{aligned}$$

It can be seen that the RMS delay spread is $0.8573 \mu\text{s}$, which is much more realistic compared to the maximum delay spread $\sigma_{\tau}^{\text{max}} = 5 \mu\text{s}$. This is because the initial path at $0 \mu\text{s}$ is of a significantly smaller power of -20 dB compared to the rest of the components. Since the RMS delay spread weighs each delay by the appropriate power, it is not susceptible to this distortion.

4.1.3 RMS Delay Based on Average Power Profile

In this section, we will look at generalizing the delay spread metric to a continuous average power profile. Consider the instantaneous power $|h(\tau)|^2$ corresponding to the delay τ . The average power associated with this delay can be defined as

$$\phi(\tau) = \text{E} \left\{ |h(\tau)|^2 \right\}$$

The above quantity $\phi(\tau)$ can be thought of as the average power associated with the delay τ at various instants of time. It can also be thought of as the power at delay τ for the wireless channels of different users in an area. The former is averaging over time, while the latter represents an averaging over the *ensemble* of channels. Similar to the framework in the previous section, one can define the fractional power associated with the delay τ as

$$f(\tau) = \frac{\phi(\tau)}{\int_0^{\infty} \phi(\tau) d\tau}$$

where $f(\tau)$ denotes the *power distribution density* corresponding to the delay τ , i.e., $f(\tau) \Delta\tau$ is the fraction of power in a delay interval of $\Delta\tau$ around τ . The average $\bar{\tau}$ can, therefore, be defined as

$$\bar{\tau} = \int_0^{\infty} \tau f(\tau) d\tau = \frac{\int_0^{\infty} \tau \phi(\tau) d\tau}{\int_0^{\infty} \phi(\tau) d\tau}$$

Finally, the RMS delay spread for the above power profile $\phi(\tau)$ is defined as

$$\begin{aligned}\sigma_{\tau}^{\text{RMS}} &= \sqrt{\int_0^{\infty} (\tau - \bar{\tau})^2 f(\tau) d\tau} \\ &= \sqrt{\frac{\int_0^{\infty} (\tau - \bar{\tau})^2 \phi(\tau) d\tau}{\int_0^{\infty} \phi(\tau) d\tau}}\end{aligned}$$

We illustrate the above concept of RMS delay spread for an average power profile below.

EXAMPLE 4.3

Consider the average power profile $\phi(\tau) = \alpha e^{-\tau/\beta}$, where $\alpha = 3$ dB, $\beta = 1$ μ s. Compute the RMS delay spread $\sigma_{\tau}^{\text{RMS}}$ for this profile which is schematically shown in Figure 4.7.

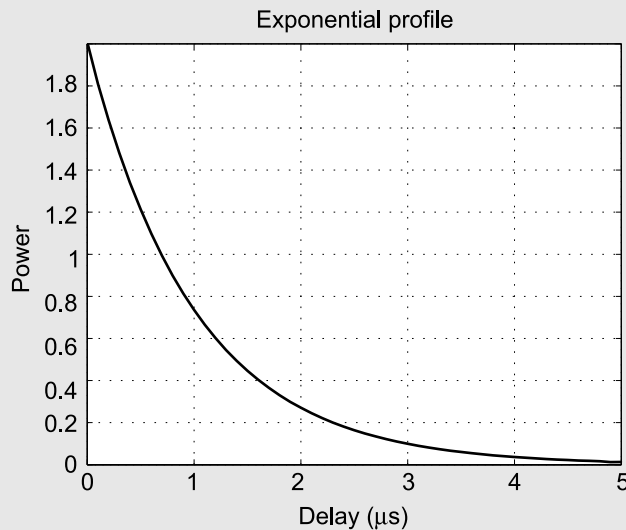


Figure 4.7: Power profile for Example 4.3

Solution: Firstly, given that α (dB) = 3 dB. Hence, we have $\alpha = 2$. Therefore, $\phi(\tau) = 2e^{-\tau/\beta}$. To compute the normalized delay profile $f(\tau)$, the normalization factor can be

computed as

$$\begin{aligned}\int_0^{\infty} \phi(\tau) d\tau &= \int_0^{\infty} 2e^{-\tau/\beta} d\tau \\ &= 2\beta e^{-\tau/\beta} \Big|_0^{\infty} \\ &= 2\beta\end{aligned}$$

Hence, the fractional power profile $f(\tau)$ can be obtained as

$$f(\tau) = \frac{2e^{-\tau/\beta}}{2\beta} = \frac{1}{\beta} e^{-\tau/\beta}$$

The average delay $\bar{\tau}$ is given as

$$\begin{aligned}\bar{\tau} &= \int_0^{\infty} \tau f(\tau) d\tau \\ &= \int_0^{\infty} \frac{\tau}{\beta} e^{-\tau/\beta} d\tau \\ &= \tau e^{-\tau/\beta} \Big|_0^{\infty} + \int_0^{\infty} e^{-\tau/\beta} d\tau \\ &= \beta e^{-\tau/\beta} \Big|_0^{\infty} \\ &= \beta = 1 \mu s\end{aligned}\tag{1}$$

where the equality in Step (1) follows from the standard *integration-by-parts* procedure. Therefore, the mean delay spread $\bar{\tau} = \beta = 1 \mu s$. To compute the RMS delay spread $\sigma_{\tau}^{\text{RMS}}$, we begin with the computation of $E\{\tau^2\}$ defined as

$$\begin{aligned}E\{\tau^2\} &= \int_0^{\infty} \tau^2 f(\tau) d\tau \\ &= \int_0^{\infty} \frac{\tau^2}{\beta} e^{-\tau/\beta} d\tau\end{aligned}\tag{2}$$

$$\begin{aligned}
&= \tau^2 e^{-\tau/\beta} \Big|_0^\infty + \int_0^\infty 2\tau e^{-\tau/\beta} d\tau \quad (3) \\
&= 2\beta\tau e^{-\tau/\beta} \Big|_0^\infty + \int_0^\infty 2\beta e^{-\tau/\beta} d\tau \\
&= 2\beta^2 e^{-\tau/\beta} \Big|_0^\infty = 2\beta^2
\end{aligned}$$

where equalities (2) and (3) follow again from integration by parts. It can then be shown that

$$\begin{aligned}
\sigma_\tau^{\text{RMS}} &= \sqrt{\text{E}\{\tau^2\} - \bar{\tau}^2} \\
&= \sqrt{2\beta^2 - \beta^2} \\
&= \beta = 1 \mu\text{s}.
\end{aligned}$$

Therefore, the RMS delay spread σ_τ^{RMS} for the above average power profile $\alpha e^{-\tau/\beta}$ can be computed as $\sigma_\tau^{\text{RMS}} = 1 \mu\text{s}$.

4.2 | Average Delay Spread in Outdoor Cellular Channels

Consider an outdoor cellular wireless communication scenario. The cell radii of typical cells are in the range of 1–5 km, i.e., outdoor wireless signal-propagation distances are of the order of a few kilometres. Consider two paths illustrated in Figure 4.8, where the direct and scatter distances are given as $d_0 = 2$ km, $d_1 = 3$ km respectively. Hence, the propagation delays τ_0 , τ_1 are given as

$$\tau_0 = \frac{2 \text{ km}}{c}, \quad \tau_1 = \frac{3 \text{ km}}{c},$$

where $c = 3 \times 10^8$ m/s. Hence, the delay spread in this case is given as

$$\begin{aligned}
\sigma_\tau^{\text{max}} &= \Delta\tau \\
&= \tau_1 - \tau_0
\end{aligned}$$

$$\begin{aligned}
 &= \frac{\Delta d}{c} \\
 &= \frac{3000 \text{ m} - 2000 \text{ m}}{3 \times 10^8} \\
 &= 3.33 \mu\text{s}
 \end{aligned}$$

The above calculation is not an exact calculation of the outdoor delay spread. However, it demonstrates that in typical outdoor cellular scenarios, where the distances and signal-propagation paths are of the orders of kilometres, the delay spreads are of the order of 1–3 μs . This value is of great importance in the design and analysis of practical wireless-communication systems. Also, similarly, corresponding to indoor distances of around 10 m, typical *indoor delay spreads* are of the order of 10–50 ns. We wish to again emphasize that these are not *exact* values and rather the approximate order of these quantities, which are helpful to know towards practical design of 3G/4G wireless-communication systems.

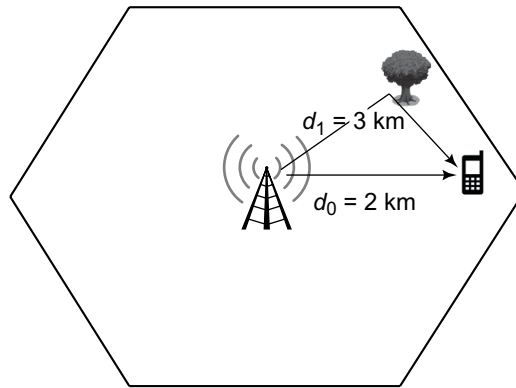


Figure 4.8 Typical delay spread in outdoor cellular channels

4.3 | Coherence Bandwidth in Wireless Communications

In this section, we introduce another important parameter of a wireless communication channel, namely, the *coherence bandwidth* B_c . Towards this end, let us define the frequency response $H(f)$ of the wireless channel as

$$H(f) = \int_0^{\infty} h(\tau) e^{-j2\pi f\tau} d\tau$$

We wish to understand the relation between these two fundamental quantities, i.e., the delay spread σ_τ and coherence bandwidth B_c of the wireless channel. Let us begin by considering a simple case corresponding to $\sigma_\tau = 0$, shown in Figure 4.13(a). In this scenario, since the delay spread is zero, the wireless channel comprises a single propagation path. Hence, the delay profile $h(\tau)$ is given as

$$h(\tau) = \delta(\tau).$$

The corresponding frequency response $H(f)$ is given as

$$H(f) = \int_0^\infty a_0 \delta(\tau) e^{-j2\pi f\tau} d\tau = 1$$

Thus, the frequency response is the constant 1 and $|H(f)| = 1$. This is basically a *flat* frequency response over the entire frequency band as shown in Figure 4.13(b), i.e., of infinite bandwidth.

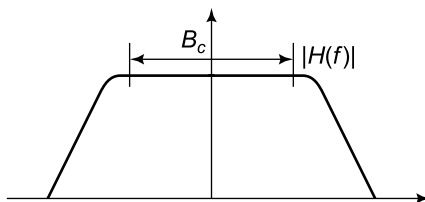


Figure 4.9 Coherence bandwidth of wireless-channel response

As the delay spread σ_τ increases in Figure 4.13(c), the time spread of this response increases, leading to a decrease in the bandwidth of the response $H(f)$ as shown in Figure 4.13(d). Finally, as the time spread of the response becomes ∞ as shown in Figure 4.13(e), the channel filter becomes an impulse $\delta(f)$ as shown in Figure 4.13(f) and the bandwidth of the channel filter reduces to 0. The coherence bandwidth B_c is then defined as the bandwidth of the response $H(f)$, i.e., the frequency band over which the response $H(f)$ is flat as shown in Figure 4.9. What is the significance of this quantity B_c ? This can be understood as follows. Consider any signal $x(t)$ transmitted over the wireless channel, with corresponding Fourier transform $X(f)$. It is well known from the theory of linear signals and systems that the output

response $Y(f)$ of the output signal $y(t)$ is given as

$$Y(f) = H(f) X(f) \quad (4.5)$$

which is shown in Figure 4.10. The impact of the coherence bandwidth B_c on the signal $x(t)$

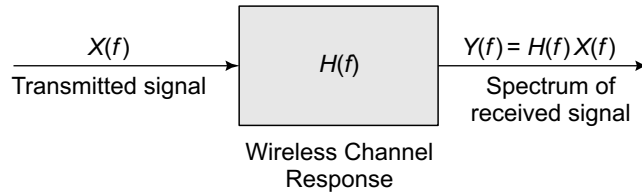


Figure 4.10 Linear input-output system model for the wireless channel

can be understood as follows. As shown in Figure 4.11, if the bandwidth B_s of the signal $x(t)$ is less than B_c , then $X(f)$ spans the *flat* part of the channel response $H(f)$. Hence, the output $Y(f) = H(f) X(f)$ is simply a scaled version of $X(f)$ corresponding to the magnitude of the flat part. Thus, the input signal spectrum $X(f)$ is *undistorted* at the output. Such a wireless channel is termed a *flat-fading* channel.

However, consider the case where the signal bandwidth B_s is greater than the coherence bandwidth B_c . In this scenario, different parts of the signal spectrum $X(f)$ experience different attenuations, i.e., the attenuation is *frequency-selective*. Thus, the output spectrum $Y(f)$ is a distorted version of the input spectrum $X(f)$. Such a wireless channel is termed a *frequency-selective* channel due to the frequency-dependent nature of the attenuation of the signal. This is schematically shown in Figure 4.12.

Thus, the impact of the frequency spectrum $H(f)$ of the wireless channel on the input signal $x(t)$ can be summarized as

$$\begin{aligned} B_s \leq B_c &\Rightarrow \text{No distortion in received signal, i.e., flat fading} \\ B_s \geq B_c &\Rightarrow \text{Distortion in received signal, i.e., frequency-selective fading} \end{aligned} \quad (4.6)$$

We now derive an empirical relationship between the delay spread and coherence bandwidth of a typical wireless channel. Consider a wireless delay profile $h(\tau) = \sum_{l=0}^{L-1} a_l \delta(\tau - \tau_l)$.

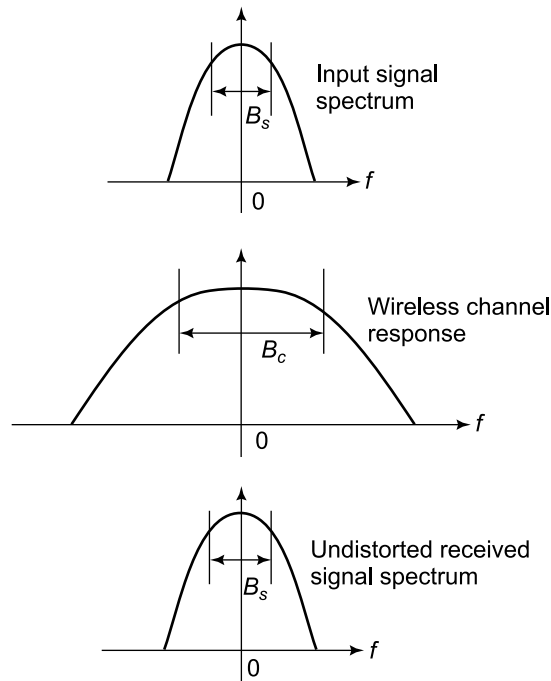


Figure 4.11 Signal bandwidth B_s less than coherence bandwidth B_c implying no distortion

The response $H(f)$ of this channel is given as

$$\begin{aligned}
 H(f) &= \int_0^{\infty} h(\tau) e^{-j2\pi f\tau} d\tau \\
 &= \int_0^{\infty} \left(\sum_{l=0}^{L-1} a_l \delta(\tau - \tau_l) \right) e^{-j2\pi f\tau} d\tau \\
 &= \sum_{l=0}^{L-1} \left(\int_0^{\infty} a_l \delta(\tau - \tau_l) e^{-j2\pi f\tau} d\tau \right) \\
 &= \sum_{l=0}^{L-1} a_l e^{-j2\pi f\tau_l}
 \end{aligned}$$

Thus, the frequency response of the channel is given as the sum of L harmonics, with the l^{th} component changing at the rate τ_l . Consider now the highest frequency harmonic corresponding to $a_{L-1} e^{-j2\pi f\tau_{L-1}}$, i.e., with phase varying at the rate τ_{L-1} . Its values at

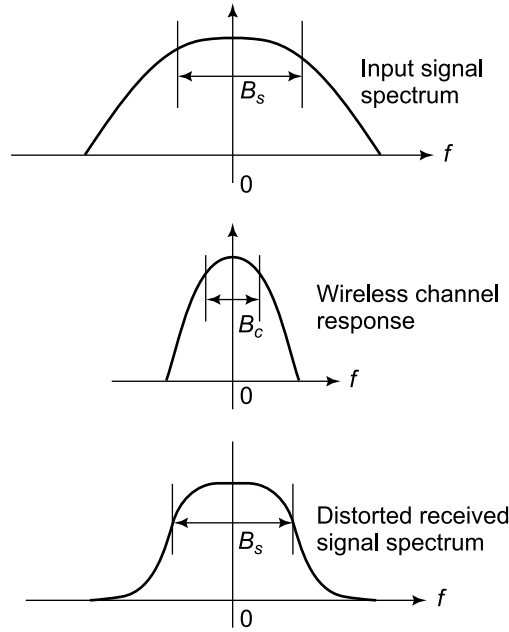


Figure 4.12 Signal bandwidth B_s greater than coherence bandwidth B_c leading to distortion in spectrum of received signal

frequencies 0 and $\frac{1}{4\tau_{L-1}}$ are given as

$$f = 0 \Rightarrow a_{L-1}e^{-j2\pi f\tau_{L-1}} = a_{L-1}e^0 = 1$$

$$f = \frac{1}{4\tau_{L-1}} \Rightarrow a_{L-1}e^{-j2\pi \frac{1}{4\tau_{L-1}}\tau_{L-1}} = a_{L-1}e^{-j\pi\frac{1}{2}} = -ja_{L-1}$$

Thus, it can be seen that as f changes from 1 to $\frac{1}{4\tau_{L-1}}$, the phase changes significantly. This leads to a significant change in the response $H(f)$ from $f = 0$ to $f = \frac{1}{4\tau_{L-1}}$. Thus, $\frac{1}{4\tau_{L-1}}$ is a point of significant change in the frequency response, where it changes significantly compared to the response at $f = 0$, as shown in Figure 4.16. Thus, the bandwidth of the response $H(f)$ is approximately given as

$$f_c = \frac{1}{4\tau_{L-1}}. \quad (4.7)$$

Hence, the coherence bandwidth of the filter $H(f)$ is approximately given as

$$B_c \approx 2 \times \frac{1}{f_c} = \frac{1}{2\tau_{L-1}} \quad (4.8)$$

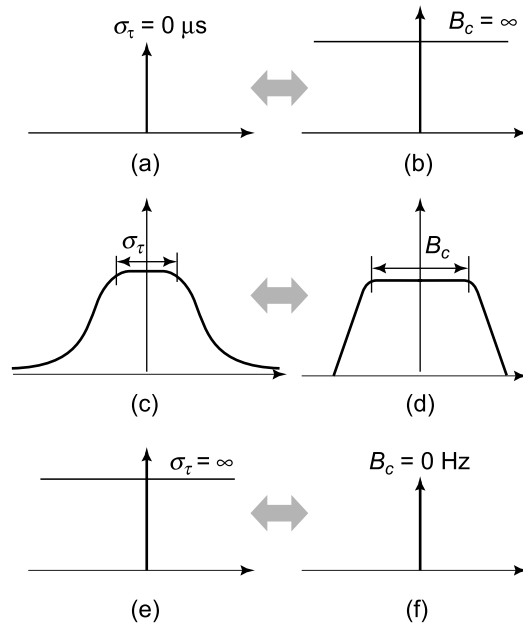


Figure 4.13 Coherence bandwidth B_c variation with delay spread σ_τ

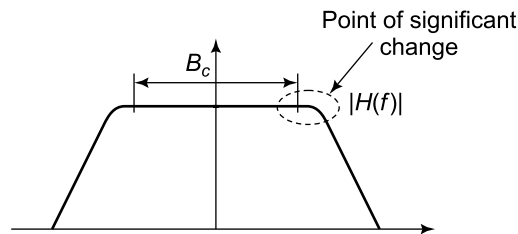


Figure 4.14 Coherence bandwidth showing point of change of response

Finally, observe that τ_{L-1} is the maximum delay spread σ_τ^{\max} of the channel. Thus, the coherence bandwidth B_c can be related to the delay spread σ_τ as

$$B_c \approx \frac{1}{\sigma_\tau}. \quad (4.9)$$

Thus, it can be seen that the above relation satisfies the intuitive property that coherence bandwidth B_c decreases as the delay spread σ_τ increases. The above relation provides a convenient handle to derive the coherence bandwidth given the delay spread of the channel.

Finally, the approximate delay spread corresponding to outdoor channels with a typical delay spread of $2 \mu s$ can be derived as

$$B_c = \frac{1}{2 \times 1 \times 10^{-6}} = 250 \text{ kHz} \tag{4.10}$$

Thus, the typical delay spread of outdoor cellular wireless channels is $B_c = 250 \text{ kHz}$. This is again very helpful towards characterizing and understanding the behaviour of typical 3G/4G wireless cellular channels.

4.4 | Relation Between ISI and Coherence Bandwidth

In this section, we will explore the relation between the *Inter-Symbol Interference (ISI)* distortion at the receiver and the coherence bandwidth B_c of the wireless channel. Consider a *Pulse Amplitude Modulated (PAM)* signal $x(t)$ of symbol time T_s transmitted by the base station. Let us also consider the presence of a scatter component at a delay of $\tau_1 = T_d$ in addition to the direct line-of-sight component with a delay $\tau_0 = 0$. This is shown in Figure 4.14. The net signal sensed by the receiver is the sum of the direct and scatter components, i.e., $x(t)$ and $x(t - \tau_0)$. Observe from Figure 4.14 that if the delay spread $\sigma_\tau = \tau_1 - \tau_0$ is comparable to the symbol time T_s , when these two signals are superposed at the receiver, the symbol s_0 from $x(t)$ adds to a different symbol from $x(t - \tau_0)$. For instance, in the figure, s_0 adds to s_{-1} , i.e., the previous symbol. Further, it can be readily seen that as the delay spread increases, and the number of interfering paths correspondingly increases, the severity of ISI increases, with several symbols superposing at the receiver. This can be clearly seen in Figure 4.15.

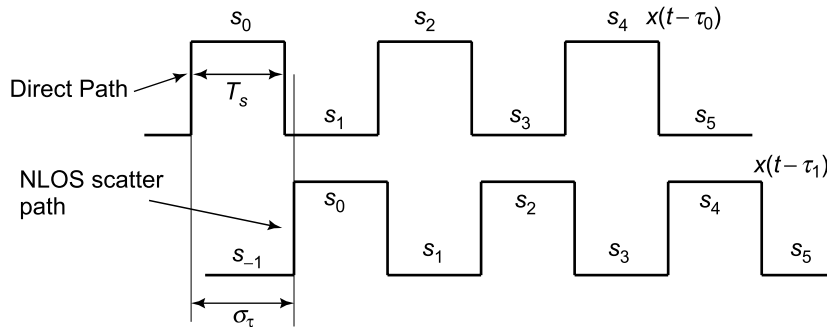


Figure 4.15 Relation between ISI and delay spread

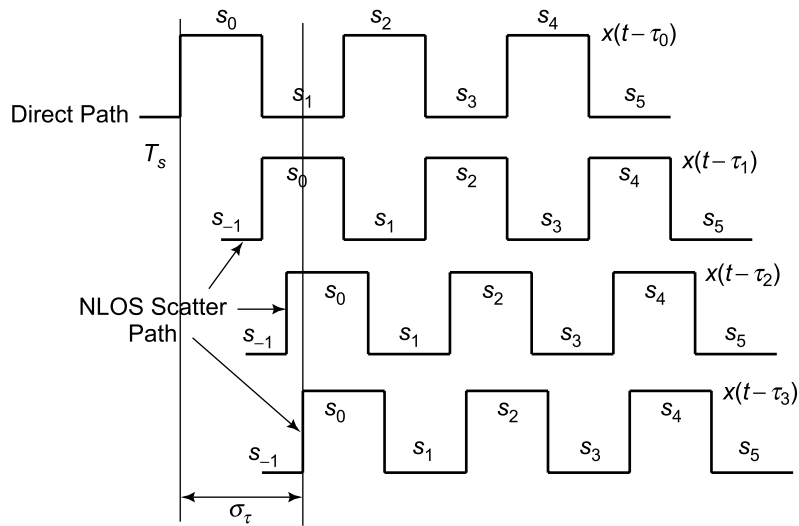


Figure 4.16 Severe ISI caused by multiple scatter components

Let us now analyze the criterion for occurrence of ISI. It can be that the ISI at the receiver is related to the interplay between the symbol time T_s and delay spread T_d . For instance, when the symbol time T_s is much larger than the delay spread T_d as shown in Figure 4.17, there is no ISI. However, as the delay spread T_d becomes comparable to T_s , it leads to ISI. Thus one can empirically state the criterion for ISI as

$$T_d \geq \frac{1}{2}T_s$$

Also, the symbol time T_s is related to the bandwidth B_s of the signal as $T_s = \frac{1}{B_s}$. Moreover, as seen earlier, the delay spread T_d is related to the coherence bandwidth B_c as $B_c = \frac{1}{2T_d}$. Thus, the criterion for inter-symbol interference above can be recast in terms of the bandwidths B_s, B_c as

$$\begin{aligned} \frac{1}{2} \frac{1}{B_c} &\geq \frac{1}{2} \frac{1}{B_s} \\ \Rightarrow B_s &\geq B_c \end{aligned}$$

which is surprisingly the same as the condition for *frequency-selective* signal distortion as illustrated in Eq. (4.6). Thus, the above analysis clearly demonstrates that the

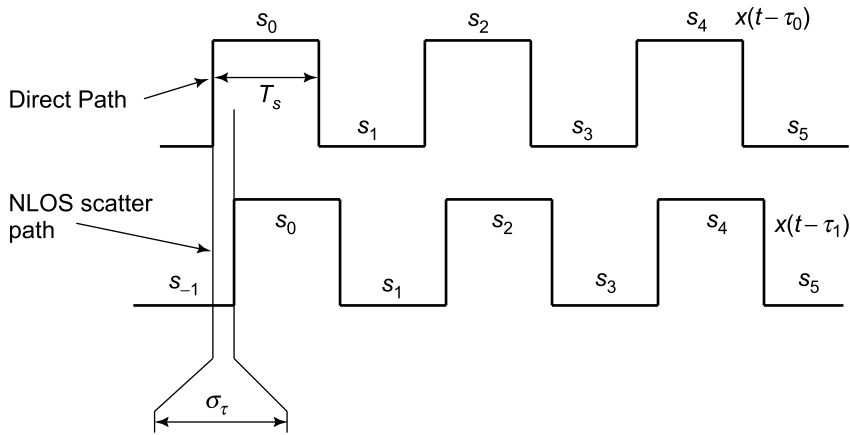


Figure 4.17 Negligible ISI when $\sigma_\tau \ll T_s$

frequency-selective distortion and inter-symbol interference are essentially both sides of the same coin. However, they have interesting interpretations in the frequency and time-domains, with each interpretation yielding insight into the behaviour of the wireless channel vis-a-vis the transmitted signal $x(t)$. In the time domain, if the delay spread is much larger compared to the symbol time, it results in inter-symbol interference. Correspondingly, in the frequency domain, this implies that the bandwidth of the signal is much larger than the coherence bandwidth of the channel. Thus, in effect, one is trying to push a signal of much higher bandwidth through a channel filter, with a much smaller bandwidth. This results in frequency-selective distortion. Thus, to correct for the inter-symbol interference at the receiver, one needs to intuitively multiply by the inverse of the channel response filter, i.e., $\frac{1}{H(f)}$, to convert the frequency selective channel into a system with a net flat-fading response. This process, termed *equalization* is the different frequency components are being equalized to a common flat-level. In the later chapters of the book, we will look at technologies to overcome such a distortion in broadband communications, i.e., when the bandwidth of the signal is much larger than the bandwidth of the channel filter. The next example illustrates the importance of this concept in understanding current 2G and 3G wireless communication systems.

EXAMPLE 4.4

Consider the 2G Global System for Mobile Communications (GSM) standard with a signal bandwidth of $B_{\text{GSM}} = 200$ kHz. Does the GSM signal experience frequency selective or flat fading? Is there inter-symbol interference at the GSM receiver? Answer the same questions as above in the context of the 3G Wideband Code Divison for Multiple Access (WCDMA) standard with a signal bandwidth $B_{\text{WCDMA}} = 5$ MHz.

Solution: To answer this, we note again the coherence bandwidth B_c corresponding to outdoor cellular wireless channels is $B_c \approx 250$ kHz, as demonstrated in Eq. (4.10). Hence, since the 2G GSM signal bandwidth $B_{\text{GSM}} = 200$ kHz $< B_c = 250$ kHz, typically the GSM signal experiences only frequency-flat and not frequency-selective fading. Further, this directly translates into an impact on the delay spread in the time domain as shown in the section above, and there is no inter-symbol interference at the GSM receiver. However, on the other hand, since the WCDMA signal bandwidth $B_{\text{WCDMA}} = 5$ MHz $> B_c = 250$ kHz, the WCDMA signal experiences frequency-selective fading, leading to inter-symbol interference at the receiver. However, interestingly, inter-symbol interference is a *boon* and not a *curse* for CDMA systems. This is due to the fact that the CDMA receiver can easily remove the effects of inter-symbol interference through the RAKE receiver. This will be elaborated in the next chapter.

4.5 | Doppler Fading in Wireless Systems

Another unique aspect of communication over wireless channels is the Doppler fading nature of such channels. The Doppler shift is a fundamental principle related to the electromagnetic radio-wave propagation. In this context, the Doppler *shift* associated with an electromagnetic wave is defined as the perceived change in the frequency of the wave due to *relative* motion between the transmitter and receiver. This is schematically shown in Figure 4.18. The perceived frequency is higher than the true frequency if the transmitter is moving towards the receiver and lower otherwise. Doppler fading is inherent in wireless communications due to the untethered nature of mobile transceivers, which enables mobility in wireless systems, leading to relative motion between the transmitter and the receiver. This is different compared to the conventional wired communications, where the tethered nature of the fixed radio-access medium does not allow for mobility.

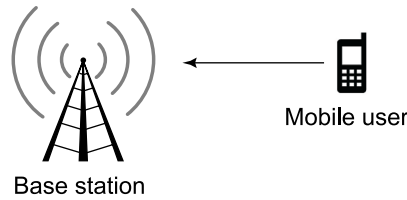


Figure 4.18 Doppler fading due to user mobility

4.5.1 Doppler Shift Computation

Consider the scenario shown pictorially in Figure 4.19, where the mobile station is moving with a velocity v at an angle θ with the line joining the mobile and base station. Let the carrier frequency be f_c . The Doppler shift for this scenario is given as

$$f_d = \left(\frac{v}{c} \cos \theta \right) f_c \quad (4.11)$$

where $c = 3 \times 10^8 \text{m/s}$ is the velocity of light, i.e., velocity of an electromagnetic wave in free space. It can be clearly seen that the Doppler shift increases with the velocity v . Moreover, it depends critically on the angle θ between the direction of motion and the line joining the transmitter and receiver. For instance, the Doppler shift is maximum when $\theta = 0, \pi$, i.e., when the relative motion is along the line joining the transmitter and receiver. However, when $\theta = \frac{\pi}{2}$, i.e., the motion is perpendicular to the receive direction, the Doppler shift is zero. Also, the Doppler shift is positive in the sense that the perceived frequency is higher if $0 \leq \theta \leq \frac{\pi}{2}$, in which case $\cos \theta > 0$. On the other hand, it is negative, leading to a lower perceived frequency that the transmit frequency is $\frac{\pi}{2} \leq \theta \leq \pi$. Example 4.5 illustrates the computation of Doppler frequency for practical wireless scenarios.

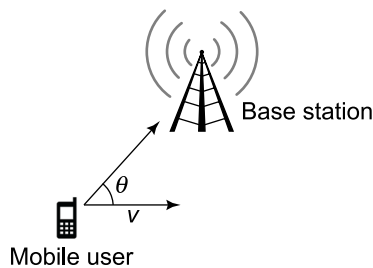


Figure 4.19 Doppler scenario

EXAMPLE 4.5

Consider a vehicle moving at 60 miles per hour at an angle of $\theta = 30^\circ$ with the line joining the base station. Compute the Doppler shift of the received signal at a carrier frequency of $f_c = 1850$ MHz.

Solution: To begin with, we convert the velocity v from units of miles per hour to the standard metres per second. Noting that a mile is equal to 1.61 km, the required velocity in meters per second can be derived as

$$\begin{aligned} 60 \text{ mph} &= 60 \times 1.61 \text{ kmph} \\ &= 60 \times 1.61 \times \frac{5}{18} \text{ m/s} \\ &= 26.8 \text{ m/s} \end{aligned}$$

Employing the expression in Eq. (4.11), the Doppler shift f_d can be computed as

$$\begin{aligned} f_d &= \frac{26.8}{3 \times 10^8} \times \cos(30^\circ) \times 1850 \times 10^6 \\ &= 143 \text{ Hz} \end{aligned}$$

Thus, the Doppler shift is $f_d = 143$ Hz. Further, since the mobile user is moving towards the base station, the Doppler shift is positive, i.e., the perceived frequency f_r is higher compared to the carrier frequency f_c and is given as $f_r = f_c + f_d = 1850 \text{ MHz} + 143 \text{ kHz}$.

4.6 | Doppler Impact on a Wireless Channel

In this section, we systematically investigate the impact of Doppler fading on the multipath wireless-channel model. Consider the impulse response of the i^{th} component of the multipath channel given as $a_i \delta(t - \tau_i)$. Let the vehicle be moving with velocity v at an angle θ with respect to the line joining the mobile and base station. This is shown schematically in Figure 3.19. Observe that the distance between the base station and the mobile is changing constantly due to the motion of the user. Therefore, as a result, the delay of the i^{th} signal component is also changing. Let the initial distance for the i^{th} signal component be d_i . The initial propagation

delay is, therefore,

$$\tau_i = \frac{d_i}{c}$$

After a small interval of time t , this distance decreases by $vt \cos \theta$, since $v \cos \theta$ is the component of the velocity in the direction of the base station. Hence, the delay of the i^{th} component after time t is correspondingly given as

$$\begin{aligned} \tau_i(t) &= \frac{d_i - vt \cos \theta}{c} \\ &= \frac{d_i}{c} - \frac{vt}{c} \cos \theta \\ &= \tau_i - \frac{vt}{c} \cos \theta \end{aligned}$$

Recall from knowledge of the previous chapter that the flat-fading wireless-channel coefficient has been defined as

$$h = \sum_{i=0}^{L-1} a_i e^{-j2\pi f_c \tau_i}$$

The equivalent model for the flat-fading channel coefficient h taking into account the velocity v of the user can now be derived by simply replacing the delay τ_i of the i^{th} component by $\tau_i(t)$. Naturally, the resulting channel coefficient is a function of the time t . This model for the time-varying channel coefficient h is given as

$$\begin{aligned} h(t) &= \sum_{i=0}^{L-1} a_i e^{-j2\pi f_c \left(\tau_i - \frac{v \cos \theta}{c} t \right)} \\ &= \sum_{i=0}^{L-1} e^{-j2\pi f_c \tau_i} e^{j2\pi f_c \frac{v \cos \theta}{c} t} \\ &= \sum_{i=0}^{L-1} a_i e^{-j2\pi f_c \tau_i} e^{j2\pi f_d t} \end{aligned} \tag{4.12}$$

where the last equality follows by substituting $f_d = f_c \frac{v \cos \theta}{c}$. Observe now that the quantity $e^{j2\pi f_d t}$ represents the time-varying phase of the wireless channel. The rate of variation of the phase is given by the Doppler frequency f_d . Thus, to summarize, the mobility of the user in a wireless communication system leads to a Doppler shift, which in turn results in a *time-varying*

wireless channel coefficient. This time-varying nature of the wireless channel is also termed *time selectivity* and the time-varying wireless channel is termed a *time-selective* channel. The reader can readily observe that just as frequency selectivity refers to different signal attenuations in different bands, time selectivity refers to different attenuations at different instants of time. Further, a channel can be both time- and frequency-selective. Such channels are termed *doubly selective* wireless channels.

4.7 | Coherence Time of the Wireless Channel

Similar to the notion of a coherence bandwidth described in the sections above for a frequency-selective channel, we now define the concept of a coherence time interval T_c for a time-varying channel. Consider the i^{th} multipath component of the time-varying channel coefficient in Eq. (4.12), which is given as

$$a_i(t) = a_i e^{-j2\pi f_c \tau_i} e^{j2\pi f_d t}$$

The value of this i^{th} component corresponding to $t = 0, \frac{\pi}{2}$ can be obtained as

$$t = 0 \Rightarrow a_i(0) = a_i e^{-j2\pi f_c \tau_i}$$

$$t = \frac{1}{4f_d} \Rightarrow a_i e^{-j2\pi f_c \tau_i} e^{j2\pi f_d \frac{1}{4f_d}} = j a_i e^{-j2\pi f_c \tau_i}$$

Thus, empirically, one can say that the channel changes significantly from time $t = 0$ to $t = \frac{1}{4f_d}$ since the phase changes by $\frac{\pi}{2}$. This time duration in which the channel changes significantly due to the mobility of the user is termed the *coherence time*, T_c . Further, although f_d depends on the angle of motion θ , a conservative estimate, i.e., minimum coherence time can be obtained by setting $\theta = \frac{\pi}{2}$, in other words, corresponding to the fastest rate of change f_d for a given velocity v . This value of the coherence time T_c can be defined as

$$T_c = \frac{1}{4f_d^{\max}}, \quad f_d^{\max} = \frac{v}{c} f_c$$

The impact of coherence time can be understood as follows. Consider a wireless channel which is changing with time. The coherence time T_c is the approximate duration of time for which

the wireless channel can be assumed to be constant. This can also be expressed as

$$T_c = \frac{1}{2B_d} \quad (4.13)$$

where $B_d = 2f_d$ is the Doppler spread of the wireless channel. Example 4.6 gives an idea of the order of the coherence time for practical 3G/4G wireless systems.

EXAMPLE 4.6

Consider the scenario described above in Example 4.5, i.e., a mobile user in a vehicle moving at 60 miles per hour. Compute the coherence time T_c at the carrier frequency $f_c = 1.85$ GHz.

Solution: To compute the coherence time T_c , we start by computing the maximum Doppler shift f_d^{\max} corresponding to $\theta = 0^\circ$. Following a procedure similar to the one in Example 4.5, this can be obtained as

$$\begin{aligned} f_d^{\max} &= \frac{26.8}{3 \times 10^8} \times 1850 \times 10^6 \\ &= 165 \text{ Hz} \end{aligned}$$

Hence, the corresponding Doppler spread is given as $B_d = 2 \times f_d^{\max} = 330$ Hz. Hence, the coherence time T_c is given from the relation in Eq. (4.13) as

$$\begin{aligned} T_c &= \frac{1}{2 \times 330} \\ &= 1.5 \text{ ms} \end{aligned}$$

Thus, as can be seen from the example above, the value of T_c in practical wireless systems, at vehicular velocities around 60 mph and carrier frequencies in the 2 GHz range is of the order of milliseconds (ms). Thus, the Doppler spread of a wireless system gives the wireless-system designer an idea of the rate of change of the wireless-channel coefficient. Also, it can be readily seen that a larger Doppler spread B_d corresponds to a smaller coherence time T_c leading to a faster rate of channel variation.

4.8 | Jakes Model for Wireless Channel Correlation

In this section, we derive an expression for the time correlation of the wireless channel coefficient. Let X, Y be two complex-valued random variables. The correlation between these random variable is defined as $E\{XY^*\}$. A higher correlation between X, Y indicates a greater degree of similarity between the values assumed by X, Y . Let $a_i(t)$ denote the channel response corresponding to the i^{th} path in the multipath channel profile at time instant t . As seen already, $a_i(t)$ can be expressed as

$$a_i(t) = a_i e^{-j2\pi f_c \tau_i} e^{j2\pi f_d t}$$

The channel coefficient $a_i(t + \Delta t)$, at time Δt later is given as

$$a_i(t + \Delta t) = a_i e^{-j2\pi f_c \tau_i} e^{j2\pi f_d (t + \Delta t)}$$

The impact of the channel time correlation coefficient on the rate of channel variation can be understood as follows. If the correlation between $a_i(t), a_i(t + \Delta t)$ is larger, it means that $a_i(t + \Delta t)$ is very similar to $a_i(t)$ and hence, the channel is varying slowly. On the other hand, if the correlation is small, it implies that $a_i(t + \Delta t)$ has changed significantly compared to $a_i(t)$ and, therefore, the rate of channel variation is faster. Thus, the time correlation coefficient, also termed the *temporal correlation coefficient* is key to understanding the rate of channel variation. Let this correlation as a function of Δt be denoted by $\psi(\Delta t)$. Therefore, $\psi(\Delta t)$ can be defined as

$$\begin{aligned} \psi(\Delta t) &= E\{a_i(t) a_i^*(t + \Delta t)\} \\ &= E\left\{a_i e^{-j2\pi f_c \tau_i} e^{j2\pi f_d t} \left(a_i e^{-j2\pi f_c \tau_i} e^{j2\pi f_d (t + \Delta t)}\right)^*\right\} \\ &= E\left\{|a_i|^2 e^{-j2\pi f \Delta t}\right\} \\ &= E\left\{|a_i|^2\right\} E\left\{e^{-j2\pi f \Delta t}\right\} \end{aligned}$$

We set the quantity $\mathbb{E}\{|a_i|^2\} = 1$ to derive the normalized correlation or, basically, the correlation coefficient. This is, therefore, given as

$$\begin{aligned}\psi(\Delta t) &= \mathbb{E}\left\{e^{-j2\pi f \Delta t}\right\} \\ &= \mathbb{E}\left\{e^{-j2\pi f_c \frac{v}{c} \cos \theta \Delta t}\right\} \\ &= \mathbb{E}\left\{e^{-j2\pi f_d^{\max} \cos \theta \Delta t}\right\}\end{aligned}$$

where $f_d^{\max} = \frac{v}{c} f_c$ as defined above. Notice now that the correlation coefficient depends on θ , which is a random quantity. One has to, therefore, average over the distribution of the random variable θ to derive the correlation coefficient $\psi(\Delta t)$. It is reasonable to assume that the angle θ between the velocity and direction of signal propagation is uniformly distributed over the range $[0, \pi]$, i.e., with distribution given as $f_\Theta(\theta) = \frac{1}{\pi}$. Therefore, the correlation coefficient $\psi(\Delta t)$ is obtained as

$$\begin{aligned}\psi(\Delta t) &= \int_0^\pi \mathbb{E}\left\{e^{-j2\pi f_d^{\max} \cos \theta \Delta t}\right\} f_\Theta(\theta) d\theta \\ &= \frac{1}{\pi} \int_0^\pi \mathbb{E}\left\{e^{-j2\pi f_d^{\max} \cos \theta \Delta t}\right\} d\theta \\ &= J_0(2\pi f_d^{\max} \Delta t)\end{aligned}$$

where J_0 is the Bessel function of the 0th order. Therefore, substituting $f_d^{\max} = \frac{1}{4T_c}$, we have

$$\begin{aligned}\psi(\Delta t) &= J_0\left(2\pi \frac{1}{4T_c} \Delta t\right) \\ &= J_0\left(\frac{\pi \Delta t}{2 T_c}\right)\end{aligned}$$

The above temporal correlation model for $\psi(\Delta t)$ is a popular model for wireless communication systems and is termed *Jakes' model*. The Jakes correlation as a function of the normalized time lag $\frac{\Delta t}{T_c}$ is shown in Figure 4.20.

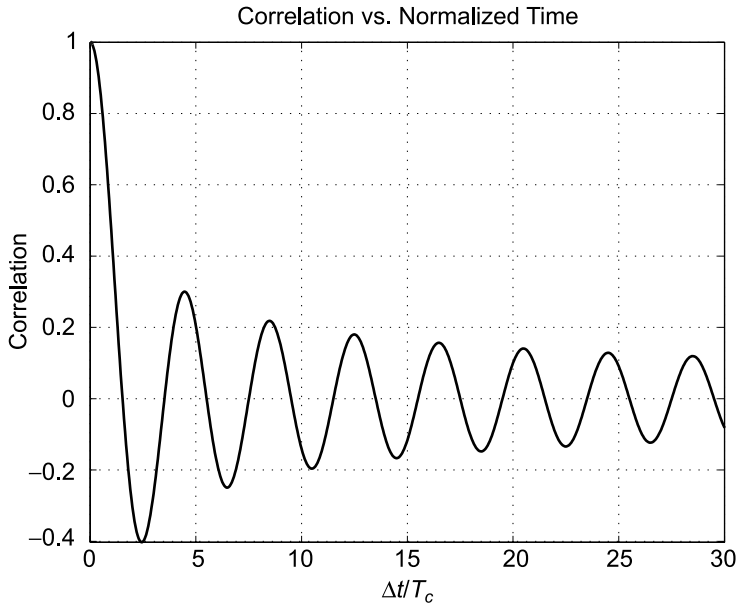


Figure 4.20 Jakes' correlation as a function of $\frac{\Delta t}{T_c}$

The Doppler spectrum corresponding to the temporal correlation function $\psi(\Delta t)$ is given by its Fourier transform as

$$\begin{aligned}
 S_H(f) &= \int_{-\infty}^{\infty} \psi(\Delta t) e^{-j2\pi f \Delta t} d(\Delta t) \\
 &= \int_{-\infty}^{\infty} J_0(2\pi f_d^{\max} \Delta t) e^{-j2\pi f \Delta t} d(\Delta t) \\
 &= \frac{1}{\pi f_d^{\max}} \frac{\text{rect}\left(\frac{f}{2f_d^{\max}}\right)}{\sqrt{1 - \left(\frac{f}{f_d^{\max}}\right)^2}}, \tag{4.14}
 \end{aligned}$$

where the function $\text{rect}(\cdot)$ is defined as

$$\text{rect}(x) = \begin{cases} 1 & |x| \leq \frac{1}{2} \\ 0 & |x| > \frac{1}{2} \end{cases} \tag{4.15}$$

i.e., $\text{rect}(x)$ is basically a pulse of height 1 between $x = -\frac{1}{2}$ and $x = \frac{1}{2}$. The Doppler spectrum $S_H(f)$ of Eq. (4.14), which is associated with the Jakes' temporal correlation model, is termed

the *Jakes' spectrum* and is very popular in the context of wireless communications to model the correlation function of time-varying wireless channels. A figure of the Jakes spectrum is shown in Figure 4.21. It can be seen that the spectrum is 'U' shaped and restricted between $-f_d^{\max}$ and f_d^{\max} . Hence, this is colloquially also termed a *U-shaped Doppler spectrum* spectrum of Doppler spread $2f_d^{\max} = 2\frac{v}{c}f_c$.

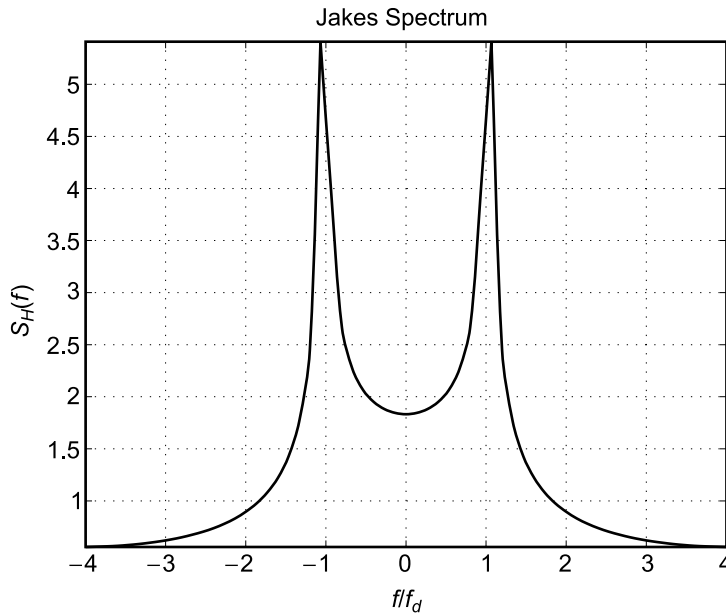


Figure 4.21 Jakes' spectrum as a function of normalized frequency $\frac{f}{f_d}$

4.9 | Implications of Coherence Time

What is the implication of a large or small coherence time T_c on the design of the wireless-communication system? This can be understood as follows. As described in the previous chapter, one needs to estimate the channel coefficient h at the receiver to decode the transmitted symbol $x(k)$. Further, since the channel is changing significantly at every coherence time duration, the channel estimation has to be carried out at least once in every coherence time interval. This is achieved by inserting *training* or *pilot* symbols in the frame of transmitted information symbols. For example, in the 2G GSM standard, 26 training symbols are inserted in the middle of a frame of 156-symbols length. This is also termed a *midamble* and schematically shown in Figure 4.22.

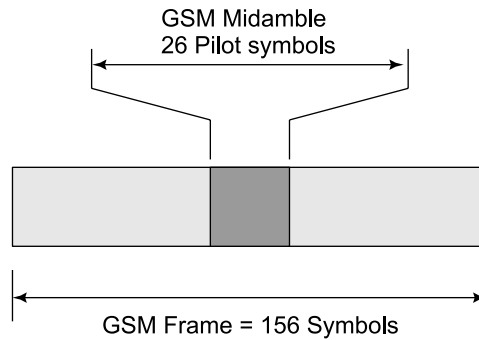


Figure 4.22 Midamble of 26 pilot symbols in GSM frame of length of 156-symbols

In this context, one can also now distinguish between a *fast-fading* versus a *slow-fading* channel. If the coherence time T_c is greater than the time interval between two channel estimation instants, i.e., the channel is estimated at least once in every coherence time interval, it is termed a *slow-fading* channel. On the other hand, if the coherence time is lower than the duration between two successive channel estimation instants, i.e., the channel is changing at a rate faster than it is being estimated at the receiver, it is termed a *fast-fading* channel. This idea is captured schematically in Figure 23. To summarize,

$$T_c \geq \text{Inter-channel estimation time} \Rightarrow \text{Slow fading}$$

$$T_c < \text{Inter-channel estimation time} \Rightarrow \text{Fast fading}$$

The relation between the various parameters such as flat-fading, frequency-selective fading, fast-fading, slow-fading, etc., is comprehensively summarized in Figure 4.23. As shown in the figure, the delay spread σ_τ and coherence time T_c are key parameters in characterizing a wireless channel. For a very low T_c and σ_τ , coherence time is smaller than T_e , the inter-channel estimation time; and σ_τ is less than T_s , the symbol time. The channel is *fast-fading* and *flat-fading*. As the coherence time T_c rises to the point $T_c > T_e$, with $\sigma_\tau < T_s$, the channel becomes *slow-fading* and *flat-fading*. On the other hand, if σ_τ , the delay spread, rises to $\sigma_\tau > T_s$, i.e., the delay spread becomes larger than the symbol time, while the coherence time $T_c < T_e$, the channel is *fast-fading* and *frequency-selective fading*. Finally, for the case of high T_c and σ_τ , i.e., $T_c > T_e$ and $\sigma_\tau > T_s$, the channel is *slow-fading* and *frequency-selective fading*.

Also, one important aspect of wireless channels is worth noting. As calculated in the sections above, the typical value of the delay spread σ_τ in the wireless channels is of the order of μs , while the typical value of the coherence time T_c is of the order of ms . Thus, the coherence time T_c is several times larger compared to the delay spread σ_τ i.e., $\sigma_\tau \ll T_c$.

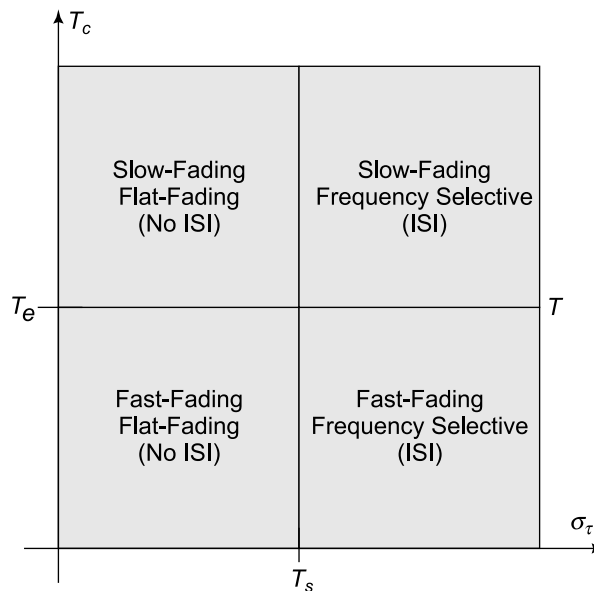


Figure 4.23 Figure summarizing relationship between key parameters of the wireless channel

This property is typical of wireless channels observed in practice and such channels are termed *underspread channels*.

PROBLEMS

1. **Jakes' Model** Employ the Jakes' model to answer the questions below.
 - (a) Find the velocity of a mobile in kmph if the correlation between the channel coefficients is 0.22 for a time interval $\Delta t = 3.9$ ms at 1.6 GHz.
 - (b) For this system, what is the joint distribution of $[h(0), h(2.9 \text{ ms})]$?
2. Fill in the blanks below.
 - (a) A wireless channel is termed underspread if _____.
 - (b) At 2 GHz and $v = 30$ km/hr the coherence time is _____.
3. Compute the RMS delay spread for the channel power profile given in Figure 4.24.
 - (a) Consider a channel with the power delay profile $P(\tau) = \alpha e^{-\tau/\beta}$, where $\alpha = 3$ dB and $\beta = 1 \mu\text{s}$. What is the RMS delay spread for this channel?
 - (b) For the above channel, what is the 3 dB coherence bandwidth?

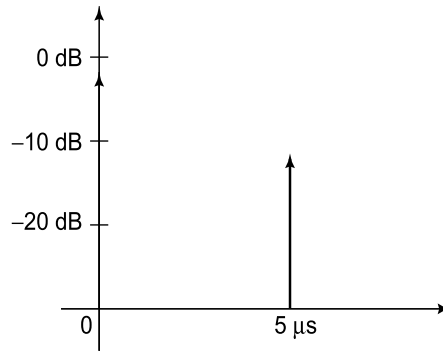


Figure 4.24 Delay profile

4. Channel Estimation

- (a) Below are the vectors corresponding to the transmitted pilot symbols and received outputs across the standard Rayleigh fading wireless channel (Single Rx/Tx antenna) as per the channel-estimation model discussed in class.

$$\mathbf{y}_p = \begin{bmatrix} -0.7850 + 0.3631i \\ 0.4072 + 0.7757i \\ 0.8004 - 0.4359i \\ 0.4464 + 0.8222i \end{bmatrix}, \quad \mathbf{x}_p = \frac{1}{\sqrt{2}} \begin{bmatrix} -1 + j \\ 1 + j \\ 1 - j \\ 1 + j \end{bmatrix}$$

Given that the noise is AWGN, what is the Maximum likelihood (ML) estimate of the fading-channel coefficient?

- (b) If the carrier frequency of the above system is 2.5 GHz, with a bandwidth of 200 kHz and frame length of 250 symbols, what is the maximum tolerable mobile terminal velocity in kmph? (*Hint*: The channel is estimated once every frame)

5. Delay Spread Consider the following **outdoor** wireless channel delay profiles given in Figure 4.25 and answer the following questions.

- (a) What is the most logical unit of time on the x -axis?
- (b) For the delay profile, compute τ_{\max} the maximum delay spread.
- (c) For the delay profile, compute τ_{rms} , the RMS delay spread.
- (d) Employing the average RMS delay spread as the metric T_d , what is the maximum possible symbol rate for ISI-free communication?

- (e) Can a GSM system ($B = 200$ kHz) work in the above environment without an equalizer?

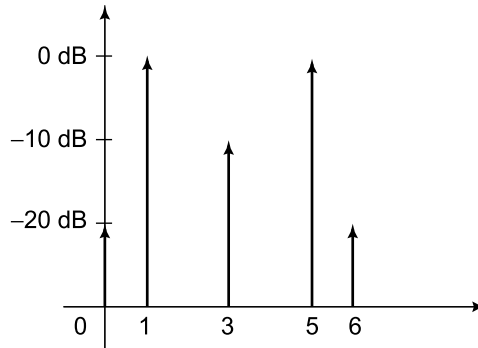


Figure 4.25 Delay profile

6. Consider a mobile moving at 80 kmph in a 3G WCDMA system at 2 GHz. The chipping rate in WCDMA is 3.84 Mchips/second. Let T_s denote the slot time, where the number of chips in a slot is 2560. Let the vector \mathbf{h} be defined as

$$\mathbf{h} = \begin{bmatrix} h(0) \\ h(T_s) \\ h(2T_s) \\ h(3T_s) \end{bmatrix} \quad (4.16)$$

where $h(t)$ denotes the channel at the time t . Compute the covariance matrix $\mathbf{h}\mathbf{h}^H$.

7. Consider a multi-path channel with the power delay profile,

$$P(\tau) = \sum_{i=0}^{N-1} \alpha_i e^{-\tau/\beta_i}$$

where $\alpha_i, \beta_i, 0 \leq i \leq N - 1$ are parameters. What is the RMS delay spread for this channel?

8. Consider a mobile communication scenario with $f_c = 2.4$ GHz and velocity $v = 40$ mph over a Rayleigh fading channel. Let $h(t) = x(t) + jy(t)$ be the channel at the time t , normalized to unit power. Employ the Jakes' model to answer the questions that follow.

- (a) Find the Doppler frequency and the **coherence** time.
 - (b) What is the joint distribution $f[h(0), h(0.3T_c)]$?
 - (c) Compute $E\{x^2(0)x^2(0.3T_c)\}$.
9. Consider a Rayleigh channel, with the channel coefficient h unknown. Compute the estimate of the channel coefficient h if the transmitted pilot symbols are given as $\mathbf{x}_p = [2, -2, 2, -2]^T$ and the received pilot symbols are given as

$$\mathbf{y}_p = [3.68 + 4.45j, -3.31 - 4.60j, 3.24 + 4.33j, -3.46 - 4.34j]^T$$

Code Division for Multiple Access (CDMA)

5.1 | Introduction to CDMA

CDMA stands for Code Division for Multiple Access and is considered a path-breaking wireless technology due to its several superior properties. It was first employed in the 2nd generation IS-95 cellular standard, which was predominantly used in North America, under the brand name **cdmaOne**. It also forms the basis for several advanced 3rd Generation i.e., 3G cellular standards such as Wideband CDMA (WCDMA), High-Speed Downlink Packet Access (HSDPA), High Speed Uplink Packet Access (HSUPA), CDMA 2000, and 1x Evolution Data Optimized (1xEV-DO). In order to understand the concepts in CDMA, it is critical to understand the concept of *multiple access*. In conventional wired communication systems, there is a dedicated wireline communication channel which is allocated exclusively to the particular device such as a telephone, etc. However, in a wireless network, mobile phones and other wireless-communication devices are required to share the common radio channel over the air. This is shown in Figure 5.1. This is because the radio channel is common for all the users/ devices and the available wireless frequency bands are limited. Thus, it is necessary to devise a mechanism for *multiple* users to *access* this common radio channel, which is termed as a *Multiple Access* (MA) technology. Thus, multiple access is at the heart of modern wireless technologies, especially 3G and 4G cellular technologies.

Several multiple-access technologies have been developed and employed for cellular applications. In fact, each generation of cellular standards is characterized by a particular multiple-access technology. For instance, the first generation, i.e., 1G cellular standards were based on *Frequency Division Multiple Access (FDMA)*. In FDMA, different users are allotted different *frequency* bands. Thus, the users are multiplexed in the frequency domain and

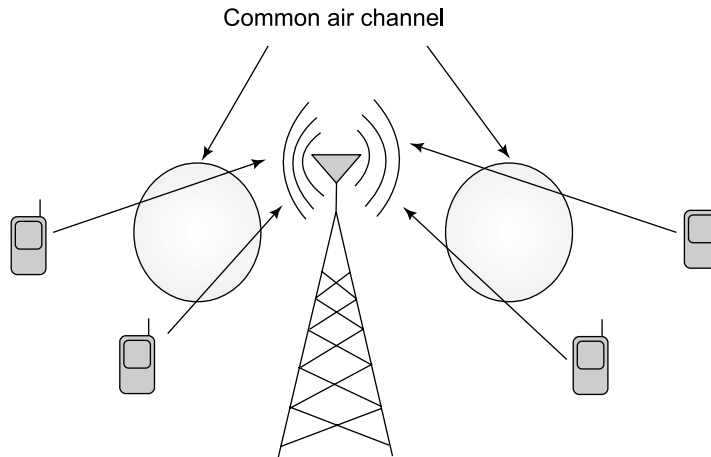


Figure 5.1 Multiple access for wireless cellular networks

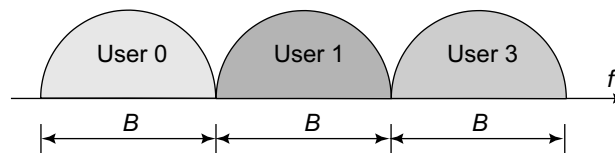


Figure 5.2 Frequency division for multiple access

they access the radio channel in their respective frequency bands of bandwidth B . This is schematically shown in Figure 5.2. On the other hand, the second generation or 2G cellular standards are based on digital *Time Division for Multiple Access (TDMA)* in which different users are allocated different *time slots* of duration T for accessing the wireless channel. Thus, the different users are multiplexed in the time domain as shown in Figure 5.3. These technologies were replaced by CDMA in successive 3G wireless technologies. The motivation and basic mechanism of CDMA is described in the next section.

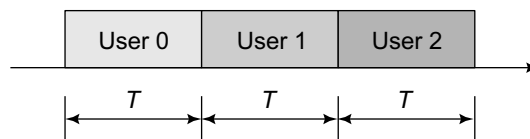


Figure 5.3 Time division for multiple access

5.2 | Basic CDMA Mechanism

CDMA, as the name suggests, is a multiple-access technology based on *code division*. In other words, different users are multiplexed using different *codes*. Consider a two-user scenario, i.e., two users accessing the radio channel simultaneously. Let a_0 denote the symbol of the user 0, while a_1 denotes the transmit symbol corresponding to the user 1. Let the code c_0 of the user 0 be given as $c_0 = [1, 1, 1, 1]$. The above code c_0 is of length $N = 4$ chips. Each element of the code is termed as a *chip*. The transmitted signal x_0 of the user 0 is then given by multiplying the code c_0 with the symbol a_0 as

$$\begin{aligned} x_0 &= a_0 \times [1, 1, 1, 1] \\ &= [a_0, a_0, a_0, a_0] \end{aligned} \quad (5.1)$$

The structure of the above transmit signal x_0 can be interpreted as follows. The symbol a_0 , of the user 0, is multiplied by the code c_0 to yield 4 chips $x_0(i)$, $0 \leq i \leq N - 1$. Similarly, let the code c_1 , given as $c_1 = [1, -1, -1, 1]$, correspond to the code of the user 1. Hence, the sequence of chips corresponding to the user 1 transmission is given as

$$\begin{aligned} x_1 &= a_1 \times [1, -1, -1, 1] \\ &= [a_1, -a_1, -a_1, a_1] \end{aligned} \quad (5.2)$$

The signals x_0, x_1 corresponding to users 1, 2 respectively are now summed to yield the net signal x as

$$x = x_1 + x_2 = [(a_0 + a_1), (a_0 - a_1), (a_0 - a_1), (a_0 + a_1)] \quad (5.3)$$

This sum, or *composite*, signal is then transmitted on the downlink from which each of the users 0, 1 detect their own signal. This is done as follows. User 1 correlates the received signal x with his code c_0 , i.e., basically multiplies each chip of the received signal x with the corresponding chip of the code $c_0 = [1, 1, 1, 1]$ and sums across the chips as follows.

$$\begin{array}{cccc} a_0 + a_1 & a_0 - a_1 & a_0 - a_1 & a_0 + a_1 \\ \times & 1 & 1 & 1 \\ \hline (a_0 + a_1) + (a_0 - a_1) + (a_0 - a_1) + (a_0 + a_1) = 4a_0 \end{array} \quad (5.4)$$

Thus, the result of the above correlation is $4a_0$, which is proportional to the transmitted symbol a_0 . Similarly, at the user 2, the received signal x is correlated with the chip sequence $c_1 =$

$[1, -1, -1, 1]$ of the user 1 as

$$\begin{array}{cccc}
 a_0 + a_1 & a_0 - a_1 & a_0 - a_1 & a_0 + a_1 \\
 \times & 1 & -1 & -1 & 1 \\
 \hline
 (a_0 + a_1) - (a_0 - a_1) - (a_0 - a_1) + (a_0 + a_1) = 4a_1
 \end{array} \tag{5.5}$$

to yield $4a_1$, which is proportional to the transmitted symbol a_1 of the user 1. Thus, unlike in GSM or FDMA, in which the signals of different users are transmitted in different time slots or frequency bands, in CDMA, all the signals of the different users are contained in the single signal x over all time and frequency. However, in CDMA, the symbols of the different users are combined using different *codes*. For instance, in the above example, the symbols a_0, a_1 of users 0, 1 are multiplied with codes c_0, c_1 prior to transmission. Thus, the users of the different signals are multiplexed over the common wireless channel employing different codes. Hence, this is termed *Code Division for Multiple Access*, i.e., multiple access based on different codes. The key operations in CDMA can be summarized as follows.

1. Multiplying or modulation the symbols of the different users with the corresponding assigned unique code, similar to the procedure illustrated in equations (5.1), (5.2).
2. Combining or adding the code-modulated signals of all the users to form the composite signal as shown in Eq. (5.3), followed by subsequent transmission of the signal.
3. Finally, correlation of the composite received signal x at each user with the corresponding code of the user to recover the transmitted symbol. This is described in Eqs (5.4), (5.5).

5.3 | Fundamentals of CDMA Codes

In fact, from the example illustrated in the previous section, the astute reader will realize that it is no accident by which we are able to recover the signals of users 0, 1. Computing the correlation r_{01} of the user codes c_0, c_1 yields

$$r_{01} = \sum_{k=0}^3 c_0(k) c_1(k)$$

$$\begin{aligned}
 &= 1 \times 1 + 1 \times (-1) + 1 \times (-1) + 1 \times 1 \\
 &= 1 + (-1) + (-1) + 1 \\
 &= 0
 \end{aligned}$$

Thus, since the correlation between the codes c_0 , c_1 is zero, the codes are, in fact, *orthogonal*. This is what helps us recover the symbols of the different users from the composite signal. This is a key property of the codes employed in CDMA wireless systems, and a fundamental principle on which the theory of CDMA is based.

Further, consider a fundamental property of the CDMA system arising because of the employment of these codes. Let the symbol rate for the symbols a_0 of the user 0 be 1 kbps. Hence, the time period T per symbol is

$$T = \frac{1}{1 \text{ kbps}} = 1 \text{ ms}$$

Hence, the corresponding bandwidth required for transmission is

$$B = \frac{1}{T} = 1 \text{ kHz}$$

However, now consider the transmission of the symbol a_0 multiplied with the corresponding code c_0 , i.e., $a_0 \times [1, 1, 1, 1] = [a_0, a_0, a_0, a_0]$. Thus, for each symbol a_0 , one has to transmit 4 chips. Thus, to keep the symbol rate constant at 1 kbps, the time of each chip T_c has to be set as $T_c = \frac{1}{4}T = 0.25 \text{ ms}$. Thus, the bandwidth required for this system is

$$B_{\text{CDMA}} = \frac{1}{T_c} = \frac{1}{0.25 \text{ ms}} = 4 \text{ kHz}$$

Thus, modulating with the code c_0 of length $N = 4$, results in an increase of the required bandwidth by a factor of N , i.e., from 1 kHz to 4 kHz. This is shown schematically in Figure 5.4. Thus, it basically results in a *spreading* of the original signal bandwidth and, hence, is termed a *spreading code*. Also, since the resulting signal occupies a large bandwidth, CDMA systems are also termed *spread spectrum* or *wideband* systems.

Also, another interesting question the reader might be interested in is the following: How many such orthogonals exist for a given spreading code length N ? The answer is there are N such orthogonal codes. For instance, consider the case $N = 4$.

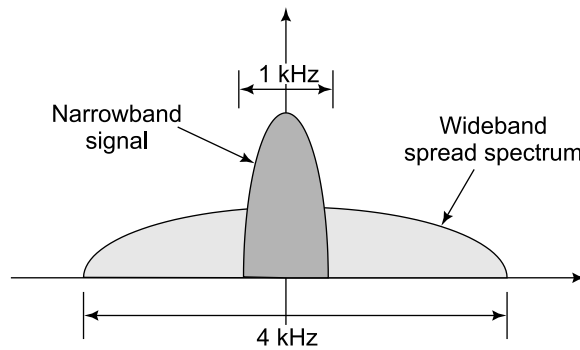


Figure 5.4 Spread spectrum communication

The different orthogonal spreading codes are

$$\begin{aligned} c_0 &= 1 \ 1 \ 1 \ 1 \\ c_1 &= 1 \ -1 \ -1 \ 1 \\ c_2 &= 1 \ -1 \ 1 \ -1 \\ c_3 &= 1 \ 1 \ -1 \ -1 \end{aligned}$$

The reader can verify that the codes c_0, c_1, c_2, c_3 are orthogonal to each other. For example, consider c_1, c_2 . The correlation r_{12} between codes c_1, c_2 is

$$\begin{aligned} r_{12} &= \sum_{k=0}^3 c_1(k) c_2(k) \\ &= 1 \times 1 + (-1) \times (-1) + (-1) \times 1 + 1 \times (-1) \\ &= 1 + 1 + (-1) + (-1) \\ &= 0 \end{aligned}$$

This implies that given a spreading sequence length N , there exist N orthogonal codes and hence, N users can be multiplexed together. This is important, since the bandwidth increases by a factor of N due to transmission employing the codes as described earlier. However, it is important to note that no inefficiency is introduced in the system because of the increase in bandwidth, because this increase in bandwidth by a factor of N is compensated by the parallel transmission of the signals corresponding to the N users over the same bandwidth. Thus, the spectral efficiency of the system is not compromised. This is schematically illustrated in Figure 5.5.

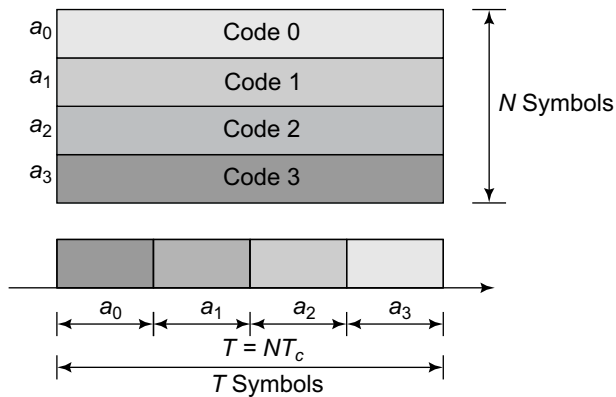


Figure 5.5 Parallel transmission of N symbols over N codes in CDMA over time interval $T = NT_c$ (above) and comparison with transmission of N symbols in time $T = NT_c$ in a conventional single carrier or time division system

5.4 | Spreading Codes based on Pseudo-Noise (PN) Sequences

Consider the code $c_2 = [1, -1, 1, -1]$. Observe that the code looks like a random sequence of $+1, -1$, or a *pseudo-noise* (PN) sequence. This is so termed since it only resembles a noise sequence, but is not actually a noise sequence. One method to generate such long spreading codes based on PN sequences for a significantly large N is through the employment of a *Linear Feedback Shift Register (LFSR)*. This is described next.

Consider the shift register architecture shown in Figure 5.6, where the element D represents delays. Thus, the digital circuit therein contains $D = 4$ delay elements or shift registers. The input on the left is denoted by X_i , and the outputs of the different delays are $X_{i-1}, X_{i-2}, X_{i-3}, X_{i-4}$. Let X_{i-4} also denote the final output of the system. Also observe that the xor $X_{i-4} \oplus X_{i-3}$ is fed back as X_i which is the input to the first shift register. Thus, the governing equation of the circuit is

$$X_i = X_{i-3} \oplus X_{i-4}$$

which is a linear equation. Thus, since it implements a *linear* relation, with *feedback* and uses delay elements or *shift registers*, such a circuit is also termed a *Linear Feedback Shift Register (LFSR)* architecture. Since the next input, i.e., X_i depends on $X_{i-1}, X_{i-2}, X_{i-3}, X_{i-4}$, this can also be thought of as the current *state* of the system. Consider initializing the system in the state $X_{i-1} = 1, X_{i-2} = 1, X_{i-3} = 1, X_{i-4} = 1$. Thus, we have the corresponding X_i given

as

$$X_i = X_{i-3} \oplus X_{i-4} = 1 \oplus 1 = 0$$

This X_i becomes X_{i-1} at the next instant and similarly, X_{i-2} , X_{i-3} are shifted to the right as X_{i-3} , X_{i-4} respectively. Continuing in this fashion, the entire sequence of state of the above LFSR is summarized. It can be seen that the LFSR goes through the sequence of 15 states 1111, 0111, 0011, 0001, 1000, 0100, 0010, 1001, 1100, 0110, 1011, 0101, 1010, 1101, 1110, before reentering the state 1111. Subsequently, the entire sequence of states repeats again. Observe that this goes through $2^D - 1 = 2^4 - 1 = 15$ states. Also note that the maximum number of possible states for $D = 4$ is $2^D = 16$. However, the LFSR can be seen to go through all the possible states except one, which is the 0000 or the all-zero state.

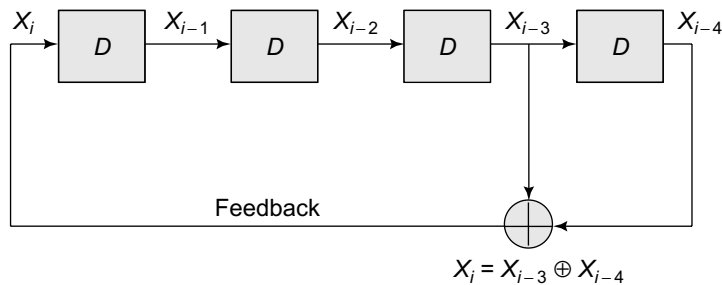


Figure 5.6 Linear feedback shift register

$$X_i = X_{i-3} \oplus X_{i-4} = 0 \oplus 0 = 0$$

Further, observe that if the LFSR is initialized in the 0000 state, it continues in the 0000 state, since the corresponding X_i is leading to the next state of 0000. Thus, the LFSR never gets out of the all zero states! Therefore, it is desired that the LFSR never enter the all-zero state. Such an LFSR circuit which goes through the maximum possible $2^D - 1$ states, without entering the all-zero state is termed a *maximum-length* shift register circuit or maximum length LFSR. The generated PN sequence is termed a *maximum-length* PN sequence. Thus, the maximum-length PN sequence is of length $2^D - 1$. For instance, for the above LFSR, the maximum-length PN sequence is the sequence of outputs X_{i-4} given as

$$\text{PN Sequence} = 111100010011010$$

We can map the bits 1, 0 to the BPSK symbols -1 , $+1$ to get the modulated PN sequence,

$$\text{PN sequence} = -1 - 1 - 1 - 1 + 1 + 1 + 1 - 1 + 1 + 1 - 1 - 1 + 1 - 1 + 1 \quad (5.6)$$

Next, we examine the properties of such PN sequences derived above.

5.4.1 Properties of PN Sequences

Property 1-Balance Property: Consider the BPSK-modulated PN sequence shown in Eq. (5.6). As already described, the PN sequence is of maximal length $2^D - 1 = 15$ corresponding to $D = 4$. Counting the number of -1 and $+1$ chips in the sequence, it can be seen that the number of -1 s is *one* more than the number of $+1$ s. This is termed the *balance* property of the PN sequence. This fundamentally arises from the noise-like properties of PN sequences. If we are generating random noise of $+1$, -1 chips, with $P(X_i = +1) = P(X_i = -1) = \frac{1}{2}$, we expect to find on an average that *half* the chips are $+1$ and the rest are -1 . In the above case, however, as the total number of chips is an odd number, i.e., 15, it is not possible to have an exactly even number of $+1$, -1 s. Hence, we observe that the number of $+1$, -1 s is close to half the total number, i.e., eight -1 s and seven $+1$ s. Thus, the balance property basically supports the notion of a noise-like PN chip sequence.

Property 2-Run-Length Property: A *run* is defined as a string of continuous values. There are a total of 8 runs in this PN sequences. For instance, the first run $-1, -1, -1, -1$ is a run of length 4. Thus, there is one run of length 4. Similarly, there is one run $+1, +1, +1$ of length 3, and two runs of length 2, viz., $-1, -1, +1, +1$. Finally, it can also be seen that there are 4 runs of length 1, viz., two runs of $+1$ and two runs of -1 . Thus, there are a total of $2^{(D-1)} = 8$ runs. Out of the 8 runs, it can be seen that 1, i.e., $\frac{1}{8}$ of the runs are of length 3, $\frac{1}{4}$ of the runs are of length 2 and $\frac{1}{2}$ of the runs are of length 1. This is termed the *run-length* property of PN sequences and can be generalized as follows. Consider a maximal length PN sequence of length $2^D - 1$. Out of the total number of runs in the sequence, $\frac{1}{2}$ of the runs are of length 1, $\frac{1}{4}$ of the runs are of length 2, $\frac{1}{8}$ of the runs are of length 3, and so on. This is again in tune with the noise-like properties of PN sequences. For instance, consider a random IID sequence of $+1, -1$. In such a sequence, one would expect the average number of $+1$ or -1 to be half the total chips. Further, the number of strings $+1, +1$ or $-1, -1$, i.e., runs of length two would be expected to comprise $\frac{1}{4}$ of the total runs. This arises since the probability of seeing two

consecutive +1, +1 symbols is

$$P(X_i = +1, X_{i+1} = +1) = \frac{1}{2} \times \frac{1}{2} = \frac{1}{4}$$

Similarly, one can explain the fraction $\frac{1}{8}$ corresponding to runs of length 3. Thus, this further supports the noiselike properties of PN sequences.

Property 3-Correlation Property: The *correlation* property is one of the most important properties of PN sequences. Consider again the BPSK chip sequence shown in Eq. (5.6) and denote it by $c_0(n)$. Let us now look at the correlation properties of this sequence. Consider the correlation $r_{00}(0)$, i.e., the correlation of the sequences c_0 with itself (the meaning of the (0) will become clear soon). This correlation is given as

$$\begin{aligned} r_{00}(0) &= \frac{1}{N} \sum_{i=0}^{N-1} c_0(i) c_0(i) \\ &= \frac{1}{N} \sum_{i=0}^{N-1} 1 \\ &= \frac{1}{N} \times N = 1 \end{aligned}$$

Now, consider a circularly shifted version of the PN sequence, shifted by $n_o = 2$. Let it be denoted by $c_0(n - 2)$. This circularly shifted sequence by 2 chips can be readily seen to be given as

$$\begin{aligned} \text{PN Sequence} &= -1 + 1, -1 - 1 - 1 - 1 + 1 + 1 \\ &\quad + 1 - 1 + 1 + 1 - 1 - 1 + 1 \end{aligned} \tag{5.7}$$

Let us denote the correlation between $c_0(n)$ and $c_0(n - 2)$ by $r_{00}(2)$, where the (2) can now be seen to represent a circular shift of 2. The correlation can be seen to be given as

$$r_{00}(2) = \frac{1}{N} \sum_{i=0}^{N-1} c_0(i) c_0(i - 2)$$

$$\begin{aligned}
&= \frac{1}{15} \{(-1) \times (-1) + (-1) \times (1) + (-1) \times (-1) + (-1) \times (-1) + (1) \times (-1) + \\
&\quad (1) \times (-1) + (1) \times (1) + (-1) \times (1) + (1) \times (1) + (1) \times (-1) + (-1) \times (1) + \\
&\quad (-1) \times (1) + (1) \times (-1) + (-1) \times (-1) + (1) \times (1)\} \\
&= \frac{1}{15} (1 - 1 + 1 + 1 - 1 - 1 + 1 - 1 + 1 - 1 - 1 - 1 - 1 + 1 + 1) \\
&= \frac{1}{15} \times (-1) = -\frac{1}{15} \\
&= -\frac{1}{N}
\end{aligned}$$

In fact, one can compute the correlation for other such nonzero delays, and can demonstrate the the correlation is always $-\frac{1}{N}$. This autocorrelation property of the PN sequence, i.e., of the sequence with a delayed version of itself, is shown pictorially in Figure 5.7. Thus, it can be seen that while the correlation of the sequence with itself corresponding to a lag of 0 is 1, for any other nonzero shift, it assumes a very low value of $-\frac{1}{N}$, which tends to the limit 0 as the spreading length $N \rightarrow \infty$. This autocorrelation property of the PN sequences can be summarized as follows.

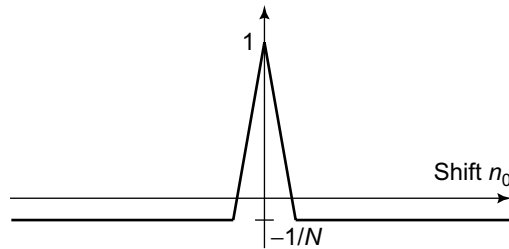


Figure 5.7 Autocorrelation of PN sequence

$$r_{00}(n_o) = \frac{1}{N} \sum_{i=0}^{N-1} = \begin{cases} 1 & \text{if } n_o = 0 \\ -\frac{1}{N} & \text{otherwise} \end{cases}$$

With this background, let us investigate the properties of random spreading sequences in the next section.

5.5 | Correlation Properties of Random CDMA Spreading Sequences

In the previous section, we have seen that CDMA spreading sequences can be chosen as PN sequences, which have noiselike properties. In other words, one can choose a chip sequence $c_k(i)$, $0 \leq i \leq N - 1$ for the user k such that $P(c_k(i) = +1) = P(c_k(i) = -1) = \frac{1}{2}$. Thus, we have,

$$E\{c_k(i)\} = \frac{1}{2} \times (+1) + \frac{1}{2} \times (-1) = 0.$$

Further, another important aspect is to choose such sequences as containing *Independent Identically Distributed (IID) chips*, i.e., satisfying the property

$$E\{c_k(i) c_k(j)\} = E\{c_k(i)\} E\{c_k(j)\} = 0 \times 0 = 0$$

The above property implies that each chip $c_k(i)$ is uncorrelated with chip $c_k(j)$. Further, one can choose independent sequences for different users, that is, to say

$$E\{c_k(i) c_l(j)\} = E\{c_k(i)\} E\{c_l(j)\}$$

Let us examine the correlation properties of such random spreading sequences. As before, let $r_{00}(k)$ denote the autocorrelation of the chip sequence of the user $k = 0$, corresponding to a lag $k \neq 0$. This can be expressed as

$$r_{00}(k) = \frac{1}{N} \sum_{i=0}^{N-1} c_0(i) c_0(i-k)$$

The average or expected valued of $r_{00}(k)$ can be seen to be given as

$$\begin{aligned} E\{r_{00}(k)\} &= E\left\{\frac{1}{N} \sum_{i=0}^{N-1} c_0(i) c_0(i-k)\right\} \\ &= \frac{1}{N} \sum_{i=0}^{N-1} E\{c_0(i) c_0(i-k)\} \end{aligned}$$

$$\begin{aligned}
&= \frac{1}{N} \sum_{i=0}^{N-1} E\{c_0(i)\} E\{c_0(i-k)\} \\
&= \frac{1}{N} \sum_{i=0}^{N-1} 0 = 0
\end{aligned}$$

Thus, the average value or the expected value of the correlation $E\{r_{00}(k)\}$ is zero for lags $k \neq 0$. This is expected from the random properties of the spreading sequence. To compute the variance of the autocorrelation $r_{00}(k)$, consider $r_{00}^2(k)$ given as

$$\begin{aligned}
r_{00}^2(k) &= \frac{1}{N^2} \left(\sum_{i=0}^{N-1} c_0(i) c_0(i-k) \right) \left(\sum_{j=0}^{N-1} c_0(j) c_0(j-k) \right) \\
&= \frac{1}{N^2} \sum_{i=0}^{N-1} \sum_{j=0}^{N-1} c_0(i) c_0(i-k) c_0(j) c_0(j-k)
\end{aligned}$$

Now, let us consider the quantity $c_0(i) c_0(i-k) c_0(j) c_0(j-k)$. It can be seen that if $i \neq j$, the expected value of this quantity can be simplified as

$$\begin{aligned}
E\{c_0(i) c_0(i-k) c_0(j) c_0(j-k)\} &= E\{c_0(i) c_0(i-k)\} E\{c_0(j) c_0(j-k)\} \\
&= E\{c_0(i)\} E\{c_0(i-k)\} E\{c_0(j)\} E\{c_0(j-k)\} \\
&= 0
\end{aligned}$$

On the other hand, if $i = j$, the same quantity can be simplified as

$$\begin{aligned}
E\{c_0(i) c_0(i-k) c_0(j) c_0(j-k)\} &= E\{c_0(i) c_0(i-k) c_0(i) c_0(i-k)\} \\
&= E\{(c_0(i))^2\} E\{(c_0(i-k))^2\} \\
&= 1 \times 1 = 1
\end{aligned}$$

Thus, the variance of $r_{00}(k)$, i.e., $E\{r_{00}^2(k)\}$ can be simplified as

$$E\{r_{00}^2(k)\} = \frac{1}{N^2} \sum_{i=0}^{N-1} \sum_{j=0}^{N-1} E\{c_0(i) c_0(i-k) c_0(j) c_0(j-k)\}$$

$$\begin{aligned}
&= \frac{1}{N^2} \sum_{i=0}^{N-1} \text{E} \{ c_0^2(i) c_0^2(i-k) \} \\
&= \frac{1}{N^2} \sum_{i=1}^{N-1} 1 = \frac{1}{N^2} \times N \\
&= \frac{1}{N}
\end{aligned}$$

Thus, the variance or basically the power of $r_{00}(k)$, the autocorrelation of the random CDMA spreading sequence is $\text{E} \{ r_{00}^2(k) \} = \frac{1}{N}$. Also, once again, the autocorrelation corresponding to a lag of $k = 0$ can be readily seen to be given as

$$\begin{aligned}
\text{E} \{ r_{00}(0) \} &= \text{E} \left\{ \frac{1}{N} \sum_{i=0}^{N-1} c_0(i) c_0(i) \right\} \\
&= \frac{1}{N} \sum_{i=0}^{N-1} \text{E} \{ c_0^2(i) \} \\
&= \frac{1}{N} \sum_{i=0}^{N-1} 1 \\
&= \frac{1}{N} \times N = 1
\end{aligned}$$

Therefore, one can succinctly summarize the autocorrelation properties of the random spreading sequence as follows. For $k = 0$, $r_{00}(k) = 1$. For $k \neq 0$, $r_{00}(k)$ is a random variable with $\text{E} \{ r_{00}(k) \} = 0$ and variance $\text{E} \{ r_{00}^2(k) \} = \frac{1}{N}$. Let us now examine the cross-correlation properties of the random CDMA spreading sequences, i.e., the correlation between the spreading sequences $c_0(i)$, $0 \leq i \leq N-1$ and $c_1(j)$, $0 \leq j \leq N-1$. We denote by $r_{01}(k)$ the cross-correlation between spreading sequences c_0 , c_1 corresponding to a lag k as

$$r_{01}(k) = \frac{1}{N} \sum_{i=0}^{N-1} c_0(i) c_1(i-k)$$

Once again, the expected value for any lag k can be computed as

$$\text{E} \{ r_{01}(k) \} = \frac{1}{N} \text{E} \left\{ \sum_{i=0}^{N-1} c_0(i) c_1(i-k) \right\}$$

$$\begin{aligned}
&= \frac{1}{N} \sum_{i=0}^{N-1} \mathbf{E} \{c_0(i) c_1(i-k)\} \\
&= \frac{1}{N} \sum_{i=0}^{N-1} \mathbf{E} \{c_0(i)\} \mathbf{E} \{c_1(i-k)\} \\
&= \frac{1}{N} \sum_{i=0}^{N-1} 0 \times 0 = 0
\end{aligned}$$

Further, the variance $\mathbf{E} \{r_{01}^2(k)\}$ for any delay k is given as

$$\begin{aligned}
\mathbf{E} \{r_{01}^2(k)\} &= \frac{1}{N^2} \mathbf{E} \left\{ \left(\sum_{i=0}^{N-1} c_0(i) c_1(i-k) \right) \left(\sum_{j=0}^{N-1} c_0(j) c_1(j-k) \right) \right\} \\
&= \frac{1}{N^2} \sum_{i=0}^{N-1} \sum_{j=0}^{N-1} \mathbf{E} \{c_0(i) c_1(i-k) c_0(j) c_1(j-k)\} \\
&= \frac{1}{N^2} \sum_{i=0}^{N-1} \mathbf{E} \{c_0^2(i)\} \mathbf{E} \{c_1^2(i-k)\} \\
&= \frac{1}{N^2} \sum_{i=0}^{N-1} 1 \\
&= \frac{1}{N^2} \times N = \frac{1}{N}
\end{aligned}$$

where we have again used the fact $\mathbf{E} \{c_0(i) c_1(i-k) c_0(j) c_1(j-k)\}$ is nonzero only if $i = j$ in the above derivation. Thus, once again, it can be seen that the cross-correlation $r_{01}(k)$ between two random CDMA spreading sequences $c_0 c_1$ is a random variable with $\mathbf{E} \{r_{01}(k)\} = 0$ and variance $\mathbf{E} \{r_{01}^2(k)\} = \frac{1}{N}$. Thus, unlike the codes introduced in Section 5.3, these random spreading codes do not satisfy the definition of *exact* orthogonality. However, they are *approximately orthogonal*, in that the average value of the correlation is zero and the power in the correlation is proportional to $\frac{1}{N}$ which tends to 0 as $N \rightarrow \infty$.

5.6 | Multi-User CDMA

Now let us analyze the performance of a multi-user CDMA system using the properties of the spreading sequences described above. Let a_0, a_1 denote the symbols of users 0, 1

respectively. Further, let the transmit powers of the users be denoted by $E\{|a_0|^2\} = P_0$ and $E\{|a_1|^2\} = P_1$. On the downlink, as described in Section 5.2, the signal $x_0(n)$ of the user 0 is derived by modulating the symbol a_0 with the spreading sequence $c_0(n)$ as

$$x_0(n) = a_0 c_0(n)$$

Similarly, the signal $x_1(n)$ is given as $x_1(n) = a_1 c_1(n)$. The net downlink multiplexed signal $x(n)$ is formed from the constituent signals $x_0(n)$, $x_1(n)$ as

$$x(n) = x_0(n) + x_1(n)$$

Assuming a simplistic AWGN channel model to begin with, the received signal at the user 0 is given in the presence of additive white Gaussian noise as

$$\begin{aligned} y(n) &= x(n) + w(n) \\ &= a_0 c_0(n) + a_1 c_1(n) + w(n) \end{aligned}$$

where the noise $w(n)$ is such that $E\{w(n)\} = 0$ and $E\{|w(n)|^2\} = \sigma_n^2$. Further, the whiteness property of the noise implies that $E\{w(n_1)w^*(n_2)\} = 0$ if $n_1 \neq n_2$. Again, as described already in Section 5.2, we correlate with the spreading code c_0 of the user 0 to recover the symbol of the user 0 as

$$\begin{aligned} d_0 &= \frac{1}{N} \sum_{i=0}^{N-1} y(n) c_0(n) \\ &= \underbrace{\frac{1}{N} \sum_{i=0}^{N-1} a_0 c_0(n) c_0(n)}_{\text{Desired user}} + \underbrace{\frac{1}{N} \sum_{i=0}^{N-1} a_1 c_1(n) c_0(n)}_{\text{Interferer}} + \underbrace{\frac{1}{N} \sum_{i=0}^{N-1} w(n) c_0(n)}_{\text{Noise}}, \end{aligned}$$

where the component $\frac{1}{N} \sum_{i=0}^{N-1} a_0 c_0(n) c_0(n)$ corresponds to the desired user signal when considering decoding at the user 0, while the component $\frac{1}{N} \sum_{i=0}^{N-1} a_1 c_1(n) c_0(n)$, which arises due to a_1 constitutes the *interference*, and is also termed *multi-user interference* in the context of CDMA. The last component $\frac{1}{N} \sum_{i=0}^{N-1} w(n) c_0(n)$ corresponds to the noise at the receiver. Below, we analyze and derive the statistical properties of each of the components described

above. We start with the signal of the desired user, which can be simplified as

$$\begin{aligned} \frac{1}{N} \sum_{i=0}^{N-1} a_0 c_0(n) c_0(n) &= a_0 \left(\frac{1}{N} \sum_{i=0}^{N-1} c_0(n) c_0(n) \right) \\ &= a_0 r_{00}(0) = a_0, \end{aligned}$$

where $r_{00}(0)$ corresponds to the autocorrelation of spreading code $c_0(n)$ of the user 0 for a delay $n_o = 0$, which was simplified above in Section 5.5. Hence, the desired signal power is given as $E\{|a_0|^2\} = P_0$. Next, we calculate the power in the multi-user interference component. This component, denoted by I_1 , i.e., interference from the user 1 can be simplified as

$$\begin{aligned} I_1 &= \frac{1}{N} \sum_{i=0}^{N-1} a_1 c_1(n) c_0(n) \\ &= a_1 \left(\frac{1}{N} \sum_{i=0}^{N-1} c_1(n) c_0(n) \right) \\ &= a_1 r_{01}(0) \end{aligned}$$

Hence, the interference power $E\{|I_1|^2\}$ can be simplified as

$$\begin{aligned} E\{|I_1|^2\} &= E\{|a_1 r_{01}(0)|^2\} \\ &= E\{|a_1|^2\} E\{|r_{01}(0)|^2\} \\ &= P_1 \times \frac{1}{N} = \frac{P_1}{N}. \end{aligned}$$

Thus, unlike the previous cases described in Eqs (5.4) and (5.5), the interference from the user 1 is not exactly zero due to the *approximate* orthogonality of the random spreading codes as described in Section 5.5. However, the interference power decays as $\frac{1}{N}$, which is significantly small for large values of spreading length N . The noise power can be calculated as follows. Let \tilde{w}_0 denote the noise, i.e.,

$$\tilde{w}_0 = \frac{1}{N} \sum_{i=0}^{N-1} w(n) c_0(n)$$

It can be readily seen that \tilde{w}_0 is a linear combination of Gaussian noise components $w(n)$ and is, therefore, Gaussian in nature. Further, the expected or average value of \tilde{w}_0 can be obtained as

$$\begin{aligned} E\{\tilde{w}_0\} &= E\left\{\frac{1}{N}\sum_{i=0}^{N-1}w(n)c_0(n)\right\} \\ &= \frac{1}{N}\sum_{i=0}^{N-1}E\{w(n)\}c_0(n) \\ &= \frac{1}{N}\sum_{i=0}^{N-1}0\times c_0(n) \\ &= 0 \end{aligned}$$

Thus, the average value of the noise is 0. Also, the average power in the noise can be calculated as

$$\begin{aligned} E\{|\tilde{w}_0|^2\} &= E\left\{\frac{1}{N^2}\left(\sum_{n=0}^{N-1}w(n)c_0(n)\right)\left(\sum_{m=0}^{N-1}w^*(m)c_0^*(m)\right)\right\} \\ &= \frac{1}{N^2}\sum_{n=0}^{N-1}\sum_{m=0}^{N-1}E\{w(n)c_0(n)w^*(m)c_0^*(m)\} \\ &= \frac{1}{N^2}\sum_{n=0}^{N-1}E\{|w_0(n)|^2|c_0(n)|^2\} \\ &= \frac{1}{N^2}\sum_{n=0}^{N-1}\sigma_n^2 = \frac{1}{N^2}\times N\sigma_n^2 \\ &= \frac{\sigma_n^2}{N} \end{aligned} \tag{5.8}$$

In the above simplification, we have used the fact that the noise samples $w(n)$ are uncorrelated. Therefore, if $n \neq m$, we have

$$\begin{aligned} E\{w(n)c_0(n)w^*(m)c_0^*(m)\} &= E\{w(n)\}E\{w^*(m)\}c_0(n)c_0^*(m) \\ &= 0 \times 0 \times c_0(n)c_0^*(m) = 0 \end{aligned}$$

Thus, the effective noise power is $\frac{1}{N}\sigma_n^2$. Hence, for the above CDMA scenario, one can define the *Signal-to-Interference-Noise power Ratio (SINR)* as

$$\begin{aligned}\text{SINR} &= \frac{\text{Signal Power}}{\text{Interference Power} + \text{Noise Power}} \\ &= \frac{P_0}{\frac{P_1}{N} + \frac{\sigma_n^2}{N}} \\ &= N \times \frac{P_0}{P_1 + \sigma_n^2}\end{aligned}\quad (5.9)$$

From the above expression, it can be clearly seen that the signal power is reduced at the receiver not only due to the noise but also due to the interference. Hence, CDMA is an *interference-limited* system, due which the interference power has to be managed for better performance. Also, notice that there is a factor of N in the numerator, which arises because the interference and noise power is suppressed by a factor of N . This is termed the *spreading gain* of the CDMA system, which is equal to the spreading length.

The above expression in Eq. (5.9) for SINR in a CDMA network can be generalized to the context of greater and two users. Consider $K + 1$ CDMA users $0, 1, \dots, K$ transmitting with powers P_0, P_1, \dots, P_K respectively on codes $c_0(n), c_1(n), \dots, c_K(N)$. Hence, the received signal $y(n)$ is given as

$$\begin{aligned}y(n) &= a_0 c_0(n) + a_1 c_1(n) + \dots + a_K c_K(n) + w(n), \\ &= \sum_{k=0}^K a_k c_k(n) + w(n)\end{aligned}$$

The corresponding SINR after for the user 0 after correlating and decoding with the spreading code $c_0(n)$ corresponding to the user 0 can be similarly obtained as

$$\begin{aligned}\text{SINR} &= \frac{P_0}{\frac{P_1}{N} + \frac{P_2}{N} + \dots + \frac{P_K}{N} + \frac{\sigma_n^2}{N}} \\ &= N \times \frac{P_0}{\sum_{k=0}^K P_k + \sigma_n^2}\end{aligned}\quad (5.10)$$

5.7 | Advantages of CDMA

In this section, we systematically investigate the advantages of CDMA-based cellular systems over 1G FDMA and 2G TDMA based cellular systems.

5.7.1 Advantage 1: Jammer Margin

An important advantage of CDMA over conventional cellular systems is *jammer* suppression. A *jammer* is basically a malicious user in a communication network who transmits with a very high power to cause interference, thus leading to disruption of communication links. This is shown schematically in Figure 5.8. Jammers are of significant concern, especially in the context of highly secure communication systems such as those used for military and defense purposes. The effect of jammer suppression in a CDMA system can be understood as follows. Consider a communication system in which the signal $x(n)$ of the power P is received in the presence of additive white Gaussian noise $w(n)$ of power σ_w^2 . The baseband system model for this communication system can be expressed as

$$y(n) = x(n) + w(n)$$

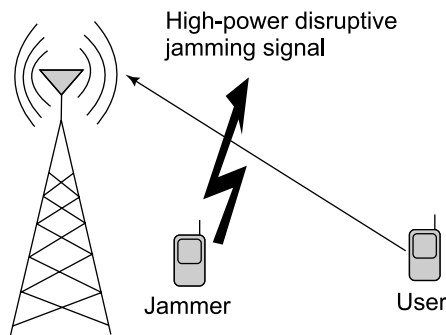


Figure 5.8 Disruption by jammer in wireless communication

Hence, the SNR at the receiver is $\text{SNR} = \frac{P}{\sigma_w^2}$. However, in the presence of a jamming signal $x_j(n)$ of power P_j , the received signal $y(n)$ is

$$y(n) = x(n) + x_j(n) + w(n)$$

Thus, the jammer interferes with the signal reception and the signal-to-interference-noise power ratio (SINR) can be calculated as $\text{SINR} = \frac{P}{P_j + \sigma_w^2}$. Thus, the jammer has a significant disruptive impact on the communication signal. Consider now a CDMA system in which the transmitted signal $x(n)$ is a spread-spectrum signal. As shown in the section above, the SINR

for a CDMA scenario is given as

$$\text{SINR} = \frac{P}{\frac{P_j}{N} + \frac{\sigma_w^2}{N}} \quad (5.11)$$

Thus, it can be seen that the jamming power P_j is suppressed by a factor of N . Moreover, as the spreading factor N increases, the jammer suppression increases, minimizing the impact of the jammer on the communication system. This is termed *jammer suppression* in CDMA systems. Hence, CDMA which is inherently tolerant to jamming attacks is highly attractive for defense applications. In fact, the earliest applications of CDMA were in the context of tactical military secure communications, which were resistant to attacks by jammers. Only later were the benefits of CDMA realized and applied in the context of civilian cellular networks. Also, it is worthwhile noting that the gain of N in this context of jammer suppression is also termed the *jammer margin*. Thus, the jammer margin is equal to N , i.e., the spreading length of the CDMA codes.

5.7.2 Advantage 2: Graceful Degradation

Graceful degradation is another key property of CDMA-based wireless networks and as we shall see soon, allows for much more efficient interference management, which ultimately leads to universal frequency reuse and higher spectral efficiency. Consider the expression for the SINR at the user 0 derived in Eq. (5.10). At this point, assume that another user, i.e., a user with index $K + 1$ joins the network. Let P_{K+1} denote the corresponding transmission power of this $(K + 1)^{\text{th}}$ user and a_{K+1} , $c_{K+1}(n)$ denote his transmitted symbol and spreading code respectively. The SINR of the user 0 now changes to

$$\begin{aligned} \text{SINR} &= \frac{P_0}{\frac{P_1}{N} + \frac{P_2}{N} + \dots + \frac{P_K}{N} + \frac{P_{K+1}}{N} + \frac{\sigma_n^2}{N}} \\ &= N \times \frac{P_0}{\sum_{k=0}^{K+1} P_k + \sigma_n^2} \end{aligned}$$

Thus, the addition of a new user $K + 1$ with power P_{K+1} only causes an incremental interference of $\frac{P_{K+1}}{N}$ at the user 0. Further, in general, at any user $i \neq (K + 1)$, the additional interference due to the introduction of this new user is $\frac{P_{K+1}}{N}$. Therefore, the addition of the new user $K + 1$ does not adversely affect any single user. Rather, the additional interference caused by this new user is *shared* amongst all the existing users in the system leading to *interference distribution*. This sharing of the interference by all the existing users leads to

a *graceful degradation* of the SINR at each user. This is termed the *graceful degradation property of CDMA systems*. This idea of graceful degradation is key to understanding the big advantage of CDMA networks, i.e., *universal frequency reuse*, which is described next.

5.7.3 Advantage 3: Universal Frequency Reuse

To understand the concept of universal frequency reuse, we have to begin by understanding the frequency allocation in convention, i.e., 1G and 2G cellular systems. Consider a cellular network organized into cells as shown in Figure 5.9. Consider two adjacent cells C_0 , C_1 shown in the figure. Assume now that the same frequency f is allotted for transmission to users in both C_0 , C_1 . Let $x_0(n)$ with power P_0 denote the signal of the user on the frequency f in the cell 0, while $x_1(n)$ with power P_1 denotes the signal of the user in the cell 1. Since both the signals are being transmitted on the identical frequency f , they will interfere with each other. More specifically, the received signal $y_0(n)$ at the user 0 is given as

$$y_0(n) = \underbrace{x_0(n)}_{\text{Signal}} + \underbrace{x_1(n)}_{\text{Interferer from } C_1} + \underbrace{w(n)}_{\text{Noise}}$$

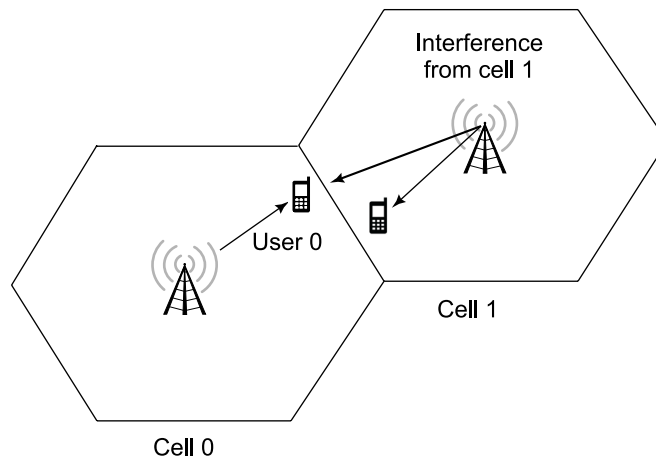


Figure 5.9 Intercell interference for the user 0 on the cell edge

Hence, the SINR at the user 0 is given as $\text{SINR} = \frac{P_0}{P_1 + \sigma_w^2}$. This is similar to the jamming interference case described in Eq. (5.11). Thus, if the same frequency f is allocated in adjacent cells, it will cause heavy interference and degradation of user SINR results from adjacent cell

interference. Thus, in a typical 1G or 2G cellular network such as GSM, only a fraction of the total available frequencies are allocated in each cell, carefully avoiding the allocation of the same frequency in adjacent cells. For instance, as can be seen from the hexagonal-lattice-based cellular structure in Figure 5.10, each hexagonal cell has 6 neighbours. Hence, to avoid adjacent cell interference, any of the frequencies allocated to C_0 cannot be allocated to its neighbours C_1, C_2, \dots, C_6 . This holds true for all the cells in the network. Hence, only $\frac{1}{7}$ of the total available frequency bands can be allocated to each cell. This factor $\frac{1}{7}$ is termed the *frequency-reuse factor* of the cellular network. Thus, since only a fraction of the frequencies are used in the cell, the total spectral efficiency is proportional to the frequency-reuse factor, resulting in a rate which is $\frac{1}{7}$ compared to that of using all the available bandwidth, since the capacity is linearly related to bandwidth.

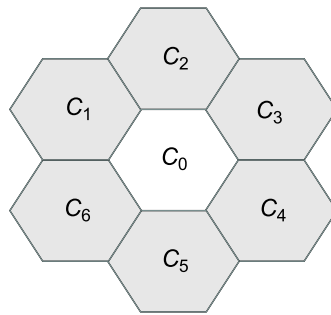


Figure 5.10 Grid or lattice of hexagonal cells

However, now consider the same scenario in the context of a CDMA network. Again, assume that the same frequency f is allotted for transmission to users in both C_0, C_1 . However, let $x_0(n)$ with power P_0 is now transmitted on code $c_0(n)$, while $x_1(n)$ with power P_1 is transmitted in the cell 1 on the random code $c_1(n)$. Hence, now similar to the jammer scenario in a CDMA system, the interference caused by the user on the identical frequency f in the adjacent cell is now reduced by a factor of N to $\frac{P_1}{N}$. Therefore, the SINR is now given as,

$$\text{SINR} = \frac{P_0}{\frac{P_1}{N} + \frac{\sigma_w^2}{N}}$$

This is the result of graceful degradation described in the previous advantage in Section 5.7.2. Thus, the interference of each user is limited to a fraction $\frac{1}{N}$ of the interferer power. Hence, basically the jammer margin in defence applications, can be used for adjacent cell interference power suppression in modern cellular networks! This is a great advantage of CDMA, which

implies that the same frequency bands can be used in all cells across the network. Another way of stating this is that the fraction of bands used in each cell is 1, i.e., all the bands. Therefore, this is termed *universal frequency reuse* or equivalently, as a cellular network with *frequency reuse factor 1*. Thus, compared to GSM, which uses only $\frac{1}{7}$ of the frequency bands in each cell, CDMA can use all the available frequency bands in each cell. This right away leads to an increase of the spectral efficiency and resulting capacity by a factor of 7. Thus, CDMA-based cellular networks have a much higher capacity compared to conventional 1G and 2G cellular networks. This has led to a widespread adoption and embrace of CDMA-based technologies for mobile communication.

5.7.4 Multipath Diversity and Rake Receiver

Another important advantage of CDMA is its ability to achieve diversity gain via multipath scatter components. This is termed *multipath diversity* and is achieved through coherent combining of the multipath-signal components employing a *rake* receiver. Consider a multipath frequency-selective channel with several delayed signal paths. We have seen in earlier chapters that such a multipath frequency-selective channel can be modelled as a *Finite Impulse Response (FIR)* channel filter with channel taps $h(0), h(1), \dots, h(L-1)$. The received symbol $y(n)$ can be expressed as

$$\begin{aligned} y(n) &= h(0)x(n) + h(1)x(n-1) + \dots + h(L-1)x(n-L+1) + w(n) \\ &= \sum_{l=0}^{L-1} h(l)x(n-l) + w(n) \end{aligned}$$

Recall that this represents a frequency-selective or intersymbol interference-limited channel since the current output $y(n)$ depends not only on the current symbol $x(n)$, but also $L-1$ previous input symbols $x(n), x(n-1), \dots, x(n-L+1)$. Consider now a CDMA signal in which $x(n) = a_0 c_0(n)$. To simplify this illustration, we currently consider a single user and this can be readily extended to multi-user scenarios as will be seen in the subsequent sections. Substituting this in the expression for $y(n)$ above, the received signal across a frequency-selective channel in a CDMA system is given as

$$y(n) = \sum_{l=0}^{L-1} h(l) a_0 c_0(n-l) + w(n)$$

As done previously, let us correlate with $c_0(n)$ to recover the symbol corresponding to the user 0. This operation can be expressed as

$$\begin{aligned}
 d(0) &= \frac{1}{N} \sum_{n=0}^{N-1} y(n) c_0^*(n) \\
 &= \frac{1}{N} \sum_{n=0}^{N-1} \left(\sum_{l=0}^{L-1} h(l) a_0 c_0(n-l) + w(n) \right) c_0^*(n) \\
 &= \frac{1}{N} \sum_{n=0}^{N-1} \sum_{l=0}^{L-1} h(l) a_0 c_0(n-l) c_0^*(n) + \underbrace{\frac{1}{N} \sum_{n=0}^{N-1} w(n) c_0^*(n)}_{\tilde{w}_0}
 \end{aligned}$$

Recall from the analysis in Eq. (5.8) that the noise \tilde{w}_0 is Gaussian of power $E\{\|\tilde{w}_0\|^2\} = \frac{\sigma_w^2}{N}$. The first term in the above expression can be split into two components: one corresponding to $l = 0$ and the other corresponding to $l \neq 0$. Simplifying, we have

$$\begin{aligned}
 d(0) &= \frac{1}{N} \sum_{n=0}^{N-1} h(0) a_0 c_0(n) c_0^*(n) + \frac{1}{N} \sum_{l=1}^{L-1} \sum_{n=0}^{N-1} h(l) a_0 c_0(n-l) c_0^*(n) + \tilde{w}_0 \\
 &= h(0) a_0 \left(\frac{1}{N} \sum_{n=0}^{N-1} c_0(n) c_0^*(n) \right) + a_0 \sum_{l=1}^{L-1} h(l) \left(\frac{1}{N} \sum_{n=0}^{N-1} c_0(n-l) c_0^*(n) \right) + \tilde{w}_0 \\
 &= h(0) a_0 r_{00}(0) + a_0 \sum_{l=1}^{L-1} h(l) r_{00}(l) + \tilde{w}_0
 \end{aligned}$$

At this point, we will employ the following simplifying approximation. Consider the quantity $r_{00}(l)$. As demonstrated in Section 5.5, for $l \neq 0$, $r_{00}(l)$ is a random variable with mean 0 and power $\frac{1}{N}$. Observe that the power tends to 0 as $N \rightarrow \infty$. Hence, for large values of N , $r_{00}(l) \approx 0$. Employing this approximation in the above expression, and noting that $r_{00}(0) = 1$, we have

$$d(0) = h(0) a_0 + \tilde{w}_0$$

Observe now a very interesting property. Even though there is intersymbol interference in the above channel, we are able to extract the signal corresponding to $h(0)$, i.e., delay 0 by correlation with the spreading code $c_0(n)$. This is once again because of the approximate orthogonality property that was introduced in the previous sections. Moreover, interestingly,

one can repeat this process by individually correlating with delayed versions of the spreading sequence $c_0(n-v)$, $1 \leq v \leq L-1$ to extract the multipath components corresponding to $h(1), h(2), \dots, h(L-1)$. Thus, correlating with $c_0(n-v)$, the resulting statistic $d(v)$ can be simplified as,

$$\begin{aligned} d(v) &= \frac{1}{N} \sum_{n=0}^{N-1} y(n) c_0^*(n-v) \\ &= \frac{1}{N} \sum_{n=0}^{N-1} \left(\sum_{l=0}^{L-1} h(l) a_0 c_0(n-l) + w(n) \right) c_0^*(n-v) \\ &= \frac{1}{N} \sum_{n=0}^{N-1} \sum_{l=0}^{L-1} h(l) a_0 c_0(n-l) c_0^*(n-v) + \underbrace{\frac{1}{N} \sum_{n=0}^{N-1} w(n) c_0^*(n-v)}_{\tilde{w}_v} \end{aligned}$$

Once again, it can be easily seen that the noise \tilde{w}_v is Gaussian with variance $E\{|\tilde{w}_v|^2\} = \frac{\tilde{w}_v^2}{N}$. Further, splitting the first term into two components corresponding to $l=v$ and $l \neq v$, one can derive the expression for $d(v)$, $1 \leq v \leq L-1$ as

$$\begin{aligned} d(v) &= \frac{1}{N} \sum_{n=0}^{N-1} h(v) a_0 c_0(n-v) c_0^*(n-v) \\ &\quad + \frac{1}{N} \sum_{l=0, l \neq v}^{L-1} \sum_{n=0}^{N-1} h(l) a_0 c_0(n-l) c_0^*(n-v) + \tilde{w}_v \\ &= h(0) a_0 \left(\frac{1}{N} \sum_{n=0}^{N-1} c_0(n-v) c_0^*(n-v) \right) \\ &\quad + a_0 \sum_{l=0, l \neq v}^{L-1} h(l) \left(\frac{1}{N} \sum_{n=0}^{N-1} c_0(n-l) c_0^*(n-v) \right) + \tilde{w}_v \\ &= h(v) a_0 r_{00}(0) + a_0 \sum_{l=1}^{L-1} h(l) r_{00}(l-v) + \tilde{w}_v \\ &\approx h(v) a_0 + \tilde{w}_v \end{aligned}$$

where we have again employed the approximation $r_{00}(l-v) \approx 0$, $l \neq v$ in the above simplification. Now, one can process that extracted components $d(0), d(1), \dots, d(L-1)$

as follows. Employing vector notation, the components can be expressed as

$$\underbrace{\begin{bmatrix} d(0) \\ d(1) \\ \vdots \\ d(L-1) \end{bmatrix}}_{\mathbf{d}} = \underbrace{\begin{bmatrix} h(0) \\ h(1) \\ \vdots \\ h(L-1) \end{bmatrix}}_{\mathbf{h}} a_0 + \underbrace{\begin{bmatrix} \tilde{w}_0 \\ \tilde{w}_1 \\ \vdots \\ \tilde{w}_{L-1} \end{bmatrix}}_{\tilde{\mathbf{w}}}$$

It can be readily seen that the above system is now similar to the multiple receive antenna system, i.e., receive diversity system with channel coefficients $h(0), h(1), \dots, h(L-1)$. The model can be, therefore, be succinctly expressed in vector notation as

$$\mathbf{d} = \mathbf{h}a_0 + \tilde{\mathbf{w}}$$

Hence, the optimal combiner is the *Maximum Ratio Combiner (MRC)* given by $\frac{\mathbf{h}}{\|\mathbf{h}\|}$. Also observe that the power of each noise component \tilde{w}_v is $E\{|\tilde{w}_v|^2\} = 1$. Denoting the symbol power $E\{|a_0|^2\}$ by P and combining the observation vector \mathbf{d} with the MRC yields the SNR

$$\begin{aligned} \text{SNR} &= \frac{\|\mathbf{h}\|^2 P}{\frac{\sigma_w^2}{N}} \\ &= N \times \underbrace{\left(|h(0)|^2 + |h(1)|^2 + \dots + |h(L-1)|^2 \right)}_{\|\mathbf{h}\|^2} \frac{P}{\sigma_w^2} \end{aligned}$$

Observe that the above expression is similar to the SNR for the multiple receive antenna system, in that there is a factor $\|\mathbf{h}\|^2$ in the numerator, where \mathbf{h} is the vector of frequency-selective channel coefficients $\mathbf{h} = [h(0), h(1), \dots, h(L-1)]^T$. This is in addition to the spreading gain factor N . Thus, this is equivalent to the performance of a system with diversity order L . This is the essence of multipath diversity and CDMA is able to exploit this multipath diversity by correlating with the spreading code $c_0(n-v)$ corresponding to different lags $0 \leq v \leq L-1$, and combining the individual components employing MRC. This receiver structure in CDMA is termed the *rake receiver* and the diversity gain thus achieved is termed *multipath diversity* since it is extracted from the multipath components. This multipath diversity arising out of rake combining is a unique feature of CDMA and

significantly improves its performance over wireless channels because of the higher diversity order of decoding.

5.8 | CDMA Near-Far Problem and Power Control

In this section, we introduce a unique aspect of the CDMA systems which is termed the *near-far* problem. Recall from Eq. (5.9) that the SINR at the user 0 of a 2 user CDMA system is given as,

$$\text{SINR} = \frac{P_0}{\frac{P_1}{N} + \frac{\sigma_n^2}{N}} \quad (5.12)$$

Consider, now a scenario where the user 1 is much closer to the base station than the user 0 as

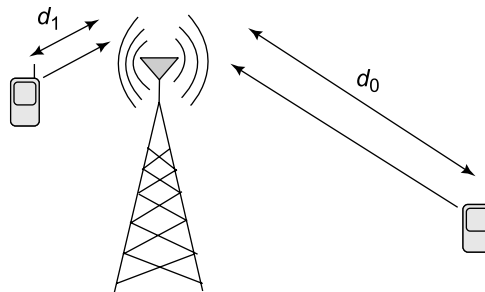


Figure 5.11 Near-far problem in CDMA networks

shown in Figure 5.11. Specifically, let $d_0 = \sqrt{N}d_1$. Let the transmitted power of each user at the base station be denoted by P_T . Since the radiated electromagnetic power decays at the rate of d^2 in free space, we have,

$$P_1 = \frac{P_T}{d_0^2} = \frac{P_T}{Nd_1^2}$$

$$P_0 = \frac{P_T}{d_1^2}$$

Substituting the values of P_0 , P_1 from above in the SINR expression in Eq. (5.12), we have

$$\begin{aligned} \text{SINR} &= \frac{\frac{P_T}{Nd_1^2}}{\frac{P_T}{Nd_1^2} + \frac{\sigma_n^2}{N}} \\ &= \frac{P_T}{P_T + d_1^2 \sigma_n^2} \end{aligned}$$

Thus, the above expression yields the surprising result that both the signal and interference power at the user 0 are of the same magnitude and the effect of the spreading gain N is lost. This phenomenon arises because the user 1, who is closer to the base station, *drowns out* the power of the user 0, i.e., there is heavy interference at the user 0. This is the *near-far problem* in CDMA systems. To avoid this near-far problem, the power that is transmitted to the different users has to be regulated in CDMA systems, i.e., lower power has to be transmitted to users closer to the base station such as the user 1, while transmitting at a higher power to users farther away such as the user 0. This is termed *power control* in CDMA systems. Power control is a very important aspect of any CDMA wireless network as CDMA systems are *interference limited* as described already in Section 5.6.

5.9 | Performance of CDMA Downlink Scenario with Multiple Users

This section will focus on developing a detailed analysis towards the characterization of downlink performance of a CDMA cellular system with multiple users. Consider the downlink scenario schematically shown in Figure 5.12, where the CDMA base station is transmitting to $K + 1$ users indexed $0, 1, \dots, K$. Let the information symbols transmitted to the $K + 1$ users be a_0, a_1, \dots, a_{K+1} . Let $c_0(n), c_1(n), \dots, c_{K+1}(n)$ be the spreading codes corresponding to the $K + 1$ users. Thus, the individual transmit signal $x_k(m)$, $0 \leq k \leq K$ is formed by $x_k(m) = a_k c_k(m)$. The composite signal corresponding to all the users is obtained by adding the individual signals corresponding to the $K + 1$ users, similar to Eq. (5.3) as

$$\begin{aligned} x(n) &= x_0(n) + x_1(n) + \dots + x_K(n) \\ &= \sum_{k=0}^K x_k(n) \\ &= \sum_{k=0}^K a_k c_k(n) \end{aligned} \tag{5.13}$$

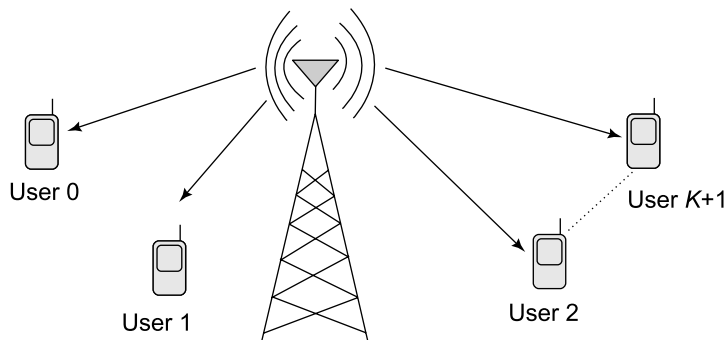


Figure 5.12 CDMA downlink scenario

Similar to the rake-receiver scenario described in Section 5.7.4, let the frequency selective channel between the base station and user 0 be characterized by the channel taps $h_0(0), h_0(1), \dots, h_0(L-1)$. The 0 in the subscript of the channel taps now denotes that this corresponds to the channel of the user 0 to distinguish it from the channels corresponding to the rest of the users. Thus, the intersymbol-interference-affected received symbol $y_0(n)$ at the user 0 corresponding to time instant n is given as

$$\begin{aligned} y(n) &= h_0(0)x(n) + h_0(1)x(n-1) + \dots + h_0(L-1)x(n-L+1) + w(n) \\ &= \sum_{l=0}^{L-1} h_0(l)x(n-l) + w(n) \end{aligned}$$

Substituting now the expression for the composite downlink signal $x(n)$ as $x(n) = \sum_{k=0}^K x_k(n) = \sum_{k=0}^K a_k c_k(n)$, one can write the expression for $y(n)$ as

$$y(n) = \underbrace{\sum_{l=0}^{L-1}}_{\text{Multipath}} \underbrace{\sum_{k=0}^K}_{\text{users}} h_0(l) a_k c_k(n-l) + w(n) \quad (5.14)$$

where the first summation above is with respect to the multipath components and the second is with respect to the $K+1$ users. Thus, since the signal of each user gives rise to L multipath components, there are a total of $(K+1)L$ multipath components in the above expression. These correspond to L components of the desired user 0 (for decoding at the user 0) and KL interfering components of the rest of the K users. Consider now correlation with the spreading code $c_0(n)$ corresponding to the user 0. The statistic $d_0(0)$, i.e., at the user 0 corresponding to

a lag of 0 can be expressed as

$$\begin{aligned} d_0(0) &= \frac{1}{N} \sum_{n=0}^{N-1} y(n) c_0^*(n) \\ &= \frac{1}{N} \sum_{n=0}^{N-1} \sum_{l=0}^{L-1} \sum_{k=0}^K h_0(l) a_k c_k(n-l) c_0^*(n) + \underbrace{\frac{1}{N} \sum_{n=0}^{N-1} w(n) c_0^*(n)}_{\tilde{w}_0(0)} \end{aligned}$$

where the noise $\tilde{w}_0(0)$ denotes the noise at the user 0 corresponding to decorrelation with lag 0, i.e., spreading code $c_0(n)$. Once again, similar to the situation in Eq. (5.8), it can be seen that the noise power is $E\{|\tilde{w}_0(0)|^2\} = \frac{\sigma_w^2}{N}$. Further, the first part comprising of the total $(K+1)L$ multipath components can be decomposed into three parts. The first comprising of the component corresponds to $k=0$ and $l=0$, i.e., the user 0 and delay 0. The second corresponds to $k=0$ and $l \neq 0$, i.e., all the other multipath components corresponding to user 0, which comprise the *Multipath Interference* (MPI) at the user 0. The third corresponds to $k \neq 0$, i.e., $1 \leq k \leq K$ and all l , i.e., $0 \leq l \leq L-1$, which are basically the multipath components of all users other than the desired user 0 and total KL in numbers. These constitute the *Multi-User Interference* (MUI) at the user 0. The MPI and MUI together constitute the total *interference* at the user 0. The above equation can, therefore, be written as

$$\begin{aligned} d_0(0) &= \frac{1}{N} \sum_{n=0}^{N-1} \sum_{l=0}^{L-1} \sum_{k=0}^K h_0(l) a_k c_k(n-l) c_0^*(n) + \underbrace{\frac{1}{N} \sum_{n=0}^{N-1} w(n) c_0^*(n)}_{\tilde{w}_0(0)} \\ &= \frac{1}{N} \underbrace{\sum_{n=0}^{N-1} h_0(0) a_0 c_0(n) c_0^*(n)}_{k=0, l=0} + \frac{1}{N} \underbrace{\sum_{n=0}^{N-1} \sum_{l=1}^{L-1} h_0(l) a_0 c_0(n-l) c_0^*(n)}_{\text{MPI: } k=0, l \neq 0} \\ &\quad + \frac{1}{N} \underbrace{\sum_{n=0}^{N-1} \sum_{l=0}^{L-1} \sum_{k=1}^K h_0(l) a_k c_k(n-l) c_0^*(n)}_{\text{MUI: } k \neq 0} + \tilde{w}_0(0) \end{aligned} \tag{5.15}$$

The above expression can be further simplified in terms of the correlation between the spreading sequences as

$$\begin{aligned}
d_0(0) &= h_0(0) a_0 \underbrace{\left(\frac{1}{N} \sum_{n=0}^{N-1} c_0(n) c_0^*(n) \right)}_{r_{00}(0)} + a_0 \sum_{l=1}^{L-1} h_0(l) \underbrace{\left(\frac{1}{N} \sum_{n=0}^{N-1} c_0(n-l) c_0^*(n) \right)}_{r_{00}(l)} \\
&+ \sum_{l=0}^{L-1} \sum_{k=1}^K h_0(l) a_k \underbrace{\left(\frac{1}{N} \sum_{n=0}^{N-1} c_k(n-l) c_0^*(n) \right)}_{r_{k0}(l)} + \tilde{w}_0(0) \\
&= \underbrace{h_0(0) a_0 r_{00}(0)}_{\text{Signal}} + \underbrace{a_0 \sum_{l=1}^{L-1} h_0(l) r_{00}(l) + \sum_{l=0}^{L-1} \sum_{k=1}^K h_0(l) a_k r_{k0}(l)}_{\text{Interference}} + \underbrace{\tilde{w}_0(0)}_{\text{noise}}
\end{aligned}$$

For additional clarity, the *signal*, *interference*, and *noise* terms have been explicitly marked in the above expression. Since the correlation $r_{00}(0) = 1$, the signal component in the above expression is

$$\text{Signal} = h_0(0) a_0 r_{00}(0) = h_0(0) a_0$$

Further, the power in the MultiPath Interference (MPI) component is

$$\begin{aligned}
\underbrace{\mathbb{E} \left\{ |\text{MPI}|^2 \right\}}_{I_{\text{MPI}}^0} &= \mathbb{E} \left\{ \left| a_0 \sum_{l=1}^{L-1} h_0(l) r_{00}(l) \right|^2 \right\} \\
&= \mathbb{E} \left\{ |a_0|^2 \right\} \sum_{l=1}^{L-1} \mathbb{E} \left\{ |h_0(l)|^2 \right\} \mathbb{E} \left\{ |r_{00}(l)|^2 \right\} \\
&= \frac{P_0}{N} \sum_{l=1}^{L-1} \mathbb{E} \left\{ |h_0(l)|^2 \right\} \tag{5.16}
\end{aligned}$$

where we have used the properties that the power of the user 0 is $\mathbb{E} \left\{ |a_0|^2 \right\} = P_0$ and $\mathbb{E} \left\{ |r_{00}(l)|^2 \right\} = \frac{1}{N}$. Interestingly, one can notice from the above expression that the multipath interference power above increases with the signal power P_0 . Thus, increasing the signal power at the base station also potentially increases the interference power. This is a unique property of *interference-limited* systems such as CDMA. The above relation for MPI power can be further

simplified as

$$\begin{aligned} I_{\text{MPI}}^0 &= \frac{P_0}{N} \left(\sum_{l=0}^{L-1} \text{E} \left\{ |h_0(l)|^2 \right\} - \text{E} \left\{ |h_0(0)|^2 \right\} \right) \\ &= \frac{P_0}{N} \|\mathbf{h}_0\|^2 - \frac{P_0}{N} |h_0(0)|^2 \end{aligned}$$

where $\|\mathbf{h}_0\|^2$ is defined as the *norm of the channel-impulse response vector* \mathbf{h}_0 , i.e.,

$$\|\mathbf{h}_0\|^2 = |h_0(0)|^2 + |h_0(1)|^2 + \dots + |h_0(L-1)|^2$$

Also, the power of the multiuser interference (MUI) component can be simplified as

$$\begin{aligned} \underbrace{\text{E} \left\{ |\text{MUI}|^2 \right\}}_{I_{\text{MUI}}^0} &= \text{E} \left\{ \left| \sum_{l=0}^{L-1} \sum_{k=1}^K h_0(l) a_k r_{k0}(l) \right|^2 \right\} \\ &= \sum_{k=1}^K \sum_{l=0}^{L-1} \text{E} \left\{ |a_k|^2 \right\} \text{E} \left\{ |h_0(l)|^2 \right\} \text{E} \left\{ |r_{k0}(l)|^2 \right\} \\ &= \sum_{k=1}^K \sum_{l=0}^{L-1} P_k \text{E} \left\{ |h_0(l)|^2 \right\} \frac{1}{N} \\ &= \frac{1}{N} \left(\sum_{l=0}^{L-1} |h_0(l)|^2 \right) \left(\sum_{k=1}^K P_k \right) \\ &= \frac{1}{N} \|\mathbf{h}_0\|^2 \left(\sum_{k=1}^K P_k \right) \end{aligned}$$

The statistic $d_0(0)$, i.e., at the user 0 derived by correlating with $c_0(n)$, i.e., corresponding to a lag of 0 can be expressed as

$$d_0(0) = h_0(0) a_0 + I^0$$

where the total interference plus noise power I^0 can be written as

$$\begin{aligned} I^0 &= I_{\text{MPI}}^0 + I_{\text{MUI}}^0 + \frac{\sigma_w^2}{N} \\ &= \frac{1}{N} \|\mathbf{h}_0\|^2 \left(\sum_{k=0}^K P_k \right) - \frac{1}{N} P_0 |h_0(0)|^2 + \frac{\sigma_w^2}{N} \end{aligned}$$

Also, similar to the rake receiver in Section 5.7.4, one can now correlate with other delayed versions of the spreading sequence $c_0(n)$ such as $c_0(1)$, $c_0(2)$, \dots , $c_0(L-1)$, corresponding to lags of $1, 2, \dots, L-1$. The resulting decision statistics $d_0(1)$, $d_0(2)$, \dots , $d_0(L-1)$, along with $d_0(0)$ can be summarized as

$$d_0(0) = h_0(0) a_0 + I^0$$

$$d_0(1) = h_0(1) a_0 + I^1$$

$$\vdots$$

$$d_0(L-1) = h_0(L-1) a_0 + I^{L-1}$$

Hence, one can perform maximum ratio combining across the statistics $d_0(0)$, $d_0(1)$, \dots , $d_0(L-1)$ to yield the decision statistic

$$\begin{aligned} d &= \frac{h_0^*(0)}{\|\mathbf{h}_0\|} d_0(0) + \frac{h_0^*(1)}{\|\mathbf{h}_0\|} d_0(1) + \dots + \frac{h_0^*(L-1)}{\|\mathbf{h}_0\|} d_0(L-1) \\ &= \sum_{l=0}^{L-1} \frac{h_0^*(l)}{\|\mathbf{h}_0\|} d_0(l) \\ &= \sum_{l=0}^{L-1} \frac{h_0^*(l)}{\|\mathbf{h}_0\|} \left(h_0(l) a_0 + I^l \right) \\ &= \underbrace{\sum_{l=0}^{L-1} \frac{h_0^*(l)}{\|\mathbf{h}_0\|} h_0(l) a_0}_{\text{Signal}} + \underbrace{\sum_{l=0}^{L-1} \frac{h_0^*(l)}{\|\mathbf{h}_0\|} I^l}_{\text{Noise + Interference}} \end{aligned}$$

The signal part of the above combined decision statistic d can be simplified as

$$\begin{aligned} \text{signal} &= \sum_{l=0}^{L-1} \frac{h_0^*(l)}{\|\mathbf{h}_0\|} h_0(l) a_0 \\ &= \frac{|h_0(0)|^2}{\|\mathbf{h}_0\|} a_0 + \frac{|h_0(1)|^2}{\|\mathbf{h}_0\|} a_0 + \dots + \frac{|h_0(L-1)|^2}{\|\mathbf{h}_0\|} a_0 \\ &= \frac{\|\mathbf{h}_0\|^2}{\|\mathbf{h}_0\|} a_0 = \|\mathbf{h}_0\| a_0 \end{aligned}$$

Hence, the signal power is

$$\|\mathbf{h}_0\|^2 \mathbb{E} \{ |a_0|^2 \} = P_0 \|\mathbf{h}_0\|^2 \quad (5.17)$$

Also, the noise plus interference power corresponding to the l^{th} branch of the combiner is

$$\begin{aligned} \frac{|h_0(l)|^2}{\|\mathbf{h}_0\|^2} \mathbb{E} \{ |I^l|^2 \} &= \frac{|h_0(l)|^2}{\|\mathbf{h}_0\|^2} \left(\frac{1}{N} \|\mathbf{h}_0\|^2 \left(\sum_{k=0}^K P_k \right) - \frac{1}{N} P_0 |h_0(l)|^2 + \frac{\sigma_w^2}{N} \right) \\ &= \frac{1}{N} \sum_{k=0}^K P_k |h_0(l)|^2 - \frac{1}{N} P_0 \frac{|h_0(l)|^4}{\|\mathbf{h}_0\|^2} + \frac{|h_0(l)|^2 \sigma_w^2}{\|\mathbf{h}_0\|^2 N} \end{aligned}$$

Finally, the sum of the total noise plus interference power across all the L branches of the combiner is given as

$$\begin{aligned} \sum_{l=0}^{L-1} \frac{|h_0(l)|^2}{\|\mathbf{h}_0\|^2} \mathbb{E} \{ |I^l|^2 \} &= \sum_{l=0}^{L-1} \left(\frac{1}{N} \sum_{k=0}^K P_k |h_0(l)|^2 - \frac{1}{N} P_0 \frac{|h_0(l)|^4}{\|\mathbf{h}_0\|^2} + \frac{|h_0(l)|^2 \sigma_w^2}{\|\mathbf{h}_0\|^2 N} \right) \\ &= \frac{1}{N} \sum_{k=0}^K P_k \|\mathbf{h}_0\|^2 - \frac{P_0}{N} \sum_{l=0}^{L-1} \frac{|h_0(l)|^4}{\|\mathbf{h}_0\|^2} + \frac{\sigma_w^2}{N} \end{aligned} \quad (5.18)$$

Hence, from the expressions for the signal and interference plus noise power from Eqs (5.17) and (5.18) respectively, the total signal to interference plus noise power at the user 0 for the downlink multi-user CDMA scenario is given as

$$\text{SINR}_0 = \frac{N P_0 \|\mathbf{h}_0\|^2}{\sum_{k=0}^K P_k \|\mathbf{h}_0\|^2 - P_0 \sum_{l=0}^{L-1} \frac{|h_0(l)|^4}{\|\mathbf{h}_0\|^2} + \sigma_w^2} \quad (5.19)$$

Observe that the factor of N above in the SINR expression represents the spreading gain of the CDMA system. Generalizing the above expression, the signal to interference plus noise power ratio SINR_u at the u^{th} user is given as

$$\text{SINR}_u = \frac{NP_u \|\mathbf{h}_u\|^2}{\sum_{k=0}^K P_k \|\mathbf{h}_u\|^2 - P_u \sum_{l=0}^{L-1} \frac{|h_u(l)|^4}{\|\mathbf{h}_u\|^2} + \sigma_w^2} \quad (5.20)$$

5.10 Performance of CDMA Uplink Scenario with Multiple Users

We now consider a CDMA uplink scenario with $K + 1$ users. Similar to the downlink multi-user scenario, let a_0, a_1, \dots, a_K denote the information symbols and $c_0(n), c_1(n), \dots, c_K(n)$ denote the spreading codes corresponding to the $K + 1$ users respectively. Hence, the spread signal transmitted by each user $x_k(m)$ can be expressed as $x_k(m) = a_k c_k(m)$. However, there is a key difference here with respect to the downlink scenario. Unlike the composite signal which is transmitted by the base station in the downlink scenario, each mobile user transmits his *individual* signal from the transmitter. These signals then traverse their respective radio channels and are superposed at the receiver as shown in Figure 5.13. Thus, the composite signal in the uplink scenario is formed by *superposition* at the receiver.

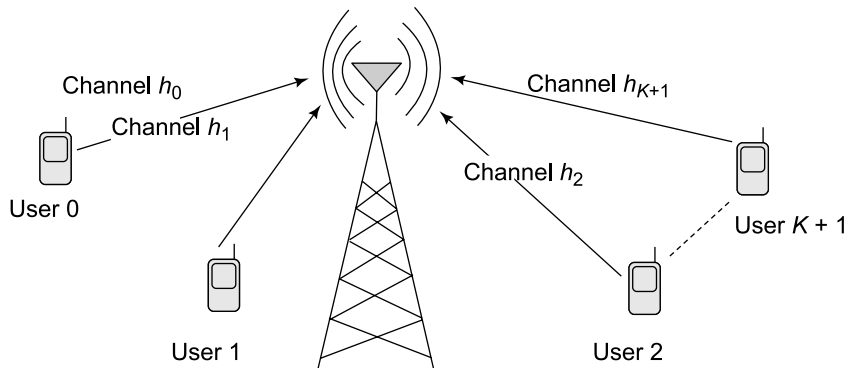


Figure 5.13 CDMA uplink scenario

To understand this better, consider the frequency-selective channel $h_k(0), h_k(1), \dots, h_k(L-1)$ between the k^{th} user and the base station. Thus, the

received signal component $y_k(n)$ of the user k at the base station is given as

$$\begin{aligned} y_k(n) &= h_k(0)x_k(n) + h_k(1)x_k(n-1) + \dots + h_k(L-1)x_k(n-L+1) \\ &= \sum_{l=0}^{L-1} h_k(l)x_k(n-l) \\ &= \sum_{l=0}^{L-1} h_k(l)a_k c_k(n-l) \end{aligned}$$

Thus, the net superposed signal $y(n)$ received at the base station is given as the sum of the components $y_0(n), y_1(n), \dots, y_K(n)$ corresponding to all the users $0, 1, \dots, K$ in the presence of noise, expressed as

$$\begin{aligned} y(n) &= y_0(n) + y_1(n) + \dots + y_K(n) + w(n) \\ &= \sum_{k=0}^K y_k(n) + w(n) \\ &= \sum_{k=0}^K \sum_{l=0}^{L-1} a_k h_k(l) c_k(n-l) + w(n) \end{aligned} \quad (5.21)$$

Observe that the key difference with respect to the downlink system model in Eq. (5.14) is that in the uplink case, the signal of each user goes through the multipath channel of that particular user, compared to the downlink case, where the signal of each user goes through the same channel $h_k(0), h_k(1), \dots, h_k(L-1)$ of the user k corresponding to the signal received at the user k . Proceeding similarly as in the downlink case, it can be easily shown that the uplink SINR_u , corresponding to the user u is given as

$$\text{SINR}_u = \frac{N P_u \|\mathbf{h}_u\|^2}{\sum_{k=0}^K P_k \|\mathbf{h}_k\|^2 - P_u \sum_{l=0}^{L-1} \frac{|h_u(l)|^4}{\|\mathbf{h}_u\|^2} + \sigma_w^2} \quad (5.22)$$

5.11 | Asynchronous CDMA

Till this point in the development of CDMA, we have implicitly assumed that the CDMA spreading sequences are aligned or *synchronized* as shown in Figure 5.14. However, frequently,

the spreading sequences at the base station in an uplink scenario are not aligned. This is due to the fact that different users are at different distances from the base station. Hence, the resulting propagation delays are different, leading to loss of synchronization at the receiver. One of the unique advantages of CDMA is the ability of asynchronous operation. The SINR corresponding to asynchronous operation in CDMA scenarios can be derived as follows.

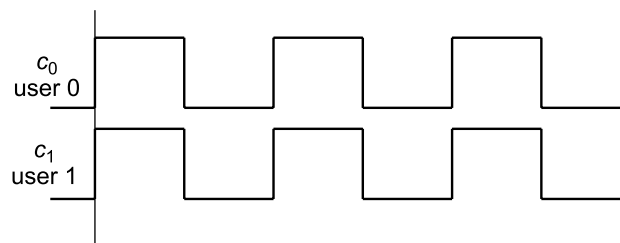


Figure 5.14 Synchronous CDMA code sequences

Consider the spreading sequences $c_0(n)$, $c_1(n)$ of users 1, 2 respectively, with the sequence $c_1(n)$ time shifted compared to $c_0(n)$. Let the fraction f , $0 \leq f \leq 1$, denote the time shift relative to the CDMA chip time as shown in Figure 5.15. It can now be seen that the asynchronous correlation between the sequences, will now comprise of two components. A fraction of the sequence $c_0(n)$, i.e., $1 - f$ will correlate with $c_1(n)$, while the fraction f will correlate with the shifted sequence $c_1(n - 1)$. Hence, the asynchronous correlation r_{01}^a can be expressed as a linear combination of the two synchronous correlations $r_{01}(0)$, $r_{01}(-1)$ as

$$r_{01}^a = (1 - f)r_{01}(0) + fr_{01}(-1)$$

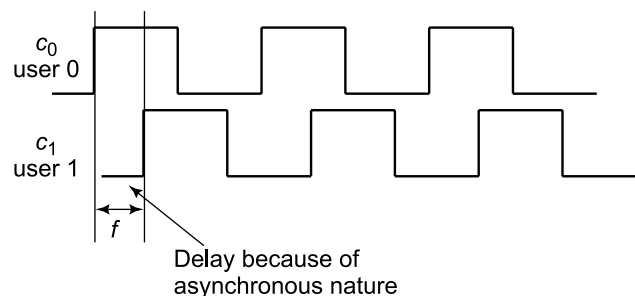


Figure 5.15 Asynchronous CDMA code sequences

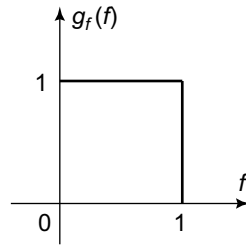


Figure 5.16 Uniform distribution of fractional shift f

Further, in a practical CDMA scenario, the parameter f is a random variable since the users are randomly distributed at various distances within a cell. Also, since $0 \leq f \leq 1$, it can be assumed to be uniformly distributed in $[0, 1]$. Thus, the distribution of f , shown in Figure 5.16, can be expressed as

$$g_F(f) = 1, 0 \leq f \leq 1$$

Further, the second moment $E\{f^2\}$ of the fractional shift random variable F can be derived as

$$\begin{aligned} E\{f^2\} &= \int_0^1 f^2 g_F(f) df \\ &= \int_0^1 f^2 df \\ &= \frac{1}{3} f^3 \Big|_0^1 = \frac{1}{3} \end{aligned}$$

Thus, we have $E\{f^2\} = \frac{1}{3}$. Further, observe that the random variable $1 - f$ is also uniformly distributed in $[0, 1]$. Hence, the variance or power of the asynchronous correlation is given as

$$\begin{aligned} E\{|r_{01}^a|^2\} &= E\{|(1-f)r_{01}(0) + fr_{01}(-1)|^2\} \\ &= E\{|1-f|^2\} E\{|r_{01}(0)|^2\} + E\{|f|^2\} E\{|r_{01}(-1)|^2\} \\ &= \frac{1}{3} \frac{1}{N} + \frac{1}{3} \frac{1}{N} \\ &= \frac{2}{3} \frac{1}{N} \end{aligned}$$

Thus, the power in the asynchronous correlation is $\frac{2}{3}$ that of the power in the synchronous correlation, which is $\frac{1}{N}$. Employing the above property, the SINR of the user u for the asynchronous CDMA uplink scenario SINR_u^a can be derived from the synchronous SINR in Eq. (5.22) as

$$\text{SINR}_u^a = \frac{NP_u \|\mathbf{h}_u\|^2}{\frac{2}{3} \sum_{k=0}^K P_k \|\mathbf{h}_k\|^2 - \frac{2}{3} P_u \sum_{l=0}^{L-1} \frac{|h_u(l)|^4}{\|\mathbf{h}_u\|^2} + \sigma_w^2} \quad (5.23)$$

PROBLEMS

1. BER in Multipath Fading Channels A wireless mobile is in an environment such that it is receiving exactly 4 independently Rayleigh faded multipath signal components. The average power of each component is -1 dB. Let the signal power be $P = 15$ dB and noise power $\sigma_n^2 = 3$ dB. Consider different scenarios as given below for BPSK transmission.

- (a) *Scenario 1:* The user is mobile and the delay spread is much smaller than the symbol time. What is the exact probability of bit error in this case ?
- (b) *Scenario 2:* The user is mobile and the delay spread is much larger than the symbol time and each of the multipath components can be *resolved* using a rake receiver, i.e., the receiver can detect the signal corresponding to each multipath component. What is the approximate BER in this case?
- (c) *Scenario 3:* Subsequently, the user arrives at a position where the channel coefficients corresponding to the different multipath components are $0.9 + 0.1j, 0.75 - 0.2j, -1.1 - 0.15j, -0.6 + 0.5j$. After this point, there is no motion and the transmitter, receiver, and scatterers are static. What is the exact BER from this point onwards for each of the scenarios above (ie small and large delay spreads)?

2. Multiuser CDMA Consider a $K = 2$ user uplink CDMA system. Let the users channel profiles be given as

$$\mathbf{h}_0 = [1 + 0.6j, 0.6 - 0.2j]^T$$

$$\mathbf{h}_1 = [1 - 0.2j, 0.8 + 0.4j, -0.2 + 0.1j]^T$$

where each element is the channel coefficient corresponding to some multipath delay. Consider spreading sequences of length $N = 64$, and user powers $P_0 = -3$ dB, $P_1 = -3$ dB, and noise power $\sigma_n^2 = 3$ dB.

- (a) Compute the corresponding rake SNRs for the desired user 0 corresponding to both an asynchronous and chip aligned multipath synchronous uplink.
- (b) What is the diversity order of for the user 0 in both the above modes?
- (c) What is the approximate BER of the user 0 for QPSK transmission corresponding to both the above modes?

3. Consider a MISO-CDMA system with t transmit antennas modelled as

$$y(k) = \mathbf{h}^H \mathbf{x}(k) + n(k)$$

with the standard vector of channel coefficients $\mathbf{h} = [h_1, h_2, \dots, h_t]^T$. Consider the following transmission scheme. A different spreading code is used to modulate the transmit symbol on each transmit antenna, i.e., the k^{th} transmitted chip on l^{th} transmit antenna is given as $s(0) c_l(k)$. Let the length of each spreading sequence be N .

- (a) Demonstrate the optimal demodulation scheme for the above MISO-CDMA system.
- (b) Derive the SNR at the receiver under the assumption of long spreading codes.
- (c) What is the diversity order of the above scheme?
- (d) Now consider a different transmit scheme where the transmitted chip is given as $s(0) c(k)$, i.e., the same spreading sequence is employed on each transmit antenna. Derive the BER for this scheme. What is the problem with this scheme?

4. **Beamforming in Multiple Antenna CDMA Receivers** Consider an M antenna SIMO CDMA system, where the frequency-selective fading channel between the transmit antenna and the i^{th} receive antenna is given as the FIR filter with channel taps $h_i(0), h_i(1), \dots, h_i(L-1)$.

- (a) Derive the optimal SNR maximizing receiver structure for the above system and clearly describe each step in the derivation.
- (b) What is the SNR at the output of the above system and the associated diversity order?
- (c) Consider a two-antenna system with channel taps $[0.51 + 0.99i, -0.04 + 1.00i, 0.50 + 0.47i]$, $[-0.14 - 0.85i, -0.08 + 0.50i, 1.05 + 1.15i]$ for the first and second antennas respectively. What is the instantaneous bit-error rate of the system at transmit SNR $P/\sigma_n^2 = -20$ dB and spreading length $N = 256$?
- (d) What is the average BER of the system if each tap is Rayleigh of average power unity?

- 5. Multi-user CDMA** Consider a multi-user CDMA scenario with $K = 15$ users and noise power $\sigma_n^2 = 0$ dB. Let all users have equal received power P and the wireless channel of each user is a multipath channel with $L = 4$ independent multipath components of unit power each. Answer the questions below. Let the tolerable BPSK BER required for voice communication be 10^{-3} . Assume spreading length $N = 256$ and ignore multipath interference.
- For a downlink scenario and *stationary* users, compute the power P required for voice calls.
 - For a downlink scenario and *mobile* users, compute the power P required for voice calls (*Hint*: Use the appropriate diversity BER approximation).
 - For an uplink asynchronous scenario and *mobile* users, compute the power P required for voice calls.
 - For an uplink asynchronous scenario and *mobile* users with a voice activity factor of 50%, compute the power P required for voice calls.
- 6. Alamouti-Coded CDMA** Consider a single-user CDMA scenario $t = 2$ transmit antennas and $r = 1$ receive antenna. Let the multipath channel between the i^{th} transmit antenna $i = 1, 2$ and the receive antenna be given as $[h_i(0), h_i(1), \dots, h_i(L-1)]$. Consider the following Alamouti CDMA transmission scheme with spreading sequence $c(k)$, $1 \leq k \leq N$, of spreading length N . The symbol vector $[x_1, x_2]^T$ is transmitted for the first N chips on code $c(k)$ followed by $[-x_2, x_1]^H$ for the next N chips. Ignore multipath interference and answer the questions below.
- Clearly describe the system model for the above system.
 - Describe the optimum decoding rule at the receiver.
 - What is the associated decoding SNR.
 - What is the diversity order associated with this scheme?
- 7. Multi-Antenna CDMA** Consider the receive (Rx) diversity system described in the class which is given as

$$\mathbf{y}(n) = \mathbf{h}x(n) + \mathbf{w}(n)$$

where $\mathbf{y}(n)$, \mathbf{h} , $\mathbf{w}(n)$ are complex L -dimensional vectors and $x(n)$ is the transmitted scalar complex symbol. The noise $\mathbf{w}(n)$ is AWG with covariance $\text{E}\{\mathbf{w}(n)\mathbf{w}(n)^H\} = \sigma_n^2\mathbf{I}$. Each entry of \mathbf{h} is IID Rayleigh with $\text{E}\{|h_i|^2\} = 1$. Consider now a K -user scenario, with signal $x_i(n)$, the signal of the i^{th} user $0 \leq i \leq K-1$ given as $x_i(n) = a_i c_i(n)$, where

$c_i(n)$ denotes the spreading code of the user i . The signal power is $E\{|a_i|^2\} = P$ and each $c_i(n) = \pm 1$. Consider *approximately* orthogonal PN sequences of length N with the *correlation properties* discussed in class (*Hint: Do NOT neglect multi-user interference*). Let the *composite* signal $x(n)$ transmitted on the downlink (DL) be given as

$$x(n) = \sum_{i=0}^{K-1} x_i(n) = \sum_{i=0}^{K-1} a_i c_i(n)$$

Answer the questions that follow.

- (a) Consider decoding at the user 0. What is the test statistic r_l at the l^{th} antenna of user 0?
- (b) What is the *total noise plus interference* power associated with r_l ?
- (c) What is the combiner \mathbf{w} and the SNR at the output of the optimal combiner?
- (d) Using a suitable approximation, derive the average BER at the receiver?
- (e) Compute the average BER for $P = -10$ dB, $\sigma_n^2 = 0$ dB, for spreading length $N = 1024$, $K = 15$ users, and number of antennas $L = 4$ with $E\{|h_i|^2\} = 1$.

8. Multi-Antenna CDMA Consider the receive (Rx) diversity system described in the class which is given as

$$\mathbf{y}(n) = \mathbf{h}x(n) + \mathbf{w}(n)$$

where $\mathbf{y}(n)$, \mathbf{h} , $\mathbf{w}(n)$ are complex L -dimensional vectors and $x(n)$ is the transmitted scalar complex symbol. The noise $\mathbf{w}(n)$ is AWG with covariance $E\{\mathbf{w}(n)\mathbf{w}(n)^H\} = \sigma_n^2 \mathbf{I}$. Each entry of \mathbf{h} is IID Rayleigh with $E\{|h_i|^2\} = 1$. Consider now a K -user scenario, with signal $x_i(n)$, the signal of the i^{th} user $0 \leq i \leq K-1$ given as $x_i(n) = a_i c_i(n)$, where $c_i(n)$ denotes the spreading code of user i . The signal power is $E\{|a_i|^2\} = P$ and each $c_i(n) = \pm 1$. Consider *exactly* orthogonal spreading codes of length N , i.e., $\sum_{n=0}^{N-1} c_i(n) c_j(n) = 0$. Let the *composite* signal $x(n)$ transmitted on the downlink (DL) be given as

$$x(n) = \sum_{i=0}^{K-1} x_i(n) = \sum_{i=0}^{K-1} a_i c_i(n)$$

Answer the questions that follow.

- (a) Consider decoding at the user 0. What is the test statistic r_l at the l^{th} antenna of the user 0?
- (b) What is the noise power associated with r_l ?
- (c) What is the optimal combiner \mathbf{w} and the SNR at the output of the optimal combiner?
- (d) What is the instantaneous and average BER at the receiver?
- (e) Compute the average BER at SNR $\frac{P}{\sigma_n^2} = 20$ dB, for spreading length $N = 256$ and number of antennas $L = 4$.

9. Multi-Antenna CDMA Consider a frequency-selective multiple receive antenna system with M receive antennas and a single transmit antenna which is given as

$$\mathbf{y}(n) = \sum_{l=0}^{L-1} \mathbf{h}(l) x(n-l) + \mathbf{w}(n)$$

where $\mathbf{y}(n)$, $\mathbf{h}(l)$, $\mathbf{w}(n)$ are complex M -dimensional vectors and $x(n)$ is the transmitted scalar complex symbol. The noise $\mathbf{w}(n)$ is AWG with covariance $E\{\mathbf{w}(n)\mathbf{w}(n)^H\} = \sigma_n^2 \mathbf{I}$. Each entry of $\mathbf{h}(l)$ is IID Rayleigh with $E\{|h_i(l)|^2\} = 1$. Consider now a K -user scenario, with signal $x_i(n)$, the signal of the i^{th} user $0 \leq i \leq K-1$ given as $x_i(n) = a_i c_i(n)$, where $c_i(n)$ denotes the spreading code of the user i . The signal power is $E\{|a_i|^2\} = P$ and each $c_i(n) = \pm 1$. Consider *exactly* orthogonal spreading codes of length N for all users i, j , and shifts l , i.e., $\sum_{n=0}^{N-1} c_i(n-l) c_j(n-v) \neq 0$ only if $i = j$ and $l = v$. Let the *composite* signal $x(n)$ transmitted on the downlink (DL) be given as

$$x(n) = \sum_{i=0}^{K-1} x_i(n) = \sum_{i=0}^{K-1} a_i c_i(n)$$

Answer the questions that follow.

- (a) Consider decoding at the user 0. Verbally describe how many test statistics are there at each antenna and what they are.
- (b) What are these test statistics at the m^{th} antenna of the user 0?
- (c) What is the noise power associated with each test statistic?
- (d) What is the optimal combiner \mathbf{w} of all these statistics and the SNR at the output of the optimal combiner?
- (e) What is the instantaneous and average BER at the receiver?

- (f) Compute the average BER at SNR $\frac{P}{\sigma_n^2} = -20$ dB, for spreading length $N = 256$ and number of antennas $M = 4$ and $L = 4$.
- (g) Now consider a binary orthogonal modulation scheme in which we either transmit $a_0 c_0^A(n)$ or $a_0 c_0^B(n)$ for the user 0, where the codes $c_0^A(n)$, $c_0^B(n)$ are both orthogonal and their shifts are also orthogonal with each other and the rest of the users. Calculate the error probability with the coherent rake for this case. (No need to derive the entire receiver. You can give the answer based on prior knowledge.)

10. Diversity Coding and CDMA Consider a scheme that transmits the vector $\mathbf{x}(n) = \mathbf{R}\mathbf{u}c_0(n)$, over two spreading code times. The vector \mathbf{u} and the matrix \mathbf{R} are

$$\mathbf{u} = \begin{bmatrix} u_1 \\ u_2 \end{bmatrix}, \quad \mathbf{R} = \begin{bmatrix} 1 & \frac{1}{2} \\ 1 & \frac{1}{2} \end{bmatrix},$$

and u_1, u_2 are BPSK symbols, each of power P . Assume the scenario is fast-fading, so that the frequency-selective channels $h_i(0), h_i(1), \dots, h_i(L-1)$ for these two spreading code times $i = 0, 1$ are independent. Also assume that the code c_0 and its shifts are *exactly* orthogonal. This is an instance of *time and multipath* diversity. Let the noise power be σ_n^2 . If $y_0(n), y_1(n)$ are the received signal for the first and second intervals of length N chips, essentially the model for this system is given as

$$\begin{bmatrix} y_0(n) \\ y_1(n) \end{bmatrix} = \sum_{l=0}^{L-1} \begin{bmatrix} h_0(l) & 0 \\ 0 & h_1(l) \end{bmatrix} \mathbf{R}\mathbf{u}c_0(n-l) + \begin{bmatrix} w_0(n) \\ w_1(n) \end{bmatrix}$$

- (a) Demonstrate that the decorrelated statistics $d_0(l), d_1(l)$ for time instants 0, 1 respectively corresponding to decorrelation with $c_0(n-l)$ are given as

$$\begin{bmatrix} d_0(l) \\ d_1(l) \end{bmatrix} = \begin{bmatrix} h_0(l) & 0 \\ 0 & h_1(l) \end{bmatrix} \mathbf{R}\mathbf{u} + \begin{bmatrix} \tilde{w}_0(l) \\ \tilde{w}_1(l) \end{bmatrix}$$

- (b) Employing the statistics corresponding to all l above, i.e., $0 \leq l \leq L-1$, derive the average *confusion* probability $P_{\mathbf{x}_A \rightarrow \mathbf{x}_B}$, where $\mathbf{x}_A, \mathbf{x}_B$ are defined as (2.0)

$$\mathbf{x}_A = \mathbf{R} \begin{bmatrix} \sqrt{P} \\ \sqrt{P} \end{bmatrix}, \quad \mathbf{x}_B = \mathbf{R} \begin{bmatrix} -\sqrt{P} \\ \sqrt{P} \end{bmatrix}$$

- (c) What is the diversity order of this system?
- (d) Compute this average confusion probability for $L = 4$, $P = 30$ dB and $\sigma_n^2 = 3$ dB.
11. The coherent performance of antipodal signalling-based rake receiver has been discussed in class. Now consider a binary orthogonal modulation based DS spread spectrum system: we either transmit $x_A = \sqrt{P}c_A(n)$ or $x_B = \sqrt{P}c_B(n)$ which are both orthogonal and their shifts are also orthogonal with each other. Calculate the average error probability expression with the coherent rake for this case considering an L tap frequency-selective channel with IID Rayleigh taps of average power unity, noise power σ_n^2 , and spreading length N .
12. **MISO CDMA** Consider a 1×4 flat-fading MISO CDMA system with code sequence of length $N = 8$ and channel vector \mathbf{h} . Assume perfect channel information available at the transmitter and answer the questions below. Transmit power = P with BPSK modulation and noise power $\sigma_n^2 = 3$ dB.
- (a) What is the optimal transmit symbol from each transmit antenna?
- (b) If the instantaneous channel vector $\mathbf{h} = [1, \frac{1}{2}, \frac{1}{2}, 1]$, what is P required for instantaneous BER 10^{-6} ?
- (c) If the channel coefficients are IID Rayleigh with average power of 3 dB, what is P required for the average BER 10^{-6} ?
13. Consider a BPSK-modulated single-user CDMA system with $N = 128$ and noise power $\sigma^2 = 3$ dB. Also for simplicity, assume that the spreading sequences for different shifts are *exactly* orthogonal. Answer the questions that follow.
- (a) Consider an AWGN channel and derive the transmit power required to achieve BER of 10^{-6} .
- (b) Consider a two-tap channel with channel taps $1 + j$, $2 - j$ and derive the transmit power required to achieve *instantaneous* BER of 10^{-6} . Assume a rake receiver.
- (c) Consider a two-tap Rayleigh fading channel with each tap of average power unity and derive the transmit power required to achieve *average* BER of 10^{-6} . Assume a rake receiver.

Multiple-Input Multiple-Output Wireless Communications

6.1 Introduction to MIMO Wireless Communications

Multiple-Input Multiple-Output (MIMO) wireless communications employ multiple antennas at the transmitter and the receiver. A schematic of a MIMO system with multiple antennas is shown in Figure 6.1. As MIMO systems have multiple antennas, they can be employed to increase the reliability of the signal through *diversity combining* as described in the previous chapters. This leads to diversity gain and a net decrease in the bit-error rate of the wireless communication system. In addition, a unique aspect of MIMO wireless systems is that they enable a several-fold increase in the data rate of the wireless communication system by transmitting several information streams in parallel. This is termed *spatial multiplexing*. This can be thought of as transmitting multiple *parallel* streams in space through different spatial modes, i.e., multiplexing information streams in the space dimension as illustrated in Figure 6.1.

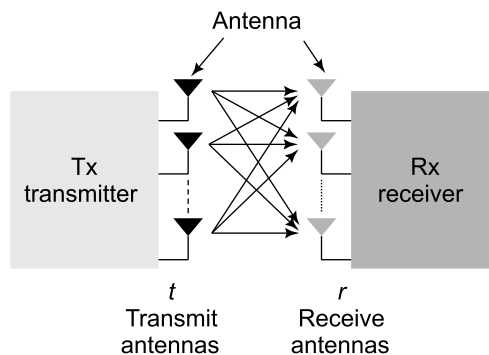


Figure 6.1 MIMO system schematic

6.2 MIMO System Model

Consider a MIMO wireless system with t transmit antennas and r receive antennas. Such a MIMO system is also termed an $r \times t$ system. Let x_1, x_2, \dots, x_t denote the t symbols transmitted from the t transmit antennas in the MIMO system, i.e., x_i denotes the symbol transmitted from the i^{th} transmit antenna $1 \leq i \leq t$. These transmit symbols can be stacked to form the t -dimensional vector, also termed the *transmit vector*,

$$\mathbf{x} = \begin{bmatrix} x_1 \\ x_2 \\ \vdots \\ x_t \end{bmatrix}$$

Corresponding to this transmission, let y_1, y_2, \dots, y_r denote the r received symbols across the r receive antennas in the MIMO systems, which can be stacked as the r -dimensional receive symbol vector,

$$\mathbf{y} = \begin{bmatrix} y_1 \\ y_2 \\ \vdots \\ y_r \end{bmatrix}$$

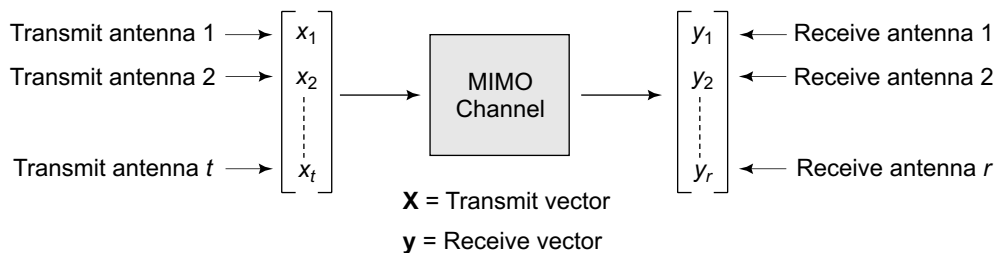


Figure 6.2 MIMO system input-output schematic

This is shown schematically in Figure 6.2. Let the complex coefficient h_{ij} represent the fading channel coefficient between the i^{th} receive antenna and the j^{th} transmit antenna. Thus, there are a net of rt channel coefficients in this wireless scenario corresponding to all possible

combinations of the r receive antennas and t transmit antennas. These can be arranged in a matrix form as

$$\mathbf{H} = \begin{bmatrix} h_{11} & h_{12} & \dots & h_{1t} \\ h_{21} & h_{22} & \dots & h_{2t} \\ \vdots & \vdots & \ddots & \vdots \\ h_{r1} & h_{r2} & \dots & h_{rt} \end{bmatrix}$$

where the $r \times t$ dimensional matrix \mathbf{H} is termed the MIMO channel matrix. Let the additive noise at the receive antenna i be denoted by n_i , i.e., n_1, n_2, \dots, n_r denote the additive noise at the r receive antennas. Thus, the net MIMO input output system model can be represented in vector form as

$$\underbrace{\begin{bmatrix} y_1 \\ y_2 \\ \vdots \\ y_r \end{bmatrix}}_{\mathbf{y}} = \underbrace{\begin{bmatrix} h_{11} & h_{12} & \dots & h_{1t} \\ h_{21} & h_{22} & \dots & h_{2t} \\ \vdots & \vdots & \ddots & \vdots \\ h_{r1} & h_{r2} & \dots & h_{rt} \end{bmatrix}}_{\mathbf{H}} \underbrace{\begin{bmatrix} x_1 \\ x_2 \\ \vdots \\ x_t \end{bmatrix}}_{\mathbf{x}} + \underbrace{\begin{bmatrix} n_1 \\ n_2 \\ \vdots \\ n_r \end{bmatrix}}_{\mathbf{n}}$$

This is succinctly represented using matrix notation as

$$\mathbf{y} = \mathbf{H}\mathbf{x} + \mathbf{n}$$

Observe that the receive symbol y_1 is given as

$$y_1 = h_{11}x_1 + h_{12}x_2 + \dots + h_{1t}x_t + n_1$$

from which it can be seen that all the symbols x_1, x_2, \dots, x_t interfere at y_1 received at the receive antenna 1. Similarly, the receive symbol y_2 is given as

$$y_2 = h_{21}x_1 + h_{22}x_2 + \dots + h_{2t}x_t + n_2$$

from which it can be once again seen that x_1, x_2, \dots, x_t interfere at y_2 received at the receive antenna 2. This is, in general, true for all the receive antennas, i.e., at each receive antenna i , the receive symbol y_i is a linear of all the transmit symbols x_1, x_2, \dots, x_t from the t transmit

antennas, observed in additive noise n_i . For the special case of $t = 1$, i.e., single transmit antenna and multiple receive antennas, this is termed as *Single-Input Multiple-Output (SIMO)* system or the receive diversity system as seen earlier. This can be modelled as

$$\underbrace{\begin{bmatrix} y_1 \\ y_2 \\ \vdots \\ y_r \end{bmatrix}}_{\mathbf{y}} = \underbrace{\begin{bmatrix} h_1 \\ h_2 \\ \vdots \\ h_r \end{bmatrix}}_{\mathbf{h}} x + \underbrace{\begin{bmatrix} n_1 \\ n_2 \\ \vdots \\ n_r \end{bmatrix}}_{\mathbf{n}}$$

Similarly, for the case of one receive antenna, i.e., $r = 1$ and multiple transmit antennas, it is termed a *Multiple-Input Single-Output (MISO)* system model or a transmit diversity system. Its system model is given as

$$y = \underbrace{\begin{bmatrix} h_1 & h_1 & \dots & h_t \end{bmatrix}}_{\mathbf{h}^T} \underbrace{\begin{bmatrix} x_1 \\ x_2 \\ \vdots \\ x_t \end{bmatrix}}_{\mathbf{x}} + n$$

Finally, for $r = t = 1$, i.e., a single receive and transmit antenna, it reduces to the single-input single-output (SISO) system, modelled as

$$y = hx + n$$

As the reader might recall, this was the first system model that was introduced to model the Rayleigh fading wireless -channel-based wireless communication. The *covariance* matrix of the noise \mathbf{R}_n of the noise vector \mathbf{n} defined as

$$\begin{aligned} \mathbf{R}_n &= \mathbb{E} \{ \mathbf{n} \mathbf{n}^H \} \\ &= \mathbb{E} \left\{ \begin{bmatrix} n_1 \\ n_2 \\ \vdots \\ n_L \end{bmatrix} \begin{bmatrix} n_1^* & n_2^* & \dots & n_L^* \end{bmatrix} \right\} \end{aligned}$$

$$\begin{aligned}
&= \begin{bmatrix} \mathbb{E}\{|n_1|^2\} & \mathbb{E}\{n_1 n_2^*\} & \dots & \mathbb{E}\{n_1 n_r^*\} \\ \mathbb{E}\{n_2 n_1^*\} & \mathbb{E}\{|n_2|^2\} & \dots & \mathbb{E}\{n_2 n_r^*\} \\ \vdots & \vdots & \ddots & \vdots \\ \mathbb{E}\{n_r n_1^*\} & \mathbb{E}\{n_r n_2^*\} & \dots & \mathbb{E}\{|n_r|^2\} \end{bmatrix} \\
&= \begin{bmatrix} \sigma_n^2 & 0 & 0 & \dots & 0 \\ 0 & \sigma_n^2 & 0 & \dots & 0 \\ \vdots & \vdots & \vdots & \ddots & \vdots \\ 0 & 0 & 0 & \dots & \sigma_n^2 \end{bmatrix} \\
&= \sigma_n^2 \mathbf{I}_r
\end{aligned}$$

The noise vector \mathbf{n} with the covariance structure above is termed *spatially* uncorrelated additive noise, since the noise samples at the different antennas i, j are independent, i.e., $\mathbb{E}\{n_i n_j^*\} = 0$ if $i \neq j$. Finally, to denote the transmission and reception across different time instants, one can add the time index k to the MIMO system model to frame the net model as

$$\underbrace{\begin{bmatrix} y_1(k) \\ y_2(k) \\ \vdots \\ y_r(k) \end{bmatrix}}_{\mathbf{y}(k)} = \underbrace{\begin{bmatrix} h_{11} & h_{12} & \dots & h_{1t} \\ h_{21} & h_{22} & \dots & h_{2t} \\ \vdots & \vdots & \ddots & \vdots \\ h_{r1} & h_{r2} & \dots & h_{rt} \end{bmatrix}}_{\mathbf{H}} \underbrace{\begin{bmatrix} x_1(k) \\ x_2(k) \\ \vdots \\ x_t(k) \end{bmatrix}}_{\mathbf{x}(k)} + \underbrace{\begin{bmatrix} n_1(k) \\ n_2(k) \\ \vdots \\ n_r(k) \end{bmatrix}}_{\mathbf{n}(k)}$$

Thus, the vectors $\mathbf{y}(k)$, $\mathbf{x}(k)$, $\mathbf{n}(k)$ define the receive, transmit, and noise vectors of the MIMO wireless communication system at the time instant k . Notice that above we have assumed the channel matrix \mathbf{H} to be constant or, in other words, not dependent on the time instant k . This is also termed a slow fading or *quasi-static* channel matrix, indicating that the channel coefficients are constant over the block of MIMO vectors that are transmitted. Lastly, we also assume that any two noise samples across two different time instants are uncorrelated, i.e., $\mathbb{E}\{n_i(k) n_j^*(l)\} = 0$ if $k \neq l$. Hence, the noise covariance matrix is given as

$$\mathbb{E}\{\mathbf{n}(k) \mathbf{n}(l)^H\} = \sigma^2 \delta(k-l) \mathbf{I}_r$$

where the delta function $\delta(k-l) = 1$ if $k = l$ and 0 otherwise.

This noise process, which is uncorrelated across different antennas and time instants is termed *spatio-temporally* uncorrelated noise.

6.3 | MIMO Zero-Forcing (ZF) Receiver

We will now describe the process to recover the transmitted signal vector \mathbf{x} from the received vector \mathbf{y} at the MIMO receiver. This can be considered as solving the system of linear equations,

$$\mathbf{y} = \mathbf{H}\mathbf{x}$$

where x_1, x_2, \dots, x_t are the t unknowns and there are r equations corresponding to the r observations y_1, y_2, \dots, y_r . Consider a simplistic scenario, where $r = t$, i.e., the number of receive antennas is equal to the number of transmit antennas. In this case, the matrix \mathbf{H} is square. Further, if the matrix \mathbf{H} is now invertible, the estimate $\hat{\mathbf{x}}$ of the transmit vector \mathbf{x} is still given as

$$\hat{\mathbf{x}} = \mathbf{H}^{-1}\hat{\mathbf{y}}$$

However, frequently, one has more receive antennas than transmit antennas, i.e., $r > t$. In this scenario, the system $\mathbf{y} = \mathbf{H}\mathbf{x}$ is given as

$$\underbrace{\begin{bmatrix} y_1(k) \\ y_2(k) \\ \vdots \\ \vdots \\ y_r(k) \end{bmatrix}}_{\mathbf{y}(k)} = \underbrace{\begin{bmatrix} h_{11} & h_{12} & \dots & h_{1t} \\ h_{21} & h_{22} & \dots & h_{2t} \\ \vdots & \vdots & \ddots & \vdots \\ \vdots & \vdots & \ddots & \vdots \\ \vdots & \vdots & \ddots & \vdots \\ h_{r1} & h_{r2} & \dots & h_{rt} \end{bmatrix}}_{\mathbf{H}} \underbrace{\begin{bmatrix} x_1(k) \\ x_2(k) \\ \vdots \\ x_t(k) \end{bmatrix}}_{\mathbf{x}(k)}$$

from which it can be seen that the matrix \mathbf{H} has more rows than columns. Such a matrix is popularly known as a *tall* matrix due to its structure. In this situation, one cannot exactly solve for \mathbf{x} since there are more equations r than unknowns t . Hence, one can resort to choosing the

vector \mathbf{x} which minimizes the estimation error $f(\hat{\mathbf{x}})$,

$$f(\mathbf{x}) = \|\mathbf{y} - \mathbf{H}\mathbf{x}\|^2$$

The above error function is also termed the *least-squares* error function and the resulting estimator is termed the *least-squares estimator*. To simplify the analysis going forward, we consider real vectors/matrices \mathbf{y} , \mathbf{x} , \mathbf{H} . The case for complex quantities will be dealt later. The above error function can be expanded as

$$\begin{aligned} f(\mathbf{x}) &= \|\mathbf{y} - \mathbf{H}\mathbf{x}\|^2, \\ &= (\mathbf{y} - \mathbf{H}\mathbf{x})^T (\mathbf{y} - \mathbf{H}\mathbf{x}) \\ &= (\mathbf{y}^T - \mathbf{x}^T \mathbf{H}^T) (\mathbf{y} - \mathbf{H}\mathbf{x}) \\ &= \mathbf{y}^T \mathbf{y} - \mathbf{x}^T \mathbf{H}^T \mathbf{y} - \mathbf{y}^T \mathbf{H}\mathbf{x} + \mathbf{x}^T \mathbf{H}^T \mathbf{H}\mathbf{x} \\ &= \mathbf{y}^T \mathbf{y} - 2\mathbf{x}^T \mathbf{H}^T \mathbf{y} + \mathbf{x}^T \mathbf{H}^T \mathbf{H}\mathbf{x} \end{aligned} \quad (6.1)$$

where we have used the relation $\mathbf{y}^T \mathbf{H}\mathbf{x} = (\mathbf{y}^T \mathbf{H}\mathbf{x})^T = \hat{\mathbf{x}}^T \mathbf{H}^T \mathbf{y}$ in the above simplification. This is due to the fact that $\mathbf{y}^T \mathbf{H}\mathbf{x}$ is a scalar and, hence, is equal to its transpose. To find the minimum of the error function $f(\mathbf{x})$ with respect to \mathbf{x} , we have to set the derivative with respect to \mathbf{x} equal to 0. For this purpose, the concept of a vector derivative is briefly described below. Consider a multidimensional function $g(\mathbf{x})$. The vector derivative of $g(\mathbf{x})$ with respect to \mathbf{x} is defined as

$$\frac{\partial g(\mathbf{x})}{\partial \mathbf{x}} = \begin{bmatrix} \frac{\partial g(\mathbf{x})}{\partial x_1} \\ \frac{\partial g(\mathbf{x})}{\partial x_2} \\ \vdots \\ \frac{\partial g(\mathbf{x})}{\partial x_t} \end{bmatrix}$$

which is basically a t -dimensional vector with the i^{th} component equal to the derivative of $f(\mathbf{x})$ with respect to x_i . This can be better understood with the aid of an example. Consider any vector $\mathbf{c} = [c_1, c_2, \dots, c_t]^T$. Let the function $g(\mathbf{x})$ be defined as

$$g(\mathbf{x}) = \mathbf{c}^T \mathbf{x} = c_1 x_1 + c_2 x_2 + \dots + c_t x_t$$

Hence, it can be seen that, $\frac{\partial g(\mathbf{x})}{\partial x_i} = c_i$. Therefore, it can be readily deduced that in this case

$$\frac{\partial g(\mathbf{x})}{\partial \mathbf{x}} = \begin{bmatrix} \frac{\partial g(\mathbf{x})}{\partial x_1} \\ \frac{\partial g(\mathbf{x})}{\partial x_2} \\ \vdots \\ \frac{\partial g(\mathbf{x})}{\partial x_t} \end{bmatrix} = \begin{bmatrix} c_1 \\ c_2 \\ \vdots \\ c_t \end{bmatrix} = \mathbf{c}$$

In fact, it can also be seen that since $\mathbf{c}^T \mathbf{x} = \mathbf{x}^T \mathbf{c}$, we have

$$\frac{\partial \mathbf{c}^T \mathbf{x}}{\partial \mathbf{x}} = \frac{\partial \mathbf{x}^T \mathbf{c}}{\partial \mathbf{x}} = \mathbf{c}$$

Going back to the expansion of the error function $f(\mathbf{x})$ from Eq. (6.1), it can be seen that the derivative of each component with respect to \mathbf{x} can be computed as follows. Consider the quantity $\mathbf{y}^T \mathbf{y} = \|\mathbf{y}\|^2$. Observe that this does not depend on \mathbf{x} . Hence, we have $\frac{\partial \mathbf{y}^T \mathbf{y}}{\partial \mathbf{x}} = 0$. Consider the component $2\mathbf{x}^T \mathbf{H}^T \mathbf{y}$. This is in the form of $\mathbf{x}^T \mathbf{c}$, where $\mathbf{c} = 2\mathbf{H}^T \mathbf{y}$. Hence, the derivative of this component with respect to \mathbf{x} is given as $\frac{\partial (2\mathbf{x}^T \mathbf{H}^T \mathbf{y})}{\partial \mathbf{x}} = 2\mathbf{H}^T \mathbf{y}$. Now, consider the last component $\mathbf{x}^T \mathbf{H}^T \mathbf{H} \mathbf{x}$. This can be differentiated employing the product rule as

$$\begin{aligned} \frac{\partial (\mathbf{x}^T \mathbf{H}^T \mathbf{H} \mathbf{x})}{\partial \mathbf{x}} &= \mathbf{H}^T \mathbf{H} \mathbf{x} + (\mathbf{x}^T \mathbf{H}^T \mathbf{H})^T \\ &= 2\mathbf{H}^T \mathbf{H} \mathbf{x} \end{aligned}$$

Hence, employing the above results, the derivative for the error function $f(\mathbf{x})$ can be simplified as

$$\frac{\partial f(\mathbf{x})}{\partial \mathbf{x}} = -2\mathbf{H}^T \mathbf{y} + 2\mathbf{H}^T \mathbf{H} \mathbf{x}$$

At the optimal estimate of the transmit vector $\hat{\mathbf{x}}$ where the above error is minimized, we must have the derivative equal to 0. Using this condition,

$$\begin{aligned} \left. \frac{\partial f(\mathbf{x})}{\partial \mathbf{x}} \right|_{\mathbf{x}=\hat{\mathbf{x}}} &= 0 \\ -2\mathbf{H}^T \mathbf{y} + 2\mathbf{H}^T \mathbf{H} \hat{\mathbf{x}} &= 0 \\ \mathbf{H}^T \mathbf{H} \hat{\mathbf{x}} &= \mathbf{H}^T \mathbf{y} \\ \hat{\mathbf{x}} &= (\mathbf{H}^T \mathbf{H})^{-1} \mathbf{H}^T \mathbf{y} \end{aligned}$$

Finally, for the case of complex vectors/matrices \mathbf{x} , \mathbf{y} , \mathbf{H} , the transpose in the above expression can be replaced by the Hermitian operator to yield

$$\hat{\mathbf{x}} = (\mathbf{H}^H \mathbf{H})^{-1} \mathbf{H}^H \mathbf{y}$$

The above decoder for the MIMO wireless system to decode the transmitted symbol vector \mathbf{x} from the received symbol vector \mathbf{y} is termed the *zero-forcing receiver* or simply the *ZF receiver*. Hence, the zero-forcing decoder can be expressed as

$$\hat{\mathbf{x}}_{\text{ZF}} = \underbrace{(\mathbf{H}^H \mathbf{H})^{-1} \mathbf{H}^H}_{\mathbf{F}_{\text{ZF}}} \mathbf{y} \quad (6.2)$$

The matrix $\mathbf{F}_{\text{ZF}} = (\mathbf{H}^H \mathbf{H})^{-1} \mathbf{H}^H$ is also termed the *zero-forcing receiver matrix* and the estimate $\hat{\mathbf{x}}_{\text{ZF}}$ is, therefore, given as

$$\hat{\mathbf{x}}_{\text{ZF}} = \mathbf{F}_{\text{ZF}} \mathbf{y}$$

6.3.1 Properties of the Zero-Forcing Receiver Matrix \mathbf{F}_{ZF}

Consider the matrix product $\mathbf{F}_{\text{ZF}} \mathbf{H}$, which can be simplified as

$$\begin{aligned} \mathbf{F}_{\text{ZF}} \mathbf{H} &= (\mathbf{H}^H \mathbf{H})^{-1} \mathbf{H}^H \mathbf{H} \\ &= (\mathbf{H}^H \mathbf{H})^{-1} (\mathbf{H}^H \mathbf{H}) = \mathbf{I}_t \end{aligned} \quad (6.3)$$

where \mathbf{I}_t denotes the identity matrix of dimension t . Thus, multiplying the matrix \mathbf{F}_{ZF} with the channel matrix indeed produces the identity matrix. In this sense, the matrix \mathbf{F}_{ZF} acts as an inverse of the channel matrix \mathbf{H} . However, observe that for $r > t$, the matrix \mathbf{H} is rectangular and strictly speaking does NOT have a matrix inverse. Hence, this matrix \mathbf{F}_{ZF} is termed the *pseudo-inverse* of \mathbf{H} . Observe that it is, however, not the inverse of the matrix \mathbf{H} in the usual sense. For instance, if \mathbf{F}_{ZF} to be the inverse of \mathbf{H} , it must also satisfy the property that $\mathbf{H} \mathbf{F}_{\text{ZF}} = \mathbf{I}$. However, we have,

$$\mathbf{H} \mathbf{F}_{\text{ZF}} = \mathbf{H} (\mathbf{H}^H \mathbf{H})^{-1} \mathbf{H}^H \neq \mathbf{I}_t$$

Thus, the matrix product $\mathbf{H} \mathbf{F}_{\text{ZF}}$ is not equal to the identity matrix in general. Further, the matrix inverse is a unique matrix. However, it can be shown that the left or pseudo-inverse of the matrix is \mathbf{H} when $r > t$ is not unique. Thus, in general, \mathbf{F}_{ZF} is not the inverse of the

channel matrix \mathbf{H} . However, if $r = t$ and the matrix \mathbf{H} is *invertible* then the pseudo-inverse is actually equal to the inverse. This can be seen as follows.

$$\begin{aligned}\mathbf{F}_{\text{ZF}} &= \mathbf{H} (\mathbf{H}^H \mathbf{H})^{-1} \mathbf{H}^H \\ &= \mathbf{H}^{-1} (\mathbf{H}^H)^{-1} \mathbf{H}^H \\ &= \mathbf{H}^{-1}\end{aligned}$$

Thus, for this particular case, the pseudo-inverse reduces to the matrix inverse and is unique.

6.3.2 Principle of Orthogonality Interpretation of ZF Receiver

In this section, we present an intuitive-reasoning-based approach to derive the zero-forcing decoder above. Consider once again the system of equations at the receiver for $r > t$.

$$\underbrace{\begin{bmatrix} y_1(k) \\ y_2(k) \\ \vdots \\ \vdots \\ y_r(k) \end{bmatrix}}_{\mathbf{y}(k)} = \underbrace{\begin{bmatrix} h_{11} & h_{12} & \dots & h_{1t} \\ h_{21} & h_{22} & \dots & h_{2t} \\ \vdots & \vdots & \ddots & \vdots \\ \vdots & \vdots & \ddots & \vdots \\ \vdots & \vdots & \ddots & \vdots \\ h_{r1} & h_{r2} & \dots & h_{rt} \end{bmatrix}}_{\mathbf{H}} \underbrace{\begin{bmatrix} x_1(k) \\ x_2(k) \\ \vdots \\ x_t(k) \end{bmatrix}}_{\mathbf{x}(k)}$$

Denoting the column $\mathbf{h}_i = [h_{1i}, h_{2i}, \dots, h_{ri}]^T$ we denote the i^{th} column of the channel matrix \mathbf{H} . Then, the system of equations above can be succinctly represented as

$$\mathbf{y} = \underbrace{x_1 \mathbf{h}_1 + x_2 \mathbf{h}_2 + \dots + x_t \mathbf{h}_t}_{\hat{\mathbf{y}}}$$

where $\hat{\mathbf{y}}$ is the approximation of \mathbf{y} and we are interested in minimizing $\|\mathbf{y} - \hat{\mathbf{y}}\|^2$. Observe that there are t columns of the channel matrix \mathbf{H} , which are $\mathbf{h}_1, \mathbf{h}_2, \dots, \mathbf{h}_t$. Hence, they represent a t -dimensional subspace. However, the vector \mathbf{y} can lie anywhere in the r -dimensional space, and is unlikely to lie exclusively in the t -dimensional subspace represented by the columns of the channel. This is shown schematically in Figure 6.3, where approximation error $\mathbf{e} = \mathbf{y} - \hat{\mathbf{y}}$

the error is shown for different choices of $\hat{\mathbf{y}}$. It can be clearly seen that the approximation is minimum, when it is *orthogonal* to the space spanned by the columns of \mathbf{H} . This is termed the *principle of orthogonality*, which is extremely helpful in understanding the intuition behind complex estimation problems. Observe that the error vector \mathbf{e} is orthogonal to \mathbf{h}_i if $\mathbf{h}_i^H \mathbf{e} = 0$. Therefore, since \mathbf{e} is orthogonal to the subspace spanned by the columns of \mathbf{H} , it follows that it is orthogonal to each of the columns of \mathbf{H} .

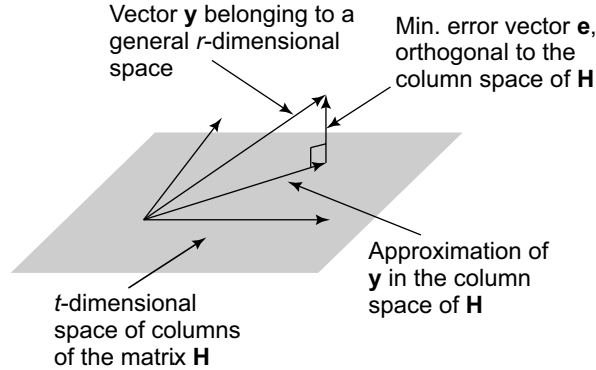


Figure 6.3 Zero-forcing: principle of orthogonality

Hence, we have

$$\begin{aligned} \mathbf{h}_1^H \mathbf{e} &= 0 \\ \mathbf{h}_2^H \mathbf{e} &= 0 \\ &\vdots \\ \mathbf{h}_t^H \mathbf{e} &= 0, \end{aligned}$$

from which it follows naturally that

$$\mathbf{H}^H \mathbf{e} = \mathbf{0}_{t \times 1}$$

We now employ the above principle of orthogonality to derive the expression for the zero-forcing estimate $\hat{\mathbf{x}}_{\text{ZF}}$ of the transmitted symbol vector \mathbf{x} . This can be derived by substituting the expression $\mathbf{e} = \mathbf{y} - \mathbf{H}\hat{\mathbf{x}}_{\text{ZF}}$ in the above result as

$$\begin{aligned} \mathbf{H}^H \underbrace{(\mathbf{y} - \mathbf{H}\hat{\mathbf{x}}_{\text{ZF}})}_{\mathbf{e}} &= 0 \\ \mathbf{H}^H \mathbf{y} - \mathbf{H}^H \mathbf{H} \hat{\mathbf{x}}_{\text{ZF}} &= 0 \end{aligned}$$

$$\mathbf{H}^H \mathbf{y} = \mathbf{H}^H \mathbf{H} \hat{\mathbf{x}}_{\text{ZF}}$$

$$\hat{\mathbf{x}}_{\text{ZF}} = (\mathbf{H}^H \mathbf{H})^{-1} \mathbf{H}^H \mathbf{y}$$

which is exactly identical to the expression for the zero-forcing MIMO decoder derived earlier in Eq. (6.2). Thus, the principle of orthogonality can be conveniently employed to deduce the expression for the optimal ZF MIMO decoder while also giving valuable insights into the decoding procedure.

EXAMPLE 6.1

Compute the MIMO zero-forcing receiver for the channel matrix \mathbf{H} given as

$$\mathbf{H} = \begin{bmatrix} 2 & 3 \\ 1 & 3 \\ 4 & 2 \end{bmatrix} \quad (6.4)$$

Solution: It can be seen that the MIMO channel matrix above is of size 3×2 , implying that the number of receive antennas is $r = 3$, while the number of transmit antennas is $t = 2$. Thus, the MIMO system model can be described as

$$\underbrace{\begin{bmatrix} y_1 \\ y_2 \\ y_3 \end{bmatrix}}_{\mathbf{y}} = \underbrace{\begin{bmatrix} 2 & 3 \\ 1 & 3 \\ 4 & 2 \end{bmatrix}}_{\mathbf{H}} \underbrace{\begin{bmatrix} x_1 \\ x_2 \end{bmatrix}}_{\mathbf{x}} + \underbrace{\begin{bmatrix} n_1 \\ n_2 \\ n_3 \end{bmatrix}}_{\mathbf{n}}$$

Thus, as can be seen from the model above, the transmit vector \mathbf{x} is of dimension 2×1 , while the receive and noise vectors \mathbf{y} , \mathbf{n} respectively are of dimension 3×1 . The above MIMO system model can also be explicitly written to describe the signal received at each receive antenna as

$$y_1 = 2x_1 + 3x_2 + n_1$$

$$y_2 = x_1 + 3x_2 + n_2$$

$$y_3 = 4x_1 + 2x_2 + n_3$$

which basically represents a system of $r = 3$ equations for $t = 2$ unknowns x_1, x_2 . To compute the zero-forcing decoder \mathbf{F}_{ZF} , we first compute the matrix $(\mathbf{H}^H \mathbf{H})^{-1} \mathbf{H}^H$. Observe that $\mathbf{H}^H \mathbf{H}$ can be simplified as

$$\begin{aligned} \mathbf{H}^H \mathbf{H} &= \begin{bmatrix} 2 & 1 & 4 \\ 3 & 3 & 2 \end{bmatrix} \begin{bmatrix} 2 & 3 \\ 1 & 3 \\ 4 & 2 \end{bmatrix} \\ &= \begin{bmatrix} 21 & 17 \\ 17 & 22 \end{bmatrix} \end{aligned}$$

Hence, the expression for $(\mathbf{H}^H \mathbf{H})^{-1}$ can be simplified as

$$\begin{aligned} (\mathbf{H}^H \mathbf{H})^{-1} &= \frac{1}{21 \times 22 - 17 \times 17} \begin{bmatrix} 22 & -17 \\ -17 & 21 \end{bmatrix} \\ &= \frac{1}{173} \begin{bmatrix} 22 & -17 \\ -17 & 21 \end{bmatrix} \end{aligned}$$

Thus, the zero-forcing receiver matrix $\mathbf{F}_{ZF} = (\mathbf{H}^H \mathbf{H})^{-1} \mathbf{H}^H$ can be expressed as

$$\begin{aligned} \mathbf{F}_{ZF} &= (\mathbf{H}^H \mathbf{H})^{-1} \mathbf{H}^H \\ &= \frac{1}{173} \begin{bmatrix} 22 & -17 \\ -17 & 21 \end{bmatrix} \begin{bmatrix} 2 & 1 & 4 \\ 3 & 3 & 2 \end{bmatrix} \\ &= \frac{1}{173} \begin{bmatrix} -7 & -29 & 54 \\ 29 & 46 & -26 \end{bmatrix} \\ &= \begin{bmatrix} -0.04 & -0.17 & 0.31 \\ 0.17 & 0.27 & -0.15 \end{bmatrix} \end{aligned} \tag{6.5}$$

Thus, the zero-forcing estimate of the transmit vector is given as

$$\begin{aligned}\hat{\mathbf{x}}_{ZF} &= \mathbf{F}_{ZF}\mathbf{y} \\ &= (\mathbf{H}^H\mathbf{H})^{-1}\mathbf{H}^H\mathbf{y} \\ &= \begin{bmatrix} -0.04 & -0.17 & 0.31 \\ 0.17 & 0.27 & -0.15 \end{bmatrix} \begin{bmatrix} y_1 \\ y_2 \\ y_3 \end{bmatrix}\end{aligned}$$

These expressions can now be explicitly written for the estimate of each of the transmit symbols \hat{x}_1, \hat{x}_2 as

$$\hat{x}_1 = -0.04y_1 - 0.17y_2 + 0.31y_3$$

$$\hat{x}_2 = +0.17y_1 + 0.27y_2 - 0.15y_3$$

It can also be confirmed that the zero-forcing receiver matrix matrix \mathbf{F}_{ZF} is of dimension 2×3 , i.e., $t \times r$.

One of the chief disadvantages of the zero-forcing receivers is *noise amplification*. This can be understood as follows. Consider the SISO wireless system for $r = t = 1$. We have the system model given as

$$y = hx + n$$

Hence, the zero-forcing receiver is given as $f_{ZF} = (h^*h)^{-1}h^* = h^{-1} = \frac{1}{h}$. Hence, the zero-forcing estimate of the transmitted symbol x is given as

$$\begin{aligned}\hat{x}_{ZF} &= f_{ZF} \times y \\ &= \frac{1}{h}(hx + n) \\ &= x + \frac{n}{h}\end{aligned}\tag{6.6}$$

Observe that if the fading coefficient h is close to zero then the factor $\frac{n}{h}$ is very high. This is termed *noise amplification*, which significantly distorts the performance of the receiver. The MMSE receiver which is proposed next addresses this problem.

6.4 MIMO MMSE Receiver

In this section, we develop the *Minimum Mean-Squared Error (MMSE)* receiver for the MIMO wireless communication system. The MMSE receiver is based on a *Bayesian* approach, meaning that the transmit vector \mathbf{x} is assumed to be random in nature. Thus, if $\hat{\mathbf{x}}_{\text{MMSE}}$ denotes the estimated symbol vector, the MMSE receiver minimizes the average or mean of the squared error

$$E \left\{ \|\hat{\mathbf{x}}_{\text{MMSE}} - \mathbf{x}\|^2 \right\}$$

Thus, it is aptly named minimum mean-squared error estimator. To illustrate the development of the MMSE receiver, we consider a single-input multiple-output (SIMO) wireless system, i.e., $t = 1$, and generalize the result to the case of a MIMO system. Hence, consider the SIMO system model given as

$$\mathbf{y} = \mathbf{h}x + \mathbf{n}$$

where x is now a scalar transmitted symbol. Thus, the basic problem can be interpreted as estimating the symbol x given the vector $\mathbf{y} = [y_1, y_2, \dots, y_r]^T$. Let $\mathbf{c} = [c_1, c_2, \dots, c_r]^T$. One can now define a linear estimator of x as

$$\hat{x} = \mathbf{c}^T \mathbf{y} \tag{6.7}$$

$$= \begin{bmatrix} c_1 & c_2 & \dots & c_r \end{bmatrix} \begin{bmatrix} y_1 \\ y_2 \\ \vdots \\ y_r \end{bmatrix}$$

$$= c_1 y_1 + c_2 y_2 + \dots + c_r y_r$$

Such an estimator as above is termed as a *linear* estimator, since the estimate is a linear function of \mathbf{y} . We now wish to find the best or optimal linear estimator $\hat{\mathbf{x}}_{\text{MMSE}}$, which minimizes the mean squared error and hence is also termed the *Linear Minimum Mean Squared Estimator (LMMSE)*. This is frequently also referred to simply as the MMSE, although strictly speaking belongs to the specific class of linear estimators. The average mean squared error is defined as

$$E \left\{ \|\hat{\mathbf{x}} - \mathbf{x}\|^2 \right\}$$

Employing the form in Eq. (6.7), the resulting equation can be simplified as

$$\begin{aligned}
\mathbb{E} \left\{ \|\hat{\mathbf{x}} - \mathbf{x}\|^2 \right\} &= \mathbb{E} \left\{ (\mathbf{c}^T \mathbf{y} - \mathbf{x}) (\mathbf{c}^T \mathbf{y} - \mathbf{x})^T \right\} \\
&= \mathbb{E} \left\{ (\mathbf{c}^T \mathbf{y} - \mathbf{x}) (\mathbf{y}^T \mathbf{c} - \mathbf{x}^T) \right\} \\
&= \mathbb{E} \left\{ \mathbf{c}^T \mathbf{y} \mathbf{y}^T \mathbf{c} - \mathbf{x} \mathbf{y}^T \mathbf{c} - \mathbf{c}^T \mathbf{y} \mathbf{x} + \mathbf{x} \mathbf{x}^T \right\} \\
&= \mathbf{c}^T \underbrace{\mathbb{E} \{ \mathbf{y} \mathbf{y}^T \}}_{\mathbf{R}_{yy}} \mathbf{c} - \underbrace{\mathbb{E} \{ \mathbf{x} \mathbf{y}^T \}}_{\mathbf{R}_{xy}} \mathbf{c} - \mathbf{c}^T \underbrace{\mathbb{E} \{ \mathbf{y} \mathbf{x} \}}_{\mathbf{R}_{yx}} + \mathbb{E} \{ \mathbf{x} \mathbf{x}^T \} \mathbf{R}_{xx} \\
&= \mathbf{c}^T \mathbf{R}_{yy} \mathbf{c} - 2\mathbf{c}^T \mathbf{R}_{yx} + \mathbf{R}_{xx}
\end{aligned}$$

where the covariance matrix \mathbf{R}_{yy} is defined as $\mathbf{R}_{yy} = \mathbb{E} \{ \mathbf{y} \mathbf{y}^H \}$. Similarly, $\mathbf{R}_{yx} = \mathbb{E} \{ \mathbf{y} \mathbf{x} \} = \mathbf{R}_{xy}^T$ and $\mathbf{R}_{xx} = \mathbb{E} \{ \mathbf{x} \mathbf{x}^T \}$. Also note that we have used the fact $\mathbf{c}^T \mathbf{R}_{yx} = (\mathbf{c}^T \mathbf{R}_{yx})^T = \mathbf{R}_{xy} \mathbf{c}$. Hence, the average MSE as a function of the receive beamformer \mathbf{c} , denoted by $\overline{\text{MSE}}(\mathbf{c})$, is given as

$$\overline{\text{MSE}}(\mathbf{c}) = \mathbf{c}^T \mathbf{R}_{yy} \mathbf{c} - 2\mathbf{c}^T \mathbf{R}_{yx} + \mathbf{R}_{xx}$$

Thus, the optimal beamformer \mathbf{c} which minimizes the average or mean squared error can be obtained by differentiating $\overline{\text{MSE}}(\mathbf{c})$ with respect to \mathbf{c} and setting equal to zero as

$$\begin{aligned}
\frac{\partial \overline{\text{MSE}}(\mathbf{c})}{\partial \mathbf{c}} &= 0 \\
\frac{\partial}{\partial \mathbf{c}} (\mathbf{c}^T \mathbf{R}_{yy} \mathbf{c} - 2\mathbf{c}^T \mathbf{R}_{yx} + \mathbf{R}_{xx}) &= 0 \\
2\mathbf{R}_{yy} \mathbf{c} - 2\mathbf{R}_{yx} &= 0 \\
\mathbf{c} &= \mathbf{R}_{yy}^{-1} \mathbf{R}_{yx}
\end{aligned}$$

Thus, the optimal LMMSE beamforming vector \mathbf{c} is given as $\mathbf{c} = \mathbf{R}_{yy}^{-1} \mathbf{R}_{yx}$. This is also termed in signal processing as the optimal *Wiener* filter. The above can be generalized in the case of complex vectors by replacing the transpose by the Hermitian operation.

Hence, the MMSE estimate of x is given as

$$\begin{aligned}\hat{\mathbf{x}}_{\text{MMSE}} &= \mathbf{c}^H \mathbf{y} \\ &= (\mathbf{R}_{yy}^{-1} \mathbf{R}_{yx})^H \mathbf{y} \\ &= \mathbf{R}_{xy} \mathbf{R}_{yy}^{-1} \mathbf{y}\end{aligned}$$

We now compute the MMSE receiver for the MIMO wireless system. Consider again the MIMO system model given as

$$\mathbf{y} = \mathbf{H}\mathbf{x} + \mathbf{n}$$

Let the transmit symbols x_i , $1 \leq i \leq t$ be such that each is of power P_d , i.e., $\text{E}\{|x_i|^2\} = P_d$, with elements on different transmit antennas being uncorrelated, i.e., $\text{E}\{x_i x_j^*\} = 0$ when $i \neq j$. Hence, the covariance \mathbf{R}_{xx} of the transmit symbols is given as

$$\begin{aligned}\mathbf{R}_{xx} &= \text{E}\{\mathbf{x}\mathbf{x}^H\} \\ &= \text{E}\left\{\begin{bmatrix} x_1 \\ x_2 \\ \vdots \\ x_t \end{bmatrix} \begin{bmatrix} x_1^* & x_2^* & \dots & x_t^* \end{bmatrix}\right\} \\ &= \begin{bmatrix} \text{E}\{|x_1|^2\} & \text{E}\{x_1 x_2^*\} & \dots & \text{E}\{x_1 x_t^*\} \\ \text{E}\{x_2 x_1^*\} & \text{E}\{|x_2|^2\} & \dots & \text{E}\{x_2 x_t^*\} \\ \vdots & \vdots & \ddots & \vdots \\ \text{E}\{x_t x_1^*\} & \text{E}\{x_t x_2^*\} & \dots & \text{E}\{|x_t|^2\} \end{bmatrix} \\ &= \begin{bmatrix} P_d & 0 & 0 & \dots & 0 \\ 0 & P_d & 0 & \dots & 0 \\ \vdots & \vdots & \vdots & \ddots & \vdots \\ 0 & 0 & 0 & \dots & P_d \end{bmatrix} \\ &= P_d \mathbf{I}_t\end{aligned}$$

Hence, \mathbf{R}_{yy} , the covariance of the receive vector \mathbf{y} can be simplified as

$$\begin{aligned}
 \mathbf{R}_{yy} &= \mathbb{E} \{ \mathbf{y} \mathbf{y}^H \} \\
 &= \mathbb{E} \{ (\mathbf{H}\mathbf{x} + \mathbf{n}) (\mathbf{H}\mathbf{x} + \mathbf{n})^H \} \\
 &= \mathbb{E} \{ \mathbf{H}\mathbf{x}\mathbf{x}^H\mathbf{H} + \mathbf{n}\mathbf{x}^H\mathbf{H}^H + \mathbf{H}\mathbf{x}\mathbf{n}^H + \mathbf{n}\mathbf{n}^H \} \\
 &= \underbrace{\mathbf{H} \mathbb{E} \{ \mathbf{x}\mathbf{x}^H \} \mathbf{H}}_{\mathbf{R}_{xx}} + \underbrace{\mathbb{E} \{ \mathbf{n}\mathbf{x}^H \}}_0 \mathbf{H}^H + \mathbf{H} \underbrace{\mathbb{E} \{ \mathbf{x}\mathbf{n}^H \}}_0 + \underbrace{\mathbb{E} \{ \mathbf{n}\mathbf{n}^H \}}_{\mathbf{R}_{nn}} \\
 &= \underbrace{P_d \mathbf{H}\mathbf{H}^H + \sigma_n^2 \mathbf{I}_r}_{\mathbf{R}_{yy}}
 \end{aligned}$$

where we have used the fact that $\mathbb{E} \{ \mathbf{n}\mathbf{x}^H \} = \mathbb{E} \{ \mathbf{x}\mathbf{n}^H \} = \mathbf{0}$, since the noise at the receiver and transmit symbols are uncorrelated, in the above simplification. Further, the cross-covariance matrix \mathbf{R}_{yx} can be simplified as

$$\begin{aligned}
 \mathbf{R}_{yx} &= \mathbb{E} \{ \mathbf{y} \mathbf{x}^H \} \\
 &= \mathbb{E} \{ (\mathbf{H}\mathbf{x} + \mathbf{n}) \mathbf{x}^H \} \\
 &= \mathbb{E} \{ \mathbf{H}\mathbf{x}\mathbf{x}^H + \mathbf{n}\mathbf{x}^H \} \\
 &= \mathbf{H} \underbrace{\mathbb{E} \{ \mathbf{x}\mathbf{x}^H \}}_{\mathbf{R}_{xx}} + \underbrace{\mathbb{E} \{ \mathbf{n}\mathbf{x}^H \}}_0 \\
 &= P_d \mathbf{H}
 \end{aligned}$$

Thus, the optimal MMSE receiver is given as

$$\begin{aligned}
 \mathbf{C} &= \mathbf{R}_{yy}^{-1} \mathbf{R}_{yx} \\
 &= (P_d \mathbf{H}\mathbf{H}^H + \sigma_n^2 \mathbf{I})^{-1} P_d \mathbf{H} \\
 &= P_d (P_d \mathbf{H}\mathbf{H}^H + \sigma_n^2 \mathbf{I})^{-1} \mathbf{H}
 \end{aligned}$$

Hence, the MMSE estimate $\hat{\mathbf{x}}_{\text{MMSE}}$ of the transmit vector \mathbf{x} is given as

$$\begin{aligned}
 \hat{\mathbf{x}}_{\text{MMSE}} &= \mathbf{C}^H \mathbf{y} \\
 &= P_d \mathbf{H}^H (P_d \mathbf{H}\mathbf{H}^H + \sigma_n^2 \mathbf{I})^{-1} \mathbf{y}
 \end{aligned} \tag{6.8}$$

We now derive an alternative structure for the MIMO MMSE receiver. Observe that, we have,

$$\begin{aligned} P_d \mathbf{H}^H \mathbf{H} \mathbf{H}^H + \sigma_n^2 \mathbf{H}^H &= P_d \mathbf{H}^H \mathbf{H} \mathbf{H}^H + \sigma_n^2 \mathbf{H}^H \\ \Rightarrow (P_d \mathbf{H}^H \mathbf{H} + \sigma_n^2 \mathbf{I}) \mathbf{H}^H &= \mathbf{H}^H (P_d \mathbf{H} \mathbf{H}^H + \sigma_n^2 \mathbf{I}) \\ \Rightarrow \mathbf{H}^H (P_d \mathbf{H} \mathbf{H}^H + \sigma_n^2 \mathbf{I})^{-1} &= (P_d \mathbf{H}^H \mathbf{H} + \sigma_n^2 \mathbf{I})^{-1} \mathbf{H}^H \end{aligned}$$

Thus, the MIMO MMSE receiver in Eq. (6.8) can also be expressed as

$$\begin{aligned} \hat{\mathbf{x}}_{\text{MMSE}} &= P_d \mathbf{H}^H (P_d \mathbf{H} \mathbf{H}^H + \sigma_n^2 \mathbf{I})^{-1} \mathbf{y} \\ &= P_d (P_d \mathbf{H}^H \mathbf{H} + \sigma_n^2 \mathbf{I})^{-1} \mathbf{H}^H \mathbf{y} \end{aligned} \quad (6.9)$$

Thus, the above expression is an alternative form of implementation of the MIMO MMSE receiver. Observe that the matrix $\mathbf{H} \mathbf{H}^H + \sigma_n^2 \mathbf{I}$ is of dimension $r \times r$, while $P_d \mathbf{H}^H \mathbf{H} + \sigma_n^2 \mathbf{I}$ is $t \times t$ dimensional. Thus, if $r > t$, inversion of the latter matrix is of a lower computation complexity. Since this is frequently the case in MIMO wireless systems, the alternative MIMO MMSE receiver version is more popular for implementation.

6.4.1 Robustness of MMSE to Noise Amplification

Further, the MMSE receiver does not lead to noise amplification, as is the case with the ZF receiver, which was seen in Eq. (6.6). Consider the SISO case for which $\mathbf{H} = h$. The system model is given as

$$y = hx + n$$

The MMSE estimate of x is given from Eq. (6.8) as

$$\begin{aligned} \hat{x}_{\text{MMSE}} &= P_d \frac{h^*}{P_d h h^* + \sigma_n^2} y \\ &= P_d \frac{h^*}{P_d |h|^2 + \sigma_n^2} y \end{aligned}$$

Thus, it can be seen that for $|h| \approx 0$, the MMSE receiver becomes

$$\hat{x}_{\text{MMSE}} \approx P_d \frac{h^*}{\sigma_n^2} y$$

Thus, since it does not lead to division by a quantity close to 0, unlike the ZF, it does not lead to noise enhancement.

6.4.2 Low and High SNR Properties of the MMSE Receiver

In this section, we explore the low and high SNR behaviour of the MMSE receiver, which provides valuable insights into its nature. Consider the expression for the MMSE receiver in Eq. (6.9). Observe that at high SNR, i.e., $\frac{P_d}{\sigma_n^2} \rightarrow \infty$, the term $P_d \mathbf{H}^H \mathbf{H}$ dominates over $\sigma_n^2 \mathbf{I}_t$. Hence, we have

$$P_d \mathbf{H}^H \mathbf{H} + \sigma_n^2 \mathbf{I} \approx P_d \mathbf{H}^H \mathbf{H}$$

Employing this approximation in the MMSE receiver in Eq. (6.9), we have

$$\begin{aligned} \hat{\mathbf{x}}_{\text{MMSE}} &= P_d (P_d \mathbf{H}^H \mathbf{H} + \sigma_n^2 \mathbf{I})^{-1} \mathbf{H}^H \mathbf{y} \\ &\approx P_d (P_d \mathbf{H}^H \mathbf{H})^{-1} \mathbf{H}^H \mathbf{y} \\ &= (\mathbf{H}^H \mathbf{H})^{-1} \mathbf{H}^H \mathbf{y} \end{aligned}$$

which is identical to the MIMO zero-forcing receiver from Eq. (6.2). Thus, at high SNR, the MMSE receiver reduces to the MIMO zero-forcing receiver. On the other hand, at low SNR, i.e., as $\frac{P_d}{\sigma_n^2} \rightarrow 0$, the term $P_d \mathbf{H}^H \mathbf{H}$ is negligible compared to $\sigma_n^2 \mathbf{I}_t$. Thus, we have

$$P_d \mathbf{H}^H \mathbf{H} + \sigma_n^2 \mathbf{I}_t \approx \sigma_n^2 \mathbf{I}_t$$

Employing the above approximation at low SNR, the MMSE receiver can be simplified as

$$\begin{aligned} \hat{\mathbf{x}}_{\text{MMSE}} &= P_d (P_d \mathbf{H}^H \mathbf{H} + \sigma_n^2 \mathbf{I})^{-1} \mathbf{H}^H \mathbf{y} \\ &\approx P_d (\sigma_n^2 \mathbf{I})^{-1} \mathbf{H}^H \mathbf{y} \\ &= \frac{P_d}{\sigma_n^2} \mathbf{H}^H \mathbf{y} \end{aligned}$$

which reduces to the *matched filter*, i.e., proportional to \mathbf{H}^H . Thus, the optimal MMSE receiver can be approximated as the zero-forcing receiver at high SNR, while at low SNR, it behaves similar to the matched filter. This behaviour of the MMSE decoder is schematically represented in Figure 6.4.

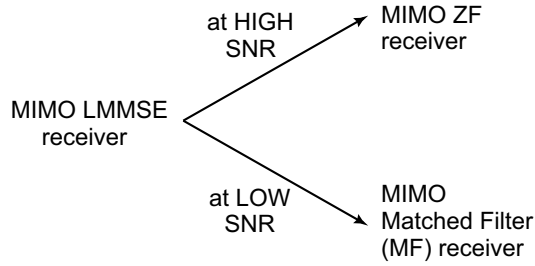


Figure 6.4 MIMO MMSE receiver: asymptotic behaviour

6.5 | Singular Value Decomposition (SVD) of the MIMO Channel

In this section, we will begin to explore the *Singular Value Decomposition* (SVD) of the MIMO channel matrix \mathbf{H} , which is a very important tool to understand the behaviour of a MIMO wireless communication system. Consider an $r \times t$ MIMO channel \mathbf{H} with $r \geq t$, i.e., number of receive antennas greater than or equal to the number of transmit antennas. The SVD of the channel matrix \mathbf{H} is given as

$$\begin{aligned}
 \mathbf{H} &= \underbrace{\begin{bmatrix} u_{11} & u_{12} & \dots & u_{1t} \\ u_{21} & u_{22} & \dots & u_{2t} \\ \vdots & \vdots & \ddots & \vdots \\ \underbrace{u_{r1}}_{\mathbf{u}_1} & \underbrace{u_{r2}}_{\mathbf{u}_2} & \dots & \underbrace{u_{rt}}_{\mathbf{u}_t} \end{bmatrix}}_{\mathbf{U}} \underbrace{\begin{bmatrix} \sigma_1 & 0 & \dots & 0 \\ 0 & \sigma_2 & \dots & 0 \\ \vdots & \vdots & \ddots & \vdots \\ 0 & 0 & \dots & \sigma_t \end{bmatrix}}_{\mathbf{\Sigma}} \\
 & \underbrace{\begin{bmatrix} v_{11}^* & v_{21}^* & \dots & v_{t1}^* \\ v_{12}^* & v_{22}^* & \dots & v_{t2}^* \\ \vdots & \vdots & \ddots & \vdots \\ v_{1t}^* & v_{2t}^* & \dots & v_{tt}^* \end{bmatrix}}_{\mathbf{V}^H} \begin{matrix} \left. \vphantom{\begin{matrix} v_{11}^* \\ v_{12}^* \\ \vdots \\ v_{1t}^* \end{matrix}} \right\} \mathbf{v}_1^H \\ \left. \vphantom{\begin{matrix} v_{21}^* \\ v_{22}^* \\ \vdots \\ v_{2t}^* \end{matrix}} \right\} \mathbf{v}_2^H \\ \left. \vphantom{\begin{matrix} v_{t1}^* \\ v_{t2}^* \\ \vdots \\ v_{tt}^* \end{matrix}} \right\} \mathbf{v}_t^H \end{matrix} \\
 &= \mathbf{U}\mathbf{\Sigma}\mathbf{V}^H \tag{6.10}
 \end{aligned}$$

where the matrices \mathbf{U} , $\mathbf{\Sigma}$, \mathbf{V} , which are $r \times t$, $t \times t$ and $t \times t$ dimensional respectively, satisfy important properties, which we examine next. The columns of the matrix \mathbf{U} and \mathbf{V} are unit-

norm, i.e., we have

$$\|\mathbf{u}_i\|^2 = \|\mathbf{v}_i\|^2 = 1, 1 \leq i \leq t$$

Further, the columns of matrix \mathbf{U} and \mathbf{V} are orthogonal, i.e.,

$$\mathbf{u}_i^H \mathbf{u}_j = \mathbf{v}_i^H \mathbf{v}_j = 0, i \neq j, 1 \leq i, j \leq t$$

Thus, the columns of matrices \mathbf{U} and \mathbf{V} are orthonormal. As a result, the $t \times t$ dimensional square matrix \mathbf{V} is unitary, i.e.,

$$\mathbf{V}^H \mathbf{V} = \mathbf{V} \mathbf{V}^H = \mathbf{I}_t$$

Further, since if $r = t$, the matrix \mathbf{U} is also a unitary matrix. Otherwise, \mathbf{U} simply satisfies the relation $\mathbf{U}^H \mathbf{U} = \mathbf{I}_t$. Further, the quantities $\sigma_1, \sigma_2, \dots, \sigma_t$ are known as the singular values of the matrix Σ . These singular values are non-negative and *ordered*, i.e., each $\sigma_i \geq 0$ and

$$\sigma_1 \geq \sigma_2 \geq \dots \geq \sigma_t$$

Finally, an important property of the singular values is that the number of nonzero singular values is equal to the rank of the matrix \mathbf{H} . Below, we illustrate some examples of singular value decomposition to give insights into the structure of the SVD.

6.5.1 Examples of Singular Value Decomposition

EXAMPLE 6.2

Consider a 2×1 SIMO wireless system with channel matrix \mathbf{H} given as

$$\mathbf{H} = \begin{bmatrix} 1 \\ 1 \end{bmatrix} \quad (6.11)$$

This can be simplified as

$$\begin{aligned} \mathbf{H} &= \begin{bmatrix} 1 \\ 1 \end{bmatrix}, = \begin{bmatrix} \frac{1}{\sqrt{2}} \\ \frac{1}{\sqrt{2}} \end{bmatrix} \sqrt{2} \\ &= \underbrace{\begin{bmatrix} \frac{1}{\sqrt{2}} \\ \frac{1}{\sqrt{2}} \end{bmatrix}}_{\mathbf{U}} \underbrace{\begin{bmatrix} \sqrt{2} \end{bmatrix}}_{\Sigma} \underbrace{\begin{bmatrix} 1 \end{bmatrix}}_{\mathbf{V}^H} \end{aligned}$$

This is a simple example of the SVD and yet illustrates several important properties. For instance, $\mathbf{U} = \left[\frac{1}{\sqrt{2}}, \frac{1}{\sqrt{2}} \right]^T$, which is of dimension $r \times t$, i.e., 2×1 . Further, \mathbf{U} only has a single column $\mathbf{u}_1 = \left[\frac{1}{\sqrt{2}}, \frac{1}{\sqrt{2}} \right]^T$, which is unit-norm, i.e., $\|\mathbf{u}_1\|^2 = 1$. Further, the singular value $\sigma_1 = \sqrt{2}$, which is greater than 0. Also, the number of nonzero singular values is 1, which is equal to the rank of the matrix. The rank of the matrix is easily seen to be equal to 1 in this case since it is simply a column vector. Also observe that $\mathbf{V} = [1]$. Hence, we trivially have

$$\mathbf{V}^H \mathbf{V} = \mathbf{V} \mathbf{V}^H = 1 = \mathbf{I}_1$$

Thus, the above decomposition satisfies all the properties of the SVD. Next, we define a slightly more nuanced example to illustrate the concept of SVD.

EXAMPLE 6.3

Let the 2×2 channel matrix \mathbf{H} be given as

$$\mathbf{H} = \begin{bmatrix} 1 & 0 \\ 0 & \sqrt{5} \end{bmatrix}$$

In this example, it is very intuitive to simplify \mathbf{H} simply as

$$\mathbf{H} = \underbrace{\begin{bmatrix} 1 & 0 \\ 0 & 1 \end{bmatrix}}_{\mathbf{U}} \underbrace{\begin{bmatrix} 1 & 0 \\ 0 & \sqrt{5} \end{bmatrix}}_{\mathbf{\Sigma}} \underbrace{\begin{bmatrix} 1 & 0 \\ 0 & 1 \end{bmatrix}}_{\mathbf{V}^H}$$

and claim that $\sigma_1 = 1$, $\sigma_2 = \sqrt{5}$ are the singular values of \mathbf{H} . However, this is incorrect since $\sigma_1 < \sigma_2$, meaning that the above is not a valid SVD. However, one can recast \mathbf{H} as follows.

$$\mathbf{H} = \underbrace{\begin{bmatrix} 0 & 1 \\ 1 & 0 \end{bmatrix}}_{\mathbf{U}} \underbrace{\begin{bmatrix} \sqrt{5} & 0 \\ 0 & 1 \end{bmatrix}}_{\mathbf{\Sigma}} \underbrace{\begin{bmatrix} 0 & 1 \\ 1 & 0 \end{bmatrix}}_{\mathbf{V}^H}$$

where the matrices \mathbf{U} , \mathbf{V} are 2×2 permutation matrices which flip the rows and columns of the inner diagonal matrix respectively. It can also be observed that $\mathbf{V}\mathbf{V}^H = \mathbf{V}^H\mathbf{V} = \mathbf{I}_t$. Also, in this case, since $r = t$, we also have $\mathbf{U}\mathbf{U}^H = \mathbf{U}^H\mathbf{U} = \mathbf{I}_t$. Further, $\sigma_1 = \sqrt{5} > \sigma_2 = 1 > 0$. Thus, the singular values are positive and ordered. Hence, this is a valid SVD of the channel matrix \mathbf{H} . This example demonstrates how an otherwise seemingly simple diagonal matrix can have an SVD that is not straightforward to compute.

EXAMPLE 6.4

We now look at another example of a channel matrix \mathbf{H} and compute its SVD. Let \mathbf{H} be given as

$$\mathbf{H} = \begin{bmatrix} 1 & 2 \\ 1 & -2 \end{bmatrix}$$

Observe that in this case, the columns of \mathbf{H} , i.e., $\mathbf{h}_1 = [1, 1]^T$ and $\mathbf{h}_2 = [2, -2]^T$ are orthogonal since $\mathbf{h}_1^H \mathbf{h}_2 = 1 \times 2 + 1 \times (-2) = 0$. This fact can be employed to compute the SVD. Thus, the matrix \mathbf{H} can be decomposed in steps as

$$\begin{aligned} \mathbf{H} &= \begin{bmatrix} 1 & 2 \\ 1 & -2 \end{bmatrix} \\ &= \begin{bmatrix} 1 & 1 \\ 1 & -1 \end{bmatrix} \times \begin{bmatrix} 1 & 0 \\ 0 & 2 \end{bmatrix} \\ &= \begin{bmatrix} 1 & 1 \\ -1 & 1 \end{bmatrix} \times \begin{bmatrix} 2 & 0 \\ 0 & 1 \end{bmatrix} \times \begin{bmatrix} 0 & 1 \\ 1 & 0 \end{bmatrix} \end{aligned}$$

The above decomposition has a structure that looks very close to the SVD. It now remains to normalize the columns of the left and right matrices to generate orthonormal vectors. This can be done as follows.

$$\mathbf{H} = \underbrace{\begin{bmatrix} \frac{1}{\sqrt{2}} & \frac{1}{\sqrt{2}} \\ -\frac{1}{\sqrt{2}} & \frac{1}{\sqrt{2}} \end{bmatrix}}_{\mathbf{U}} \underbrace{\begin{bmatrix} 2\sqrt{2} & 0 \\ 0 & \sqrt{2} \end{bmatrix}}_{\mathbf{\Sigma}} \underbrace{\begin{bmatrix} 0 & 1 \\ 1 & 0 \end{bmatrix}}_{\mathbf{V}^H}$$

It can be seen that the singular values are $\sigma_1 = 2\sqrt{2} > \sigma_2 = \sqrt{2} > 0$. Further, the number of nonzero singular values and, hence, the rank is 2. Since $r = t = 2$, the matrices \mathbf{U} , \mathbf{V} are both square 2×2 , unitary and contain orthonormal columns.

6.6 | Singular Value Decomposition and MIMO Capacity

The singular value decomposition is central to understanding the spatial multiplexing properties of the MIMO channel and deriving the fundamental limit on the capacity of the MIMO channel. Consider the $r \times t$ MIMO wireless system,

$$\mathbf{y} = \mathbf{H}\mathbf{x} + \mathbf{n}$$

Let the SVD of the channel matrix \mathbf{H} be given as $\mathbf{H} = \mathbf{U}\mathbf{\Sigma}\mathbf{V}^H$. Thus, replacing \mathbf{H} with its SVD, the above MIMO system model is given as

$$\mathbf{y} = \underbrace{\mathbf{U}\mathbf{\Sigma}\mathbf{V}^H}_{\mathbf{H}}\mathbf{x} + \mathbf{n}$$

At the receiver, multiplying by \mathbf{U}^H , we have

$$\begin{aligned} \underbrace{\mathbf{U}^H\mathbf{y}}_{\tilde{\mathbf{y}}} &= \mathbf{U}^H(\mathbf{U}\mathbf{\Sigma}\mathbf{V}^H\mathbf{x} + \mathbf{n}) \\ \tilde{\mathbf{y}} &= \underbrace{\mathbf{U}^H\mathbf{U}}_{\mathbf{I}_t}\mathbf{\Sigma}\mathbf{V}^H\mathbf{x} + \underbrace{\mathbf{U}^H\mathbf{n}}_{\tilde{\mathbf{n}}} \\ &= \mathbf{\Sigma}\mathbf{V}^H\mathbf{x} + \tilde{\mathbf{n}} \end{aligned}$$

This operation of multiplying by \mathbf{U}^H at the receiver is a part of the signal processing at the receiver or *receive processing*. Further, prior to transmission, let the transmit vector \mathbf{x} be generated as $\mathbf{x} = \mathbf{V}\tilde{\mathbf{x}}$, where the vector $\tilde{\mathbf{x}}$ contains the transmit symbols. This operation is termed as *transmit precoding*. Thus, substituting this expression for \mathbf{x} above, we have

$$\tilde{\mathbf{y}} = \mathbf{\Sigma}\mathbf{V}^H\mathbf{x} + \tilde{\mathbf{n}}$$

$$\begin{aligned}
&= \mathbf{\Sigma} \mathbf{V}^H \mathbf{V} \tilde{\mathbf{x}} + \tilde{\mathbf{n}} \\
&= \mathbf{\Sigma} \tilde{\mathbf{x}} + \tilde{\mathbf{n}}
\end{aligned}$$

The above equivalent system model of the MIMO system after the receive and transmit processing operations can be explicitly written as

$$\begin{bmatrix} \tilde{y}_1 \\ \tilde{y}_2 \\ \vdots \\ \tilde{y}_t \end{bmatrix} = \begin{bmatrix} \sigma_1 & 0 & \dots & 0 \\ 0 & \sigma_2 & \dots & 0 \\ \vdots & \vdots & \ddots & \vdots \\ 0 & 0 & \dots & \sigma_t \end{bmatrix} \begin{bmatrix} \tilde{x}_1 \\ \tilde{x}_2 \\ \vdots \\ \tilde{x}_t \end{bmatrix} + \begin{bmatrix} \tilde{n}_1 \\ \tilde{n}_2 \\ \vdots \\ \tilde{n}_t \end{bmatrix}$$

The above system can, in fact, be written in a much simpler *decoupled* form as

$$\begin{aligned}
\tilde{y}_1 &= \sigma_1 \tilde{x}_1 + \tilde{n}_1 \\
\tilde{y}_2 &= \sigma_2 \tilde{x}_2 + \tilde{n}_2 \\
&\vdots \\
\tilde{y}_t &= \sigma_t \tilde{x}_t + \tilde{n}_t
\end{aligned} \tag{6.12}$$

Thus, the above equivalent system represents the *parallelization* of the MIMO channel with t information streams being transmitted in parallel. As can be seen, there is no interference between the t information streams carrying symbols $\tilde{x}_1, \tilde{x}_2, \dots, \tilde{x}_t$. This is termed *spatial multiplexing*, where the t independent information streams are being multiplexed over the multiple spatial dimensions, arising due to the presence of multiple transmit and receive antennas in the system. Also, the covariance of the modified noise $\tilde{\mathbf{n}}$ can be derived as

$$\begin{aligned}
\mathbf{R}_{\tilde{\mathbf{n}}} &= \mathbf{E} \{ \tilde{\mathbf{n}} \tilde{\mathbf{n}}^H \} \\
&= \mathbf{E} \{ \mathbf{U}^H \mathbf{n} (\mathbf{U}^H \mathbf{n})^H \} \\
&= \mathbf{E} \{ \mathbf{U}^H \mathbf{n} \mathbf{n}^H \mathbf{U} \} \\
&= \mathbf{U}^H \underbrace{\mathbf{E} \{ \mathbf{n} \mathbf{n}^H \}}_{\sigma_n^2 \mathbf{I}} \mathbf{U}
\end{aligned}$$

$$\begin{aligned}
&= \mathbf{U}^H \sigma_n^2 \mathbf{I} \mathbf{U} = \sigma_n^2 \underbrace{\mathbf{U}^H \mathbf{U}}_{\mathbf{I}_t} \\
&= \sigma_n^2 \mathbf{I}_t
\end{aligned} \tag{6.13}$$

Thus, once again, the noise $\tilde{\mathbf{n}}$ has a covariance proportional to the identity matrix, indicating equal variance, uncorrelated noise components. Further, the variance of each noise component \tilde{n}_i , $1 \leq i \leq t$ is equal to σ_n^2 . Consider now the i^{th} parallel MIMO channel above. This is given as

$$\tilde{y}_i = \sigma_i \tilde{x}_i + \tilde{n}_i.$$

Hence, the SNR of the system is given as $\sigma_i^2 \frac{\text{E}\{|x_i|^2\}}{\sigma_n^2} = \sigma_i^2 \frac{P_i}{\sigma_n^2}$, where P_i is the power of the i^{th} data stream x_i . Thus, the MIMO system can be viewed as a collection of t parallel channels each with noise power σ_n^2 and power gain σ_i^2 . This is schematically shown in Figure 6.5. From the above expression for the SNR of the i^{th} channel, the Shannon capacity C_i of the channel

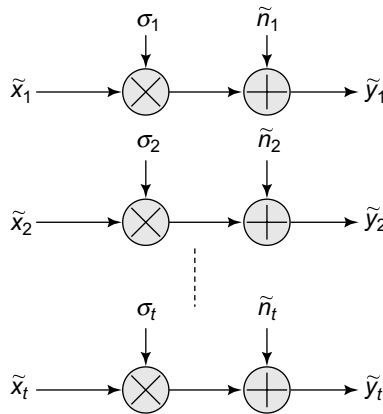


Figure 6.5 MIMO SVD parallel channels

can be derived as

$$C_i = \log_2 \left(1 + \frac{P_i \sigma_i^2}{\sigma_n^2} \right)$$

Thus, the MIMO system can be thought of as a collection of t parallel data pipes, with capacities

$$C_1 = \log_2 \left(1 + \frac{P_1 \sigma_1^2}{\sigma_n^2} \right)$$

$$C_2 = \log_2 \left(1 + \frac{P_2 \sigma_2^2}{\sigma_n^2} \right)$$

⋮

$$C_t = \log_2 \left(1 + \frac{P_t \sigma_t^2}{\sigma_n^2} \right)$$

Thus, the net MIMO C capacity is given as the sum of the individual capacities

$$C = \sum_{i=1}^t \log_2 \left(1 + \frac{P_i \sigma_i^2}{\sigma_i^2} \right)$$

The total power P at the transmitter can be allocated to the individual streams to maximize the net capacity. Thus, one can maximize the above sum capacity subject to the power constraint

$$P_1 + P_2 + \dots + P_t \leq P$$

Next, we describe computation of the optimal MIMO capacity.

6.6.1 Optimal MIMO Capacity

Thus, the optimal MIMO power allocation problem can be formulated as

$$\begin{aligned} \max. \quad & \sum_{i=1}^t \log_2 \left(1 + \frac{P_i \sigma_i^2}{\sigma_i^2} \right) \\ \text{s.t.} \quad & \sum_{i=1}^t P_i \leq P \end{aligned}$$

where s.t. in the above problem statement stands for *subject to* and denotes the optimization constraint. We employ the standard Lagrange-multiplier-based technique for the above constrained optimization problem. Denoting the Lagrange multiplier by λ , the Lagrangian cost

function $f(\bar{P}, \lambda)$ for the above optimization problem can be formulated as

$$f(\bar{P}, \lambda) = \sum_{i=1}^t \log_2 \left(1 + \frac{P_i \sigma_i^2}{\sigma_n^2} \right) + \lambda \left(P - \sum_{i=1}^t P_i \right)$$

where $\bar{P} = [P_1, P_2, \dots, P_t]^T$. Differentiating $f(\bar{P}, \lambda)$ with respect to P_i and setting equal to 0, we obtain

$$\begin{aligned} \frac{\partial}{\partial P_i} f(\bar{P}, \lambda) &= 0 \\ \frac{\frac{\sigma_i^2}{\sigma_n^2}}{1 + \frac{P_i \sigma_i^2}{\sigma_n^2}} - \lambda &= 0 \end{aligned}$$

Solving the above equation yields

$$\begin{aligned} \frac{\sigma_i^2}{\sigma_n^2} \frac{1}{\lambda} &= 1 + \frac{P_i \sigma_i^2}{\sigma_n^2} \\ P_i &= \left(\frac{1}{\lambda} - \frac{\sigma_n^2}{\sigma_i^2} \right)^+ \end{aligned}$$

where the function $x^+ = x$ if $x \geq 0$ and 0 otherwise. This is because of the fact that each power $P_i \geq 0$, i.e., power cannot be negative. It now remains to find the Lagrange multiplier λ , which can be found from the constraint equation as

$$\begin{aligned} \sum_{i=1}^t P_i &= P \\ \sum_{i=1}^t \left(\frac{1}{\lambda} - \frac{\sigma_n^2}{\sigma_i^2} \right)^+ &= P \end{aligned} \tag{6.14}$$

The above optimal power allocation is also termed *water filling*. This can be seen as follows. Consider a vessel with t bars and the height of the i^{th} bar equal to $\frac{\sigma_n^2}{\sigma_i^2}$. If water is poured into this vessel to the level $\frac{1}{\lambda}$ then the level of water at the i^{th} bar is $\left(\frac{1}{\lambda} - \frac{\sigma_n^2}{\sigma_i^2} \right)^+$. This is shown schematically in Figure 6.6. Observe that the power allocated is proportional to the singular value, i.e., larger the σ_i , larger is the power allocated. Further, also observe that due to the nature of water filling, weak channels with low σ_i are not allocated any power.

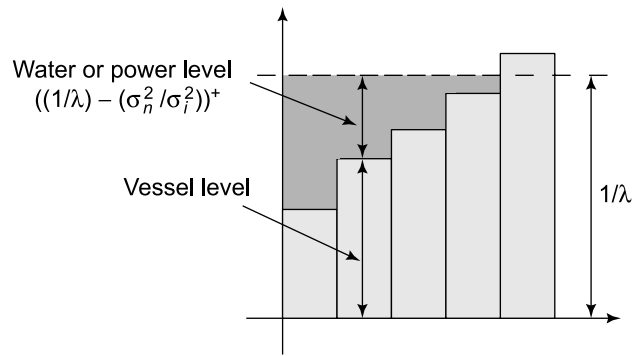


Figure 6.6 MIMO water-filling capacity

Observe that the water-filling equation in Eq. (6.14) above is nonlinear due to the x^+ function. It can be solved iteratively as follows. Set $N = t$ initially. Assume $\frac{1}{\lambda} - \frac{\sigma_n^2}{\sigma_i^2}$ for $1 \leq i \leq N$. Solve the equation

$$\sum_{i=1}^N \left(\frac{1}{\lambda} - \frac{\sigma_n^2}{\sigma_i^2} \right) = P$$

Now, check if $\frac{1}{\lambda} - \frac{\sigma_n^2}{\sigma_N^2} \geq 0$. If this is the case then the λ computed yields the desired power allocation. However, if $\frac{1}{\lambda} - \frac{\sigma_n^2}{\sigma_N^2} < 0$, then set $P_N = 0$ and $N = t - 1$ and repeat the process as above. Example clarifies this concept of MIMO capacity and optimal power allocation.

EXAMPLE 6.5

Consider the MIMO channel matrix \mathbf{H} given as

$$\mathbf{H} = \begin{bmatrix} 2 & -6 & 0 \\ 3 & 4 & 0 \\ 0 & 0 & 2 \end{bmatrix}$$

Considering a transmit power of $P = -1.25$ dB and noise power $\sigma_n^2 = 3$ dB, compute the MIMO capacity and optimal power allocation.

Solution: The above MIMO channel matrix is 3×3 , i.e., a MIMO system with $r = t = 3$ antennas. We also have, $\sigma_n^2 = 3 \text{ dB} = 2$ and $P = -1.25 \text{ dB} = 0.75$. Observe that the columns of the channel matrix \mathbf{H} are orthogonal. For instance, if $\mathbf{c}_1, \mathbf{c}_2$ denote the first two columns of \mathbf{H} , we have

$$\begin{aligned}\mathbf{c}_1^H \mathbf{c}_2 &= 2 \times (-6) + 3 \times (4) \\ &= 0\end{aligned}$$

Hence, the SVD of the channel matrix \mathbf{H} is given as

$$\begin{aligned}\mathbf{H} &= \begin{bmatrix} 2 & -6 & 0 \\ 3 & 4 & 0 \\ 0 & 0 & 2 \end{bmatrix} \\ &= \begin{bmatrix} \frac{2}{\sqrt{13}} & -\frac{6}{\sqrt{52}} & 0 \\ \frac{3}{\sqrt{13}} & \frac{4}{\sqrt{52}} & 0 \\ 0 & 0 & 1 \end{bmatrix} \\ &= \underbrace{\begin{bmatrix} -\frac{6}{\sqrt{52}} & \frac{2}{\sqrt{13}} & 0 \\ \frac{4}{\sqrt{52}} & \frac{3}{\sqrt{13}} & 0 \\ 0 & 0 & 1 \end{bmatrix}}_{\mathbf{U}} \underbrace{\begin{bmatrix} \sqrt{52} & 0 & 0 \\ 0 & \sqrt{13} & 0 \\ 0 & 0 & 2 \end{bmatrix}}_{\mathbf{\Sigma}} \underbrace{\begin{bmatrix} 0 & 1 & 0 \\ 1 & 0 & 0 \\ 0 & 0 & 1 \end{bmatrix}}_{\mathbf{V}^H}\end{aligned}$$

Thus, the singular values $\sigma_1, \sigma_2, \sigma_3$ for the above channel matrix are given as

$$\sigma_1 = \sqrt{52} \Rightarrow \sigma_1^2 = 52$$

$$\sigma_2 = \sqrt{13} \Rightarrow \sigma_2^2 = 13$$

$$\sigma_3 = 2 \Rightarrow \sigma_3^2 = 4$$

It can be seen that the channel matrix \mathbf{H} has 3 nonzero singular values. Hence, the rank of the channel matrix is 3. The channel capacity C in terms of the powers P_1, P_2, P_3 assigned to the

different channel singular modes is given as

$$\begin{aligned} C &= \log_2 \left(1 + \frac{P_1 \sigma_1^2}{\sigma_n^2} \right) + \log_2 \left(1 + \frac{P_2 \sigma_2^2}{\sigma_n^2} \right) + \log_2 \left(1 + \frac{P_3 \sigma_3^2}{\sigma_n^2} \right) \\ &= \log_2 \left(1 + \frac{P_1 \times 52}{2} \right) + \log_2 \left(1 + \frac{P_2 \times 13}{2} \right) + \log_2 \left(1 + \frac{P_3 \times 4}{2} \right) \end{aligned}$$

The above expression for capacity has to be maximized for total power $P_1 + P_2 + P_3 = 0.75$. We set $N = t = 3$ and solve the Lagrangian in Eq. (6.14) as

$$\begin{aligned} \left(\frac{1}{\lambda} - \frac{1}{26} \right) + \left(\frac{1}{\lambda} - \frac{2}{13} \right) + \left(\frac{1}{\lambda} - \frac{1}{2} \right) &= 0.75 \\ \frac{1}{\lambda} &= \frac{0.75 + \frac{1}{26} + \frac{2}{13} + \frac{1}{2}}{3} \\ \frac{1}{\lambda} &= 0.48 \end{aligned}$$

Let us now compute the power allocation to the channel 3, i.e., P_3 , which is given as, $P_3 = \frac{1}{\lambda} - \frac{1}{2} = 0.48 - 0.5 = -0.02 \leq 0$. Thus, since the power P_3 is coming out to be negative, this is not a possible allocation. This implies that the power bar corresponding to the channel 3 lies above the water level $\frac{1}{\lambda}$, as per the schematic shown in Figure 6.6. Thus, the singular mode 3 is allotted 0 power in the optimal allocation. Hence, we now set $N = 2$ and resolve the equation for the Lagrangian variable λ as

$$\begin{aligned} \left(\frac{1}{\lambda} - \frac{1}{26} \right) + \left(\frac{1}{\lambda} - \frac{2}{13} \right) &= 0.75 \\ \frac{1}{\lambda} &= \frac{0.75 + \frac{1}{26} + \frac{2}{13}}{2} \\ &= 0.4712 \end{aligned}$$

Recomputing the powers P_1, P_2 , we have

$$\begin{aligned} P_1 &= 0.4712 - \frac{1}{26} = 0.4327 > 0 \\ P_2 &= 0.4712 - \frac{2}{13} = 0.3174 > 0 \end{aligned}$$

Thus, since $P_1, P_2 > 0$, this is a feasible power allocation. Hence, we have, $P_1 = 0.4327 = -3.63$ dB and $P_2 = 0.3174 = -4.98$ dB. As already described, $P_3 = 0$. Therefore, the capacity C is given as

$$\begin{aligned} C_{\max} &= \log_2 \left(1 + \frac{52 \times 0.4327}{2} \right) + \log_2 \left(1 + \frac{13 \times 0.3174}{2} \right) \\ &= 5.23 \text{ b/s/Hz} \end{aligned}$$

where the units b/s/Hz is read as *bits per second per hertz*. The optimal MIMO transmission scheme can now be derived as follows. Observe from the SVD of $\mathbf{H} = \mathbf{U}\mathbf{\Sigma}\mathbf{V}^H$ computed above that the matrix \mathbf{V} is given as

$$\underbrace{\begin{bmatrix} 0 & 1 & 0 \\ 1 & 0 & 0 \\ 0 & 0 & 1 \end{bmatrix}}_{\mathbf{V}} = \underbrace{\begin{bmatrix} \mathbf{v}_1 & \mathbf{v}_2 & \mathbf{v}_3 \end{bmatrix}}$$

As described in Section 6.6, the transmit vector \mathbf{x} is given as

$$\begin{aligned} \mathbf{x} &= \begin{bmatrix} \mathbf{v}_1 & \mathbf{v}_2 & \mathbf{v}_3 \end{bmatrix} \begin{bmatrix} \tilde{x}_1 \\ \tilde{x}_2 \\ \tilde{x}_3 \end{bmatrix} \\ &= \mathbf{v}_1 \tilde{x}_1 + \mathbf{v}_2 \tilde{x}_2 \end{aligned}$$

where $\tilde{x}_3 = 0$ since $P_3 = 0$. Also, we have $\sqrt{P_1} = 0.66$ and $\sqrt{P_2} = 0.56$. Therefore, the net transmit vector \mathbf{x} is given as

$$\mathbf{x} = \begin{bmatrix} 0 \\ 1 \\ 0 \end{bmatrix} \underbrace{\tilde{x}_1}_{\sqrt{P_1} b_1} + \begin{bmatrix} 1 \\ 0 \\ 0 \end{bmatrix} \underbrace{\tilde{x}_2}_{\sqrt{P_2} b_2}$$

$$= \begin{bmatrix} 0 \\ 1 \\ 0 \end{bmatrix} 0.66 b_1 + \begin{bmatrix} 1 \\ 0 \\ 0 \end{bmatrix} 0.56 b_2$$

where b_1, b_2 are unit power-transmit symbols belonging to an appropriate transmit constellation such as BPSK, QPSK, etc. Thus, one can compute the optimal power allocation corresponding to the capacity of the MIMO channel to derive the optimal precoded transmit vectors for the MIMO system.

6.7 | Asymptotic MIMO Capacity

We now describe a simple scenario to illustrate the asymptotic capacity of the MIMO channel. Let the transmit covariance matrix $\mathbf{R}_x = \text{E} \{ \mathbf{x}(k) \mathbf{x}^H(k) \}$. It can then be demonstrated that the capacity of the MIMO channel, for a general transmit covariance matrix \mathbf{R}_x is given as

$$C = \log_2 \left| \mathbf{I} + \frac{1}{\sigma_n^2} \mathbf{H} \mathbf{R}_x \mathbf{H}^H \right|$$

where the notation $|\mathbf{A}|$ above denotes the determinant of the matrix \mathbf{A} . Consider now equal power allocation, i.e., transmit covariance given as $\mathbf{R}_x = \frac{P_t}{t} \mathbf{I}$, where the transmit power P_t is equally allocated to all the t transmit antennas. Also, let us look at a special scenario of $t \gg r$, corresponding to a much larger number of transmit than receive antennas. Substituting the value of $\mathbf{R}_x = \frac{P_t}{t} \mathbf{I}$, the above MIMO capacity C reduces to

$$C = \log_2 \left| \mathbf{I} + \frac{P_t}{t \sigma_n^2} \mathbf{H} \mathbf{H}^H \right|$$

Let us now examine the structure of the matrix $\mathbf{H} \mathbf{H}^H$. Let the r columns of the matrix \mathbf{H}^H be denoted by $\mathbf{h}_1, \mathbf{h}_2, \dots, \mathbf{h}_r$.

Hence, $\mathbf{H}\mathbf{H}^H$ can be simplified as

$$\begin{aligned} \mathbf{H}\mathbf{H}^H &= \begin{bmatrix} \mathbf{h}_1^H \\ \mathbf{h}_2^H \\ \vdots \\ \mathbf{h}_r^H \end{bmatrix} \begin{bmatrix} \mathbf{h}_1 & \mathbf{h}_2 & \dots & \mathbf{h}_r \end{bmatrix} \\ &= \begin{bmatrix} \mathbf{h}_1^H \mathbf{h}_1 & \mathbf{h}_1^H \mathbf{h}_2 & \dots & \mathbf{h}_1^H \mathbf{h}_r \\ \mathbf{h}_2^H \mathbf{h}_1 & \mathbf{h}_2^H \mathbf{h}_2 & \dots & \mathbf{h}_2^H \mathbf{h}_r \\ \vdots & \vdots & \ddots & \vdots \\ \mathbf{h}_r^H \mathbf{h}_1 & \mathbf{h}_r^H \mathbf{h}_2 & \dots & \mathbf{h}_r^H \mathbf{h}_r \end{bmatrix} \end{aligned}$$

Observe now that all the vectors \mathbf{h}_i , $1 \leq i \leq r$ are t -dimensional. Further, considering a rich scattering environment, they consist of uncorrelated random flat-fading channel coefficients.

Hence, we have

$$\begin{aligned} \mathbf{h}_i^H \mathbf{h}_i &= \sum_{k=1}^t |h_{ik}|^2 \\ &\rightarrow t\mathbb{E}\{|h_{ik}|^2\} \\ &\approx t \end{aligned}$$

where we have assumed that all channel coefficients h_{ik} are independent identically distributed with $\mathbb{E}\{|h_{ik}|^2\} = 1$. Further, the quantities $\mathbf{h}_i^H \mathbf{h}_j$, for $i \neq j$ can be approximated as

$$\begin{aligned} \mathbf{h}_i^H \mathbf{h}_j &= \sum_{k=1}^t h_{ik}^* h_{jk} \\ &\rightarrow 0 \\ &\approx 0 \end{aligned}$$

since the elements h_{ik} and h_{jk} are uncorrelated. Hence, the matrix $\mathbf{H}\mathbf{H}^H$ for $t \gg r$, can be approximated as

$$\begin{aligned} \mathbf{H}\mathbf{H}^H &= \begin{bmatrix} t & 0 & \dots & 0 \\ 0 & t & \dots & 0 \\ \vdots & \vdots & \ddots & \vdots \\ 0 & 0 & \dots & t \end{bmatrix} \\ &= t\mathbf{I}_r \end{aligned}$$

Therefore, the asymptotic MIMO capacity C_a is given as

$$\begin{aligned} \log_2 \left| \mathbf{I} + \frac{P_t}{t\sigma_n^2} \times t\mathbf{I}_r \right| &= \log_2 \left| \mathbf{I} + \frac{P_t}{\sigma_n^2} \mathbf{I}_r \right| \\ &= r \log_2 \left(1 + \frac{P_t}{\sigma_n^2} \right) \end{aligned}$$

The above simplification can be better seen as follows. Consider $\mathbf{I}_r + \frac{P_t}{\sigma_n^2} \mathbf{I}_r$, which can be written as

$$\mathbf{I}_r + \frac{P_t}{\sigma_n^2} \mathbf{I}_r = \begin{bmatrix} 1 + \frac{P_t}{\sigma_n^2} & 0 & \dots & 0 \\ 0 & 1 + \frac{P_t}{\sigma_n^2} & \dots & 0 \\ \vdots & \vdots & \ddots & \vdots \\ 0 & 0 & \dots & 1 + \frac{P_t}{\sigma_n^2} \end{bmatrix} \quad (6.15)$$

It can be readily seen that the determinant of the above matrix is $\left(1 + \frac{P_t}{\sigma_n^2}\right)^r$. Hence, the capacity is simplified as, $\log_2 \left(1 + \frac{P_t}{\sigma_n^2}\right)^r = r \log_2 \left(1 + \frac{P_t}{\sigma_n^2}\right)$. Also, it can be seen that in this case, since $t \gg r$, we have $\min\{r, t\} = r$. The asymptotic capacity can, therefore, also be written as

$$C_a = (\min\{r, t\}) \log_2 \left(1 + \frac{P_t}{\sigma_n^2}\right)$$

from which it can be seen that the capacity increases **linearly** with the minimum of the number of transmit or receive antennas, which also indicates the number of degrees of freedom of

the MIMO system. Further, also observe that this gain is achieved with a constant transmit power P_t , i.e., one does not need to increase the net transmit power to achieve a higher throughput using MIMO. This indicates the power of employing MIMO in broadband wireless communication systems. The throughput can be increased significantly without any need for a higher transmit power.

6.8 | Alamouti and Space-Time Codes

In this section, we describe a power set of codes which are termed *space-time* codes for error protection coding in MIMO communication systems. In a traditional error-control coding framework, the block code is applied only over the time dimension or basically over a block of concatenated symbols. However, due to the nature of the MIMO system, one can exploit the spatial dimension as well. That is to say, the one can additionally encode the symbols over the spatial dimension or across the multiple antennas, in addition to coding over the time dimension. This gives rise to the paradigm of space-time encoding, which leads to a significantly superior performance in MIMO systems and multiple-antenna systems in general.

We begin with a basic introduction to the Alamouti code which is described for a 1×2 system, i.e., for a system with $r = 1$ receive antenna and $t = 2$ transmit antennas. This is an example of a MISO system, which is a special case of the MIMO system, and has been described in the beginning of this chapter. Let the 1×2 channel matrix be denoted by $[h_1, h_2]$, where h_1, h_2 denote the channel coefficients between transmit antennas 1, 2 and the single receive antenna respectively. Hence, the system model can be represented as

$$y = \begin{bmatrix} h_1 & h_2 \end{bmatrix} \begin{bmatrix} x_1 \\ x_2 \end{bmatrix} + n \quad (6.16)$$

where x_1, x_2 are the symbols transmitted from the two transmit antennas and n denotes the additive white Gaussian noise at the receiver. Before we discuss the Alamouti code, let us discuss another possible mode of transmission, which is termed *beamforming*. Consider now a symbol x which is transmitted as follows. Let x_1 be generated as $\frac{h_1^*}{\|\mathbf{h}\|}x$ and similarly, x_2 be generated as $x_2 = \frac{h_2^*}{\|\mathbf{h}\|}x$. Here, $\|\mathbf{h}\|$ denotes the norm of vector \mathbf{h} and is defined as

$\|\mathbf{h}\| = \sqrt{|h_1|^2 + |h_2|^2}$. Thus, the transmit vector is now given as

$$\begin{bmatrix} x_1 \\ x_2 \end{bmatrix} = \begin{bmatrix} \frac{h_1^*}{\|\mathbf{h}\|} \\ \frac{h_2^*}{\|\mathbf{h}\|} \end{bmatrix} x$$

This is termed *transmit beamforming*, i.e., transmitting the symbol x in the direction given by the vector

$$\begin{bmatrix} \frac{h_1^*}{\|\mathbf{h}\|} \\ \frac{h_2^*}{\|\mathbf{h}\|} \end{bmatrix}.$$

Substituting the above expression for the beamformed symbol in Eq. (6.16), the output y is given as

$$\begin{aligned} y &= \begin{bmatrix} h_1 & h_2 \end{bmatrix} \begin{bmatrix} \frac{h_1^*}{\|\mathbf{h}\|} \\ \frac{h_2^*}{\|\mathbf{h}\|} \end{bmatrix} x + n, \\ &= \left(\frac{|h_1|^2}{\|\mathbf{h}\|} + \frac{|h_2|^2}{\|\mathbf{h}\|} \right) x + n, \\ &= \|\mathbf{h}\| x + n \end{aligned}$$

Observe that the SNR for the above system is, therefore, given as

$$\text{SNR} = \frac{\|\mathbf{h}\|^2 P}{\sigma_n^2} \quad (6.17)$$

which is identical to that of the receive diversity with *Maximum Ratio Combining (MRC)*. Thus, the above example seems to indicate that the performance that can be achieved through multiple antennas at the transmitter is equivalent to that achieved with multiple antennas at the receiver. However, a close examination reveals the following point. Consider again the transmit vector given as

$$\begin{bmatrix} x_1 \\ x_2 \end{bmatrix} = \begin{bmatrix} \frac{h_1^*}{\|\mathbf{h}\|} \\ \frac{h_2^*}{\|\mathbf{h}\|} \end{bmatrix} x$$

Observe that to perform this at the transmitter requires knowledge of the channel coefficients h_1, h_2 at the transmitter, which is termed *Channel State Information* (CSI) in the context of wireless communications. However, the channel coefficients h_1, h_2 are estimated at the receiver. To implement beamforming at the transmitter, information about these channel coefficients has to be *fed back* to the transmitter. This is a challenging task. Therefore, one cannot always count on possessing the knowledge of the channel at the transmitter. The Alamouti space-time code is an ingenious scheme which overcomes this constraint through a novel transmission procedure and is described next.

6.8.1 Alamouti Code: Procedure

The Alamouti code is a space-time code proposed for a 1×2 MISO system. The interesting aspect of the Alamouti-code is that it achieves a diversity order of 2 without CSI at the transmitter. Consider two symbols x_1, x_2 . In an Alamouti-coded system, in the first transmit instant, the symbol x_1 is transmitted from the transmit antenna 1, while x_2 is transmitted from the transmit antenna 2. Therefore, the transmit symbol vector in the first time instant is given as

$$\begin{bmatrix} x_1 \\ x_2 \end{bmatrix}$$

Further, the received symbol $y(1)$ at the receiver corresponding to this transmission is given as

$$y(1) = \begin{bmatrix} h_1 & h_2 \end{bmatrix} \begin{bmatrix} x_1 \\ x_2 \end{bmatrix} + n(1) \quad (6.18)$$

In the second time instant, the symbol $-x_2^*$ is transmitted from the first transmit antenna, while x_1^* is transmitted from the second transmit antenna. As we will see later, this is the unique aspect of the Alamouti code which enables it to achieve diversity gain of the order 2 at the receiver. Therefore, the transmit symbol vector in the second time instant is given as

$$\begin{bmatrix} -x_2^* \\ x_1^* \end{bmatrix}$$

Further, the received symbol $y(2)$ can be expressed as

$$y(2) = \begin{bmatrix} h_1 & h_2 \end{bmatrix} \begin{bmatrix} -x_2^* \\ x_1^* \end{bmatrix} + n(2) \quad (6.19)$$

Consider the conjugate of $y(2)$ at the receiver, the above equation can be simplified as

$$\begin{aligned} y^*(2) &= \begin{bmatrix} h_1^* & h_2^* \end{bmatrix} \begin{bmatrix} -x_2 \\ x_1 \end{bmatrix} + n^*(2) \\ &= \begin{bmatrix} -h_1^* & h_2^* \end{bmatrix} \begin{bmatrix} x_2 \\ x_1 \end{bmatrix} + n^*(2) \\ &= \begin{bmatrix} h_2^* & -h_1^* \end{bmatrix} \begin{bmatrix} x_1 \\ x_2 \end{bmatrix} + n^*(2) \end{aligned} \quad (6.20)$$

Now, the received symbols $y(1)$ and $y^*(2)$ from equations (6.18) and (6.20) above can be stacked to write the combined system model for the first and second time instants in the Alamouti code as

$$\underbrace{\begin{bmatrix} y(1) \\ y^*(2) \end{bmatrix}}_{\mathbf{y}} = \underbrace{\begin{bmatrix} h_1 & h_2 \\ h_2^* & -h_1^* \end{bmatrix}}_{\mathbf{H}} \begin{bmatrix} x_1 \\ x_2 \end{bmatrix} + \underbrace{\begin{bmatrix} n(1) \\ n^*(2) \end{bmatrix}}_{\mathbf{n}} \quad (6.21)$$

Thus, both the symbols have been stacked which effectively converts the Alamouti coded system into a 2×2 MIMO system, with the channel matrix

$$\begin{bmatrix} h_1 & h_2 \\ h_2^* & -h_1^* \end{bmatrix} \quad (6.22)$$

Further, the noise $n^*(2)$ is statistically identical to $n(2)$, i.e., $n^*(2)$ is zero mean circularly symmetric Gaussian noise with variance σ_n^2 . Moreover, observe a *very important property* of

the Alamouti channel matrix. Consider the columns $\mathbf{c}_1, \mathbf{c}_2$ of the channel matrix given as

$$\mathbf{c}_1 = \begin{bmatrix} h_1 \\ h_2^* \end{bmatrix}, \mathbf{c}_2 = \begin{bmatrix} h_2 \\ -h_1^* \end{bmatrix}$$

Then, we have, $\mathbf{c}_1^H \mathbf{c}_2$ given as

$$\begin{aligned} \mathbf{c}_1^H \mathbf{c}_2 &= \begin{bmatrix} h_1^* & h_2 \end{bmatrix} \begin{bmatrix} h_2 \\ -h_1^* \end{bmatrix} \\ &= h_1^* h_2 - h_2 h_1^* \\ &= 0 \end{aligned}$$

It can, therefore, be seen that the columns $\mathbf{c}_1, \mathbf{c}_2$ are orthogonal. This tremendously simplifies the receive processing of the Alamouti code. Consider now beamforming using the vector \mathbf{w}_1 defined in terms of \mathbf{c}_1 as

$$\begin{aligned} \mathbf{w}_1 &= \frac{1}{\|\mathbf{c}_1\|} \mathbf{c}_1 \\ &= \frac{1}{\|\mathbf{h}\|} \begin{bmatrix} h_1 \\ h_2^* \end{bmatrix} \end{aligned}$$

One can now employ this as a receive beamformer to derive the processed symbol as

$$\begin{aligned} \mathbf{w}_1^H \mathbf{y} &= \begin{bmatrix} \frac{h_1^*}{\|\mathbf{h}\|} & \frac{h_2}{\|\mathbf{h}\|} \end{bmatrix} \begin{bmatrix} h_1 & h_2 \\ h_2^* & -h_1^* \end{bmatrix} \begin{bmatrix} x_1 \\ x_2 \end{bmatrix} + \mathbf{w}_1^H \mathbf{n} \\ &= \begin{bmatrix} \|\mathbf{h}\| & 0 \end{bmatrix} \begin{bmatrix} x_1 \\ x_2 \end{bmatrix} + \tilde{n}_1 \\ &= \|\mathbf{h}\| x_1 + \tilde{n}_1 \end{aligned}$$

Further, since \mathbf{w}_1 is a unit-norm vector, $\tilde{n}_1 = \mathbf{w}_1^H \mathbf{n}$ is Gaussian noise with variance σ_n^2 . Therefore, the SNR at the receiver is given as

$$\begin{aligned} \text{SNR} &= \frac{\|\mathbf{h}\|^2}{\sigma_n^2} \text{E} \left\{ |x_1|^2 \right\} \\ &= \frac{\|\mathbf{h}^2\|}{\sigma_n^2} P_1, \end{aligned}$$

where $\|\mathbf{h}\|^2 = |h_1|^2 + |h_2|^2$. Therefore, the diversity gain or diversity order of BER at the receiver is 2, since it is analogous to the maximum ratio combiner with 2 antennas shown in Eq. (6.17). Similarly, to decode x_2 , the beamformer \mathbf{w}_2 is given as

$$\mathbf{w}_2 = \frac{\mathbf{c}_2}{\|\mathbf{c}_2\|} = \frac{1}{\|\mathbf{h}\|} \begin{bmatrix} h_2 \\ -h_1^* \end{bmatrix}$$

Thus, the SNR of the decoded streams of the Alamouti code is $\frac{\|\mathbf{h}^2\|}{\sigma_n^2} P_1$, $\frac{\|\mathbf{h}^2\|}{\sigma_n^2} P_2$, where P_1 , P_2 are the power allocated to x_1 , x_2 respectively. However, it may be noted that the total transmit power P is fixed. This has to be allocated to the individual streams. Therefore, we have $P_1 = P_2 = \frac{P}{2}$. Hence, the net output SNR of each stream is

$$\text{SNR} = \frac{P}{2} \frac{\|\mathbf{h}^2\|}{\sigma_n^2} = \frac{1}{2} \frac{\|\mathbf{h}^2\|}{\sigma_n^2} P$$

or in other words, equal to half that with CSI at the transmitter as can be seen from Eq. (6.17). Thus, the absence of CSI results in a loss of 3 dB in output SNR corresponding to this factor of $\frac{1}{2}$. Also, the orthogonality of the columns \mathbf{c}_1 , \mathbf{c}_2 of the effective channel matrix is a key property of the Alamouti code. Hence, the Alamouti code is also termed an *Orthogonal Space-Time Block Code* (OSTBC). The term *space-time* refers to the fact that the Alamouti code involves two symbols x_1 , x_2 which are transmitted over two antennas over two instants of time. Therefore, the symbols are coded across both the space and time dimensions, leading to the name "space-time" code. This is schematically shown in Figure 6.7. Further, also note that the Alamouti code transmits a net of two symbols x_1 , x_2 in time instants. Therefore, on an average it transmits one symbol per time instant. Hence, the net rate of the code is 1 symbol per time instant, i.e., the rate $R = 1$. Such a code is termed a *full rate code*. Therefore, the Alamouti code is a full-rate code. Example 6.6 given below clarifies the various operations in the Alamouti code.

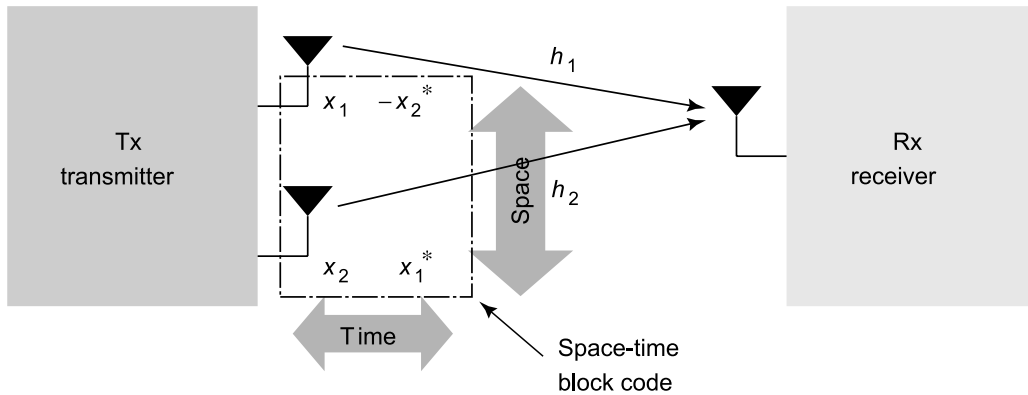


Figure 6.7 Alamouti orthogonal space-time block code

EXAMPLE 6.6

Consider the 1×2 wireless system given as

$$y = \begin{bmatrix} 1 + j & 3 + 4j \end{bmatrix} \begin{bmatrix} x_1 \\ x_2 \end{bmatrix} + n$$

Clearly, indicate the processing at the transmitter and the receiver for the above system with the Alamouti code.

Solution: Firstly, it can be readily seen that the channel coefficients h_1, h_2 are $1 + j, 3 + 4j$, corresponding to the channels of transmit antennas 1, 2 respectively. Therefore, corresponding to the transmission of symbols x_1, x_2 from the first and second transmit antennas in the first time instant, we have the received symbol $y(1)$ given as

$$y(1) = \begin{bmatrix} 1 + j & 3 + 4j \end{bmatrix} \begin{bmatrix} x_1 \\ x_2 \end{bmatrix} + n(1)$$

as described in Eq. (6.18). Further, corresponding to the transmission of $-x_2^*$, x_1^* from the first and second transmit antennas in the second time instant, we have

$$y(2) = \begin{bmatrix} 1+j & 3+4j \end{bmatrix} \begin{bmatrix} -x_2^* \\ x_1^* \end{bmatrix} + n(2)$$

which can be simplified by considering the conjugate $y^*(2)$ of $y(2)$ as,

$$\begin{aligned} y^*(2) &= \begin{bmatrix} 1-j & 3-4j \end{bmatrix} \begin{bmatrix} -x_2 \\ x_1 \end{bmatrix} + n^*(2) \\ &= \begin{bmatrix} -1+j & 3-4j \end{bmatrix} \begin{bmatrix} x_2 \\ x_1 \end{bmatrix} + n^*(2) \\ &= \begin{bmatrix} 3-4j & -1+j \end{bmatrix} \begin{bmatrix} x_1 \\ x_2 \end{bmatrix} + n^*(2) \end{aligned}$$

as given in Eq. (6.20). Therefore, stacking now $y(1)$, $y^*(2)$, we have

$$\underbrace{\begin{bmatrix} y(1) \\ y^*(2) \end{bmatrix}}_{\mathbf{y}} = \underbrace{\begin{bmatrix} 1+j & 3+4j \\ 3-4j & -1+j \end{bmatrix}}_{\mathbf{H}} \begin{bmatrix} x_1 \\ x_2 \end{bmatrix} + \mathbf{n}$$

where \mathbf{H} above indicates the effective Alamouti channel matrix and \mathbf{y} is the effective received vector. Therefore, the columns \mathbf{c}_1 , \mathbf{c}_2 are given as

$$\mathbf{c}_1 = \begin{bmatrix} 1+j \\ 3-4j \end{bmatrix}, \quad \mathbf{c}_2 = \begin{bmatrix} 3+4j \\ -1+j \end{bmatrix}$$

It can now be easily verified that the columns \mathbf{c}_1 , \mathbf{c}_2 are orthogonal. Consider $\mathbf{c}_1^H \mathbf{c}_2$, which can be simplified as

$$\begin{aligned}\mathbf{c}_1^H \mathbf{c}_2 &= (1+j)^*(3+4j) + (3-4j)^*(-1+j) \\ &= (1-j)(3+4j) + (3+4j)(-(1-j)) \\ &= (1-j)(3+4j) - (3+4j)(1-j) \\ &= 0\end{aligned}$$

Beamformer to detect x_1 is given as

$$\mathbf{w}_1 = \frac{\mathbf{c}_1}{\|\mathbf{c}_1\|} = \frac{1}{\sqrt{27}} \begin{bmatrix} 1+j \\ 3-4j \end{bmatrix}$$

To detect x_1 , one has to perform the receive beamforming operation $\mathbf{w}_1^H \mathbf{y}$. Similarly, \mathbf{w}_2 , the beamformer to detect x_2 is given as

$$\mathbf{w}_2 = \frac{\mathbf{c}_2}{\|\mathbf{c}_2\|} = \frac{1}{\sqrt{27}} \begin{bmatrix} 3+4j \\ -1+j \end{bmatrix}$$

Therefore, x_2 can be detected by performing the operation $\mathbf{w}_2^H \mathbf{y}$ at the receiver.

6.9 | Another OSTBC Example

We now describe another example of an OSTBC for a 1×3 , i.e., a system with 1 receive and 3 transmit antennas. Consider the channel matrix $\begin{bmatrix} h_1 & h_2 & h_3 \end{bmatrix}$ corresponding to this 1×3 system. Consider the transmission of 4 symbols x_1, x_2, x_3, x_4 over the wireless channel. The corresponding coded block for the OSTBC is given as

$$\begin{bmatrix} x_1 & -x_2 & -x_3 & -x_4 & x_1^* & -x_2^* & -x_3^* & -x_4^* \\ x_2 & x_1 & x_4 & -x_3 & x_2^* & x_1^* & x_4^* & -x_3^* \\ x_3 & -x_4 & x_1 & x_2 & x_3^* & -x_4^* & x_1^* & x_2^* \end{bmatrix} \quad (6.23)$$

Each column in the above code block gives the three symbols transmitted over each of the 3 transmit antennas. Observe, that there are 8 time instants in total in the above block. Therefore, the four symbols, i.e., x_1, x_2, x_3, x_4 are being transmitted over a total of 8 time instants. Therefore, the net rate of the code is $\frac{4}{8} = \frac{1}{2}$. Consider the first received symbols $y(1)$. This can be expressed as

$$\begin{aligned} y(1) &= \begin{bmatrix} h_1 & h_2 & h_3 \end{bmatrix} \begin{bmatrix} x_1 \\ x_2 \\ x_3 \end{bmatrix} \\ &= h_1x_1 + h_2x_2 + h_3x_3 + 0x_4 \\ &= \begin{bmatrix} h_1 & h_2 & h_3 & 0 \end{bmatrix} \begin{bmatrix} x_1 \\ x_2 \\ x_3 \\ x_4 \end{bmatrix} \end{aligned}$$

Further, the second received symbol $y(2)$ is given as

$$\begin{aligned} y(2) &= \begin{bmatrix} h_1 & h_2 & h_3 \end{bmatrix} \begin{bmatrix} -x_2 \\ x_1 \\ -x_4 \end{bmatrix} \\ &= -h_1x_2 + h_2x_1 - h_3x_4 + 0x_3 \\ &= \begin{bmatrix} h_2 & -h_1 & 0 & -h_3 \end{bmatrix} \begin{bmatrix} x_1 \\ x_2 \\ x_3 \\ x_4 \end{bmatrix} \end{aligned} \tag{6.24}$$

Thus, proceeding similarly, the received symbols $y(1), y(2), y(3), y(4)$ and the complex conjugates of the symbols $y(5), y(6), y(7), y(8)$ can be stacked to obtain the effective system

model

$$\underbrace{\begin{bmatrix} y(1) \\ y(2) \\ y(3) \\ y(4) \\ y^*(5) \\ y^*(6) \\ y^*(7) \\ y^*(8) \end{bmatrix}}_{\mathbf{y}} = \underbrace{\begin{bmatrix} h_1 & h_2 & h_3 & 0 \\ h_2 & -h_1 & 0 & -h_3 \\ h_3 & 0 & -h_1 & h_2 \\ 0 & h_3 & -h_2 & -h_1 \\ h_1^* & h_2^* & h_3^* & 0 \\ h_2^* & -h_1^* & 0 & -h_3^* \\ h_3^* & 0 & -h_1^* & h_2^* \\ 0 & h_3^* & -h_2^* & -h_1^* \end{bmatrix}}_{\mathbf{H}} \begin{bmatrix} x_1 \\ x_2 \\ x_3 \\ x_4 \end{bmatrix}. \quad (6.25)$$

Therefore, it can be seen that the effective channel matrix \mathbf{H} represents an equivalent 8×4 MIMO system. Further, the different columns of \mathbf{H} are orthogonal. For instance, consider the $\mathbf{c}_1^H \mathbf{c}_2$ corresponding to columns \mathbf{c}_1 , \mathbf{c}_2 . This can be simplified as

$$\begin{aligned} \mathbf{c}_1^H \mathbf{c}_2 &= \begin{bmatrix} h_1^* & h_2^* & h_3^* & 0 & h_1 & h_2 & h_3 & 0 \end{bmatrix} \begin{bmatrix} h_2 \\ -h_1 \\ 0 \\ h_3 \\ h_2^* \\ h_1^* \\ 0 \\ h_3^* \end{bmatrix} \\ &= h_1^* h_2 - h_2^* h_1 + 0 + 0 + h_1 h_2^* - h_2 h_1^* + 0 + 0 \\ &= 0 \end{aligned}$$

Hence, the columns are orthogonal. Therefore, this is an example of an $R = \frac{1}{2}$ OSTBC, i.e., orthogonal space-time block code.

6.10 | Nonlinear MIMO Receiver: V-BLAST

Previously, we have seen the zero-forcing (ZF) and minimum mean squared error (MMSE) receivers, which are **linear** MIMO receivers. We now look at the first nonlinear MIMO receiver, termed V-BLAST, short for *Vertical Bell Labs Layered Space-Time* receiver. V-BLAST employs *Successive Interference Cancellation* (SIC) in which the impact of each estimated symbol is cancelled prior to the detection of the next symbol. This SIC principle on which V-BLAST is based leads to its nonlinear nature. Consider the MIMO system model given as

$$\begin{aligned} \mathbf{y} &= \mathbf{H}\mathbf{x} + \mathbf{n} \\ &= \begin{bmatrix} \mathbf{h}_1 & \mathbf{h}_2 & \dots & \mathbf{h}_t \end{bmatrix} \begin{bmatrix} x_1 \\ x_2 \\ \vdots \\ x_t \end{bmatrix} + \mathbf{n} \end{aligned} \quad (6.26)$$

The vectors $\mathbf{h}_1, \mathbf{h}_2, \dots, \mathbf{h}_t$ correspond to the t columns of the channel matrix \mathbf{H} . Consider now the left-inverse or pseudo-inverse of the channel matrix \mathbf{Q} described in Eq. (6.3). Let this matrix be denoted by the $t \times r$ matrix \mathbf{Q} , i.e., $\mathbf{Q}\mathbf{H} = \mathbf{I}_t$. Further, let the matrix \mathbf{Q} be written as

$$\mathbf{Q} = \begin{bmatrix} \mathbf{q}_1^H \\ \mathbf{q}_2^H \\ \vdots \\ \mathbf{q}_t^H \end{bmatrix}$$

where $\mathbf{q}_1^H, \mathbf{q}_2^H, \dots, \mathbf{q}_t^H$ denote the t rows of the matrix \mathbf{Q} . Therefore, $\mathbf{Q}\mathbf{H} = \mathbf{I}_t$ can be written as

$$\begin{bmatrix} \mathbf{q}_1^H \\ \mathbf{q}_2^H \\ \vdots \\ \mathbf{q}_t^H \end{bmatrix} \begin{bmatrix} \mathbf{h}_1 & \mathbf{h}_2 & \dots & \mathbf{h}_t \end{bmatrix} = \mathbf{I}_t$$

$$\Rightarrow \begin{bmatrix} \mathbf{q}_1^H \mathbf{h}_1 & \mathbf{q}_1^H \mathbf{h}_2 & \dots & \mathbf{q}_1^H \mathbf{h}_t \\ \mathbf{q}_2^H \mathbf{h}_1 & \mathbf{q}_2^H \mathbf{h}_2 & \dots & \mathbf{q}_2^H \mathbf{h}_t \\ \vdots & \vdots & \ddots & \vdots \\ \mathbf{q}_t^H \mathbf{h}_1 & \mathbf{q}_t^H \mathbf{h}_2 & \dots & \mathbf{q}_t^H \mathbf{h}_t \end{bmatrix} = \begin{bmatrix} 1 & 0 & \dots & 0 \\ 0 & 1 & \dots & 0 \\ \vdots & \vdots & \ddots & \vdots \\ 0 & 0 & \dots & 1 \end{bmatrix} \quad (6.27)$$

Therefore, we have,

$$\begin{aligned} \mathbf{q}_1^H \mathbf{h}_1 &= \mathbf{q}_2^H \mathbf{h}_2 = \dots = \mathbf{q}_t^H \mathbf{h}_t = 0 \\ \mathbf{q}_1^H \mathbf{h}_2 &= \mathbf{q}_1^H \mathbf{h}_3 = \dots = \mathbf{q}_{t-1}^H \mathbf{h}_t = 0 \end{aligned}$$

The above property can be basically summarized as

$$\mathbf{q}_i^H \mathbf{h}_j = \begin{cases} 1 & \text{if } i = j \\ 0 & \text{if } i \neq j \end{cases} \quad (6.28)$$

From Eq. (6.26), observe that the system model can be explicitly given in terms of the columns of the channel matrix \mathbf{H} as

$$\mathbf{y} = \mathbf{h}_1 x_1 + \mathbf{h}_2 x_2 + \dots + \mathbf{h}_t x_t + \mathbf{n}$$

Employing now the fact that $\mathbf{q}_1^H \mathbf{h}_1 = 1$ and $\mathbf{q}_1^H \mathbf{h}_2, \mathbf{q}_1^H \mathbf{h}_3, \dots$, is zero, one can use \mathbf{q}_1 as a receive beamformer. Therefore, performing $\mathbf{q}_1^H \mathbf{y}$ at the receiver, we have

$$\begin{aligned} \tilde{y}_1 &= \mathbf{q}_1^H \mathbf{y} \\ &= \mathbf{q}_1^H (\mathbf{h}_1 x_1 + \mathbf{h}_2 x_2 + \dots + \mathbf{h}_t x_t + \mathbf{n}) \\ &= \underbrace{\mathbf{q}_1^H \mathbf{h}_1}_1 x_1 + \underbrace{\mathbf{q}_1^H \mathbf{h}_2}_0 x_2 + \dots + \underbrace{\mathbf{q}_1^H \mathbf{h}_t}_0 x_t + \underbrace{\mathbf{q}_1^H \mathbf{n}}_{\tilde{n}_1} \\ &= x_1 + \tilde{n}_1 \end{aligned}$$

Thus, \tilde{y}_1 can now be employed to decode x_1 . Now, the interference caused by x_1 is removed from \mathbf{y} to form \check{y}_2 as

$$\begin{aligned}
 \check{y}_2 &= \mathbf{y} - \mathbf{h}_1 x_1 \\
 &= \mathbf{h}_1 x_1 + \mathbf{h}_2 x_2 + \dots + \mathbf{h}_t x_t + \mathbf{n} - \mathbf{h}_1 x_1 \\
 &= \mathbf{h}_2 x_2 + \dots + \mathbf{h}_t x_t + \mathbf{n} \\
 &= \underbrace{\begin{bmatrix} \mathbf{h}_2 & \mathbf{h}_3 & \dots & \mathbf{h}_t \end{bmatrix}}_{\mathbf{H}^{(2)}} \underbrace{\begin{bmatrix} x_2 \\ x_3 \\ \vdots \\ x_t \end{bmatrix}}_{\mathbf{x}^{(2)}} + \mathbf{n} \\
 &= \mathbf{H}^{(2)} \mathbf{x}^{(2)} + \mathbf{n}
 \end{aligned}$$

The above system model can now be seen to correspond to a reduced MIMO system with channel matrix $\mathbf{H}^{(2)}$ of r rows and $t - 1$ columns. Thus, it represents an $r \times (t - 1)$ MIMO system, with x_2, x_3, \dots, x_t denoting the $t - 1$ transmit symbols. Now, consider $\mathbf{Q}^{(2)}$ as the zero-forcing receiver for $\mathbf{H}^{(2)}$ and repeat the above process by decoding x_2 , and so on. The advantage of this scheme is that the diversity order and the associated diversity gain progressively increases as we proceed through the scheme for decoding the different transmit symbols x_1 through x_t . In fact, in the last stage, when only one symbol x_t is left for decoding, the effective system model is given as

$$\check{y}_t = \mathbf{H}^{(t)} x_t + \mathbf{n}$$

Notice that the effective channel $\mathbf{H}^{(t)}$ is the column vector \mathbf{h}_t . This can be decoded by receive beamforming along \mathbf{h}_t , in other words, maximum ratio combining. In V-BLAST, streams that are decoded later experience progressively higher diversity. Example 6.7 clearly illustrates the working of the V-BLAST MIMO receiver.

EXAMPLE 6.7

Consider the 2×2 MIMO system given below and describe the various stages of the V-BLAST receiver.

$$\underbrace{\begin{bmatrix} y_1 \\ y_2 \end{bmatrix}}_{\mathbf{y}} = \underbrace{\begin{bmatrix} 1 & 2 \\ 1 & 3 \end{bmatrix}}_{\mathbf{H}} \underbrace{\begin{bmatrix} x_1 \\ x_2 \end{bmatrix}}_{\mathbf{x}} + \underbrace{\begin{bmatrix} n_1 \\ n_2 \end{bmatrix}}_{\mathbf{n}} \quad (6.29)$$

Solution: The channel matrix \mathbf{H} is given as

$$\mathbf{H} = \begin{bmatrix} 1 & 2 \\ 1 & 3 \end{bmatrix}$$

Therefore, the left inverse of \mathbf{H} , i.e., $\mathbf{Q} = \mathbf{H}^\dagger$ is given as $\mathbf{Q} = \mathbf{H}^{-1}$ since the matrix \mathbf{H} is square and invertible. Therefore, we have

$$\mathbf{Q} = \mathbf{H}^{-1} = \begin{bmatrix} 3 & -2 \\ -1 & 1 \end{bmatrix}$$

It can be clearly seen that the rows of the matrix \mathbf{Q} are $\mathbf{q}_1^H = \begin{bmatrix} 3 & -2 \end{bmatrix}$, $\mathbf{q}_2^H = \begin{bmatrix} -1 & 1 \end{bmatrix}$. Further, it can be readily seen that $\mathbf{q}_1^H \mathbf{h}_1$ is given as

$$\mathbf{q}_1^H \mathbf{h}_1 = \begin{bmatrix} 3 & -2 \end{bmatrix} \begin{bmatrix} 1 \\ 1 \end{bmatrix} = 1$$

and $\mathbf{q}_1^H \mathbf{h}_2$ can be simplified as

$$\mathbf{q}_1^H \mathbf{h}_2 = \begin{bmatrix} 3 & -2 \end{bmatrix} \begin{bmatrix} 2 \\ 3 \end{bmatrix} = 0$$

Therefore, the first row \mathbf{q}_1^H is orthogonal to \mathbf{h}_2 , i.e., the second column of the channel matrix \mathbf{H} . Therefore, decoding in \mathbf{q}_1^H in the first stage of V-BLAST, we have

$$\begin{aligned}\tilde{y}_1 &= \mathbf{q}_1^H \mathbf{y} \\ &= \begin{bmatrix} 3 & -2 \end{bmatrix} \left(\begin{bmatrix} 1 & 2 \\ 1 & 3 \end{bmatrix} \begin{bmatrix} x_1 \\ x_2 \end{bmatrix} + \begin{bmatrix} n_1 \\ n_2 \end{bmatrix} \right) \\ &= \begin{bmatrix} 1 & 0 \end{bmatrix} \begin{bmatrix} x_1 \\ x_2 \end{bmatrix} + \underbrace{\mathbf{q}_1^H \mathbf{n}}_{\tilde{n}_1} \\ &= x_1 + \tilde{n}_1\end{aligned}$$

Therefore, the symbol x_1 can be detected from \tilde{y}_1 . The interference caused by this can now be canceled from the received signal \mathbf{y} to form $\check{\mathbf{y}}_2$ as

$$\begin{aligned}\check{\mathbf{y}}_2 &= \mathbf{y} - \mathbf{h}_1 x_1 \\ &= \begin{bmatrix} 1 & 2 \\ 1 & 3 \end{bmatrix} \begin{bmatrix} x_1 \\ x_2 \end{bmatrix} + \begin{bmatrix} n_1 \\ n_2 \end{bmatrix} - \begin{bmatrix} 1 \\ 1 \end{bmatrix} x_1 \\ &= \begin{bmatrix} 2 \\ 3 \end{bmatrix} x_2 + \mathbf{n}\end{aligned}$$

It can now be seen that the above system corresponds effectively to a receive diversity system with 2 receive antennas and a single transmit antenna. In fact, the optimum receiver scheme is to perform maximum ratio combining with the receive beamformer $\mathbf{w} = \begin{bmatrix} 2 & 3 \end{bmatrix}^T$. The diversity order of decoding this stream is, therefore, equal to 2.

6.11 | MIMO Beamforming

In this section, we describe beamforming in the context of a MIMO wireless system. Beamforming basically implies that only spatial dimension is used for transmission amongst

the many dimensions that are available. Consider the MIMO system given as

$$\begin{aligned} \mathbf{y} &= \mathbf{H}\mathbf{x} + \mathbf{n} \\ &= \mathbf{U}\mathbf{\Sigma}\mathbf{V}^H\mathbf{x} + \mathbf{n} \\ &= \begin{bmatrix} \mathbf{u}_1 & \mathbf{u}_2 & \dots & \mathbf{u}_t \end{bmatrix} \begin{bmatrix} \sigma_1 & 0 & \dots & 0 \\ 0 & \sigma_2 & \dots & 0 \\ \vdots & \vdots & \ddots & \vdots \\ 0 & 0 & \dots & \sigma_t \end{bmatrix} \begin{bmatrix} \mathbf{v}_1^H \\ \mathbf{v}_2^H \\ \vdots \\ \mathbf{v}_t^H \end{bmatrix} \mathbf{x} + \mathbf{n} \end{aligned}$$

where $\mathbf{H} = \mathbf{U}\mathbf{\Sigma}\mathbf{V}^H$ is the singular value decomposition (SVD) of the channel matrix \mathbf{H} as described in Section 6.6. Observe now that the right and left singular vectors \mathbf{v}_1 , \mathbf{u}_1 respectively, which correspond to the largest singular value σ_1 , represent the dominant transmit and receive modes of the MIMO system. Hence, one can transmit a single symbol \tilde{x}_1 from the transmitter by beamforming along the vector \mathbf{v}_1 as

$$\mathbf{x} = \mathbf{v}_1\tilde{x}_1$$

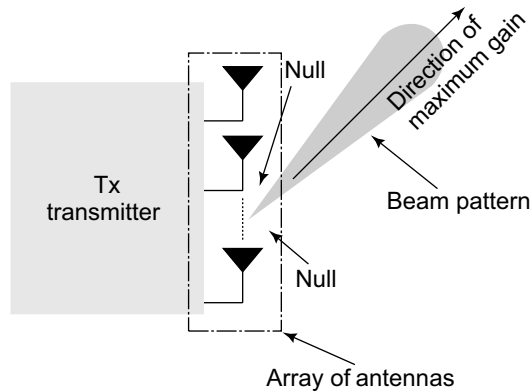


Figure 6.8 MIMO beamforming

Thus, the symbol \tilde{x}_1 is being transmitted along the abstract direction represented by the vector \mathbf{v}_1 in t dimensional space as shown in Figure 6.8. Substituting this in the MIMO system

model, we have

$$\begin{aligned} \mathbf{y} &= \begin{bmatrix} \mathbf{u}_1 & \mathbf{u}_2 & \dots & \mathbf{u}_t \end{bmatrix} \begin{bmatrix} \sigma_1 & 0 & \dots & 0 \\ 0 & \sigma_2 & \dots & 0 \\ \vdots & \vdots & \ddots & \vdots \\ 0 & 0 & \dots & \sigma_t \end{bmatrix} \begin{bmatrix} \mathbf{v}_1^H \\ \mathbf{v}_2^H \\ \vdots \\ \mathbf{v}_t^H \end{bmatrix} \mathbf{v}_1 \tilde{x}_1 + \mathbf{n} \\ &= \begin{bmatrix} \mathbf{u}_1 & \mathbf{u}_2 & \dots & \mathbf{u}_t \end{bmatrix} \begin{bmatrix} \sigma_1 & 0 & \dots & 0 \\ 0 & \sigma_2 & \dots & 0 \\ \vdots & \vdots & \ddots & \vdots \\ 0 & 0 & \dots & \sigma_t \end{bmatrix} \begin{bmatrix} \mathbf{v}_1^H \mathbf{v}_1 \\ \mathbf{v}_2^H \mathbf{v}_1 \\ \vdots \\ \mathbf{v}_t^H \mathbf{v}_1 \end{bmatrix} \tilde{x}_1 + \mathbf{n} \end{aligned}$$

It can now be seen that $\mathbf{v}_1^H \mathbf{v}_1 = 1$, while $\mathbf{v}_2^H \mathbf{v}_1 = \dots = \mathbf{v}_t^H \mathbf{v}_1 = 0$, since \mathbf{v}_i , $2 \leq i \leq t$ are orthogonal to \mathbf{v}_1 . Therefore, the received signal \mathbf{y} can be further simplified as

$$\begin{aligned} \mathbf{y} &= \begin{bmatrix} \mathbf{u}_1 & \mathbf{u}_2 & \dots & \mathbf{u}_t \end{bmatrix} \begin{bmatrix} \sigma_1 & 0 & \dots & 0 \\ 0 & \sigma_2 & \dots & 0 \\ \vdots & \vdots & \ddots & \vdots \\ 0 & 0 & \dots & \sigma_t \end{bmatrix} \begin{bmatrix} 1 \\ 0 \\ \vdots \\ 0 \end{bmatrix} \tilde{x}_1 + \mathbf{n} \\ &= \begin{bmatrix} \mathbf{u}_1 & \mathbf{u}_2 & \dots & \mathbf{u}_t \end{bmatrix} \begin{bmatrix} \sigma_1 \\ 0 \\ \vdots \\ 0 \end{bmatrix} \tilde{x}_1 + \mathbf{n} \\ &= \sigma_1 \mathbf{u}_1 \tilde{x}_1 + \mathbf{n} \end{aligned}$$

Thus, it can be readily seen that the received vector \mathbf{y} effectively corresponds to a multiple receive antenna system with the effective channel vector \mathbf{u}_1 . One can now perform MRC at the receiver using the beamforming vector \mathbf{u}_1 as,

$$\tilde{y}_1 = \mathbf{u}_1^H \mathbf{y}$$

$$\begin{aligned}
&= \mathbf{u}_1^H (\sigma_1 \mathbf{u}_1 \tilde{x}_1 + \mathbf{n}) \\
&= \sigma_1 \mathbf{u}_1^H \mathbf{u}_1 \tilde{x}_1 + \underbrace{\mathbf{u}_1^H \mathbf{n}}_{\tilde{n}_1} \\
&= \sigma_1 \tilde{x}_1 + \tilde{n}_1
\end{aligned}$$

Further, it can be seen from Eq. (6.13) that the variance of the noise $\tilde{n}_1 = \mathbf{u}_1^H \mathbf{n}$ is σ_n^2 . Thus, the SNR at the receiver is given as

$$\text{SNR} = \sigma_1^2 \frac{\text{E} \{ |\tilde{x}_1|^2 \}}{\sigma_n^2} = \sigma_1^2 \frac{P}{\sigma_n^2}$$

where $P = \text{E} \{ |\tilde{x}_1|^2 \}$ is the transmit power corresponding to the symbol \tilde{x}_1 . It can be seen from the above expression that the net transmit power P is amplified by a factor of σ_1^2 corresponding to the largest singular value σ_1 . This MIMO beamforming scheme is termed *Maximum Ratio Transmission (MRT)*. Since only one dimension is being used in this scheme, it results in a simplistic transmission and reception scheme compared to spatial multiplexing MIMO schemes such as MIMO-ZF, MIMO-MMSE, MIMO V-BLAST, etc. However, since it is transmitting along the MIMO spatial dimension with channel gain σ_1 corresponding to the largest singular value, it leads to a high SNR at the receiver. Further, two additional points are worth of being noted about the maximum ration transmission scheme. Firstly, it is capacity optimal at low SNR. Secondly, it achieves the full diversity order of MIMO communication, i.e., rt , where r , t denote the number of receive and transmit antennas respectively.

PROBLEMS

1. Fill in the blanks below.

- (a) The Alamouti scheme belongs to a class of codes known as _____.
- (b) At low SNR, the performance of the MIMO MMSE receiver is equivalent to that of ____.

2. Using the properties of singular values or otherwise, compute the singular values of the channel matrix below.

$$\mathbf{H} = \begin{bmatrix} 1 & 2 & 3.5 \\ 1 & 2 & 3.5 \\ 1 & 2 & 3.5 \end{bmatrix}$$

3. Consider the MIMO channel matrix given below and $\sigma_n^2 = 3$ dB for the system.

$$\mathbf{H} = \begin{bmatrix} 1 & 3 & 0 \\ 1 & 3 & 0 \\ 0 & 0 & 2 \end{bmatrix}$$

- (a) Compute the SVD of the above MIMO channel matrix.
 (b) What is the capacity optimal transmit scheme for a transmit power of 3 dB?
4. **MIMO Decoding** Consider the MIMO channel matrix below.

$$\mathbf{H} = \begin{bmatrix} 1 & -0.8 \\ 0.2 & -1 \end{bmatrix}$$

Consider a transmit power of $P = -3$ dB on each transmit antenna, i.e., $E\{|x_i|^2\} = -3$ dB on each transmit antenna. Let the transmit constellation be BPSK on each transmit antenna.

- (a) Derive the ZF receiver decoding matrix for the above MIMO system.
 (b) Let a received noisy output vector of the above MIMO channel be given as

$$y = \begin{bmatrix} -1.50 \\ 0.27 \end{bmatrix} \quad (6.30)$$

Employing ZF decoding, compute the linear estimate and the decoded transmitted symbols on each transmit antenna.

- (c) What is the vector transmit constellation corresponding to BPSK?

(d) Employ the optimal ML decoder and compute the decoded vector belonging to the transmit constellation above corresponding to the received vector in Eq. (6.30). Illustrate the steps clearly (*Hint*: Mind the transmit power on each antenna).

(e) Of both the decoded vectors above, which one do you think is the correct transmit vector?

5. Answer the questions below.

(a) Compute the SVD of the following 3×2 channel matrix.

$$\mathbf{H} = \begin{bmatrix} 1 & 1 \\ 2 & -2 \\ 3 & 1 \end{bmatrix}$$

(b) Consider BPSK transmission for the above MIMO system with SNR $\frac{P_d}{\sigma_n^2} = 10$ dB. Derive the MMSE MIMO receiver for the above system.

(c) Let a received vector in the above system be given by

$$\begin{bmatrix} -1.71 \\ 12.55 \\ 6.08 \end{bmatrix}$$

Compute the MMSE decoded transmit BPSK vector corresponding to this received vector.

6. **MIMO and Games** Consider an $r \times t$ flat-fading MIMO system characterized by the channel matrix \mathbf{H} . Assume that the transmitter has to select one transmit antenna for transmission and the receiver has to select one receive antenna for reception. Answer the questions that follow.

(a) What is the diversity order of a cooperative transmit/receive antenna selection scenario in which the receive and transmit antennas are chosen such that

$$i, j = \arg \max_{i,j} |h_{i,j}|$$

(b) Consider a game in which the (disruptive) transmitter is trying to choose the worst possible antenna for transmission while the (angel) receiver is trying to choose the best possible antenna. What is the diversity order of the resulting system, if it can be shown that *an* equilibrium (because it is not *the* equilibrium) selection strategy in this

scenario is given by the minimax rule

$$i, j = \arg \min_j \max_i |h_{i,j}|$$

(c) Repeat the above problem with a disruptive receiver and angel transmitter.

7. Channel Estimation in Alamouti-Coded Systems Consider the following QPSK modulated pilot symbols which are Alamouti-coded and transmitted across a 1×2 MISO system.

$$\frac{1}{\sqrt{2}} [1 + j, -1 + j, -1 - j, 1 - j]$$

Compute the least-squares estimate of the channel coefficients if the *total* transmitter power is 20 dB and the received pilot outputs corresponding to the Alamouti-coded pilot inputs are

$$[11.15 - 0.66j, -2.23 + 2.70j, -13.54 + 0.99j, 3.03 - 2.44j]$$

8. MIMO Capacity Consider the MIMO channel with channel matrix \mathbf{H} given as

$$\mathbf{H} = \begin{bmatrix} 2 & -6 & 0 \\ 3 & 4 & 0 \\ 0 & 0 & 2 \end{bmatrix}$$

(a) Compute the SVD of the above matrix and illustrate how you would do maximum-ratio transmission (MRT) in this scenario.

(b) Compute the capacity and optimal power allocation for a total transmit power $P_T = -1.25$ dB and noise power $\sigma_n^2 = 3$ dB.

9. Optimal MIMO Power Allocation Consider the MIMO channel matrix \mathbf{H} given below and answer the questions that follow.

$$\mathbf{H} = \begin{bmatrix} 0 & -2 & 5 \\ 1 & 2 & 4 \\ -2 & 1 & 2 \end{bmatrix} \begin{bmatrix} 0 & 0 & 1 \\ 1 & 0 & 0 \\ 0 & 1 & 0 \end{bmatrix} \begin{bmatrix} 1 & -1 & 1 \\ 1 & 2 & 1 \\ -1 & 0 & 1 \end{bmatrix}$$

(a) Compute the SVD of \mathbf{H} .

- (b) Only for this part, assume a transmit power of 10 dB at the transmitter and a receiver noise power $\sigma_n^2 = 0$ dB. Compute the optimal power allocation and the optimal transmit scheme for spatially multiplexing streams x_1, x_2, x_3 .
- (c) Assume BPSK modulation and unit power loading on each mode corresponding to each \mathbf{v}_i . Let the received vector be $[36, 16, 13]^T$. Decode the transmitted BPSK symbol vector.

10. MIMO SIC Receiver Consider the MIMO channel \mathbf{H} given below and answer the questions that follow.

$$\mathbf{H} = \begin{bmatrix} 1 & 1 \\ 2 & 1 \\ 3 & 4 \end{bmatrix}$$

- (a) Derive the MIMO zero-forcing receiver.
- (b) Consider BPSK symbol transmission with unit power for each symbol and received vector $[0.8622, -0.6812, -0.3077]^T$. Decode the transmitted BPSK vector employing VBLAST SIC and clearly illustrate the process.

11. Optimal MIMO Power Allocation Consider the MIMO channel matrix \mathbf{H} given below and answer the questions that follow.

$$\mathbf{H} = \begin{bmatrix} 1 & -1 & -1 & -1 \\ 1 & -1 & 1 & 1 \\ 1 & 1 & -1 & 1 \\ 1 & 1 & 1 & -1 \end{bmatrix} \begin{bmatrix} 0 & 0 & 2 \\ 5 & 0 & 0 \\ 0 & 0 & 0 \\ 0 & 3 & 0 \end{bmatrix} \begin{bmatrix} 2 & 6 & 3 \\ 3 & 2 & -6 \\ 6 & -3 & 2 \end{bmatrix}$$

- (a) Compute the SVD of \mathbf{H} .
- (b) Only for this part, assume a transmit power of 2 dB at the transmitter and a receiver noise power $\sigma_n^2 = 0$ dB. Compute the optimal power allocation and the optimal transmit scheme for spatially multiplexing streams x_1, x_2, x_3 .
- (c) Assume QPSK modulation and unit power loading on each mode corresponding to each \mathbf{v}_i . Let the received vector be $[490 + 196j, 196 + 490j, -294, -294j]^T$. Decode the transmitted QPSK symbol vector.
- (d) Derive the MMSE-ZF receiver for the above MIMO channel in terms of the SVD component matrices (*Hint*: Employ properties of the SVD for simplification).

12. Consider a MISO-CDMA system with t transmit antennas modelled as

$$y(k) = \mathbf{h}^H \mathbf{x}(k) + n(k)$$

with the standard vector of channel coefficients $\mathbf{h} = [h_1, h_2, \dots, h_t]^T$. Consider the following transmission scheme. A different spreading code is used to modulate the transmit symbol on each transmit antenna, i.e., the k^{th} transmitted chip on the l^{th} transmit antenna is given as $s(0) c_l(k)$. Let the length of each spreading sequence be N .

- (a) Demonstrate the optimal demodulation scheme for the above MISO-CDMA system.
- (b) Derive the SNR at the receiver under the assumption of long spreading codes.
- (c) What is the diversity order of the above scheme.
- (d) Now consider a different transmit scheme where the transmitted chip is given as $s(0) c(k)$, i.e., the same spreading sequence is employed on each transmit antenna. Derive the BER for this scheme. What is the problem with this scheme?

13. Answer the questions below.

- (a) Compute the SVD of the following 3×2 channel matrix.

$$\mathbf{H} = \begin{bmatrix} 1 & 1 \\ 2 & -2 \\ 3 & 1 \end{bmatrix}$$

(6.31)

- (b) Consider BPSK transmission for the above MIMO system with SNR $\frac{P_d}{\sigma_n^2} = 10$ dB. Derive the MMSE MIMO receiver for the above system.
- (c) Compute the MMSE decoded transmit BPSK vector corresponding to the received vector in the above system be given as

$$\begin{bmatrix} -1.71 \\ 12.55 \\ 6.08 \end{bmatrix}$$

14. Consider an $r \times t$ MIMO system, i.e., one with r receive and t transmit antennas. The channel matrix \mathbf{H} consists of uncorrelated Rayleigh fading channel coefficients with

$E\{|h_{ij}|^2\} = 1$. Consider a transmission scheme in which the same symbol $x(k)$ is transmitted from each of the t transmit antennas at the time instant k . Also $x(k)$ is BPSK $\pm\sqrt{P}$. For this scheme, answer the questions below.

- Derive the optimal receiver for this scheme.
- Compute the signal-to-noise power ratio (SNR) at the receiver.
- Derive the *average* BER and diversity order of detection.
- Compute the average BER for SNR = 35 dB and a 3×2 MIMO system.

15. Consider the 3×3 MIMO channel matrix \mathbf{H} given below.

$$\mathbf{H} = \begin{bmatrix} 3 & 0 & -8 \\ 0 & 1 & 0 \\ 4 & 0 & 6 \end{bmatrix}$$

Consider a transmit power of $P = -1.75$ dB and receiver noise power $\sigma_n^2 = 3$ dB. Answer the questions below.

- Derive the SVD of the channel matrix \mathbf{H} above. (2.0)
- Compute the optimal power allocation for MIMO rate maximization and the associated MIMO channel capacity.
- Illustrate the optimal transmission scheme clearly demonstrating the precoding operation at the transmitter.

16. Optimal MIMO Power Allocation: Consider the MIMO channel matrix \mathbf{H} given below and answer the questions that follow.

$$\mathbf{H} = \begin{bmatrix} 1 & 1 & 1 \\ 2 & 0 & -1 \\ 1 & -1 & 1 \end{bmatrix} \begin{bmatrix} 0 & 2 & 0 \\ 3 & 0 & 0 \\ 0 & 0 & 1 \end{bmatrix} \begin{bmatrix} 2 & 2 & -1 \\ 2 & -1 & 2 \\ -1 & 2 & 2 \end{bmatrix}$$

- Compute the SVD of \mathbf{H} .
- Only for this part assume a transmit power of -3 dB at the transmitter and a receiver noise power $\sigma_n^2 = 0$ dB. Compute the optimal power allocation.
- Demonstrate the optimal transmit precoding scheme for spatially multiplexing streams x_1, x_2, x_3 .

- (d) Assume QPSK modulation and unknown power loading on each mode corresponding to each \mathbf{v}_i . Decode the transmitted QPSK symbol on the second mode for the received vector,

$$\begin{bmatrix} -0.36 - 0.18j \\ -0.45 + 0.45j \\ 0.18 + 0.36j \end{bmatrix}$$

17. **MIMO Receivers** Consider a 3×2 MIMO system with total transmit power $P = 10$ dB and per receiver noise variance $\sigma_n^2 = 3$ dB. Answer the questions that follow for the MIMO channel matrix be as given below.

$$\begin{bmatrix} 1 & 2 \\ 2 & 1 \\ 1 & 2 \end{bmatrix}$$

- (a) Derive the MIMO-ZF receiver matrix.
 (b) The SNR at the receiver for decoding each symbol $x_1(k)$, $x_2(k)$ at the receiver.
 (c) Illustrate the MIMO V-BLAST receiver procedure, i.e., the beamformer at each stage.
 (d) Calculate the SNR at the receiver for the symbol decoded at each stage.
18. **MIMO System** Consider the instantaneous MIMO channel matrix \mathbf{H} given below and answer the questions that follow.

$$\mathbf{H} = \begin{bmatrix} 1 & -2 & 2 \\ 2 & -1 & -2 \\ 2 & 2 & 1 \end{bmatrix}$$

- (a) What property do the columns \mathbf{c}_1 , \mathbf{c}_2 , \mathbf{c}_3 of this matrix satisfy?
 (b) Compute the SVD of the above channel matrix.
 (c) What is the corresponding MIMO zero-forcing receiver matrix ?
 (d) If the transmit power of BPSK modulated symbols is $P = 5$ dB per transmit antenna and noise power $\sigma_n^2 = 3$ dB, what is the **instantaneous** bit error rate for the zero forcing decoder?
 (e) If the transmit power of BPSK modulated symbols is $P = 5$ dB per transmit antenna and noise power $\sigma_n^2 = 3$ dB, what is the **instantaneous** bit error rate for the second

decoded stream in the V-BLAST decoder, assuming the decoding operation proceeds in the order of the transmit antennas? Make the simplifying assumption that there is no error propagation.

- (f) If the transmit power of BPSK modulated symbols is $P = 5$ dB per transmit antenna and noise power $\sigma_n^2 = 3$ dB, what is the **exact** (NOT PEP) **instantaneous** bit error rate for the maximum likelihood decoder?
- (g) Considering a transmit power of $P = 30$ dB, $\sigma_n^2 = -3$ dB, and BPSK symbols, what is the **average** BER for zero-forcing with elements of the channel matrix \mathbf{H} IID Rayleigh of average power unity?
- (h) Considering a transmit power of $P = 30$ dB, $\sigma_n^2 = -3$ dB, and BPSK symbols, what is the **average** BER for the second decoded stream in the V-BLAST decoder, assuming the decoding operation proceeds in the order of the transmit antennas, with elements of the channel matrix \mathbf{H} IID Rayleigh of average power unity? Make the simplifying assumption that there is no error propagation.
19. Considering space-time block code matrices $\sqrt{P}\mathbf{X}_A$, $\sqrt{P}\mathbf{X}_B$ and L transmit antennas with IID Rayleigh fading-channel coefficients of average power unity, derive the determinant criterion discussed in class for space-time code design as

$$\mathcal{P}\{\mathbf{X}_A \rightarrow \mathbf{X}_B\} \leq \frac{K}{SNR^L \det\left((\mathbf{X}_A - \mathbf{X}_B)(\mathbf{X}_A - \mathbf{X}_B)^H\right)} \quad (6.32)$$

where K is an appropriate constant.

20. **MIMO Decoding** Consider the instantaneous MIMO channel matrix below.

$$\mathbf{H} = \begin{bmatrix} 4 & 3 \\ 3 & 2 \end{bmatrix}$$

Consider a transmit power of $P = E\{|x_i|^2\} = 25$ dB on each transmit antenna and noise variance $\sigma_n^2 = 3$ dB. Let the transmit constellation be BPSK on each transmit antenna.

- (a) Find the MIMO zero-forcing receiver for the above channel matrix \mathbf{H} .
- (b) Compute the instantaneous BER for BPSK decoding.
- (c) If each h_{ij} is IID Rayleigh with $E\{|h_{ij}|^2\} = 1$, compute the average BER for BPSK decoding.

21. Consider the MIMO channel matrix \mathbf{H} given below and answer the questions that follow.

$$\mathbf{H} = \begin{bmatrix} 1 & 3 \\ 2 & -2 \\ 1 & 1 \end{bmatrix}$$

- (a) Find the SVD of \mathbf{H} .
 (b) Compute the zero-forcing receiver for \mathbf{H} .
 (c) Find a projection matrix for the column space of \mathbf{H} .
22. Corresponding to a MISO space-time block coded system with L antennas and code matrices $\mathbf{X}_A, \mathbf{X}_B$, derive the determinant criterion for space-time code design as

$$\mathcal{P}\{\mathbf{X}_A \rightarrow \mathbf{X}_B\} = \frac{K}{\text{SNR}^L \det [(\mathbf{X}_A - \mathbf{X}_B)(\mathbf{X}_A - \mathbf{X}_B)^*]}$$

where K is an appropriate constant. When is the diversity order L achieved.

23. Consider a 2×2 Alamouti-coded MIMO system with total transmit power P and noise variance σ^2 with i.i.d. noise samples across antennas and time. Consider the channel matrix \mathbf{H} given as below and answer the questions that follow for BPSK modulated transmission.

$$\mathbf{H} = \begin{bmatrix} h_{11} & h_{12} \\ h_{21} & h_{22} \end{bmatrix}$$

- (a) Illustrate the decoding process at the receiver and derive the SNR for each symbol.
 (b) Consider the instantaneous channel matrix \mathbf{H} with $h_{11} = h_{22} = 2$ and $h_{12} = h_{21} = 1$ and derive an expression for the instantaneous BER as a function of the SNR P/σ^2 .
 (c) What is the SNR required for an instantaneous BER of 10^{-6} ?
 (d) Consider now each channel coefficient to be Rayleigh with average power 2, i.e., $E\{|h_{ij}|^2\} = 2$. Derive the exact expression for the average BER as a function of P/σ^2 .
 (e) Consider now each channel coefficient to be Rayleigh with average power 2, i.e., $E\{|h_{ij}|^2\} = 2$. Derive a suitable approximation for the average BER as a function of P/σ^2 .
 (f) What is the diversity order of the above system?

- (g) Employing the approximation above derive the SNR required to achieve an average BER of 10^{-6} .
24. Consider a $r \times t$ MIMO version of the repetition code in which the transmitted symbol on antenna j is $x(j) = \sqrt{j}u$, where u is the BPSK symbol $\pm\sqrt{P}$ for $1 \leq j \leq t$. The AWGN noise is i.i.d across antennas of variance σ^2 and channel coefficients h_{ij} are i.i.d Rayleigh fading coefficients with $E\{|h_{ij}|^2\} = 1$. Derive an expression for the **exact** BER of this system with *optimal* combining at the receiver. What is the associated diversity order?

Orthogonal Frequency-Division Multiplexing

7.1 | Introduction

Orthogonal Frequency-Division Multiplexing (OFDM) forms the basis for 4G, i.e., Fourth Generation wireless communication systems. OFDM is used in 4G wireless cellular standards such as Long-Term Evolution (LTE) and WiMAX (Worldwide Interoperability for Microwave Access). OFDM is a key broadband wireless technology which supports data rates in excess of 100 Mbps. Similarly, the wireless local area (LAN) standards such as 802.11 a/g/n are based on OFDM. Next we describe multicarrier transmission, which is the motivation and key idea behind OFDM.

7.2 | Motivation and Multicarrier Basics

Consider a bandwidth $B = 2W$ available for communication, where W is the one-sided bandwidth, or, in other words, the maximum frequency. For a single carrier communication system, the symbol time T is given as

$$T = \frac{1}{B}$$

basically implying that symbols can be transmitted at intervals of $\frac{1}{B}$ seconds each. Therefore, the symbol rate is given as

$$\text{Rate} = \frac{1}{1/B} = B \quad (7.1)$$

Such a system is termed a single-carrier communication system. In such a system, a single carrier is employed for the entire baseband bandwidth of B . Therefore, roughly speaking, the symbols are transmitted as symbol $X(0)$ from $0 \leq t < T$, symbol $X(1)$ from $T \leq t < 2T$, and so on, i.e., roughly one symbol transmitted every $T = \frac{1}{B}$ seconds.

Consider now dividing the total bandwidth B into N sub-bands of bandwidth B/N each as shown in Figure 7.1. Each subcarrier can now be represented by a subcarrier. Therefore, the subcarriers are placed at $\dots, -\frac{B}{N}, 0, \frac{B}{N}, \dots$, as shown in the figure. For instance, consider the bandwidth $B = 256$ kHz with $N = 64$ subcarriers. The bandwidth per sub-band is equal to $\frac{256}{64} = 4$ kHz, which is also the frequency spacing between the subcarriers. We now implement a multi-carrier transmission system as follows. Consider the i^{th} subcarrier at the frequency $f_i = i\frac{B}{N}$, with $-\left(\frac{N}{2} - 1\right) \leq i \leq \frac{N}{2}$. Let X_i denote the data transmitted on the i^{th} subcarrier. Then, the signal $s_i(t)$ corresponding to the i^{th} subcarrier is given as

$$s_i(t) = X_i e^{j2\pi f_i t} = X_i e^{j2\pi i \frac{B}{N} t}$$

where f_i is the i^{th} subcarrier centre frequency, as described above, and $e^{j2\pi f_i t}$ is the i^{th} subcarrier. The above equation shows the data modulation process over the i^{th} subcarrier. The N different data symbols X_i are modulated over the N different subcarriers with centre frequencies f_i . Hence, there are a total of N data streams. Next we illustrate the scheme for multicarrier transmission.

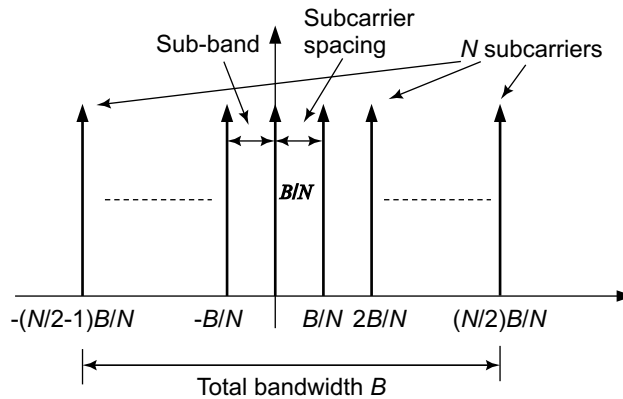


Figure 7.1 Multi-carrier concept

7.2.1 Multicarrier Transmission

Consider now the different modulated signals $s_i(t)$ corresponding to the N different subcarriers. These signals are then superposed and transmitted to form the *composite* signal $s(t)$ given as

$$\begin{aligned} s(t) &= \sum_i s_i(t) \\ &= \sum_i X_i e^{j2\pi f_i t} \\ &= \sum_i X_i e^{j2\pi i \frac{B}{N} t} \end{aligned} \quad (7.2)$$

This composite signal $s(t)$ is then transmitted over the wireless channels. Thus, N different data streams are transmitted over N subcarriers in *parallel* in this multicarrier system. At the receivers, the individual data streams have then to be isolated from the composite signal $s(t)$ above. This is accomplished as follows. Consider the signal $y(t)$ received as

$$y(t) = s(t) = \sum_i X_i e^{j2\pi f_i t}$$

For simplicity, to illustrate the demodulation procedure at the receiver, we have assumed noise to be absent above. We will consider the general case of a noisy received signal later. From the expression for the composite signal $s(t)$ in Eq. (7.2), it can be readily seen that the expression on the right-hand side is indeed the Fourier series representation $s(t)$, corresponding to the fundamental frequency $f_0 = (B/N)$ and the various X_i representing the Fourier coefficients. Indeed, all the frequencies $i \frac{B}{N}$ are multiples of the fundamental frequency $f_0 = \frac{1}{T_0} = \frac{B}{N}$. Therefore, to extract X_l , which is the Fourier coefficient corresponding to the frequency $f_l = l f_0$, one needs to follow the procedure similar to compute the Fourier series as

$$\begin{aligned} f_0 \int_0^{T_0} y(t) \left(e^{j2\pi f_l t} \right)^* dt &= \frac{B}{N} \int_0^{\frac{N}{B}} \left(\sum_i X_i e^{j2\pi i \frac{B}{N} t} \right) e^{-j2\pi l \frac{B}{N} t} dt \\ &= \frac{B}{N} \sum_i \int_0^{\frac{N}{B}} X_i e^{j2\pi(i-l) f_0 t} dt \end{aligned}$$

$$\begin{aligned}
&= \underbrace{\frac{B}{N} \int_0^{\frac{N}{B}} X_l dt}_{i=l} + \frac{B}{N} \sum_{i \neq l} \int_0^{\frac{N}{B}} X_i e^{j2\pi(i-l)f_0 t} dt \\
&= X_l + \frac{B}{N} \sum_{i \neq l} X_i \underbrace{\int_0^{\frac{N}{B}} e^{j2\pi(i-l)f_0 t} dt}_{=0} \\
&= X_l
\end{aligned}$$

where we have used the fact that $\int_0^{T_0} e^{j2\pi(i-l)f_0 t} dt = 0$ for $i \neq l$, since this is basically integrating a sinusoid of frequency $(i-l)f_0$, which is a multiple of the fundamental frequency f_0 over the period T_0 . Therefore, since there are an integer number of cycles of the sinusoid of frequency $(i-l)f_0$, this integral is 0. In fact, this basically implies that the different sinusoids $e^{j2\pi i f_0 t}$ and $e^{j2\pi l f_0 t}$ are *orthogonal*. It is this key property of *orthogonality* which helps extract the different streams X_i modulated over the different subcarriers. This property of orthogonality can be summarized as

$$\int_0^{N/B} e^{j2\pi(i-l)\frac{B}{N}t} dt = \begin{cases} 0 & i \neq l \\ \frac{N}{B} & i = l \end{cases}$$

Therefore, all the subcarriers other than the l^{th} subcarrier are orthogonal to the l^{th} subcarrier. Further, observe that multiplying with $(e^{j2\pi f_0 t})^*$ and integrating is basically *coherent* demodulation, i.e., demodulation with the carrier matched to the subcarrier frequency $f_l = l\frac{B}{N}$. Thus, X_l , the data modulated on the different subcarriers, can be conveniently recovered by coherently demodulating with each of the subcarriers corresponding to $l = -(\frac{N}{2} - 1), \dots, \frac{N}{2}$. The above scheme of transmission on multiple orthogonal subcarriers and the associated data recovery at the receiver is termed *MultiCarrier Modulation (MCM)*. Also observe that the window of time associated with detection of this multicarrier signal is $\frac{N}{B} = \frac{1}{f_0} = T_0$, which is basically the time period of integration. Hence, MCM basically transmits N symbols using N subcarriers in a time period of $\frac{N}{B}$. The symbol rate is, therefore, $\frac{N}{N/B} = B$. Thus, the overall symbol rate in single carrier vs multicarrier systems is unchanged. The transmitter and receiver block schematics for this MCM system are shown in figures 7.2 and 7.3 respectively.

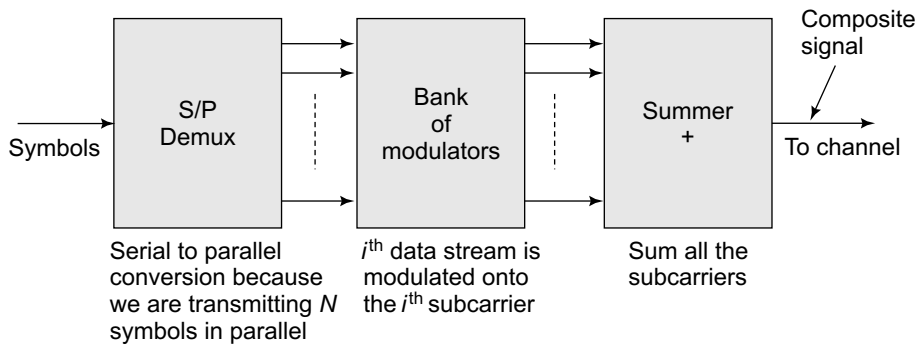


Figure 7.2 Multicarrier modulation transmitter

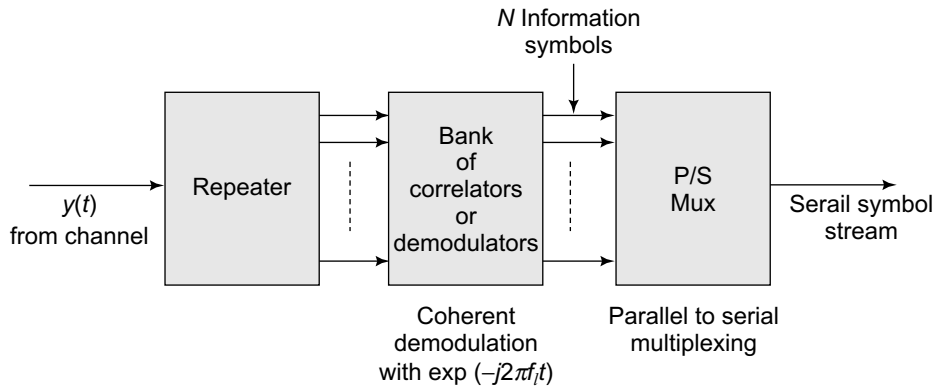


Figure 7.3 Multi-carrier modulation receiver

It is very important now to note the following fact. Observe from Eq. (7.1) and the above rate for an MCM system. It is clear that the symbol rate in both these systems is exactly identical, i.e., B . The single-carrier system transmits each symbol in time $\frac{1}{B}$, while the MCM system transmits N symbols in parallel in time $\frac{N}{B}$. What then is the advantage of an MCM system over the single-carrier system? To understand this, consider an example with a transmission bandwidth of $B = 1.024$ MHz, i.e., 1024 kHz. As seen in an earlier chapter, notice that this bandwidth B is much greater than the coherence bandwidth B_c which is typically around 250 kHz, i.e., $B_c \approx 250$ kHz. Therefore, since the transmission bandwidth $B \gg B_c$, the single-carrier system experiences *frequency-selective* fading and inter-symbol interference. However, consider an OFDM system with employs $N = 256$ subcarriers in the same bandwidth. The bandwidth per subcarrier is $B_s = \frac{1024}{256} = 4$ kHz. It can be readily seen that the subcarrier bandwidth of 4 kHz is significantly lower than the coherence

bandwidth of 250 kHz. Thus, since $\frac{B}{N} \ll B_c$, each subcarrier experiences *flat fading*. Hence, there is no inter-symbol interference in the data transmitted on any of the subcarriers. Thus, the most critical and key benefit of this MCM system is that through parallel transmission using multiple narrowband subcarriers, it eliminates the *Inter-Symbol interference (ISI)*, thus avoiding distortion of the received symbols.

However, the above MCM system suffers from a significant bottleneck. Implementing the bank of N modulators and N demodulators with closely spaced subcarrier frequencies is an extremely challenging task. This was solved by the key idea proposed by Weinstein and Ebert in 1972, in the paper titled "Data Transmission by Frequency Division Multiplexing using the Discrete Fourier Transform". Both of them were engineers at Bell Telephone Laboratories. Their idea can be described as follows. Consider the MCM transmit signal $s(t)$. Observe that it is band-limited to the bandwidth B (total bandwidth). Therefore, the Nyquist sampling rate is B and the associated sampling time is $T_s = \frac{1}{B}$. Consider now the composite MCM signal given in Eq. (7.2). The u^{th} sample at time instant $uT_s = \frac{u}{B}$ is given as

$$s(uT_s) = x(u) = \sum_i X_i e^{j2\pi i \frac{B}{N} \frac{u}{B}}$$

$$x(u) = \underbrace{\sum_i X_i e^{j2\pi \frac{i u}{N}}}_{\text{DFT}}$$

Observe from the expression above that the sample $x(u)$ is basically the *Inverse Discrete Fourier Transform (IDFT)* coefficient of the information symbols $X(0), X(1), \dots, X(N-1)$ at the u^{th} time point. Thus, the *Inverse Fast Fourier Transform (IFFT)* can be conveniently employed to generate the sample MCM signal. This scheme of generating the composite transmit signal through IDFT was proposed by Weinstein and Ebert in 1971. Thus, it drastically reduces the complexity of implementing an OFDM system since it eliminates the need for the bank of modulators corresponding to the different subcarrier frequencies. This technique, where the MCM signal is generated by employing the IFFT operation is termed *Orthogonal Frequency Division Multiplexing*, or **OFDM**. At the receiver, to recover the information symbols, one can correspondingly employ an FFT operation. Schematic figures of the OFDM transmitter and receiver with the IFFT and FFT blocks are given in figures 7.4 and 7.5 respectively.

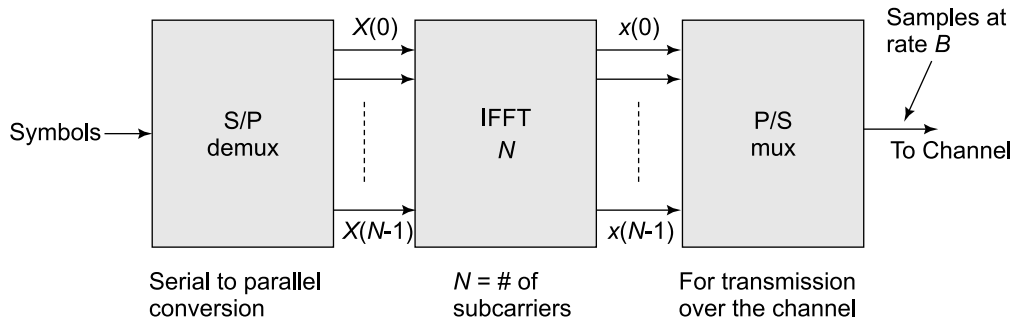


Figure 7.4 OFDM transmitter schematic with IFFT

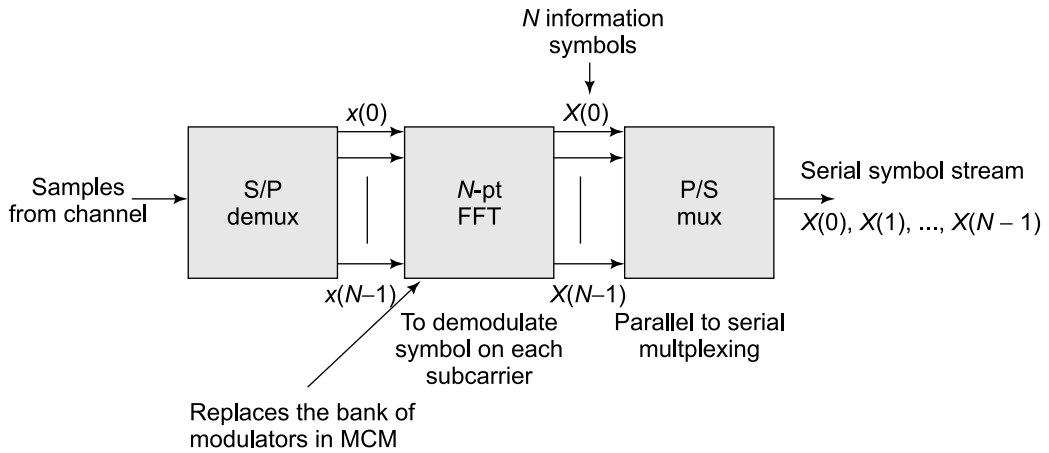


Figure 7.5 OFDM receiver schematic with FFT

7.2.2 Cyclic Prefix in OFDM

In this section, we explain the concept of *cyclic prefix*, which is an important component of an OFDM system. Consider a frequency-selective channel modelled with channel taps $h(0), h(1), \dots, h(L-1)$. Thus, the received symbol y at a given time instant n can be expressed as

$$y(n) = h(0)x(n) + \underbrace{h(1)x(n-1) + \dots + h(L-1)x(n-L+1)}_{\text{ISI component}},$$

from which it can be seen that the received symbol $y(n)$ at the time instant n experiences inter symbol interference from the previous $L-1$ transmitted symbols. Consider now two OFDM symbols as follows. Let $x(0), x(1), \dots, x(N-1)$ denote the IFFT samples of the modulated symbols $X(0), X(1), \dots, X(N-1)$, while $\tilde{x}(0), \tilde{x}(1), \dots, \tilde{x}(N-1)$ denote the

IFFT samples of the previous modulated symbol block $\tilde{X}(0), \tilde{X}(1), \dots, \tilde{X}(N-1)$. Thus, the samples corresponding to these two blocks of OFDM symbols are transmitted sequentially as

$$\underbrace{\tilde{x}(0), \tilde{x}(1), \dots, \tilde{x}(N-1)}_{\text{Previous block}}, \underbrace{x(0), x(1), \dots, x(N-1)}_{\text{Current block}}$$

Now, consider the received symbol $y(0)$ corresponding to the transmission of $x(0)$. This can be expressed as

$$y(0) = h(0)x(0) + \underbrace{h(1)\tilde{x}(N-1) + \dots + h(L-1)\tilde{x}(N-L+1)}_{\text{ISI from previous OFDM symbol}}$$

It can be seen from the above equation that the received symbol $y(0)$ experiences inter-symbol interference from $\tilde{x}(N-1), \tilde{x}(N-2), \dots, \tilde{x}(N-(L-1))$. Thus, there is *inter-OFDM symbol interference* in this new OFDM system. The initial samples of the current OFDM symbol block are being subject to interference from the $N-1$ samples of the previous OFDM block. This is shown in Figure 7.6. Similarly, the received symbol $y(1)$ is given as

$$y(1) = h(0)x(1) + h(1)x(0) \underbrace{h(2)\tilde{x}(N-1) + \dots + h(L-1)\tilde{x}(N-L+2)}_{\text{ISI from previous OFDM symbol}},$$

which can again be seen to experience inter-OFDM symbol interference from the previous OFDM block symbols $\tilde{x}(N-1), \tilde{x}(N-2), \dots, \tilde{x}(N-L+2)$. Let us now consider a modified transmission scheme as follows. To each transmitted OFDM sample stream, we pad the last L_c symbols to make the transmitted stream as follows.

$$\underbrace{\tilde{x}(0), \tilde{x}(1), \dots, \tilde{x}(N-1)}_{\text{Previous block}}, \underbrace{x(N-L_c), x(N-L_c+1), \dots, x(N-1)}_{\text{Cyclic prefix}}, \underbrace{x(0), x(1), \dots, x(N-1)}_{\text{Current block}}$$

Initial samples, of subject to inter OFDM symbol interference

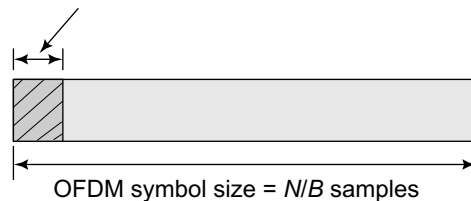


Figure 7.6 Inter-OFDM symbol interference

Observe that we are prefixing the transmitted sample block $x(0), x(1), \dots, x(N-1)$ of the current block with the L_c samples $x(N-L_c), x(N-L_c+1), \dots, x(N-1)$. Further, this prefix is *cyclic* in nature, since the same samples from the end of the block are being *cycled* towards the beginning. Therefore, this is known as the *cyclic prefix* and is an important aspect of OFDM systems. Consider now the received symbol corresponding to $x(0)$. This is given as

$$y(0) = h(0)x(0) + \underbrace{h(1)x(N-1) + \dots + h(L-1)x(N-L+1)}_{\text{ISI from same OFDM symbol}}$$

The inter-symbol interference can be seen to now be from $x(N-1), x(N-2), \dots, x(N-L+1)$, if $L_c \geq L-1$. Thus, with the cyclic prefix of appropriate length, i.e., $L_c \geq L-1$, inter-OFDM symbol interference can be avoided and inter-symbol interference is restricted to samples from the same OFDM symbol. Therefore, the samples $y(0), y(1), \dots, y(N-1)$ are given as

$$y(0) = h(0)x(0) + h(1)x(N-1) + \dots + h(L-1)x(N-L+1)$$

$$y(1) = h(0)x(1) + h(1)x(0) + \dots + h(L-1)x(N-L+2)$$

⋮

$$y(N-1) = h(0)x(N-1) + h(1)x(N-2) + \dots + h(L-1)x(N-L)$$

It can now be clearly seen that the output $y(n)$ is a circular convolution between the channel filter $h(n)$ and the input $x(n)$.

This can, therefore, be expressed as

$$[y(0), y(1), \dots, y(N-1)] = [h(0), h(1), \dots, h(L-1), 0, \dots, 0] *_N [x(0), x(1), \dots, x(N-1)]$$

where $*_N$ denotes circular convolution of modulo N . Therefore, the output y can be written as

$$y = h *_N x$$

Therefore, taking the DFT of $y(n)$ at the output, we have

$$Y(k) = H(k)X(k), \quad 0 \leq k \leq N-1 \quad (7.3)$$

where $Y(k)$, $0 \leq k \leq N - 1$, denotes the N -point DFT of $y(n)$. Similarly, $X(k)$ denotes the N -point DFT of $x(n)$. Further, observe that the samples $x(n)$ have been generated as the IDFT of $X(n)$. Therefore, the DFT of the samples $x(n)$ yields back the original transmitted symbols $X(n)$. The coefficients $H(k)$ denotes the DFT of the zero-padded channel filter,

$$h(0), h(1), \dots, h(L-1), \underbrace{0, \dots, 0}_{(N-L)}. \quad (7.4)$$

Thus, observe that Eq. (7.3) represents the flat-fading channel across the k^{th} subcarrier in the OFDM system. The quantity $Y(k)$ represents the output symbol, while $H(k)$ denotes the equivalent flat-fading channel coefficient. This holds true for each subcarrier k , i.e., for $0 \leq k \leq N - 1$. Thus, the frequency-selective fading channel is converted into a group of narrowband flat-fading channels, one channel across each subcarrier. Observe that if a single carrier system was used, and the symbols $X(0), X(1), \dots, X(N-1)$ were transmitted directly then the received symbol $y(n)$ would be given as

$$y(n) = h(0)X(n) + h(1)X(n-1) + \dots + h(L-1)X(n-L+1)$$

Each symbol $X(n)$ would experience inter-symbol interference of $L-1$ past symbols. Therefore, using this novel scheme of OFDM, we have been able to totally eliminate the inter-symbol interference arising out of the frequency-selective nature of the channel. The set of parallel flat-fading channels can be summarized by the expressions

$$\begin{aligned} Y(0) &= H(0)X(0) \\ Y(1) &= H(1)X(1) \\ &\vdots \\ Y(N-1) &= H(N-1)X(N-1) \end{aligned}$$

This conversion of the frequency-selective wideband channel into N narrowband flat-fading channels is shown schematically in Figure 7.7. Also, the modified transmitter and receiver schematics with the blocks corresponding to the cyclic prefix are given in Figures 7.8 and 7.9 respectively. Now, considering the noise at the receiver, the received symbol $Y(k)$ can be expressed as

$$Y(k) = H(k)X(k) + N(k) \quad (7.5)$$

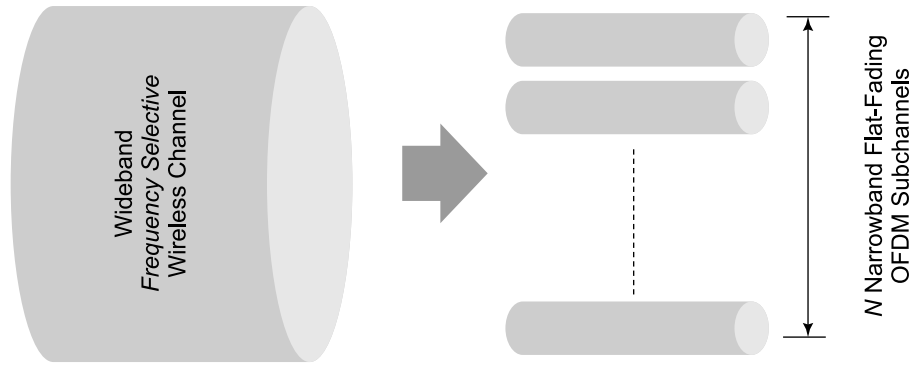


Figure 7.7 OFDM parallel subchannels

where $N(k)$ denotes the noise across the k^{th} subcarrier. A simple detection scheme for $X(k)$ is to use the zero-forcing detector for the subcarrier as

$$\hat{X}(k) = \frac{1}{H(k)} Y(k) = X(k) + \underbrace{\frac{N(k)}{H(k)}}_{\tilde{N}(k)}$$

Further, for a simplistic BPSK or QPSK-modulated transmission, the coherent or matched filter detector can be simply obtained by multiplying with $H^*(k)$, i.e., the complex conjugate of $H(k)$ as

$$H^*(k) Y(k) = |H(k)|^2 X(k) + \underbrace{H^*(k) N(k)}_{N'(k)}$$

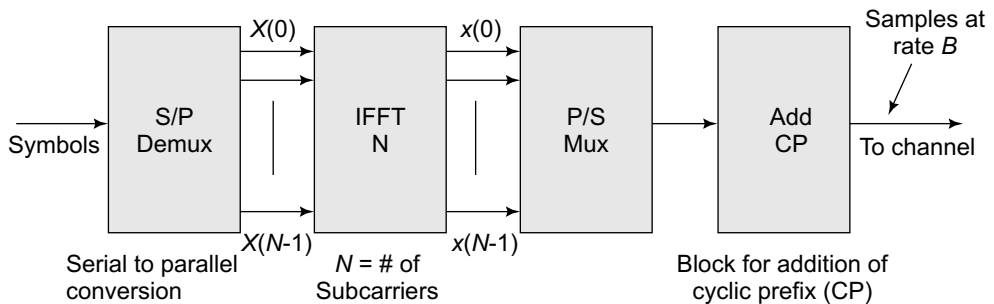


Figure 7.8 OFDM transmitter schematic with CP

Also, one can employ the MMSE detector as

$$\hat{X}_{\text{MMSE}}(k) = \frac{H^*(k)}{|H(k)|^2 + \sigma_n^2} Y(k)$$

The above equation gives the MMSE receiver across the k^{th} subcarrier in this OFDM system.

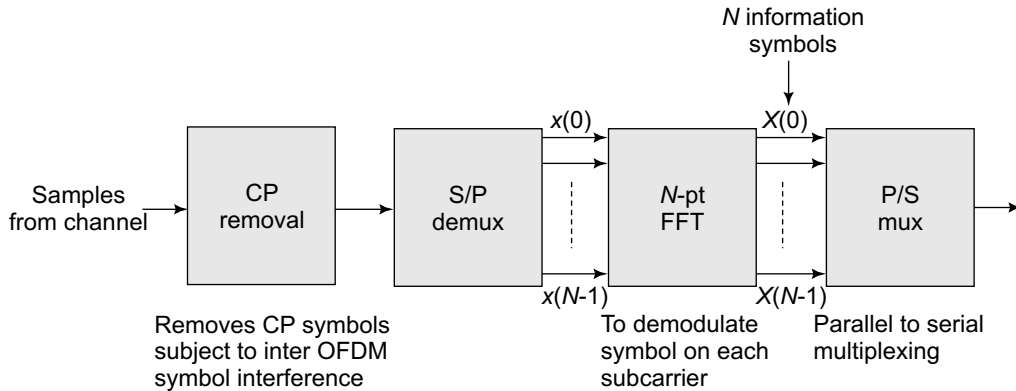


Figure 7.9 OFDM receiver schematic with CP

7.2.3 Impact of Cyclic Prefix on Data Rate

Consider the transmitted samples $x(n)$ with the cyclic prefix, as given below.

$$\underbrace{x(N - L_c), x(N - L_c + 1), \dots, x(N - 1)}_{\text{Cyclic prefix}} \underbrace{x(0), x(1), \dots, x(N - 1)}_{\text{Current block}}.$$

The minimum required length of the cyclic prefix is $L - 1$ as was described in the previous section. Also, observe that $L - 1$ is the delay spread of the wireless channel. Therefore, it follows that the length of the cyclic prefix should be greater than the delay spread of the channel. However, since the samples in the tail, i.e., $x(N - L_c), x(N - L_c + 1), \dots, x(N - 1)$ are simply repeated in the beginning, they do not constitute any additional information. Hence, the effect of the addition of a long CP is lost in the throughput of the system. More specifically,

the loss in efficiency can be calculated as

$$\begin{aligned} \text{Loss in efficiency} &= \frac{\text{Cyclic prefix}}{\text{Total OFDM symbol length}} \\ &= \frac{L - 1}{N + L - 1} \\ &= \frac{L - 1}{N + L - 1} \end{aligned}$$

However, as the block length N becomes very large, we have

$$\lim_{N \rightarrow \infty} \frac{L - 1}{N + L - 1} \rightarrow 0$$

Thus, the loss in throughput approaches 0 as the number of subcarriers N increases, for a fixed length of the delay spread L . Also observe that as the number of subcarriers N increases, the symbol time $\frac{N}{B}$ increases as shown in Figure 7.10. Increasing N results in increasing OFDM symbol time, thus restricting the ISI to a small fraction of the OFDM symbol block, i.e., the fraction $\frac{L}{N}$ is progressively smaller. However, as the block length N increases, the decoding delay at the receiver also increases as one has to wait for arrival of the entire block of N samples before it can be demodulated. Hence, there is a trade-off for increasing N vs decoding delay. Now, we present another intuitive framework to understand the effect of various parameters. As we have said previously, the duration of the cyclic prefix has to be greater than the delay spread.

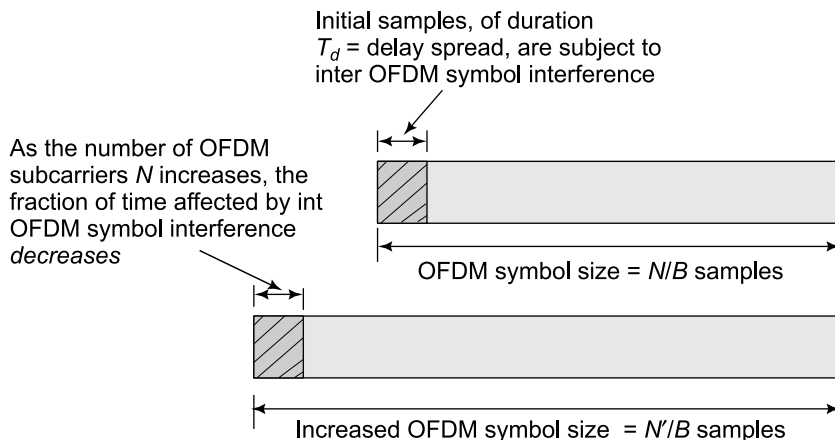


Figure 7.10 Inter OFDM symbol interference with increasing OFDM symbol time

Therefore, we need

$$L_c \times T_s \geq T_d$$

where T_s denotes the sample time and T_d denotes the delay spread. Also, the sample time $T_s = \frac{1}{B}$, where B is the total bandwidth of the system and $T_d = \frac{1}{B_c}$, where B_c is the coherence bandwidth of the system. The above condition implies

$$\begin{aligned} L_c &\geq \frac{T_d}{T_s}, \\ &= \frac{B}{B_c} \end{aligned}$$

Combining this with the earlier condition that $N \gg L_c$ for efficiency in terms of the effective data rate, we have

$$N \gg L_c \geq \frac{B}{B_c}.$$

This can also be recast as $B_c \gg \frac{B}{N}$. Interestingly, this is the same condition for frequency flat fading across each subcarrier since this implies that the subcarrier bandwidth $\frac{B}{N}$ is required to be much less than the coherence bandwidth B_c . Thus, an appropriately designed OFDM system converts a frequency-selective fading channel into a set of parallel narrowband flat-fading channels across the subcarriers. The example next illustrates an OFDM system design example.

7.3 | OFDM Example

In this section, we consider a practical WiMAX example to illustrate the impact of the various parameters in the design of a complete OFDM system. As already stated in the beginning, WiMAX, which stands for Worldwide Interoperability for Microwave Access, is a prominent 4G wireless standard. The total number of subcarriers $N = 256$, with a bandwidth of 15.625 kHz per subcarrier. Therefore,

$$\begin{aligned} \frac{B}{N} &= 15.625 \text{ kHz} \\ \Rightarrow B &= N \times 15.625 = 256 \times 15.625 \\ &= 4 \text{ MHz} \end{aligned}$$

Also, observe that the subcarrier bandwidth is less than the coherence bandwidth, i.e., $B_s = 15.625 \text{ kHz} \ll B_c = 250 \text{ kHz}$. Therefore, each subcarrier experiences frequency flat fading. The OFDM symbol time without CP is

$$\frac{N}{B} = \frac{256}{4 \times 10^6} = 64 \mu\text{s}.$$

The raw OFDM symbol time, corresponding to the $N = 256$ IFFT samples, is $64 \mu\text{s}$. WiMAX employs a cyclic prefix which is 12.5% of the symbol time. Therefore, the duration of the cyclic prefix is

$$\begin{aligned} \text{Duration of cyclic prefix} &= 12.5\% \text{ of symbol time} \\ &= \frac{12.5}{100} \times 64 \mu\text{s}, \\ &= 8 \mu\text{s} \end{aligned}$$

Thus, the total transmitted OFDM symbol duration with cyclic prefix is $64 \mu\text{s} + 8 \mu\text{s} = 72 \mu\text{s}$. Also, the number of samples in the CP is

$$\begin{aligned} \# \text{ Samples in CP} &= \frac{\text{CP duration}}{\text{Sample time}} \\ &= \frac{8 \mu\text{s}}{1/B} \\ &= 8 \mu\text{s} \times 4 \times 10^6 \\ &= 32 \end{aligned}$$

Thus, the length of the cyclic prefix $L_c = 32$ samples and the total number of samples is $256 + 32 = 288$. This break-up of the OFDM symbol in terms of the regular samples and the cyclic prefix is shown in Figure 7.11. Finally, the loss in spectral efficiency is

$$\begin{aligned} \text{Loss in spectral efficiency} &= \frac{32}{288} \\ &= \frac{8 \mu\text{s}}{72 \mu\text{s}} \\ &= 11.1\% \end{aligned}$$

This is the loss in spectral efficiency arising because of the addition of the cyclic prefix.

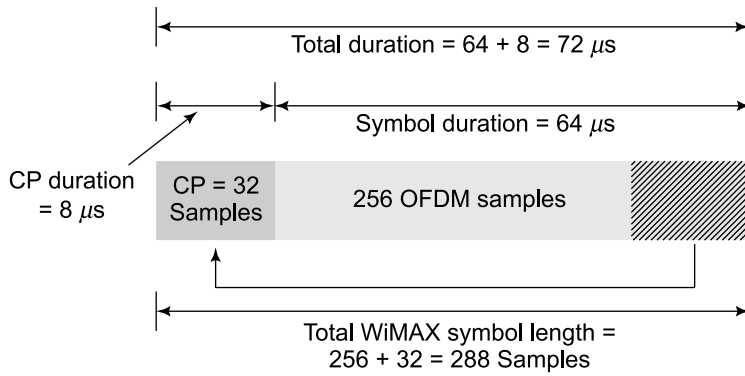


Figure 7.11 WiMAX OFDM symbol with cyclic prefix

7.4 Bit-Error Rate (BER) for OFDM

Consider the OFDM subcarrier system model given in Eq. (7.5), i.e.,

$$Y(k) = H(k)X(k) + N(k) \quad (7.6)$$

where $N(k)$ is the subcarrier noise obtained from the FFT of the noise samples at the output of the receiver as

$$N(k) = \sum_{m=0}^{N-1} n(m) e^{-j2\pi \frac{km}{N}}$$

where N is the number of subcarriers, and $n(0), n(1), \dots, n(N-1)$ are additive noise samples for each of the output samples $y(0), y(1), \dots, y(N-1)$. We now deduce the statistical properties of these noise samples $N(k)$, which are required to characterize the BER performance of the OFDM system. Firstly, observe that the noise $N(k)$ is the linear combination of Gaussian noise samples $n(0), n(1), \dots, n(N-1)$. Hence, it is Gaussian in nature. Further, the mean or expected value of $N(k)$ is given as

$$\begin{aligned} E\{N(k)\} &= E\left\{\sum_{m=0}^{N-1} n(m) e^{-j2\pi \frac{km}{N}}\right\} \\ &= \sum_{m=0}^{N-1} E\{n(m)\} e^{-j2\pi \frac{km}{N}} \end{aligned}$$

Further, the variance σ_N^2 of the noise sample $N(k)$ is given as

$$\begin{aligned}
 \sigma_N^2 &= \text{E} \left\{ |N(k)|^2 \right\} \\
 &= \text{E} \left\{ \left(\sum_{m=0}^{N-1} n(m) e^{-j2\pi \frac{km}{N}} \right) \left(\sum_{l=0}^{N-1} n(l) e^{-j2\pi \frac{kl}{N}} \right)^* \right\} \\
 &= \text{E} \left\{ \sum_{m=0}^{N-1} \sum_{l=0}^{N-1} n(m) n^*(l) e^{-j2\pi(m-l)\frac{k}{N}} \right\} \tag{7.7}
 \end{aligned}$$

Observe that since the noise samples $n(m)$ are independent identically distributed Gaussian of variance σ_n^2 , it follows that $\text{E} \{n(m) n^*(l)\} = 0$ if $m \neq l$ and σ_n^2 if $m = l$. Therefore, the above expression for the noise variance can be simplified as

$$\begin{aligned}
 \sigma_N^2 &= \sum_{m=0}^{N-1} \sum_{l=0}^{N-1} \text{E} \{n(m) n^*(l)\} e^{-j2\pi(m-l)\frac{k}{N}} \\
 &= \sum_{m=0}^{N-1} \sigma_n^2 \\
 &= N\sigma_n^2
 \end{aligned}$$

Further, let us assume that each of the channel taps $h(0), h(1), \dots, h(L-1)$ is Rayleigh fading in nature, i.e., has a complex symmetric Gaussian distribution of mean 0 and variance 1. Therefore, the channel coefficient across the k^{th} subcarrier is given as

$$H(k) = \sum_{m=0}^{N-1} h(m) e^{-j2\pi \frac{km}{N}}$$

As can be seen, $H(k)$ is a linear combination of Gaussian random variables $h(k)$, $0 \leq k \leq L-1$. Therefore, $H(k)$ is indeed complex Gaussian i.e. has a Rayleigh fading envelope. Further, since each $h(k)$ is zero mean, $H(k)$ also has mean zero. Further, identical to the development of the noise variance above, it follows on similar lines that the channel power

gain $E \left\{ |H(k)|^2 \right\}$ is

$$\begin{aligned} E \left\{ |H(k)|^2 \right\} &= E \left\{ \left| \sum_{m=0}^{L-1} h(m) e^{-j2\pi \frac{km}{N}} \right|^2 \right\} \\ &= \sum_{m=0}^{L-1} E \left\{ |h(m)|^2 \right\} \left| e^{-j2\pi \frac{km}{N}} \right|^2 \\ &= L \end{aligned}$$

Therefore, the system model in Eq. (7.6) represents a standard Rayleigh fading channel of power gain L with receiver noise $N(k)$ of variance $N\sigma_n^2$. Therefore, the average SNR is $\frac{LP}{N\sigma_n^2}$. Hence, the BER is given by the standard expression for that of a Rayleigh fading wireless channel as

$$\text{BER}_{\text{OFDM}} = \frac{1}{2} \left(1 - \sqrt{\frac{\frac{LP}{N\sigma_n^2}}{2 + \frac{LP}{N\sigma_n^2}}} \right)$$

7.5 | MIMO-OFDM

MIMO-OFDM is a combination of the Multiple-Input Multiple-Output (MIMO) wireless technology with that of OFDM, to further increase the rate in broadband multi-antenna wireless systems. Similar to OFDM, MIMO-OFDM converts a frequency-selective MIMO channel into multiple parallel flat fading MIMO channels. Hence, MIMO-OFDM significantly simplifies baseband receive processing by eliminating the need for a complex MIMO equalizer. We have already seen that the frequency-selective SISO channel is modelled as an FIR channel filter, with the output $y(n)$ at time instant n given as

$$\begin{aligned} y(n) &= \sum_{l=0}^{L-1} h(l) x(n-l) + w(n), \\ &= h(0)x(n) + \underbrace{h(1)x(n-1) + \dots + h(L-1)x(n-L+1)}_{\text{ISI from previous symbols}} + w(n) \end{aligned}$$

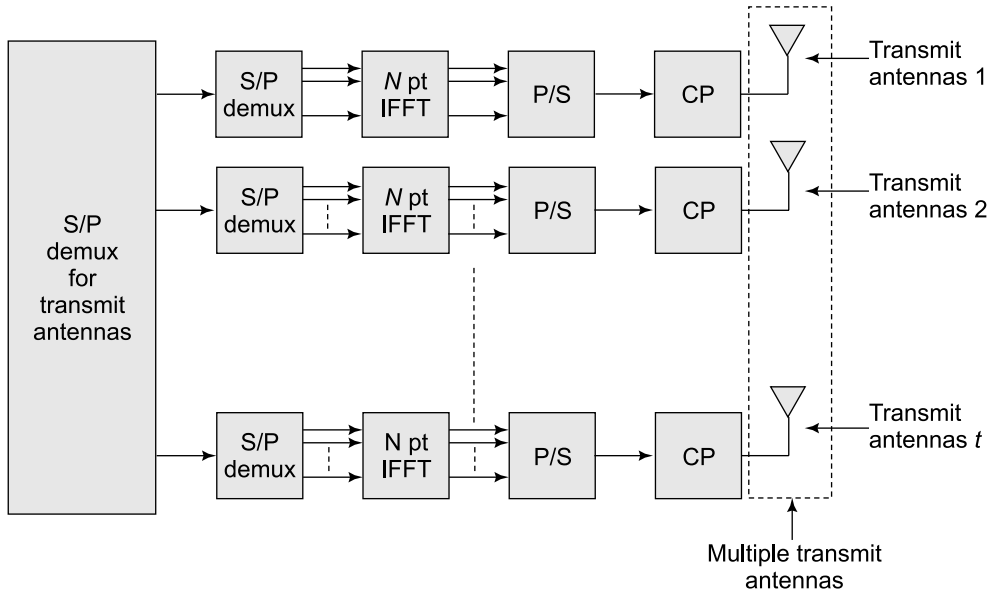


Figure 7.12 MIMO OFDM transmitter schematic

where $w(n)$ denotes the noise. Hence, a MIMO frequency-selective channel can be modelled as a MIMO FIR filter, which can be described as

$$\begin{aligned}
 \mathbf{y}(n) &= \sum_{l=0}^{L-1} \mathbf{H}(l) \mathbf{x}(n-l) + \mathbf{w}(n) \\
 &= \mathbf{H}(0) \mathbf{x}(n) + \underbrace{\mathbf{H}(1) \mathbf{x}(n-1) + \dots + \mathbf{H}(L-1) \mathbf{x}(n-L+1)}_{\text{ISI from previous symbol vectors}} + \mathbf{w}(n)
 \end{aligned}$$

Therefore, the symbol vector $\mathbf{y}(n)$ at the time instant n is affected by inter-symbol vector interference from $\mathbf{x}(n-1)$, $\mathbf{x}(n-2)$, \dots , $\mathbf{x}(n-L+1)$. This is an L -tap frequency-selective MIMO channel. As can be seen, in a MIMO frequency-selective channel, the interference occurs between current and previous transmit symbol vectors. In a MIMO-OFDM system, one needs to perform the IFFT operation at each transmit antenna. The schematic figures showing clearly the processing at the transmitter and receiver of the MIMO-OFDM system are shown in figures 7.12 and 7.13 respectively. Hence, employing MIMO-OFDM, the MIMO frequency-selective channel can be converted into a set of parallel flat-fading MIMO channels.

These can be described as,

$$\begin{aligned}\tilde{\mathbf{y}}(0) &= \tilde{\mathbf{H}}(0) \tilde{\mathbf{x}}(0) \\ \tilde{\mathbf{y}}(1) &= \tilde{\mathbf{H}}(1) \tilde{\mathbf{x}}(1) \\ &\vdots \\ \tilde{\mathbf{y}}(N-1) &= \tilde{\mathbf{H}}(N-1) \tilde{\mathbf{x}}(N-1)\end{aligned}$$

The model across the k^{th} subcarrier is $\tilde{\mathbf{y}}(k) = \tilde{\mathbf{H}}(k) \tilde{\mathbf{x}}(k)$, where $\tilde{\mathbf{y}}(k)$ and $\tilde{\mathbf{x}}(k)$ are the received and transmitted symbol vectors corresponding to the k^{th} subcarrier, and $\tilde{\mathbf{H}}(k)$ is the flat-fading channel matrix corresponding to the subcarrier k . Each of the received vectors $\tilde{\mathbf{y}}(0), \tilde{\mathbf{y}}(1), \dots, \tilde{\mathbf{y}}(N-1)$ can be processed by a simple MIMO zero-forcing receiver or a MIMO-MMSE receiver for detection of the vectors $\tilde{\mathbf{x}}(0), \tilde{\mathbf{x}}(1), \dots, \tilde{\mathbf{x}}(N-1)$. The zero-forcing MIMO receiver is given as

$$\begin{aligned}\hat{\mathbf{x}}_{\text{ZF}}(k) &= \left(\tilde{\mathbf{H}}(k) \right)^\dagger \tilde{\mathbf{y}}(k) \\ &= \left(\tilde{\mathbf{H}}^H(k) \tilde{\mathbf{H}}(k) \right)^{-1} \tilde{\mathbf{H}}^H(k) \tilde{\mathbf{y}}(k)\end{aligned}$$

Also, the MMSE receiver for the subcarrier k of the MIMO-OFDM system is given as

$$\begin{aligned}\hat{\mathbf{x}}_{\text{MMSE}}(k) &= \left(\tilde{\mathbf{H}}(k) \right)^\dagger \tilde{\mathbf{y}}(k) \\ &= P_d \left(P_d \tilde{\mathbf{H}}^H(k) \tilde{\mathbf{H}}(k) + \sigma_w^2 \mathbf{I} \right)^{-1} \tilde{\mathbf{H}}^H(k) \tilde{\mathbf{y}}(k)\end{aligned}$$

where P_d denotes the data power. The channel matrices $\tilde{\mathbf{H}}(0), \tilde{\mathbf{H}}(1), \dots, \tilde{\mathbf{H}}(N-1)$ corresponding to the OFDM subcarriers are given as follows. Let $h_{u,v}(k), \tilde{h}_{u,v}(k)$ denote the $(u, v)^{\text{th}}$ entries of the matrices $\mathbf{H}(k), \tilde{\mathbf{H}}(k)$ respectively. Then, $\tilde{h}_{u,v}(k)$ is given as the N -point DFT of the zero-padded coefficients

$$h_{u,v}(0), h_{u,v}(1), \dots, h_{u,v}(L-1), \underbrace{0, \dots, 0}_{(N-L)}$$

In effect, the channel matrix $\tilde{\mathbf{H}}(k)$ is the k^{th} frequency point corresponding to the FFT of the zero padded channel matrices $[\mathbf{H}(0), \mathbf{H}(1), \dots, \mathbf{H}(L-1), \mathbf{0}_{r \times t}, \dots, \mathbf{0}_{r \times t}]$.

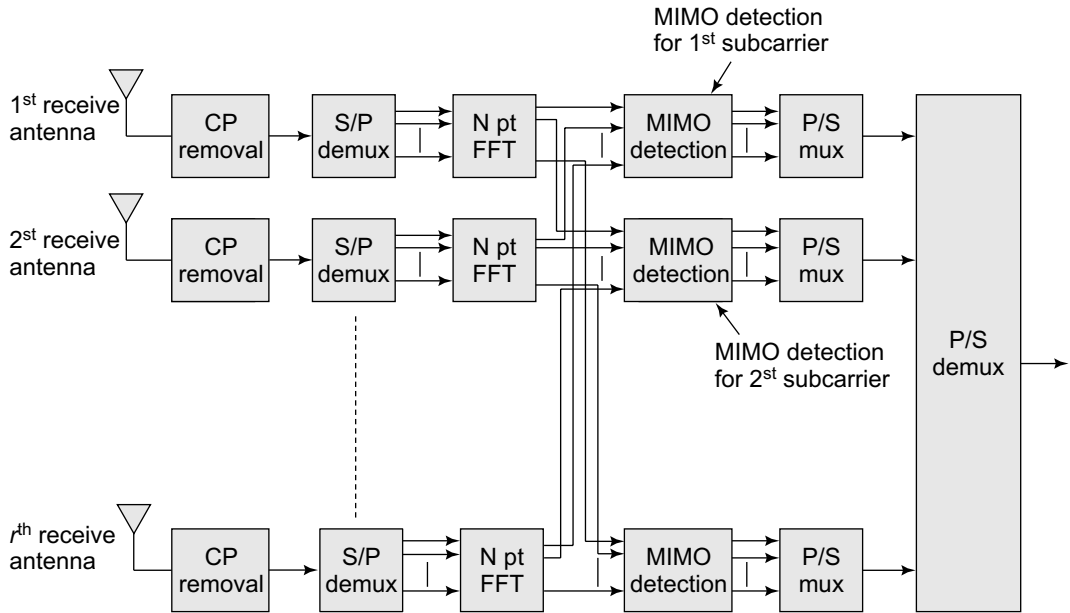


Figure 7.13 MIMO-OFDM receiver schematic

7.6 Effect of Frequency Offset in OFDM

OFDM divides the available wideband amongst a set of orthogonal overlapping subcarriers. Hence, the presence of a carrier-frequency offset can introduce severe distortion in an OFDM system, as it results in a loss of orthogonality amongst the subcarriers. Hence, the presence of a carrier-frequency offset introduces *Inter-Carrier Interference (ICI)* in OFDM systems. In this section, we characterize the effect of frequency offset on the performance of the OFDM system. Consider a frequency offset Δf such that

$$\epsilon = \frac{\Delta f}{B/N}$$

where ϵ denotes the normalized frequency offset, normalized with respect to the subcarrier bandwidth B/N . Corresponding to the frequency offset ϵ , the baseband received samples $y(n)$ are given as

$$y(n) = \frac{1}{N} \sum_{k=-\frac{N}{2}}^{\frac{N}{2}} X(k) H(k) e^{j2\pi n \frac{k+\epsilon}{N}} + w(n) \quad (7.8)$$

To verify the above equation, set $\epsilon = 0$. The above equation then reduces to

$$y(n) = \frac{1}{N} \sum_{k=-\frac{N}{2}}^{\frac{N}{2}} X(k) H(k) e^{j2\pi n \frac{k}{N}} + w(n)$$

Performing now the FFT of $y(0), y(1), \dots, y(N-1)$ at the receiver, $Y(l)$, which corresponds to the symbol received on the l^{th} subcarrier, is given as

$$\begin{aligned} Y(l) &= \frac{1}{N} \sum_n y(n) e^{-j2\pi \frac{nl}{N}} \\ &= \frac{1}{N} \sum_n \sum_{k=-\frac{N}{2}}^{\frac{N}{2}} X(k) H(k) e^{j2\pi n \frac{k}{N}} e^{-j2\pi \frac{nl}{N}} + \underbrace{\frac{1}{N} \sum_n w(n) e^{-j2\pi \frac{nl}{N}}}_{W(l)} \\ &= \frac{1}{N} \sum_n \sum_{k=-\frac{N}{2}}^{\frac{N}{2}} X(k) H(k) e^{j2\pi n \frac{k-l}{N}} + W(l) \\ &= X(l) H(l) + \frac{1}{N} \sum_{k=-\frac{N}{2}, k \neq l}^{\frac{N}{2}} X(k) H(k) \underbrace{\left(\sum_n e^{j2\pi n \frac{k-l}{N}} \right)}_0 + W(l) \\ &= X(l) H(l) + W(l) \end{aligned}$$

where we have used the fact that $\sum_n e^{j2\pi n \frac{k-l}{N}} = 0$ if $k \neq l$. Thus, in the absence of a carrier-frequency offset, i.e., $\epsilon = 0$, the system in Eq. (7.8) reduces to the earlier flat-fading OFDM system across each subcarrier, i.e.,

$$Y(l) = X(l) H(l) + W(l)$$

Now consider the received symbols $y(n)$ in the presence of a carrier-frequency offset

$$y(n) = \frac{1}{N} \sum_{k=-\frac{N}{2}}^{\frac{N}{2}} X(k) H(k) e^{j2\pi n \frac{k+\epsilon}{N}} + w(n)$$

Therefore, the demodulated symbol $Y(l)$ in the presence of a carrier-frequency offset is given as

$$\begin{aligned}
 Y(l) &= \frac{1}{N} \sum_n y(n) e^{-j2\pi \frac{nl}{N}} \\
 &= \frac{1}{N} \sum_n \sum_{k=-\frac{N}{2}}^{\frac{N}{2}} X(k) H(k) e^{j2\pi n \frac{k-l+\epsilon}{N}} + \underbrace{\frac{1}{N} \sum_n w(n) e^{-j2\pi \frac{nl}{N}}}_{W(l)} \\
 &= \frac{1}{N} \sum_n X(l) H(l) e^{j2\pi n \frac{\epsilon}{N}} + \frac{1}{N} \sum_{k=-\frac{N}{2}, k \neq l}^{\frac{N}{2}} \sum_n X(k) H(k) e^{j2\pi n \frac{k-l+\epsilon}{N}} + W(l) \\
 &= X(l) H(l) + W(l)
 \end{aligned}$$

To simplify the above expression, we will use the result below

$$\sum_{n=0}^{N-1} e^{j\theta n} = \frac{\sin\left(\frac{N\theta}{2}\right)}{\sin\left(\frac{\theta}{2}\right)} e^{j\tilde{\phi}}$$

where $e^{j\tilde{\phi}}$ is a phase factor, which does not affect the power at the output. Using the relation above, the expression for $Y(l)$ can be simplified as

$$Y(l) = \underbrace{H(l) X(l) \frac{\sin(\pi\epsilon)}{\sin\left(\frac{\pi\epsilon}{N}\right)} \frac{1}{N} e^{j\tilde{\phi}_l}}_{\text{Desired signal}} + \underbrace{\sum_{k=-\frac{N}{2}, k \neq l}^{\frac{N}{2}} H(k) X(k) \left(\frac{\sin(\pi\epsilon)}{N \sin\left(\pi \frac{l-k+\epsilon}{N}\right)} \right) e^{j\tilde{\phi}_{kl}}}_{\text{Inter-carrier interference } I_l} + W(l)$$

The SINR is given as

$$\begin{aligned}
 \text{SINR} &= \frac{\text{Signal power}}{\text{Interference} + \text{Noise power}} \\
 &= \frac{\text{Signal power}}{\text{E}\left\{|I_l|^2\right\} + \sigma_n^2}
 \end{aligned}$$

The desired signal power can be calculated as

$$\text{Signal power} = \text{E}\left\{|H(l)|^2\right\} \text{E}\left\{|X(l)|^2\right\} \left(\frac{\sin(\pi\epsilon)}{N \sin\left(\frac{\pi\epsilon}{N}\right)} \right)^2$$

For a large value of N , i.e., number of subcarriers, we have

$$\begin{aligned}\lim_{N \rightarrow \infty} \sin\left(\frac{\pi\epsilon}{N}\right) &\approx \frac{\pi\epsilon}{N} \\ \Rightarrow N \sin\frac{\pi\epsilon}{N} &\rightarrow N \frac{\pi\epsilon}{N} = \pi\epsilon\end{aligned}$$

Hence, the signal power for a large number of subcarriers N is given as

$$\begin{aligned}\text{Signal Power} &= E\left\{|H(l)|^2\right\} P \left(\frac{\sin(\pi\epsilon)}{\pi\epsilon}\right)^2 \\ &= P |H|^2 \left(\frac{\sin(\pi\epsilon)}{\pi\epsilon}\right)^2\end{aligned}$$

where $P = E\left\{|X(l)|^2\right\}$ is the power of the transmitted data symbols and $|H|^2 = E\left\{|H(l)|^2\right\}$ denotes the average channel-power gain across each subcarrier. The interference power is given as,

$$E\left\{|I_l|^2\right\} = E\left\{|X(l)|^2\right\} E\left\{|H(l)|^2\right\} \sum_{k=-\frac{N}{2}, k \neq l}^{k=\frac{N}{2}} \left(\frac{\sin(\pi\epsilon)}{N \sin\left(\pi \frac{l-k+\epsilon}{N}\right)}\right)^2$$

Setting $k - l = u$ and letting $N \rightarrow \infty$, we have

$$\begin{aligned}E\left\{|I_l|^2\right\} &= P |H|^2 \sum_{u=-\infty, u \neq 0}^{\infty} \left(\frac{\sin \pi\epsilon}{N \sin \pi \frac{u}{N}}\right)^2 \\ &= P |H|^2 (\sin \pi\epsilon)^2 \sum_{u=-\infty, u \neq 0}^{\infty} \left(\frac{1}{N \sin \pi \frac{u}{N}}\right)^2\end{aligned}$$

Employing the inequality $\sin \theta \geq \frac{2\theta}{\pi}$, we have

$$\begin{aligned}\sin \frac{\pi u}{N} &\geq \frac{2\pi u/N}{\pi} = \frac{2u}{N} \\ \Rightarrow N \sin \frac{\pi u}{N} &\geq 2u\end{aligned}\tag{7.9}$$

The interference power $E \left\{ |I_l|^2 \right\}$ can, therefore, be approximated as

$$\begin{aligned}
 E \left\{ |I_l|^2 \right\} &\leq P |H|^2 (\sin \pi \epsilon)^2 \sum_{u=-\infty, u \neq 0}^{\infty} \left(\frac{1}{2u} \right)^2 \\
 &= P |H|^2 2 (\sin \pi \epsilon)^2 \sum_{u=1}^{\infty} \left(\frac{1}{2u} \right)^2 \\
 &= \frac{1}{2} P |H|^2 (\sin \pi \epsilon)^2 \underbrace{\sum_{u=1}^{\infty} \left(\frac{1}{u} \right)^2}_{\frac{\pi^2}{6}} \\
 &= \frac{\pi^2}{12} P |H|^2 \sin^2 \pi \epsilon \\
 &= 0.822 P |H|^2 \sin^2 \pi \epsilon
 \end{aligned}$$

Hence, the SINR in the presence of carrier-frequency offset of ϵ is given as

$$\text{SINR} = \frac{P |H|^2 \left(\frac{\sin \pi \epsilon}{\pi \epsilon} \right)^2}{0.822 P |H|^2 \sin^2 \pi \epsilon + \sigma_n^2} \quad (7.10)$$

Example 7.1 illustrates the effect of ICI in reducing the SINR at the output of the OFDM receiver.

EXAMPLE 7.1

Consider $|H|^2 = 1$, and data power $P = 10$ dB with noise power $\sigma_n^2 = 0$ dB. Derive the SNR/SINR with and without a carrier-frequency offset of $\epsilon = 5\% = 0.05$ in a WiMAX system.

Solution: If the carrier-frequency offset $\epsilon = 0$, the SNR at the receiver is given as

$$\text{SNR} = \frac{P |H|^2}{\sigma_n^2} = 10 \text{ dB}$$

Considering now a carrier-frequency offset of $\epsilon = 0.05$ and employing the expression in Eq. (7.10), the SINR is given as

$$\text{SINR} = \frac{10 \times \left(\frac{\sin \pi 0.05}{\pi 0.05} \right)^2}{0.82210 \times \sin^2(\pi 0.05) + 1} = 8.25$$

Therefore, the reduction in SINR is a factor of 1.75 or, basically, 17.5%. Further, the WiMAX subcarrier bandwidth is 15.625 kHz. The absolute value of the frequency offset Δf , is therefore,

$$\Delta f = \epsilon B_s = 0.05 \times 15.625 \approx 0.78 \text{ kHz}$$

Further, considering a typical 4G carrier frequency of 2.4 GHz, the carrier-frequency offset as a fraction of the centre frequency is

$$\frac{0.78 \times 10^3}{2.4 \times 10^9} = \frac{1}{3} \times 10^{-6}$$

This is also termed as 0.33 ppm or parts per million with respect to the carrier frequency since $1 \times 10^{-6} = \frac{1}{1000000}$ is equivalent to 1 part per million.

7.7 | OFDM–Peak-to-Average Power Ratio (PAPR)

The *Peak-to-Average Power Ratio (PAPR)* is a critical problem in OFDM systems, which needs to be handled effectively in order to limit the distortion at the receiver. Consider a non-OFDM or single-carrier system with BPSK modulated symbols. For example, let the symbol stream $x(0), x(1), x(2), \dots$ be given as $+a, -a, +a, \dots$ and so on. The power in each symbol equals a^2 . Further, also observe that this is the peak power at any given instant of time. Therefore, we have

$$\text{Peak power} = \text{Average power} = E \left\{ |x(k)|^2 \right\} = a^2$$

Thus, since the peak and average power are equal, the peak-to-average power ratio, or PAPR, is given as

$$\begin{aligned} \text{PAPR} &= \frac{\text{Peak power}}{\text{Average power}} \\ &= \frac{a^2}{a^2} \\ &= 1 = 0 \text{ dB} \end{aligned}$$

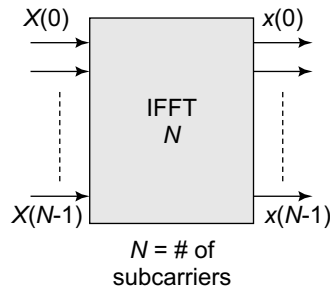


Figure 7.14 OFDM subcarrier loading

The above relation clearly shows that there is no significant deviation of the instantaneous power level from the mean power level. Now, consider an OFDM system in which the different information symbols $X(0), X(1), X(2), \dots$ given by $+a, -a, +a, \dots$ for instance, are loaded onto the subcarriers. This is shown schematically in Figure 7.14. The actual samples transmitted over the wireless channel are $x(0), x(1), x(2), \dots, x(N-1)$, which are the IFFT samples of the information symbols $X(0), X(1), X(2), \dots, X(N-1)$. Consider the k^{th} IFFT sample $x(k)$ given as

$$x(k) = \frac{1}{N} \sum_{i=0}^{N-1} X(i) e^{j2\pi \frac{ki}{N}}$$

where $X(i)$ denotes the information symbols. The average power in the symbols is given as

$$\text{Average power} = E \left\{ |x(k)|^2 \right\}$$

$$\begin{aligned}
&= \frac{1}{N} \sum_{i=0}^{N-1} \mathbb{E} \left\{ |X(i)|^2 \right\} \underbrace{\mathbb{E} \left\{ \left| e^{j2\pi \frac{ki}{N}} \right|^2 \right\}}_1 \\
&= \frac{1}{N^2} \sum_{i=0}^{N-1} \mathbb{E} \left\{ |X(i)|^2 \right\} \\
&= \frac{1}{N^2} \sum_{i=0}^{N-1} a^2 \\
&= \frac{1}{N^2} a^2 N = \frac{a^2}{N}
\end{aligned}$$

As can be seen from the above equation, the average power of transmission is $\frac{a^2}{N}$. The peak power can be found as follows. Observe that the peak of the OFDM sample arises for all symbols $X(i) = +a$ or $X(i) = -a$. This can be verified as follows.

$$\begin{aligned}
|x(k)| &= \left| \frac{1}{N} \sum_{i=0}^{N-1} X(i) e^{j2\pi \frac{ki}{N}} \right| \\
&\leq \frac{1}{N} \sum_{i=0}^{N-1} \left| X(i) e^{j2\pi \frac{ki}{N}} \right| \\
&= \frac{1}{N} \sum_{i=0}^{N-1} \underbrace{|X(i)|}_a \underbrace{\left| e^{j2\pi \frac{ki}{N}} \right|}_1 \\
&= \frac{1}{N} \sum_{i=0}^{N-1} a \\
&= a
\end{aligned}$$

Therefore, the peak power is given as a^2 . Hence, the peak-to-average power ratio in an OFDM system is given as

$$\text{OFDM PAPR} = \frac{a^2}{a^2/N} = N$$

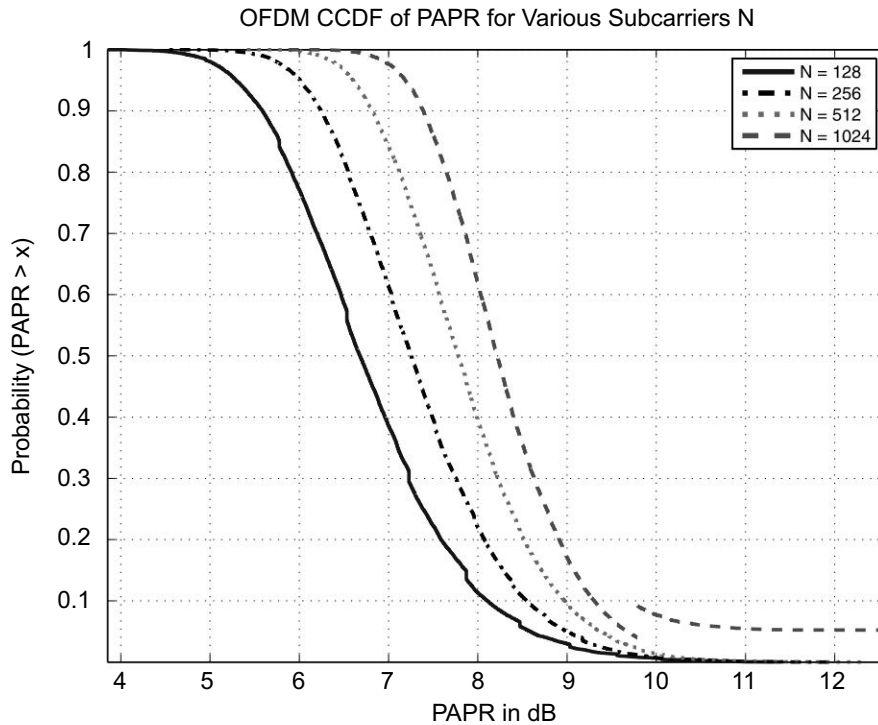


Figure 7.15 OFDM PAPR for various number of subcarriers N

From the above expression, it can be seen that the peak-to-average power ratio in an OFDM system is N , which is significantly higher compared to that of the single-carrier system, which is 1. Further, interestingly, this PAPR rises with N , i.e., the number of subcarriers. Larger the number of subcarriers, larger is the PAPR. This high PAPR of the OFDM arises because of the IFFT operation. The data symbols across the subcarriers can add up to produce a high peak valued signal as seen above. For instance, in an OFDM system with 512 subcarriers and BPSK modulation, the PAPR at the output can be as high as 10 dB. The PAPR of an OFDM system is characterized using the CCDF, i.e., the complementary cumulative distribution function. The CCDF $\bar{F}_X(x)$ of a random variable X is given as the probability that $X > x$, expressed as

$$\bar{F}_X(x) = \Pr(X > x)$$

Naturally, the CCDF is related to the CDF, i.e., cumulative distribution function $F_X(x)$ of X as

$$\begin{aligned}
 F_X(x) &= \Pr(X \leq x) \\
 &= 1 - \Pr(X > x) \\
 &= 1 - F_X(x)
 \end{aligned}$$

The CCDF of the PAPR then shows the probability that the PAPR, which is a random quantity, exceeds a particular threshold. A plot of the CCDF of the PAPR for various values of N , the total number of subcarriers, is shown in Figure 7.15.

The impact of PAPR on the OFDM system hardware can be understood as follows. Every communication system has a receiver amplifier, which serves to amplify the amplitude of the receive signal, in order to boost its strength. However, the characteristic of the amplifier is linear only for a limited amplitude range of the signal. Typically, the amplifier operates around a bias point, as shown in Figure 7.16, which is roughly around the average power of the signal. As long as the signal amplitude is restricted to the *dynamic range* of the amplifier around this bias point, for which the amplifier characteristic is linear, there is no nonlinear distortion at the output. However, in the case of OFDM, since the peak power deviates significantly from the average power, there is a high chance that the signal crosses into the voltage region outside the

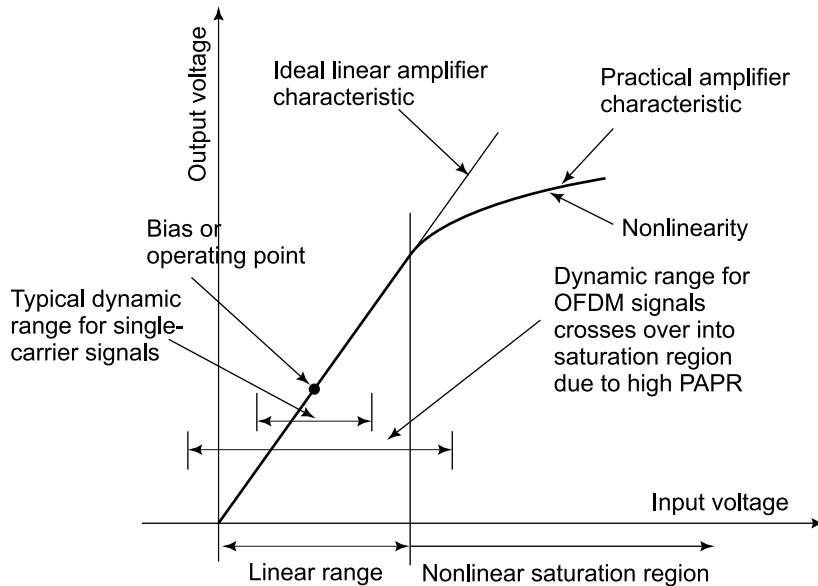


Figure 7.16 *Nonlinear amplifier characteristic*

dynamic range of the amplifier, thus resulting in a nonlinear distortion of the received signal. This nonlinear effect, arising out of amplifier saturation, leads to loss of orthogonality of the subcarriers and inter-carrier interference. The net result is a poor decoding performance and a rise in the bit-error rate. A slightly modified OFDM technique, which can significantly reduce the PAPR, is SC-FDMA, which is described next.

7.8 | SC-FDMA

SC-FDMA, which stands for *Single-Carrier Frequency Division for Multiple Access*, can be employed to reduce the peak-to-average power ratio in an OFDM system. Consider the following hypothetical modification of the OFDM transmitter, shown in Figure 7.17, by the insertion of an N -point FFT block before the N -point IFFT block. It can then be seen that the FFT and the IFFT cancel the effect of each other and the net output is the exact input symbol stream, i.e., corresponding to a single-carrier system. This drastically reduces the PAPR, since, as seen previously, the PAPR of a single-carrier system is 0 dB. However, instead of using an N -point FFT, one can use an M -point FFT, where $M < N$, to reduce the PAPR, while still retaining the properties of the OFDM system. This proposed SC-FDMA schematic is shown in Figure 7.18. Hence, introduction of the M -point FFT in SC-FDMA significantly reduces the PAPR of the system. This is the central principle of SC-FDMA.

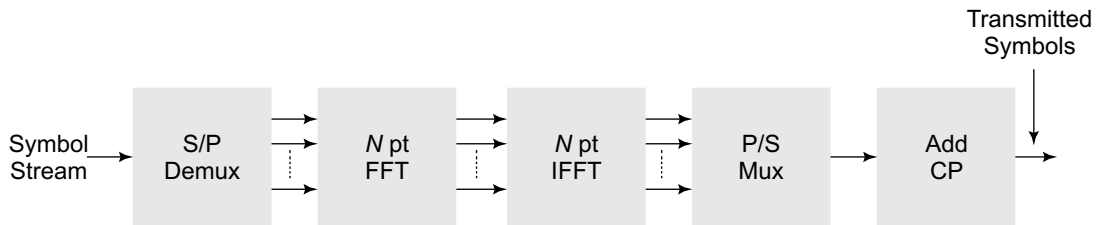


Figure 7.17 Hypothetical modification of OFDM transmitter

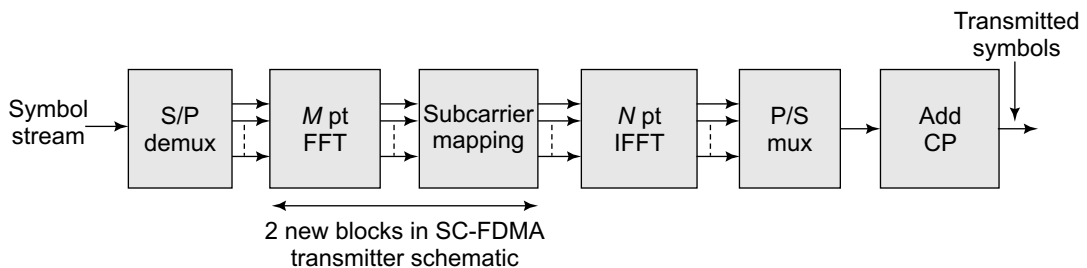


Figure 7.18 SC-FDMA transmitter schematic

7.8.1 SC-FDMA Receiver

The SC-FDMA receiver schematic is shown in Figure 7.19. The SC-FDMA receiver incorporates two new blocks compared to the OFDM receiver. The purpose of these additional blocks can be described as follows. After the N -point FFT operation at the receiver, the signals are equalized across all the subcarriers, to remove the effect of the fading-channel coefficient across the subcarriers. Following the above operation, they are demapped from the subcarriers, which are N in number, to the original FFT block size of M . Finally, the M -point FFT is performed on these samples to generate the symbol stream.

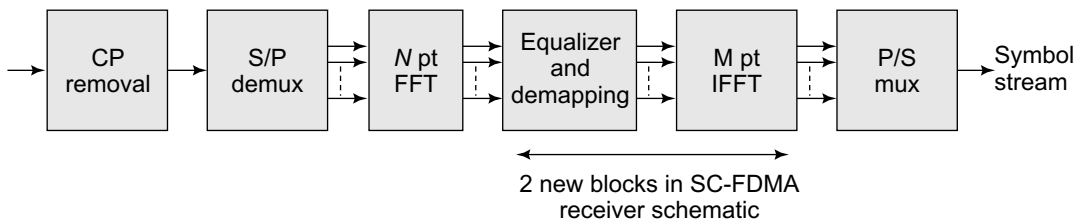


Figure 7.19 SC-FDMA receiver schematic

7.8.2 Subcarrier Mapping in SC-FDMA

Subcarrier mapping, in which the M samples at the output of the M -point FFT are mapped to the N subcarriers, is a key operation in SC-FDMA, a block representation of which can be seen in the SC-FDMA transmitter schematic in Figure 7.18. The various possible SC-FDMA subcarrier mappings are illustrated through the following example. Consider $M = 4$ SC-FDMA symbols and $N = 12$ subcarriers. Let $x(0)$, $x(1)$, $x(2)$, $x(3)$ denote the symbols and $X(0)$, $X(1)$, $X(2)$, $X(3)$ denote the corresponding $M = 4$ -point FFT samples which are to be loaded onto the subcarriers. Let the number of subcarriers be $N = 12$. In Interleaved FDMA (IFDMA) shown in Figure 7.20, the samples $X(i)$ are interleaved with zeros. In LFDMA, which is also employed in the uplink of the 4G mobile standard LTE, the samples are loaded as a block onto the subcarriers, with appropriate zero padding. This is shown in Figure 7.20. Post this subcarrier mapping, the rest of the procedure prior to transmission proceeds as shown in the SC-FDMA transmitter block.

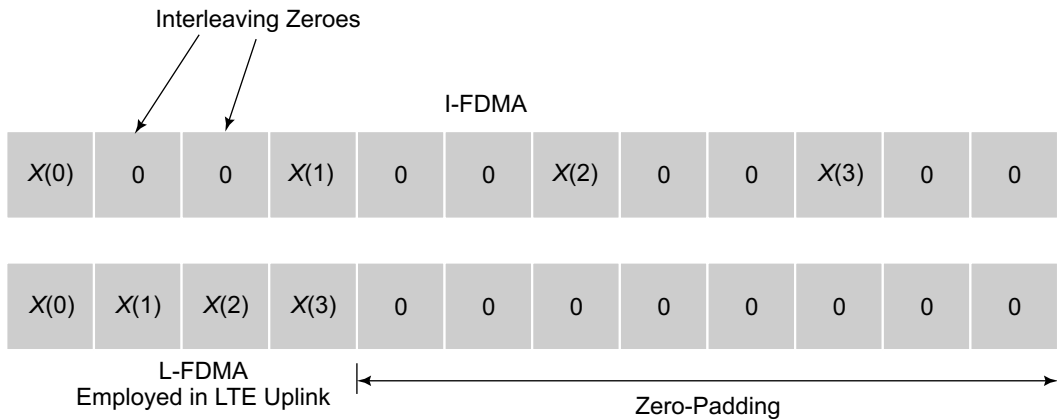


Figure 7.20 SC-FDMA various subcarrier mapping schemes

PROBLEMS

1. Consider a three-tap wireless channel $[h(0), 0, h(2)]$ (i.e., $h(1) = 0$) with each tap a uniform Rayleigh fading channel coefficient. Employ the WSSUS channel assumption. Let an OFDM system with 256 subcarriers in the 2.1 GHz band be implemented over this channel with delay spread $T_d = 8 \mu\text{s}$. The DFT operation at the receiver is given as

$$F(k) = \frac{1}{\sqrt{N}} \sum_{l=0}^{N-1} f(l) e^{-j\frac{2\pi lk}{N}}$$

- (a) With a bare minimum cyclic-prefix duration, the system has a useful bit rate of 8.6486 Mbps for QPSK transmission. What is the bandwidth of the system?
- (b) For a cyclic prefix of $12 \mu\text{s}$ duration, what is the loss in spectral efficiency for this system?
- (c) Consider the channel coefficients $H(0)$ and $H(64)$ at the 0^{th} and 64^{th} subcarriers respectively. What is their joint distribution?
- (d) It is not difficult to see that every OFDM system must satisfy a very important constraint that the wireless channel is constant during the transmission of the total OFDM symbol (i.e., useful plus cyclic). Assuming a system with 20% loss of spectral efficiency and an extreme vehicle moving at 200 km/h, what is the maximum possible number of subcarriers?

- 2. OFDM System Design** Consider an OFDM system with $N = 256$ subcarriers over a bandwidth of $B = 5$ MHz. Let the corresponding frequency selective *fading* channel have an impulse response with 3 multipath components at delays of $[0, 0.40, 1.0]$ μs , with each component of -3 dB average power. Noise power at the receiver is $\sigma_v^2 = 3$ dB. Assume that the IFFT and FFT operations are given respectively as

$$x(n) = \frac{1}{N} \sum_{k=0}^{N-1} X(k) e^{j2\pi kn/N}, \quad X(k) = \sum_{n=0}^{N-1} x(n) e^{-j2\pi kn/N}$$

In that case, the system model after FFT at the receiver becomes $Y(k) = H(k) X(k) + V(k)$, where $V(k)$ is the FFT of the AWGN. Answer the following questions.

- Describe the time-domain model of the above frequency-selective channel.
 - What is the minimum number of samples required in the cyclic prefix?
 - What is the duration of this minimum cyclic prefix?
 - If the actual cyclic prefix employed is twice the minimum length required with QPSK modulated subcarriers, what is the *effective* bit rate of the OFDM system?
 - What is the bit-error rate across each subcarrier if the total transmit power of 70 dB is distributed equally across the subcarriers?
 - What is the reduction in SNR across each subcarrier in the presence of a 5% carrier-frequency offset relative to the subcarrier bandwidth?
- 3. OFDM System Design** Consider a mobile OFDM profile with $N = 512$ subcarriers over a bandwidth of $B = 10$ MHz. Let the corresponding frequency-selective *fading* channel have an impulse response with 4 multipath components at delays of $0 \mu s, 0.60 \mu s, 1.2 \mu s, 2.4 \mu s$, with each component of average power -3 dB. Noise power at the receiver is $\sigma_n^2 = 3$ dB per sample (i.e., before FFT). Assume that the IFFT and FFT operations are given respectively as,

$$x(n) = \frac{1}{N} \sum_{k=0}^{N-1} X(k) e^{j2\pi kn/N}, \quad X(k) = \sum_{n=0}^{N-1} x(n) e^{-j2\pi kn/N}$$

In that case, the system model after FFT at the receiver becomes $Y(k) = H(k) X(k) + W(k)$, where $W(k)$ is the FFT of the AWGN. Answer the following questions.

- Describe the time-domain model of the above frequency-selective channel, i.e., what

is the length of the channel impulse response filter and what is the number of nonzero channel taps?

- (b) What is the minimum number of samples required in the cyclic prefix in this system?
 - (c) What is the duration of this minimum cyclic prefix?
 - (d) If the actual cyclic prefix employed is three times the minimum length required with QPSK-modulated subcarriers, what is the *effective* bit rate of the OFDM system?
 - (e) What is the QPSK bit-error rate across each subcarrier if the total transmit power of 80 dB is distributed equally across the subcarriers?
 - (f) What is the reduction in SNR across each subcarrier in the presence of an 8% carrier-frequency offset relative to the subcarrier bandwidth?
4. Consider an OFDM system with total passband bandwidth $B = 5$ MHz with $N = 512$ subcarriers. The channel has a maximum delay spread of $T_d = 4$ μ s. Answer the questions that follow.
- (a) What is the symbol time of a corresponding single-carrier system?
 - (b) What is the sample time of the OFDM system and the raw symbol time without the cyclic prefix?
 - (c) What is the minimum number of samples required in the cyclic prefix?
 - (d) If the length of the cyclic prefix is twice the required minimum calculated above, what is the total OFDM symbol time?
 - (e) What is the loss in efficiency due to the overhead of the cyclic prefix?
 - (f) If the modulation employed is 16-QAM, what is the effective bit rate of the above OFDM system?
 - (g) At a carrier frequency of $f_c = 2.4$ GHz, what is the maximum possible velocity of a mobile for the system to be able to function?
5. **Alamouti Coded OFDM** Consider an Alamouti-coded OFDM system with two transmit and one receive antennas. Consider symbols $X_1(k)$, $X_2(k)$ loaded onto transmit antennas 1,2 respectively on the k^{th} subcarrier of the OFDM system in the first OFDM symbol. Consider a frequency-selective channel with channel taps $h(0)$, $h(1)$, \dots , $h(L-1)$. Answer the questions that follow.
- (a) Describe the operation of the Alamouti-coded OFDM system above, i.e., the transmission on each subcarrier and the decoding operation at the receiver.
 - (b) If the transmit power is P per subcarrier, noise power σ_n^2 , find the instantaneous receive SNR expression for each symbol.

- (c) Considering the channel taps to be IID Rayleigh random variables of average power unity, derive the **average** Symbol Error Rate (SER) expressions for BPSK and 16-PSK modulation.
- (d) Compute the average SER above for both BPSK and 16-PSK for $P = 35$ dB, number of subcarriers $N = 128$, $L = 5$, and noise power $\sigma_n^2 = -3$ dB.
- (e) Considering the channel taps to be independent Rayleigh random variables of average power σ_l^2 , $0 \leq l \leq L - 1$, derive the **average** SER expressions for BPSK and 16-PSK modulation.
- (f) Compute the average SER above for both BPSK and 16-PSK for $P = 35$ dB, number of subcarriers $N = 128$, $\sigma_l^2 = l$ dB for $0 \leq l \leq 4$ and noise power $\sigma_n^2 = -3$ dB.
6. Consider a multipath channel with L i.i.d Rayleigh faded taps $h(i)$, $0 \leq i \leq L - 1$, each distributed as the symmetric complex Gaussian $\mathcal{CN}(0, 1)$. Let $H(u)$, $H(v)$ denote the complex channel coefficients corresponding to subcarriers u , v respectively in an OFDM system with N subcarriers and bandwidth B . Consider *uncorrelated scattering* and answer the questions that follow.
- (a) Express $H(u)$, $H(v)$ in terms of the channel taps.
- (b) Compute the auto-correlation $R(0)$ corresponding to the the complex channel coefficient across each subcarrier.
- (c) Derive the exact expression for the correlation between the subcarrier coefficients $H(u)$, $H(v)$.
- (d) Derive a suitable bound for the correlation between the subcarrier coefficients $H(u)$, $H(v)$ in terms of $|u - v|$ and N .
- (e) Derive an expression for the number of subcarriers per coherence bandwidth B_c in the above system. Denote this by N_c .
- (f) Let $|u - v| = \alpha N_c$. Derive a bound for the correlation between the subcarrier coefficients $H(u)$, $H(v)$ as a function of $R(0)$ and α . From this, deduce the rate at which the correlation is decreasing as a function of α .
7. Consider an OFDM system with $N = 4$ subcarriers and $L = 2$ tap wireless channel with channel coefficients $h(0)$, $h(1)$. Let noise power *per subcarrier* (i.e., after the FFT at the receiver) be $\sigma^2 = 3$ dB. Let the total transmit power be P_T . Answer the questions that follow.
- (a) Consider $h(0) = h(1) = \frac{1}{2}$ and derive the complex channel coefficients across all the subcarriers.

- (b) Consider $h(0) = h(1) = \frac{1}{2}$, $P_T = 18$ dB with equal power allocation and derive the instantaneous BER across each subcarrier for BPSK modulation.
- (c) Consider $h(0) = h(1) = \frac{1}{2}$, $P_T = 18$ dB and derive the optimal power allocation for each subcarrier.
- (d) Consider coefficients $h(0)$, $h(1)$ to be Rayleigh fading i.i.d. with average power unity and derive the average BER as a function of P_T , σ^2 for BPSK modulation with total power P_T and equal power allocation across subcarriers.

Wireless-System Planning

8.1 | Introduction

In order to plan the installation and deployment of a comprehensive wireless network, one needs to characterize the performance of the communication system in terms of the transmitted power and also the total load in terms of users that can be supported by the network. This chapter intends to focus on those aspects which are necessary to characterize the overall performance of a large wireless network.

In this context, it is well known from the theory of electromagnetic waves that the strength of the transmitted wireless radio signal decreases as the distance of propagation increases. In a typical wireless communication scenario, such as the one shown in Figure 8.1, we would like to characterize the signal strength at the mobile as a function of the distance d . Hence, we need models which predict the mean signal strength at the receiver as a function of the separation between the transmitter and the receiver. These models are also termed *large-scale-propagation* models. We begin with a discussion of the free-space-propagation model next.

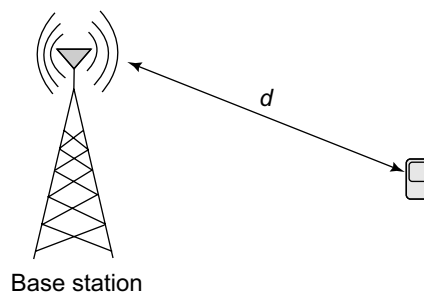


Figure 8.1 Propagation loss for a wireless signal

8.2 | Free-Space Propagation Model

The free-space propagation model predicts the received signal strength when there is an unobstructed propagation path between the transmitter and the receiver. The Friis free-space equation, which gives the received power $P_r(d)$ as a function of the distance d , is given as

$$P_r(d) = \frac{P_t G_t G_r \lambda^2}{(4\pi)^2 d^2 L} \quad (8.1)$$

where P_t is the transmitted power, G_t is the transmit antenna gain, G_r is the receive antenna gain, λ is the wavelength, and $L \geq 1$ denotes the system-loss factor. Further, the wavelength $\lambda = \frac{c}{f_c}$, where $c = 3 \times 10^8$ m/s is the velocity of light or electromagnetic waves and f_c is the carrier frequency. Let P_0 be the power received at a reference distance d_0 . We, therefore, have

$$\begin{aligned} P_0 &= \frac{P_t G_t G_r \lambda^2}{(4\pi)^2 d_0^2 L} \\ \Rightarrow P_0 d_0^2 &= \frac{P_t G_t G_r \lambda^2}{(4\pi)^2 L} \end{aligned}$$

Hence, for any distance d , we have

$$\begin{aligned} P_r(d) &= \frac{P_t G_t G_r \lambda^2}{(4\pi)^2 d^2 L} \\ &= \frac{P_0 d_0^2}{d^2} \end{aligned}$$

from which it can be seen that the received power decays as the inverse of d^2 . The number 2 in the exponent of d is also termed the *path-loss exponent*. Thus, the path-loss exponent for free space is 2, which basically means that the received power decays as the inverse of the distance squared. Converting the received power to dB, we have

$$\begin{aligned} P^{\text{dB}} &= 10 \log_{10} P = 10 \log_{10} \left(\frac{P_0 d_0^2}{d^2} \right) \\ &= 10 \log_{10} P_0 + 20 \log_{10} \left(\frac{d_0}{d} \right) \end{aligned}$$

$$\begin{aligned}
&= 10 \log_{10} P_0 - 2 \times 10 \log_{10} \left(\frac{d_0}{d} \right) \\
&= 10 \log_{10} P_0 - n \times 10 \log_{10} \left(\frac{d_0}{d} \right)
\end{aligned}$$

where $n = 2$ is the path-loss exponent for free-space propagation. However, the path-loss exponent varies from scenario to scenario and is typically greater than 2, especially in the presence of reflectors. The model described in the next section illustrates one such context.

8.3 | Ground-Reflection Scenario

Consider the *ground-reflection scenario* shown in Figure 8.2. The total received signal E_{Tot} is given as

$$E_{Tot} = E_{LOS} + E_g \quad (8.2)$$

where E_{LOS} , E_g are the received line-of-sight and ground-reflection components. The component E_{LOS} can be expressed as

$$E_{LOS} = \frac{E_0 d_0}{d_{LOS}} e^{j2\pi f_c \left(t - \frac{d_{LOS}}{c} \right)}$$

where E_0 is the transmitted signal amplitude at a reference distance d_0 , and d_{LOS} is the propagation distance for the LOS component. Since the received power decays as the inverse square of the distance, the signal amplitude is inversely proportional to the distance of propagation. Also, the quantity $2\pi f_c \left(t - \frac{d_{LOS}}{c} \right)$ denotes the phase lag of the carrier at the receiver arising due to the propagation delay corresponding to this line-of-sight component. Further, using the approximation $d_{LOS} \approx d$ for the large-scale path loss, where d is the ground distance between the transmitter and the receiver as shown in Figure 8.2, we have

$$E_{LOS} \approx \frac{E_0 d_0}{d} e^{j2\pi f_c \left(t - \frac{d_{LOS}}{c} \right)}$$

Similarly, the quantity E_g corresponding to the ground-reflection component is given as

$$E_g = -\frac{E_0 d_0}{d} e^{j2\pi f_c \left(t - \frac{d_g}{c} \right)}$$

where d_g is the distance traversed by the ground-reflected component and the – ve sign arises because of the phase inversion from ground reflection. Therefore, substituting in Eq. (8.2), it follows that

$$\begin{aligned} E_{Tot} &= E_{LOS} + E_g \\ &= \frac{E_0 d_0}{d} e^{j2\pi f_c (t - \frac{d_{LOS}}{c})} - \frac{E_0 d_0}{d} e^{t - \frac{d_g}{c}} \\ &= \frac{E_0 d_0}{d} e^{j2\pi f_c (t - \frac{d_{LOS}}{c})} \left(1 - e^{j2\pi f_c \frac{\Delta d}{c}} \right) \end{aligned} \quad (8.3)$$

where $\Delta d = d_g - d_{LOS}$ is the difference in distances. Employing the relation that $\lambda = \frac{c}{f_c}$, the above expression can be further simplified as

$$\begin{aligned} E_{Tot} &= \frac{E_0 d_0}{d} e^{j2\pi f_c (t - \frac{d_{LOS}}{c})} \left(1 - e^{j2\pi \frac{\Delta d}{\lambda}} \right) \\ &= \frac{E_0 d_0}{d} e^{j2\pi f_c (t - \frac{d_{LOS}}{c})} e^{j2\pi \frac{\Delta d}{2\lambda}} \left(e^{-j2\pi \frac{\Delta d}{2\lambda}} - e^{j2\pi \frac{\Delta d}{2\lambda}} \right) \\ &= -\frac{E_0 d_0}{d} e^{j2\pi f_c (t - \frac{d_{LOS}}{c})} e^{j2\pi \frac{\Delta d}{2\lambda}} \sin \left(2\pi \frac{\Delta d}{2\lambda} \right) \end{aligned}$$

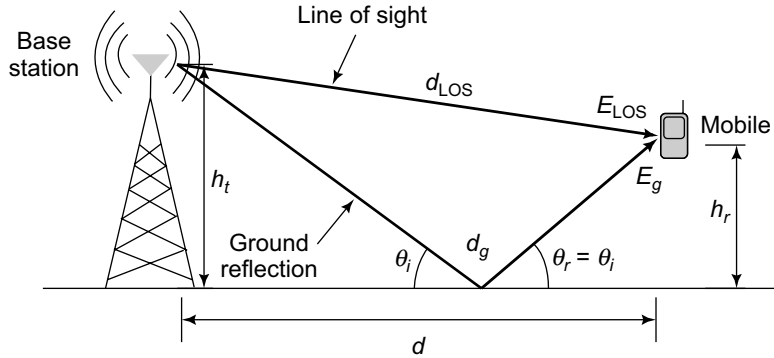


Figure 8.2 Ground-reflection model

Hence, it follows from the above expression that the magnitude $|E_{TOT}|$ of the net signal at the receiver can be simplified as

$$|E_{TOT}| = \frac{E_0 d_0}{d} \left| \sin \left(2\pi \frac{\Delta d}{2\lambda} \right) \right| \quad (8.4)$$

The difference of the distances $\Delta d = d_g - d_{LOS}$ can be further simplified as follows. It can be seen from Figure 8.3 that d_{LOS} can be expressed as

$$d_{LOS} = \sqrt{(h_t - h_r)^2 + d^2} \quad (8.5)$$

where h_t, h_r denote the heights of the transmit and receive antennas respectively. Further, as shown in Figure 8.4, it can be seen that the expression for d_g , the total distance traversed by the ground-reflected component, can be simplified as

$$d_g = \sqrt{(h_t + h_r)^2 + d^2} \quad (8.6)$$

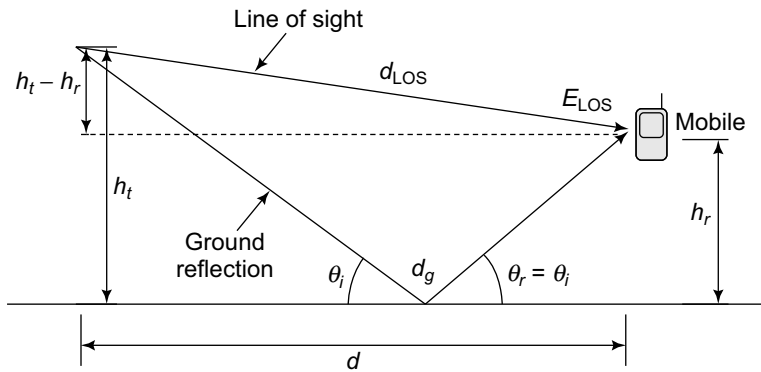


Figure 8.3 Line-of-sight distance d_{LOS} in ground-reflection model

Therefore, from the expressions for d_{LOS} , d_g from equations (8.5), (8.6) above, the resulting equation for Δd can be simplified as

$$\begin{aligned} \Delta d &= d_g - d_{LOS} \\ &= \sqrt{(h_t + h_r)^2 + d^2} - \sqrt{(h_t - h_r)^2 + d^2} \\ &= d \left(\sqrt{1 + \left(\frac{h_t + h_r}{d}\right)^2} - \sqrt{1 + \left(\frac{h_t - h_r}{d}\right)^2} \right) \end{aligned}$$

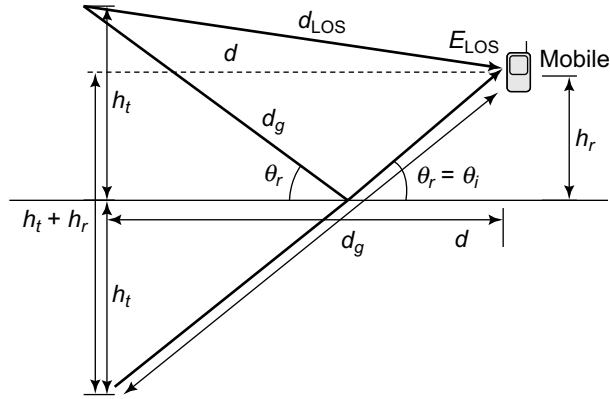


Figure 8.4 Ground-reflection distance d_g in ground-reflection model

Assuming now that $h_t, h_r \ll d$, the expression for Δd can be approximated as

$$\begin{aligned}
 \Delta d &\approx d \left\{ \left(1 + \frac{1}{2} \left(\frac{h_t + h_r}{d} \right)^2 \right) - \left(1 + \frac{1}{2} \left(\frac{h_t - h_r}{d} \right)^2 \right) \right\} \\
 &= d \left(\frac{1}{2} \frac{4h_t h_r}{d^2} \right) \\
 &= \frac{2h_t h_r}{d}
 \end{aligned} \tag{8.7}$$

Substituting the above expression for Δd in Eq. (8.4) yields

$$\begin{aligned}
 |E_{Tot}| &= \frac{2E_0 d_0}{d} \sin \left(2\pi \frac{\Delta d}{2\lambda} \right) \\
 &\approx \frac{2E_0 d_0}{d} 2\pi \frac{\Delta d}{2\lambda} \\
 &= \frac{2E_0 d_0}{d} \frac{2\pi}{2\lambda} \frac{2h_t h_r}{d} \\
 &= \frac{4\pi E_0 d_0 h_t h_r}{\lambda d^2} \propto \frac{1}{d^2}
 \end{aligned}$$

where we have used the approximation $\sin \left(2\pi \frac{\Delta d}{2\lambda} \right) \approx 2\pi \frac{\Delta d}{2\lambda}$ in the above simplification, which holds when $\Delta d \approx \frac{2h_t h_r}{d} \ll \lambda$, i.e., basically, when the distance d between the transmitter and the receiver is large in comparison to the product $h_t h_r$ of the transmit and receive antenna heights. Therefore, as seen above, since the net magnitude $|E_{Tot}|$ of the received signal is inversely proportional to $\frac{1}{d^2}$, it follows that the net received power P_{Tot} , which is proportional

to the squared magnitude, decreases as $\frac{1}{d^4}$, indicating a path-loss exponent $n = 4$. Thus, we have

$$P_{Tot} \propto \frac{1}{d^4}$$

Therefore, considering the dB power level $P^{\text{dB}} = 10 \log_{10} P_{Tot}$, we have

$$P^{\text{dB}} = \tilde{P}^{\text{dB}} - 40 \log_{10} \left(\frac{d}{\tilde{d}} \right)$$

where \tilde{P} is the received power at a reference distance \tilde{d} . Thus, the path-loss exponent can vary depending on the scenario and, therefore, the received power decays as $\frac{1}{d^n}$, where $n = 2$ for free space, while n can be significantly greater than 2 as seen in the case of the ground-reflection scenario above.

8.4 | Okumura Model

Several models have been developed to accurately model the received signal strength in practical wireless scenarios. Amongst these, the Okumura model, proposed by the Japanese engineer Yoshihisa Okumura in 1968 in the paper titled "Field Strength and its Variability in VHF and UHF Land-Mobile Radio Service", is one of the most widely used models for signal strength in urban/suburban areas. This is valid roughly in the 150-to-1920 MHz range, although it can be extrapolated for higher frequencies. According to the Okumura model, the 50th percentile or median-path loss L_{50} is given as

$$L_{50} (\text{dB}) = L_F (\text{dB}) + A_{mu} (f_c, d) - G(h_{te}) - G(h_{re}) - G_{Area} \quad (8.8)$$

where L_F denotes the free-space-propagation loss; $A_{mu} (f_c, d)$ is the correction factor; $G(h_{te})$, $G(h_{re})$ are the gain factors corresponding to the transmit and receive antenna heights h_{te} , h_{re} respectively; and G_{Area} is the gain due to the environment.

The free-space loss is derived from the Friis free space model described in Section 8.2 and is given as

$$\begin{aligned} L_F \text{ (dB)} &= \frac{P_t}{P_r} \text{ (dB)} \\ &= 10 \log_{10} \left(\frac{(4\pi)^2 d^2 L}{G_t G_r \lambda^2} \right) \end{aligned}$$

Further, when $L = G_t = G_r = 1$, we have

$$L_F \text{ (dB)} = 10 \log_{10} \left(\frac{(4\pi)^2 d^2}{\lambda^2} \right) \quad (8.9)$$

The transmit and receive antenna-height-gain factors $G(h_{te})$, $G(h_{re})$ respectively are given as

$$\begin{aligned} G(h_{te}) &= 20 \log_{10} \left(\frac{h_{te}}{200} \right) \\ G(h_{re}) &= \begin{cases} 10 \log_{10} \left(\frac{h_{re}}{3} \right) & h_{re} < 3 \text{ m} \\ 20 \log_{10} \left(\frac{h_{re}}{3} \right) & 3 \text{ m} \leq h_{re} \leq 10 \text{ m} \end{cases} \end{aligned}$$

The quantity $A_{mu}(f_c, d)$ is a correction factor as a function of the carrier frequency f_c and distance d . This has been plotted for several values of f_c , d and can be found in standard reference books. For example, from the Okumura model, the factor A_{mu} at distance $d = 5$ km and $f_c = 1.8$ GHz is given as

$$A_{mu}(1.8 \text{ GHz}, 5 \text{ km}) = 28 \text{ dB}$$

The quantity G_{Area} is a correction factor for various environments. It has been computed and plotted for different frequencies for suburban, quasi-open, and open areas, and is given in standard references. For example, the factor G_{Area} for a suburban area at 1.8 GHz is given as $G_{Area} = 12$ dB. Example 8.1 illustrates an application of the Okumura model for wireless-signal-strength computation.

EXAMPLE 8.1

Employing the Okumura model, compute the median loss at a distance of 8 km when the carrier frequency $f_c = 2.1$ GHz, $h_{te} = 40$ m, $h_{re} = 2$ m in a large city.

Solution: Given $f_c = 2.1$ GHz $= 2.1 \times 10^9$ Hz. Therefore, the wavelength λ equals

$$\lambda = \frac{3 \times 10^8}{2 \times 10^9} = 0.143 \text{ m}$$

The quantity L_F , the free-space loss, is given as

$$L_F = \frac{(4\pi)^2 \times (8 \times 10^3)^2}{0.143^2}$$

Hence, L_F , the free-space loss, is given as

$$L_F = \frac{(4\pi)^2 \times (8 \times 10^3)^2}{0.143^2}$$

Further, the free-space loss L_F in dB is

$$\begin{aligned} L_F (\text{ dB}) &= 10 \log_{10} \left(\frac{(4\pi)^2 \times (8 \times 10^3)^2}{0.143^2} \right) \\ &= 116.93 \text{ dB} \approx 117 \text{ dB} \end{aligned}$$

Since the transmit antenna height $h_{te} = 40$ m, the transmit antenna-gain factor is given as

$$G(h_{te}) = 20 \log_{10} \left(\frac{40}{200} \right) = -14 \text{ dB}$$

Further, since $h_{re} = 2$ m, the antenna-gain factor $G(h_{re})$ is given as

$$G(h_{re}) = 10 \log_{10} \left(\frac{2}{3} \right) = -1.76 \text{ dB}$$

Further, since the cell radius is 8 km, the correction factor $A_{mu}(f_c, d)$ is given as

$$A_{mu}(2.1\text{GHz}, 88\text{Km}) = 34 \text{ dB}$$

Since the environment is urban, the factor $G_{Area} = 0$. Therefore, the 50-percentile path loss L_F dB is given as

$$\begin{aligned} L_{50} \text{ dB} &= L_F + A_{mu}(f, d) - G(h_{te}) - G_{h_{re}} - G_{Area} \\ &= 117 + 34 - (-14) - (-1.76) \approx 167 \text{ dB} \end{aligned}$$

8.5 | Hata Model

The Hata model is another popular model for signal strength prediction proposed initially by the Japanese engineer Masaharu Hata in his 1980 paper titled "Empirical Formula for Propagation Loss in Land Mobile Radio Services". The Hata model presents an analytical approximation for the graphical-information-based Okumura model introduced previously. The median-path loss L_{50} (dB) for urban areas under the Hata model is given as

$$\begin{aligned} L_{50} \text{ (dB)} &= 69.55 + 26.16 \log_{10} f_c^{\text{MHz}} - a(h_{re}) - 13.82 \log_{10}(h_{te}) \\ &\quad + (44.9 - 6.55 \log_{10} h_{te}) \log_{10} d^{\text{km}} \end{aligned}$$

where f_c^{MHz} is the carrier frequency expressed in megahertz; $a(h_{re})$ is the mobile antenna-correction factor associated with the antenna height h_{re} ; h_{te} is the transmit antenna height; and d^{km} is the distance in kilometres. The transmit and receive antenna heights h_{te} , h_{re} in the Hata model are constrained as follows.

$$30 \text{ m} < h_{te} < 200 \text{ m}$$

$$1 \text{ m} < h_{re} < 10 \text{ m}$$

The mobile antenna-correction factor $a(h_{re})$ for a small-to-medium sized city is given as

$$a(h_{re}) = (1.1 \log_{10} f_c^{\text{MHz}} - 0.7) h_{re} - (1.56 \log_{10} f_c^{\text{MHz}} - 0.8) \text{ dB}$$

The correction factor for a large city is given as

$$a(h_{re}) = \begin{cases} 8.29 (\log_{10} 1.54 h_{re})^2 - 1.1 \text{ dB}, & f_c \leq 300 \text{ MHz} \\ 3.2 (\log_{10} 11.75 h_{re})^2 - 4.97 \text{ dB}, & f_c > 300 \text{ MHz} \end{cases}$$

Example 8.2 illustrates an application of the Hata model for wireless-signal-strength prediction.

EXAMPLE 8.2

Employing the Hata model, compute the median loss at a distance $d = 8$ km, when the carrier frequency $f_c = 2.1$ GHz, $h_{te} = 40$ m, $h_{re} = 2$ m for a large city.

Solution: The carrier frequency is $f_c = 2.1$ GHz. Therefore, f_c^{MHz} , i.e., the carrier-frequency in MHz is given as

$$f_c^{\text{MHz}} = \frac{2.1 \times 10^9}{10^6} = 2100$$

The distance in kilometres $d^{\text{km}} = 8$. Therefore, the correction factor $a(h_{re})$ is given as

$$a_{h_{re}} = 3.2 (\log_{10} 11.75 \times 2)^2 - 4.97 = 1.04 \text{ dB}$$

Therefore, L_{50} , i.e., the 50th percentile loss is given from the Hata model as

$$\begin{aligned} L_{50} &= 69.55 + \underbrace{26.16 \log_{10} 2100}_{86.9 \text{ dB}} - \underbrace{13.82 \log_{10} 2}_{22.14 \text{ dB}} - 1.04 + \underbrace{(44.9 - 6.55 \log_{10} 40) \log_{10} 8}_{31.07 \text{ dB}} \\ &= 69.55 + 86.90 - 22.14 - 1.04 + 31.07 \text{ dB} \\ &= 164.34 \text{ dB} \end{aligned}$$

8.6 | Log-Normal Shadowing

The surrounding environment at different locations is very different in a wireless scenario. For example, users can be shadowed by large objects such as walls or buildings. Thus, the net received signal strength is basically a random variable with the mean predicted by the path loss. This random dB deviation about the mean signal strength can be modelled as a Gaussian RV $X_\sigma \sim \mathcal{N}(0, \sigma^2)$. This is shown schematically in Figure 8.5, where the point L_{50} indicates the mean/median path loss. Hence, X_σ , the deviation about the mean is Gaussian or normally

distributed. Also, X_σ , which is in dB, is logarithmically related to the signal power. Thus, log of the received signal power is Gaussian distributed, or in other words, X_σ is a log normal Gaussian random variable with variance σ^2 . Hence, this is also termed *log-normal shadowing*. The observed path loss in dB PL^{dB} can therefore, be expressed as

$$\text{PL}^{\text{dB}} = L_{50} + X_\sigma$$

where L_{50} denotes the median-path loss. Therefore, the probability that the path loss is greater than the threshold γ is given as

$$\begin{aligned} \Pr(\text{PL}^{\text{dB}} > \gamma) &= \Pr(L_{50} + X_\sigma > \gamma) \\ &= \Pr(X_\sigma > \gamma - L_{50}) \\ &= Q\left(\frac{\gamma - L_{50}}{\sigma}\right) \end{aligned} \quad (8.10)$$

where $Q(\cdot)$ denotes the Gaussian Q -function. An application of the above log-normal shadowing principle is shown in the Example 8.3.

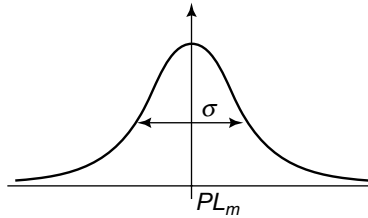


Figure 8.5 Probability density function of log-normal shadowing

EXAMPLE 8.3

Consider the previous example where $L_{50} = 167$ dB. Let the deviation σ of the log-normal shadowing be given by $\sigma = 6$ dB. Compute the threshold γ such that the path loss (PL) is greater than γ at only 5% of the locations in the cell. In other words, at 95% of the locations the path loss is less than γ .

Solution: From Eq. (8.10), we have,

$$\begin{aligned}
 Q\left(\frac{\gamma - L_{50}}{\sigma}\right) &= 5\% = 0.05 \\
 \Rightarrow \frac{\gamma - L_{50}}{\sigma} &= Q^{-1}(0.05) = 1.65v \Rightarrow \gamma &= L_{50} + \sigma \times 1.65 \\
 &= 167 \text{ dB} + 6 \text{ dB} \times 1.65 \\
 &= 177 \text{ dB}
 \end{aligned}$$

Thus, the above example tells us that the path loss is greater than 177 dB only 5% of the time. In other words, 95% of the time, the path loss is lower than 177 dB. Thus, we can say that the reliability is $\rho = 95\% = 0.95$. In general, if ρ is the required reliability, the required margin M_{dB} is given as,

$$\sigma Q^{-1}(1 - \rho)$$

which, in the above example, is given as $6 \text{ dB} \times Q^{-1}(0.05) = 6 \text{ dB} \times 1.65 \approx 10 \text{ dB}$

8.7 | Receiver-Noise Computation

Noise at the receiver arises due to thermal effects and is also known as *thermal noise*. It is very important to accurately characterize noise power to compute the signal-to-noise power ratio at the receiver and the resulting bit-error-rate performance. The *noise Power Spectral Density (PSD)* η_0 denotes the noise power per hertz of bandwidth. Hence, the total noise power is given as

$$\text{Noise power} = \eta_0 \times B$$

Further, the noise power spectral density η_0 can be derived as

$$\eta_0 = kTF \tag{8.11}$$

where $k = 1.38 \times 10^{-23}$ is the Boltzmann constant, T is the temperature in Kelvin, and F is the noise figure. Example 8.4 serves to clarify this idea.

EXAMPLE 8.4

Compute the noise power at $T = 293$ K and noise figure $F = 5$ dB. The bandwidth $B = 30$ kHz.

Solution: Given $F = 5$ dB. Therefore, the linear value of the noise figure is $F = 10^{0.5}$. Hence, from Eq. (8.11), the noise power spectral density η_0 is given as

$$\begin{aligned}\eta_0 &= kTF \\ &= 1.38 \times 10^{-23} \times 293 \times 10^{0.5} \\ &= 1.28 \times 10^{-20}\end{aligned}$$

Therefore, we have, the dB noise power spectral density given as

$$\eta_0 \text{ dB} = 10 \log_{10} \eta_0 = -199 \text{ dBW/Hz}$$

Further, the noise power σ_n^2 is given as

$$\begin{aligned}\sigma_n^2 &= \eta_0 B \\ &= 1.28 \times 10^{-20} \times 30 \times 10^3 \\ &= 3.84 \times 10^{-16}\end{aligned}$$

Therefore, the noise power in dB is

$$10 \log_{10} \sigma_n^2 = 10 \log_{10} (3.84 \times 10^{-16}) \approx -154 \text{ dB}$$

8.8 | Link-Budget Analysis

Link-budget of a wireless link is a systematic listing of power losses and gains of different intermediate components in the transceiver chain. The various additive and negative

components for the net signal power at the receiver are shown in Table 8.1 below. The + sign denotes a component which enhances or adds to the received signal strength while the – sign denotes a component which subtract from the signal strength or SNR. The final = in the last row denotes the required SNR. Therefore, the link-budget expression for the SNR required is given as

$$\text{SNR}_{\text{req}} = P_t (\text{ dB}) + G_t (\text{ dB}) - L_{50} (\text{ dB}) - M_{\text{dB}} + G_r (\text{ dB}) - L_c (\text{ dB}) - (N + 1)_{\text{dB}}$$

Therefore, the above expression can be recast to compute the required transmit power as

$$P_t (\text{ dB}) = \text{SNR}_{\text{req}} - G_t (\text{ dB}) + L_{50} (\text{ dB}) + M_{\text{dB}} - G_r (\text{ dB}) + L_c (\text{ dB}) + (N + 1)_{\text{dB}}$$

Example 8.5 illustrates a typical link-budget analysis for a wireless communication scenario.

Table 8.1 *Components of a typical wireless-link budget*

Additive(+)/Negative(–)	Component	Symbol
+	Transmitter power	P_t
+	Transmit-antenna gain	G_t
–	Median-link-propagation loss	L_{50}
–	Margin	M_{dB}
+	Mobile-receive antenna gain	G_r
–	Cabling losses	L_c
–	Receiver (noise + interference)	$N + I$
=	Required SNR	SNR_{req}

EXAMPLE 8.5

Consider a wireless-signal-propagation scenario with cell radius $d = 8$ km, carrier frequency $f_c = 2.1$ GHz, transmit antenna height $h_{te} = 40$ m, and receive antenna height $h_{re} = 2$ m. Let the standard deviation $\sigma = 6$ dB for the log-normal shadowing and it is required to achieve a reliability of $\rho = 95\%$. The temperature $T = 293$ K, bandwidth $B = 30$ kHz, noise figure $F = 5$ dB. Further, the wireless link has a receive antenna gain of 5 dB, cabling losses of 3 dB and a transmit antenna gain of 12 dB. Consider a scenario with level of interference equal to the noise power, and a Rayleigh fading channel with average power unity. Through a link-budget analysis, compute the transmit power required to achieve a bit-error rate of 10^{-4} at the receiver for BPSK modulation.

Solution: From Example 8.1, it can be seen that the median-path loss for the above scenario is L_{50} (dB) = 167 dB. For a reliability of $\rho = 95\% = 0.95$, it has been shown in Example 8.3 that the required margin $M_{dB} = 10$ dB. Also, as derived in Example 8.4, the noise power at 293 K and bandwidth 30 kHz is $3.84 \times 10^{-16} = -154$ dB. Further, it is given that the interference power I is equal to that of the noise power N , i.e., $I = N = 3.84 \times 10^{-16}$. Therefore, we have

$$N + I = 2 \times 3.84 \times 10^{-16}$$

$$(N + I) \text{ dB} = -154 \text{ dB} + 3 \text{ dB} = -151 \text{ dB}$$

The required SNR for a BER of 10^{-4} with BPSK transmission can be calculated as

$$\text{BER} = 10^{-4} = \frac{1}{2} \left(1 - \sqrt{\frac{\text{SNR}}{2 + \text{SNR}}} \right)$$

Therefore, we have

$$\frac{\text{SNR}}{2 + \text{SNR}} = (1 - 2 \times 10^{-4})^2$$

$$\text{SNR}_{\text{req}} = \frac{2(1 - 2 \times 10^{-4})^2}{1 - (1 - 2 \times 10^{-4})^2}$$

$$\approx 5 \times 10^3$$

$$\text{SNR dB} = 10 \log_{10} 5 \times 10^3 = 37 \text{ dB}$$

The various components of the link budget for this example are shown in Table 8.2. For the link-budget analysis, we have

$$37 = P_t + 12 - 167 - 10 + 5 - 3 - (-151)$$

$$P_t = 37 - 12 + 167 + 10 - 5 + 3 - 151$$

$$= 49 \text{ dBW}$$

Thus, the required transmit power at the base station is 49 dBW.

Table 8.2 *Components of a typical wireless-link budget*

Additive(+)/Negative(-)	Component	Symbol
+	Transmitter power	P_t
+	Transmit-antenna gain	12 dB
-	Median-link-propagation Loss	167 dB
-	Margin	10 dB
+	Mobile-receive antenna gain	5 dB
-	Cabling losses	3 dB
-	Receiver (noise + interference)	-151 dB
=	Required SNR	37 dB

8.9 | Teletraffic Theory

Cellular systems employ the principle of trunking to provide or meet the demands of a large number of users, with a limited number of channels. Consider an example of a cellular system with 100 supported users and 100 available channels, as shown in Figure 8.6. Such a one-to-one or dedicated channel allocation results in wastage of resources as the probability that all users are active at a given instant of time is low. Only a very small fraction of users or subscribers are likely to be active at a given point of time. Hence, practically, only a few channels are necessary to meet the demands of users as they are random in nature. This random nature for the demand

for communication or the demand to place a call is exploited by the principle of *statistical multiplexing*. For instance, consider the example of a cellular system shown in Figure 8.7 in which there are 100 users as before, with a significantly fewer number of channels. Thus, the large number of users have to share these limited number of channels, which is basically statistical multiplexing, i.e., assigning the channels to the various users based on demand.

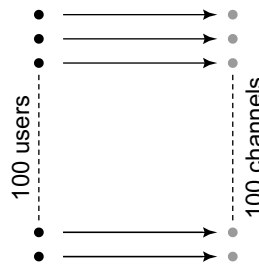


Figure 8.6 Schematic showing teletraffic system with $N = 100$ channels and $N = 100$ users

In the context of communication systems, this is also termed *trunking*. In a cellular system, a small number of wireless channels are available in each cell which are shared by a large number of subscribers in the cell. Further, in a landline or a PSTN network, very few lines are available at the exchange for a large number of subscriber home/office lines connected to the exchange. Thus, all the possible customers on these lines have to share the limited number of outgoing lines at the telephone exchange. Thus, since the number of users is much greater than the number of channels available in the cell, there is always a finite probability that all the lines are occupied. Hence, when a new user requests a channel for communication, his call is blocked as there are no channels available for communication. This probability with which calls are blocked is termed *blocking probability*, or in cellular systems, is also termed *grade of service*. The blocking probability is a key parameter of a cellular communication system. This can be derived using teletraffic theory and was proposed by the Danish engineer Erlang in 1917. The next section begins with a framework to characterize the traffic in this cellular system. The traffic per user A_0 is defined as follows:

$$A_0 = (\text{user call rate}) \times (\text{average call duration})$$

For instance, consider a per-user call rate of 2 calls per hour of 2-minute average duration each.

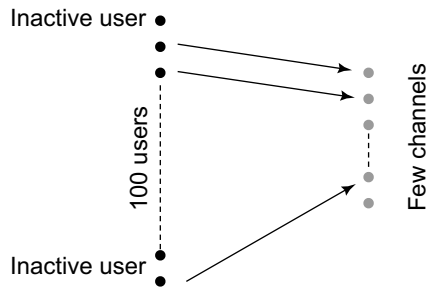


Figure 8.7 Schematic showing teletraffic system with 100 users and much fewer channels

Therefore, the traffic A_0 per user is defined as

$$\begin{aligned} A_0 &= \frac{2 \text{ calls}}{\text{hour}} \times \frac{2 \text{ hours}}{60 \text{ call}} \\ &= \frac{1}{15} \text{E} \end{aligned}$$

where E denotes the unit *erlang* of traffic. Hence, traffic is measured in units of erlangs. In the above example, the traffic is $\frac{1}{15}$ erlang. If the total number of users in the system is N , the total aggregate traffic A is given as,

$$A = NA_0$$

For instance, consider $N = 30$ users in the above system. The total traffic is given as

$$A = 30A_0 = 30 \times \frac{1}{15} \text{E} = 2\text{E}$$

Further, it can also be noted that the maximum traffic that can be supported on a single channel is given as

$$\text{Maximum traffic} = \frac{1 \text{ call}}{\text{hour}} \times \frac{1 \text{ hour}}{\text{call}} = 1\text{E}$$

Hence, a single channel can support a maximum traffic of 1 E. Hence, N channels can support a maximum of N erlangs of traffic.

8.10 | Teletraffic System Model

Assume a random-call-arrival process modeled by the Poisson distribution. Let the average call-arrival rate in this system be denoted by λ . Hence, the probability that k calls arrive in a time duration t is given as

$$P(k) = \frac{(\lambda t)^k e^{-\lambda t}}{k!} \quad (8.12)$$

The Poisson distribution is a discrete distribution defined for $k = 0, 1, \dots, \infty$. Consider now a cellular system with N available channels. Therefore, a maximum of N users can be supported. The state of the wireless system is the number of channels occupied at a given point of time. Therefore, the system can be in states S_0, S_1, \dots, S_N , where S_i denotes the state the i channels are occupied. A schematic representation of the state-space transition diagram is shown in Figure 8.8. In the state S_0 , all the channels are vacant, while in the state S_N , all the N channels are occupied. Any new calls arriving in the state S_N will, therefore, be blocked. Let P_k denote the probability of the system being in the state k , i.e., k of the N channels are occupied. Therefore, P_N denotes the probability of the system being in state N , in which any arriving call is blocked. Therefore, P_N denotes the blocking probability of the system.

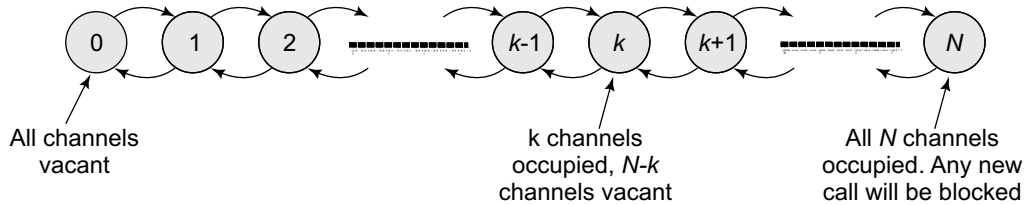


Figure 8.8 State-transition diagram for a system with N channels

8.11 | Steady-State Analysis

Consider an infinitesimally small time interval Δt . The probability that one call arrives in time interval Δt is given from Eq. (8.12) as

$$\begin{aligned} \Pr(\text{one call arrival}) &= \frac{(\lambda \Delta t)^1 e^{-\lambda \Delta t}}{1!} \\ &= (\lambda \Delta t) e^{-\lambda \Delta t} \\ &\approx \lambda \Delta t \end{aligned}$$

where the last approximation follows since $e^{-\lambda\Delta t} \approx 1$. Probability that one call arrives in the time Δt is $\lambda\Delta t$. Similarly, consider the average call time as T . Therefore, the call departure can be modeled as a Poisson process with departure $\mu = \frac{1}{T}$. Therefore, the probability of one call departure in the time ΔT is given as

$$\Pr(\text{one call departs}) = \mu\Delta t$$

Therefore, in the state k , we have k channels occupied. Hence, probability of call departure in the state k is $k\mu(\Delta t)$. Consider the time instant t . The system is in the state S_k at time $t + \Delta t$ if one of the following occurs.

1. The system is in the state S_{k-1} at the time t and one call arrives in Δt . The probability of this event is given as

$$\text{Prob} = P_{k-1} \times (\lambda\Delta t)$$

2. The system is in the state S_{k+1} at the time t and one call departs in Δt . The probability of this event is given as

$$\text{Prob} = P_{k+1} \times (k + 1) (\mu\Delta t)$$

3. The system is in the state k , and call neither arrives or departs. The probability of this event is given as

$$\text{Prob} = P_k \times (1 - \lambda\Delta t - (k + 1) \mu\Delta t)$$

Therefore, the probability P_k can be expressed as

$$P_k = P_{k-1} \times (\lambda\Delta t) + P_{k+1} \times (k + 1) (\mu\Delta t) + P_k \times (1 - \lambda\Delta t - (k + 1) \mu\Delta t)$$

Simplifying the above expression, we have

$$(\lambda + k\mu) P_k = \lambda P_{k-1} + (k + 1) \mu P_{k+1} \quad (8.13)$$

Consider now the transition diagram shown for the state S_0 given in Figure 8.8. Since no further calls can depart from S_0 , the expression for P_0 can be derived as

$$\begin{aligned} P_0 &= P_0(1 - \lambda\Delta t) + P_1\mu\Delta t \\ P_1 &= \frac{\lambda}{\mu}P_0 \end{aligned} \quad (8.14)$$

Substituting $k = 1$ in Eq. (8.13), we have

$$\begin{aligned} (\lambda + \mu)P_1 &= \lambda P_0 + 2\mu P_2 \\ (\lambda + \mu)\frac{\lambda}{\mu}P_0 &= \lambda P_0 + 2\mu P_2 \\ \frac{\lambda^2}{\mu}P_0 + \lambda P_0 &= \lambda P_0 + 2\mu P_2 \\ \Rightarrow \frac{\lambda^2}{\mu}P_0 &= 2\mu P_2 \\ \Rightarrow P_2 &= \frac{1}{2}\left(\frac{\lambda}{\mu}\right)^2 P_0 \end{aligned}$$

Proceeding similarly, it can be shown that

$$P_k = \frac{1}{k!}\left(\frac{\lambda}{\mu}\right)^k P_0$$

Employing the fact now that the total probability must equal 1, we have

$$\begin{aligned} \sum_{k=0}^N k &= 0^N = 1 \\ \Rightarrow \sum_{k=0}^N \frac{1}{k!}\left(\frac{\lambda}{\mu}\right)^k P_0 &= 1 \\ \Rightarrow P_0 &= \frac{1}{\sum_{k=0}^N \frac{1}{k!}\left(\frac{\lambda}{\mu}\right)^k} \end{aligned}$$

Therefore, finally, the blocking probability P_N or, in other words, the probability that the system is in the state N is given as

$$P_N = \left(\frac{1}{N!} \left(\frac{\lambda}{\mu} \right)^N P_0 \right) = \frac{\frac{1}{N!} \left(\frac{\lambda}{\mu} \right)^N}{\sum_{k=0}^N \frac{1}{k!} \left(\frac{\lambda}{\mu} \right)^k}$$

Let λ denote the call-arrival rate and $\mu = \frac{1}{T}$ denote the call-departure rate. The total traffic A is given as

$$\begin{aligned} \text{Total traffic} &= \text{Call-arrival rate} \times T \\ &= \lambda \times \frac{1}{\mu} = \frac{\lambda}{\mu} = A. \end{aligned}$$

Therefore, the blocking probability is given as

$$P_N = \left(\frac{1}{N!} A^N P_0 \right) = \frac{\frac{1}{N!} A^N}{\sum_{k=0}^N \frac{1}{k!} A^k}$$

Example 8.6 helps illustrate the process of computation of the blocking probability described above.

EXAMPLE 8.6

Consider a system with $N = 50$ channels. Let the blocking probability $P_N = P_B = 10^{-2} = 1\%$. What is the total traffic that can be supported?

Solution: It can be seen from the standard Erlang traffic table that the offered load for a blocking probability of 10^{-2} corresponding to number of users $N = 50$ is given as $A = 37.9E \approx 38E$.

Further, another example of the teletraffic framework described above in the context of cellular system design is given in Example 8.7.

EXAMPLE 8.7

Consider a cellular system with $N = 48$ channels per cell, and blocking probability $P_B = 0.02 = 2\%$. The traffic per user is $A_0 = 0.04$ E. The cell radius is 1 km as shown in Figure 8.9. What is the number of users that can be supported in a city of 603 km^2 area?

Solution: For $N = 48$ channels and blocking probability $P_B = 0.02$, it can be seen that the net offered load or supported traffic is given as $A = 38.4$ E. Also, since the total traffic $A = NA_0$, we have

$$N = \frac{A}{A_0} = \frac{38.4}{0.02} = 960.$$

Further, from Figure 8.9, it can be seen that the area of a typical hexagonal cell of radius 1 km is given as

$$\text{Cell area} = 6 \times 1 \times \frac{1}{\sqrt{3}} = 3.46 \text{ km}^2.$$

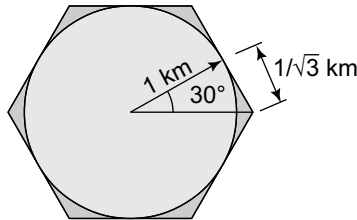


Figure 8.9 Cell for Example 8.7

Therefore, the number of cells that are required to cover the entire city is given as

$$\text{Number of cells} = \frac{\text{City area}}{\text{Cell area}} = \frac{603}{3.46} \approx 174 \text{ cells.}$$

Therefore, the total number of users that can be supported by the cellular provider is given as

$$\text{Number of users supported} = \text{Number of cells} \times \text{Number of users per cell}$$

$$\approx 174 \times 960 = 167,040$$

Thus, approximately 167,040 users can be supported by the cellular service provider in the given city for the desired blocking probability of 2%.

PROBLEMS

1. **Okumura Model** Answer the questions below on the basis of the Okumura model for path loss in wireless transmission.
 - (a) At $f_c = 700$ MHz, find the median-path loss using $d = 50$ km, $h_{te} = 80$ m and $h_{re} = 6$ m in a quasi-open area.
 - (b) If the noise power at the receiver is -155 dB, what is the exact EIRP (Effective Isotropic Radiated Power) in watts of the transmitter required to decode BPSK with a BER of 10^{-5} at 50% of the ensemble locations? Please pay attention to the nature of the wireless channel.

2. **Cellular Communication** A GSM cellular system blanketing the city of Mumbai has a cell radius of 1 km. Assuming that the cellular operator has secured a spectrum of 8.4 MHz from TRAI, answer the questions that follow.
 - (a) From Wikipedia, Mumbai has an area that is roughly 603 km^2 . What is the number of users that can be supported per cell for a GoS of 2% and per-user traffic of 0.04 E? Please pay attention to the **specific** cellular design of GSM.
 - (b) What is the maximum number of subscribers that can be served by this cellular operator in Mumbai?

3. A corporate headquarters has 50 leased telephone lines. For an average per-employee talk time of 1 minute 20 seconds per hour, what is the employee strength that can be supported for a blocking probability of 2%?

4. Consider a WCDMA system (bandwidth = 5 MHz) in a large city with Rx antenna gain of 5 dB, cabling losses of 3 dB, Tx antenna gain of 12 dB, and a processing gain of 21 dB. The system has a noise figure of 15 dB. Answer the questions that follow.
 - (a) Employing the Hata model, compute the median path loss L_{50} at the cell edge of a cellular system with a cell radius of 8 km, $f_c = 2.1$ GHz, $h_{te} = 40$ m, $h_{re} = 2$ m.
 - (b) Using an appropriate approximation, compute the average SNR at the receiver required to decode Alamouti-coded QPSK symbols with a BER of $P_e = 10^{-4}$.
 - (c) Finally, compute the transmitter power in watts required to support the above decoding at a minimum of 85% of the cell-edge locations given a variance of $X_\sigma = 6$ dB for the

log-normal shadowing. Assume a temperature of 27°C and an interference level equal to the noise level.

- 5. Cellular CDMA** Consider an IS-95 based CDMA system (bandwidth = 1.25 MHz) in a large city with Rx antenna gain of 3 dB, cabling losses of 6 dB, Tx antenna gain of 7 dB, and a processing gain of 24.08 dB. The system has a noise figure of 4 dB. Assume an ambient temperature of 27°C and answer the questions that follow.
- What is N , the length of the spreading code?
 - Employing the Hata model, compute the median-path loss L_{50} at the cell edge of a cellular system with a cell radius of 7 km, $f_c = 2.3$ GHz, $h_{te} = 35$ m, $h_{re} = 6$ m.
 - Assuming that on an average, 10 users interfere with any given user and further, each user has a voice activity factor of 50%, compute the SNR at the receiver required to decode QPSK-modulated symbols with a BER of $P_e = 10^{-3}$. Assume a simplistic line-of-sight unity gain AWGN baseband channel model for each user and that all cell-edge users (desired and interferers) have the same SNR.
 - Finally, compute the average total transmit power of the base station in watts if 100 users are connected to the base station on an average and the above decoding is supported at a minimum of 85% of the cell-edge locations given a variance of $X_\sigma = 6$ dB for the log-normal shadowing (make sure you do NOT double count the processing gain).
- 6. Cellular Capacity:** Consider a CDMA operator who operates with spreading codes of length 64. If each user on an average makes 3 calls per hour of average duration of 2 minutes per call, what is the total number of users that can be supported per cell with a blocking probability of 1%? Assume each user is allocated one spreading code for a voice call and that the users are perfectly orthogonal (i.e., neglect the effect of interference). What is the number of users for a tolerable blocking probability of 5%?
- 7. Okumura Model** Answer the questions below on the basis of the Okumura model for path loss in wireless transmission. Consider a WCDMA system of bandwidth = 5 MHz, with Rx antenna gain of 5 dB, cabling losses of 3 dB, Tx antenna gain of 12 dB, and a processing gain 21 dB. The system has a noise figure of 15 dB. Assume a temperature of 27°C and an interference level equal to the noise level.
- At $f_c = 1.8$ GHz, find the median-path loss using for $d = 20$ km, $h_{te} = 60$ m, and $h_{re} = 2$ m in a suburban area.

- (b) If this needs to be supported at a minimum of 85% of the cell-edge locations given a variance of $\sigma = 10$ dB for the log-normal shadowing, compute the power margin required.
- (c) Compute the total sum noise and interference power ($\eta + I$) at the receiver.
- (d) Using an appropriate approximation, compute the average SNR at the receiver required to decode 1×2 Alamouti-coded BPSK symbols with a BER of $P_e = 10^{-4}$ if the channel between each transmit and receive antenna is Rayleigh of average power unity. Ignore the multi-user interference in CDMA systems.
- (e) Finally, compute the transmitter power in watts required to support the above decoding.

8. Okumura Model

- (a) Employing the Okumura model, compute the median-path loss for $d = 10$ km, $h_{te} = 60$ m, and $h_{re} = 8$ m, at $f_c = 600$ MHz, in a suburban area ($G_t = G_r = L = 1$).
- (b) If the noise power at the receiver is -175 dB, what is the exact EIRP in watts required at the transmitter to decode QPSK with a BER of 10^{-4} at 95% of the ensemble locations? Assume $X_\sigma = 6$ dB, the small-scale fading is Rayleigh in nature, and that path loss is the only loss factor in the system.

9. Cellular MIMO Answer the questions below on the basis of the Okumura model for path loss in wireless transmission. Consider a MIMO wireless system of bandwidth = 200 kHz, with Rx antenna gain of 8 dB, cabling losses of 5 dB, Tx antenna gain of 5 dB. The system has a noise figure of 10 dB. Assume a temperature of 20°C and an interference level equal to $\frac{2}{3}$ of the noise level.

- (a) At $f_c = 1.5$ GHz, find the median-path loss using $d = 5$ km, $h_{te} = 30$ m and $h_{re} = 1.5$ m in a suburban area.
- (b) If this needs to be supported at a minimum of 95% of the cell-edge locations given a variance of $\sigma = 8$ dB for the log-normal shadowing, compute the power margin required.
- (c) Compute the total sum noise and interference power ($\eta + I$) at the receiver.
- (d) Using an appropriate expression, compute the average SNR at the receiver required to decode BPSK symbols with a BER of $P_e = 10^{-4}$ if the channel between each transmit and receive antenna is Rayleigh of average power unity.
- (e) Finally, compute the transmitter power in watts required to support the above decoding.

Index

1x Evolution Data Optimized (1xEV-DO), 119
1x Evolution Data Optimized (1xEVDO), 3
2G Wireless Standards, 1
3rd Generation Partnership Project (3GPP), 4

A

Additive White Gaussian Noise (AWGN), 8
Alamouti code, 201, 203
Approximate orthogonality, 135
Asymmetric Digital Subscriber Line (ADSL), 3
Asymptotic MIMO capacity, 198
Asynchronous CDMA, 155
Attenuation factor, 27
Average delay spread, 94
Average power profile, 91

B

Balance property, 127
Beamformer, 55
Beamforming, 201
Binary Phase-Shift Keying (BPSK), 8
Binary signal vector detection problem, 20
Bit Error Rate (BER), 8
Blocking probability, 284

C

Cauchy–Schwarz inequality, 56
CDMA 2000, 119
Central limit theorem, 32
Channel estimation, 46
Channel Impulse Response (CIR), 27
Channel State Information (CSI), 203
Chernoff bound, 45
Chip, 121
Code division, 121
Coherence time, 108
Coherent demodulation, 233
Complex fading channel coefficient, 31
Correlation property, 128
Critical difference, 25
Cyclic prefix, 236

D

Delay spread, 29, 84
Digital Subscriber Line (DSL), 3

Diversity combining, 165
Diversity order, 71
Diversity, 45
Doppler shift computation, 105
Doubly selective wireless channels, 108
Dynamic range, 259

E

Equalization, 103
Erlang, 285
Exact orthogonality, 133

F

Fading coefficient, 31
Fading, 25
Fast-fading channel, 114
Finite Impulse Response (FIR), 142
Flat-fading channel, 97
Flat-fading wireless channel, 30
Free-space propagation model, 268
Frequency Division for Multiple Access (FDMA), 2, 119
Frequency-reuse factor, 141
Frequency-selective channel, 97
Frequency-selective fading, 114, 234

G

Gaussian Q function, 14
Gaussian Random Variable, 6
General Packet Radio Service (GPRS), 2
Global System for Mobile (GSM), 1
Graceful degradation, 139
Grade of service, 284
Ground-reflection scenario, 269

H

Hata model, 276
Hermitian transpose, 55
High-Speed Uplink Packet Access (HSUPA), 119
High-Speed Uplink Packet Access (HSUPA), 3
High-Definition Television (HDTV), 5
High-Speed Downlink Packet Access (HSDPA), 119
High-Speed Downlink Packet Access (HSDPA), 3

I

Identically Distributed (IID) chips, 130
 Indoor delay spreads, 95
 Instantaneous amplitude, 39
 Inter-Carrier Interference (ICI), 250
 Interference distribution, 139
 Interference, 134
 Interference-limited system, 137
 Inter-OFDM symbol interference, 237
 Inter-Symbol Interference (ISI), 101, 235
 Inverse Discrete Fourier Transform (IDFT), 235
 Inverse Fast Fourier Transform (IFFT), 235

J

Jacobian determinant, 17
 Jake's model, 111
 Jakes' spectrum, 113
 Jakes' temporal correlation model, 112
 Jakes' model, 110
 Jammer margin, 138
 Jammer suppression, 139
 Jammer, 138

L

Large-scale-propagation models, 267
 Least-squares error function, 171
 Least-squares estimate, 47
 Least-squares estimator, 171
 Linear estimator, 179
 Linear Feedback Shift Register (LFSR), 125
 Linear Minimum Mean Squared Estimator (LMMSE), 179
 Linear relation, 125
 Linear Time Invariant (LTI) systems, 27
 Line-Of-Sight (LOS), 27
 Link-budget analysis, 280
 Log-normal shadowing, 277
 Long-Term Evolution (LTE), 4, 230
 LTE Advanced, 4

M

M -ary Phase Shift Keying (PSK), 17
 Matched filter, 184
 Maximal Ratio Combiner (MRC), 57
 Maximal ratio combining, 57
 Maximum Delay Spread, 85
 Maximum Ratio Combiner (MRC), 145, 202
 Maximum Ratio Transmission (MRT), 219
 Maximum-length PN sequence, 126
 Maximum-length shift register, 126

MIMO beamforming, 216
 MIMO capacity, 189
 MIMO MMSE receiver, 179
 MIMO system model, 166
 MIMO Zero-Forcing (ZF) receiver, 170
 MIMO-OFDM, 247
 Minimum Mean-Squared Error (MMSE), 179
 Motivation, 230
 Multicarrier basics, 230
 MultiCarrier Modulation (MCM), 234
 Multicarrier transmission, 232
 Multipath components, 83
 Multipath diversity, 142, 145
 Multipath fading, 25
 Multipath Interference (MPI), 25, 149
 Multiple Access (MA) technology, 119
 Multiple access, 119
 Multiple-Input Multiple-Output (MIMO), 3
 Multiple-Input Single-Output (MISO), 168
 Multi-User CDMA, 133
 Multi-user interference, 134

N

Near-far problem, 146
 Noise amplification, 178
 Noise Power Spectral Density (PSD), 279
 Nonlinear MIMO Receiver: V-BLAST, 212
 Non-Line-Of-Sight (NLOS), 27, 83
 Norm of the channel-impulse response vector, 151

O

Okumura model, 273
 Optimal MIMO capacity, 192
 Optimum beamformer, 56
 Orthogonal Frequency Division for Multiple Access (OFDMA), 3
 Orthogonal Frequency Division Multiplexing (OFDM), 3, 236
 Orthogonal Space-Time Block Code (OSTBC), 206
 Outdoor cellular channels, 94

P

Parallelization, 190
 Path delay, 27
 Path-loss exponent, 268
 Peak-to-Average Power Ratio (PAPR), 255
 Phase factor, 29
 Pilot symbols, 47
 Power control, 146

Power distribution density, 91
 Principle of orthogonality, 175
 Pseudo-inverse, 173
 Pseudo-noise (PN) sequence, 125
 Pulse Amplitude Modulated (PAM), 101

Q

Quadrature Phase Shift Keying (QPSK), 11
 Quasi-static channel matrix, 169

R

Rake Receiver, 142, 145
 Rayleigh fading wireless channel, 32
 Receive diversity, 64
 Receive processing, 189
 Receiver-noise computation, 279
 RMS delay spread, 87
 Run-length Property, 127

S

SC-FDMA receiver, 261
 SC-FDMA, 260
 Shift registers, 125
 Signal-to-Interference-Noise power Ratio (SINR), 137
 Single-carrier frequency division for multiple access, 260
 Single-Input Multiple-Output (SIMO), 51, 168
 Singular Value Decomposition (SVD), 185
 Slow-fading channel, 114
 Space-time codes, 201
 Spatial diversity, 64
 Spatial multiplexing, 165, 190
 Spatially matched filter, 57
 Spatially uncorrelated additive noise, 169
 Spread spectrum, 123
 Spreading code, 123
 Spreading gain, 137
 Standard deviation, 89
 Standard Gaussian random variable, 6
 Statistical multiplexing, 284
 Steady-state analysis, 286
 Successive Interference Cancellation (SIC), 212

Index

T

Tail probability, 14
 Tall matrix, 170
 Tapped delay-line, 27
 Teletraffic system model, 286
 Teletraffic Theory, 283
 Temporal correlation coefficient, 110
 Thermal noise, 279
 Time Division for Multiple Access (TDMA), 2, 120
 Time selectivity, 108
 Time slots, 120
 Time-selective channel, 108
 Training symbols, 46
 Transmit beamforming, 202
 Transmit precoding, 189
 Transmit vector, 166
 Trunking, 284

U

Underspread channels, 115
 Universal Frequency Reuse, 140
 Universal Mobile Telecommunications System (UMTS), 2
 U-shaped Doppler spectrum, 113

V

Vertical Bell Labs layered space-time, 212

W

Water filling, 193
 Wideband CDMA (WCDMA), 119
 Wideband systems, 123
 Wideband wireless technologies, 2
 WiMAX (Worldwide Interoperability for Microwave Access), 230
 Wireless channel correlation, 110
 Worldwide Interoperability for Microwave Access (WiMAX), 4

Z

Zero-forcing receiver, 46, 173
 Zero-forcing receiver matrix, 173
 Zero-mean circularly symmetric complex Gaussian noise, 12